Electron shuttling in haloalkaliphilic sulfide oxidizing bacteria

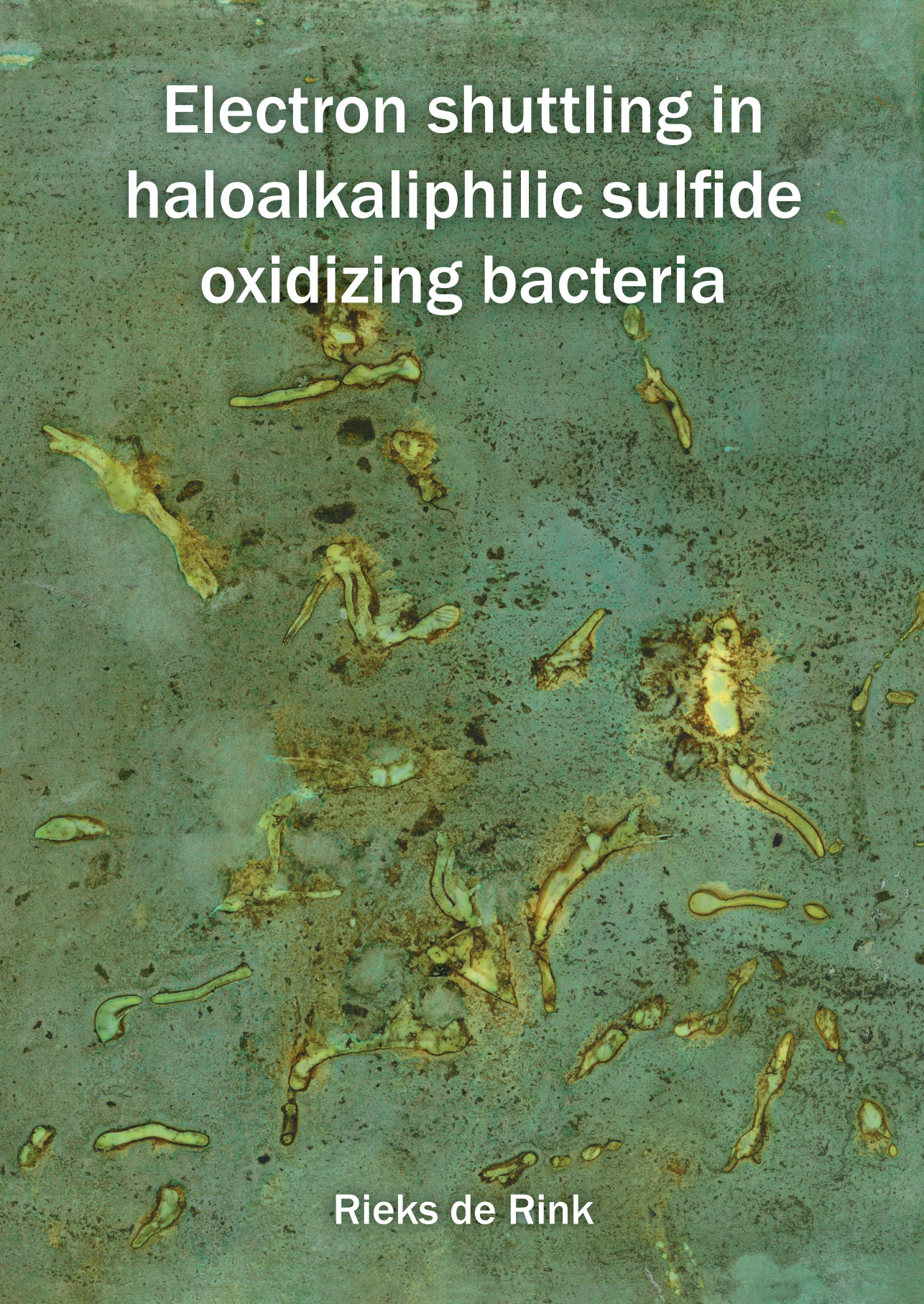

Rieks de Rink

Propositions

1. Bacteria are essential for efficient H_2S absorption from sour gas streams in the biological gas desulfurization process.
   (this thesis)

2. HA-SOB can produce electric current in a microbial electrochemical system without their substrate being present.
   (this thesis)

3. Scientific journals should not disclose the name(s) of the author(s) of manuscripts that are submitted for publication to reviewers.

4. Someone's ability to complete a PhD thesis is independent of exam grades.

5. Waste management companies should change the way of handling waste in accordance with their statement "Waste does not exist".

6. To improve the quality of life, it is more effective to invest in the reduction of air pollution than to increase the budget of the health care system.

Propositions belonging to the thesis, entitled

Electron shuttling in haloalkaliphilic sulfide oxidizing bacteria

Rieks de Rink
Wageningen, 13 October 2021

ELECTRON SHUTTLING IN HALOALKALIPHILIC SULFIDE OXIDIZING BACTERIA

Rieks de Rink

Thesis Committee

Promotor

Prof. Dr C.J.N. Buisman
Professor Biological Recovery and Reuse Technology
Wageningen University & Research

Co-promotors

Dr J.B.M. Klok
R&D manager Paqell B.V
Utrecht

Dr A. Ter Heijne
Associate professor, Environmental Technology
Wageningen University & Research

Other Members

Prof. Dr D.Z. Machado de Sousa, Wageningen University & Research
Prof. Dr F.J. Cervantes, Universidad Nacional Autónoma de México, Mexico City
Dr J.B.A. Arends, Ghent University, Belgium
Dr P.L.F. van den Bosch, Nederlandse Aardolie Maatschappij B.V., Assen

This research was conducted under the auspices of the Graduate School for Socio-Economic and Natural Sciences of the Environment (SENSE)

ELECTRON SHUTTLING IN HALOALKALIPHILIC SULFIDE OXIDIZING BACTERIA

Rieks de Rink

Thesis

Submitted in fulfilment of the requirements for the degree of doctor
at Wageningen University
By the authority of the Rector Magnificus,
Prof. Dr A.P.J. Mol,
In the presence of the
Thesis Committee appointed by the Academic Board
to be defended in public
on Wednesday 13 October
at 1:30 p.m. in the Aula

Rieks de Rink
Electron shuttling in haloalkaliphilic sulfide oxidizing bacteria
228 pages.

PhD Thesis, Wageningen University, Wageningen, the Netherlands (2021)
With references, with summaries in English and Dutch

ISBN: 978-94-6395-969-8
DOI: https://doi.org/10.18174/553335

TABLE OF CONTENTS

CHAPTER 1

General introduction

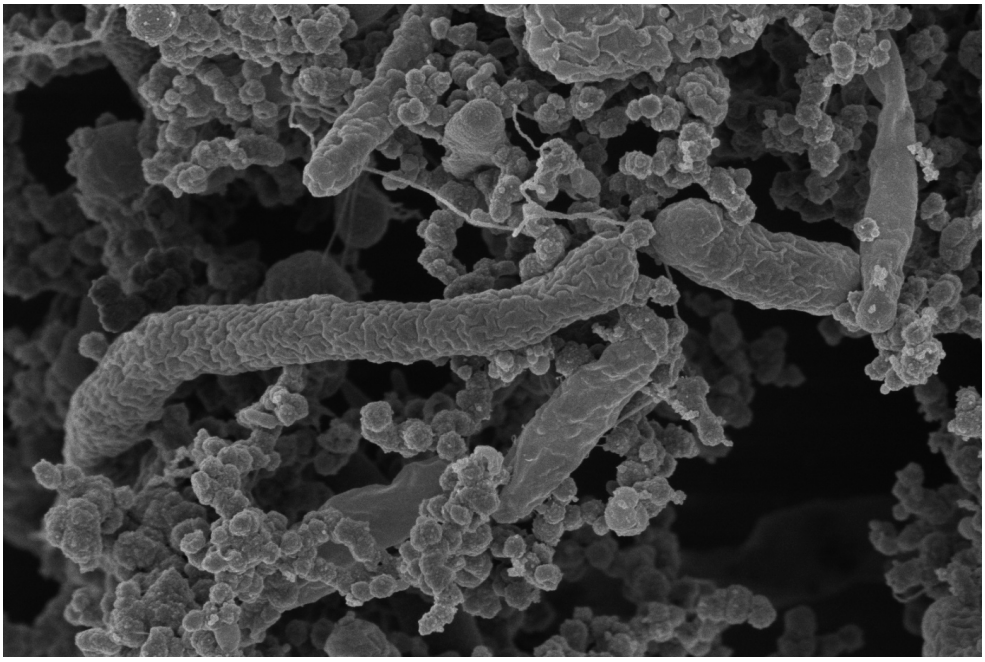

1.1 SULFUR DIOXIDE EMISSION

The use of fossil fuels for e.g. transport, electricity production and industrial production processes, is inevitably associated with air pollution, having a high impact on public health and the environment [1, 2]. One of the main air pollutants resulting from fossil fuels usage, is sulfur dioxide (SO_2). SO_2 is formed by the combustion of sulfur compounds that are present in fossil fuels and is a toxic gas, known to cause several respiratory diseases [3]. As part of the natural occurring biogeochemical sulfur cycle, SO_2 is also emitted by for example volcanoes [4, 5]. Due to the industrial revolution, the global SO_2 emission has drastically increased. The highest global man-made SO_2 emissions were reached in the 1970s with 130-140 million tons per year [6, 7], which far exceeded emission from natural sources [8, 9]. As such, SO_2 emissions from human activities severely impacts the global sulfur cycle.

In the atmosphere, part of the SO_2 is oxidized via various routes into sulfuric acid (H_2SO_4). H_2SO_4 dissolves into water droplets and is eventually removed from the atmosphere via wet deposition by rain- or snow fall [10-12]. Another part of the SO_2 is removed via dry deposition, for example in the form of particulates [8, 13]. The deposition of acidic substances from the atmosphere via either wet or dry deposition, is often referred to as 'acid rain' [2]. Acid rain leads to acidification of waters and soils and is therefore harmful for ecosystems and agriculture [11, 12].

From the 1970's onwards, implementation of specific environmental legislation in mainly the United States and Europe resulted in a decline of of SO_2 emission and sulfur deposition [14-18]. In 2014, the global SO_2 emission was estimated to be 105 million ton and it is expected that this will remain stable until 2030. However, large spatial differences in the SO_2 emission exist [7, 19, 20] and currently India is the world's largest emitter of SO_2, contributing to approximately 15% of the global SO_2 emission [19, 21].

1.2 GAS DESULFURIZATION

One of the main strategies to prevent emission of SO_2, is the removal of sulfur compounds from (fossil) fuels prior to combustion, called desulfurization. In natural gas, sulfur compounds are mainly present in the form of hydrogen sulfide (H_2S) [22], which is known for its smell of rotten eggs. H_2S is a highly toxic gas and is lethal for humans at a concentration of 500 ppm [23]. In addition, H_2S is very corrosive [24] and is explosive in a large concentration range (4-46 vol% in air) [25]. Besides natural gas, crude oil also

contains sulfur compounds [26, 27]. These are often removed in petroleum refineries via hydrodesulfurization, in which the sulfur compounds react with H_2 gas to form H_2S [28]. Another source of H_2S is 'syngas' (or synthesis gas), which is produced in the gasification of coal and biomass [29]. During the gasification, the sulfur compounds in the feedstock are converted into H_2S. Also biogas and landfill gas, which are formed during the anaerobic digestion of organic wastes, often contain H_2S [30, 31]. The aforementioned gas streams are all 'sour gas' streams that require treatment in order to prevent emission of H_2S and SO_2.

Especially for gas streams with a medium-size sulfur load (0.2 – 20 ton H_2S per day), desulfurization is challenging. For these gas streams non-regenerative scavengers, such as iron oxides, have too high operational costs (about $ 5700 / ton sulfur) [32]. For bulk removal of H_2S the combination of the amine and Claus process is typically applied. In the amine process, H_2S is removed from the gas stream in an absorber column at high pressure and a temperature of 40 – 50 °C with an aqueous alkanolamine solution [33]. The H_2S is subsequently stripped from the solution in a regenerator by heating the solvent to approximately 120 °C and decreasing the pressure to 1-2 bar. Next, the concentrated H_2S gas stream, called 'acid gas', is send to a Claus unit to convert H_2S to elemental sulfur (S^0). The Claus process consists of a thermal stage and several catalytic stages [34]. In the thermal stage, part of the H_2S is combusted to SO_2. The remainder of the H_2S reacts with the SO_2 to form S^0. Because the reaction between H_2S and SO_2 is an equilibrium reaction, complete H_2S removal is not achieved in the Claus process. Therefore, a 'tail gas' treatment step is often required to meet the sulfur emission regulations [34]. Whilst the combination of the amine and Claus process is very cost-effective for gas streams with a high sulfur load (>50 ton-S day^{-1}), the investment costs are high for gas streams with a medium-size sulfur load [32].

To remove H_2S and recover elemental sulfur from gas streams with a medium-size sulfur load, liquid redox processes, such as the Lo-cat and Sulferox process, have been developed [35]. These processes make use of aqueous solutions with chelated iron complexes as a pseudo-catalyst to convert H_2S into elemental sulfur. The catalyst is regenerated with oxygen and the sulfur is separated from the solution. These processes operate at temperatures of 20 – 60 °C and at a pH of around pH 8.5 [36, 37]. Commonly used chelating agents are EDTA and HEDTA, which are required to avoid metal precipitation. However, due to direct contact of sulfide with O_2, by-products thiosulfate and sulfate are

formed [38]. Disadvantage of these side reactions is that they result in the production of protons and thus require addition of a base to maintain the pH of the solution. Due to the nature of sulfur formed in the process, liquid redox processes often suffer from plugging problems caused by sticky sulfur [39]. Another disadvantage is the degradation of the chelating agents, resulting in the formation of insoluble iron compounds [38, 40, 41]. Hence, continuous supply of metals and chelating agents are required, resulting in high operating costs. Chelating agents such as EDTA, are present in the effluent streams of liquid redox processes. These chelating agents are not biodegradable and can inhibit biological wastewater treatment [42]. When released into the environment, these compounds disturb metal speciation and have a strong tendency to form toxic metal complexes [43]. Thus, although liquid redox processes are effective for the removal and conversion of H_2S, these processes are expensive and produce waste streams which are harmful for the environment.

1.3 BIOTECHNOLOGICAL GAS DESULFURIZATION

As a cost-effective and environmentally friendly alternative to physico-chemical technologies, a biotechnological desulfurization process has been developed. This process makes use of naturally occurring bacteria for the conversion of sulfide to elemental sulfur. The development of this process started in the late 1980s at Wageningen University and the first full-scale unit was built in 1993 in Eerbeek, the Netherlands. To date, this unit is treating biogas formed by anaerobic digestion of wastewater from paper industry [44]. The process is currently widely applied for desulfurization of various types of gas streams, such as biogas, landfill gas, high-pressure natural gas and several refinery gas streams. It is licensed by the company Paques as THIOPAQ® for applications of biogas and landfill gas, and by the company Paqell as Thiopaq O&G for application in the oil and gas industry. By 2016, more than 250 installations have been built worldwide [45].

The effluent stream of the biological desulfurization process is non-hazardous since no toxic chemicals are used. The process can be applied for gas streams with pressures up to 80 bar and is not limited to a certain inlet H_2S concentration. H_2S removal efficiencies of over 99.5% are achieved and typically, the H_2S concentration of the treated gas is <25 ppm(v) [46]. The process solution is an aqueous alkaline sodium (bi)carbonate buffer solution. The Na^+ concentration of the process solution is about 1.0 – 1.5 M and the pH is 8-9. Therefore, the solution is called ‘haloalkaline’ (halo means salt and alkaline means

high pH). In this thesis, the process is referred to as 'biological desulfurization process under haloalkaline conditions'.

The first step of the biological desulfurization process is the counter current contact of sour gas with process solution, which occurs in the absorber column (Figure 1.1). First, H_2S dissolves into the solution. Due to the alkalinity of the process solution, the dissolved H_2S is converted into predominantly soluble bisulfide (HS^-), releasing a proton. The gas stream low in H_2S ('treated gas') leaves the absorber at the top. The 'sulfide rich' solution is collected at the bottom of the absorber and is led to a bioreactor. Via compressed air, oxygen is supplied to the bioreactor, which also serves to mix the bioreactor solution. A mixed culture of bacteria uses the oxygen to convert the dissolved sulfide into predominantly elemental sulfur, forming hydroxide. This regenerates the process solution, i.e. the alkalinity that is used for the absorption of H_2S is restored. The process solution from the bioreactor is recirculated to the top of the absorber. Elemental sulfur forms solid particles as it has a very low solubility (5 µg L^{-1}) [47]. These S^0 particles are recovered from

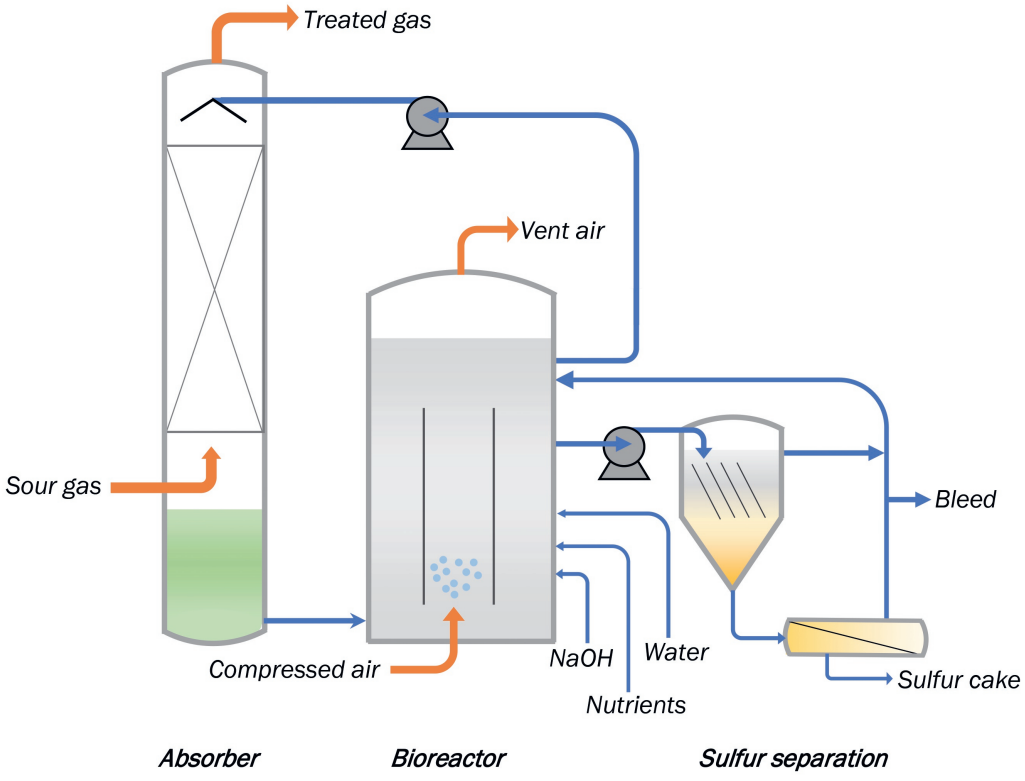

Figure 1.1: Process scheme of the biological desulfurization process under haloalkaline conditions.

the process solution in the sulfur separation section, which typically consists of a gravity settler and/or a decanter centrifuge.

Because elemental sulfur has oxidation state 0, it is commonly denoted as 'S^0'. Since the most commonly encountered form consists of rings of 8 S atoms, elemental sulfur is also referred to as 'S_8' [39, 48]. Both S^0 and S_8 are used to indicate elemental sulfur. The elemental sulfur formed in the biological desulfurization process (biosulfur) is more hydrophilic compared to chemically formed sulfur, which is hydrophobic [48-50]. Furthermore, chemical sulfur has a bright yellow color due to a small fraction of S_7 rings [51], whilst the biosulfur has a more white to grey color. The biosulfur has several applications. For example, it can be used as a substrate for microbial sulfidogenesis in metal recovery [52] and can be applied as a fertilizer or fungicide in agriculture [53, 54].

Besides elemental sulfur, the by-products sulfate (SO_4^{2-}) and thiosulfate ($S_2O_3^{2-}$) are formed in the process. This has several disadvantages. Unlike S^0, the formation of sulfate and thiosulfate from H_2S produces protons. The protons are buffered by (bi)carbonate leading to a decrease of the alkalinity of the process solution. Therefore, SO_4^{2-} and $S_2O_3^{2-}$ formation require addition of caustic soda (NaOH) to maintain the alkalinity. Since NaOH addition results in an increase of the salt concentration, water is added in addition to NaOH to control the salinity. SO_4^{2-} and $S_2O_3^{2-}$ can only be removed via a liquid effluent stream ('bleed') because they are dissolved in the process solution. Another disadvantage of sulfate and thiosulfate formation is that more O_2 is required, which results in a higher air demand of the bioreactor and thus a higher energy consumption. NaOH consumption, the production of the bleed stream and energy consumption all contribute to the operating costs of the process [45]. The environmental impact of the process would decrease when less NaOH, water and energy are required, and when less bleed would be produced. The NaOH and water consumption and the bleed stream formation are directly proportional to the by-product formation. Hence, to minimize NaOH and water consumption and the production of bleed, SO_4^{2-} and $S_2O_3^{2-}$ formation should be minimized, meaning that the formation of S^0 should be maximized. This becomes especially important when the process is applied for gas streams with a higher sulfur load.

To ensure that all sulfide is converted while minimizing formation of by-products, accurate control of the O_2 supply to the bioreactor is essential. When O_2 is supplied in excess amounts, all sulfide is converted into sulfate. Therefore, the bioreactor is operated under

oxygen-limited conditions [55, 56]. However, when O_2 supply is too low, sulfide accumulates in the bioreactor solution. This would lead to: i) increased thiosulfate formation, ii) H_2S presence in the vent air of the bioreactor, and iii) lower H_2S absorption in the absorber. In full-scale systems, the O_2 supply to the bioreactor is controlled via the online measurement of the oxidation reduction potential (ORP or redox) [57]. Although this ORP control strategy has been optimized, the maximum selectivity for S^0 formation that is achieved is limited to about 90% in current full-scale systems [58]. Selectivity is a general term to express the mole fractions of the products that are formed from a substrate. In several previous studies, the product formation has been investigated and the obtained product selectivities are shown in Table 1.1.

In most of these studies, the maximum achieved selectivity for S^0 formation was 80-90%. However, results were often obtained in relatively short experiments, meaning the number of measurements was limited. Furthermore, short experimental runs are not representative for full-scale plants, in which the specific conditions provide selection pressure for the microbial community on the long term. The composition of the microbial community, in turn, affects the process performance [62]. Hence, long-term experiments are required to study product selectivities in the biological desulfurization process.

Table 1.1: Obtained product selectivities of sulfide oxidation under haloalkaline conditions as reported in literature. In case multiple experiments / experimental stages were performed, the highest selectivity for S^0 formation is mentioned. The experiment of Roman et al. was performed in the presence of methanethiol.

Product selectivities (%)			Duration of experiment (days)	Reference
S^0	SO_4^{2-}	$S_2O_3^{2-}$		
73	*Not reported*	*Not reported*	1	Janssen et al., 1995 [59]
85	14	1	*Not reported*	Alcantara et al., 2004 [60]
83.3	1.4	15.3	5	Van den Bosch et al., 2007 [56]
88	5	7	3	Klok et al., 2012 [55]
82	2	16	1	Roman et al., 2015 [61]
92	7	1	6	Kiragosyan et al., 2019 [62]
75	*Not reported*	*Not reported*	215	Li et al., 2020 [63]
86	8.6	*Not reported*	5	Mu et al., 2021 [64]

The main objective of the research in this thesis is to increase the selectivity for sulfur formation in the biological desulfurization process. In previous research, it has been predicted that a selectivity of S^0 formation of 98% should be possible [65]. Since the ORP based control strategy has already been optimized, new strategies are required to further improve the selectivity for S^0 formation, which will be outlined below.

1.4 SULFUR (BIO)CHEMISTRY AT HALOALKALINE CONDITIONS

In order to increase the selectivity for sulfur formation in the biological desulfurization process, control of the reactions is essential. A combination of biological and chemical reactions occurs in the process. The bacteria that are active in the process form a mixed culture of haloalkaliphilic bacteria, which are adapted to high salt concentrations and high pH. These double extreme conditions naturally occur in soda lakes, which have very high concentrations of sodium (bi)carbonate due to high evaporation rates, creating a stable alkaline environment [66, 67]. Hence, the bacteria that are able to grow under the conditions of the biological desulfurization process are also found in soda lakes [67, 68]. Among these bacteria are sulfur oxidizers, sulfur reducing bacteria and sulfur disproportionators. An overview of the sulfur (bio)chemistry and the reactions that can occur in the process is provided in Table 1.2 and Figure 1.2.

The most abundant bacteria in the process are chemolithoautotrophic sulfur-compound oxidizing bacteria (SOB). These gram-negative bacteria gain metabolic energy by the oxidation of reduced sulfur compounds, such as sulfide (HS^-), thiosulfate ($S_2O_3^{2-}$) and elemental sulfur (S^0), and use an inorganic source of carbon, i.e. CO_2 / HCO_3^-. A wide phylogenetic variety of SOB exists [95]. The main reaction catalyzed by these bacteria in the biodesulfurization process is the oxidation of HS^- to S^0 (reaction 1 in Table 1.2). SOB prefer to form sulfate (SO_4^{2-}) (reaction 2), because the Gibbs free energy is higher and therefore yields more metabolic energy [71]. In many SOB, SO_4^{2-} formation occurs via S^0 (reaction 3), with sulfite (SO_3^{2-}) as intermediate [96, 97]. In the absorber, part of the HS^- chemically reacts with S^0 to form polysulfide (S_x^{2-}) (reaction 14). SOB also use S_x^{2-} as a substrate to form S^0 or SO_4^{2-} (reactions 4 and 5). HS^- and S_x^{2-} are also oxidized via a chemical reaction, forming $S_2O_3^{2-}$ (reactions 15 and 16). $S_2O_3^{2-}$ may also be formed via chemical hydrolysis of S^0 (reaction 17). With inorganic sulfur, this reaction requires a high temperature and high pH to occur (i.e. 80 °C at pH 7.6 and 20 °C at pH 11.5) [94], which does not apply for the biological desulfurization process. However, it has been suggested that freshly prepared colloidal S^0 is subject to hydrolysis under the conditions in the

biological desulfurization process [92]. $S_2O_3^{2-}$ is also used as a substrate by SOB to form SO_4^{2-} and/or S^0 (reactions 6 and 7). Lastly, organotrophic bacteria may be present. These bacteria can oxidize $S_2O_3^{2-}$ to tetrathionate ($S_4O_6^{2-}$) (reaction 8). $S_4O_6^{2-}$ can subsequently chemically react with HS^- to form S^0 and $S_2O_3^{2-}$ (reaction 18), i.e. $S_2O_3^{2-}$ is recycled.

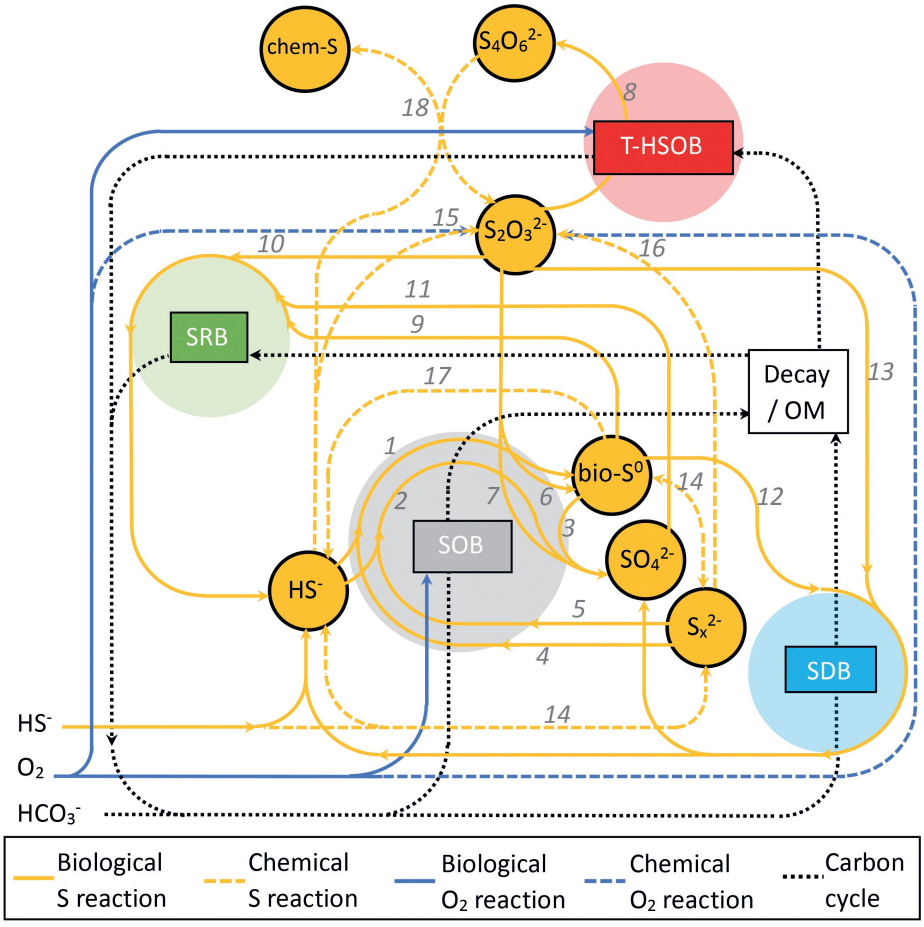

Figure 1.2: Overview of the main biological and chemical sulfur reactions that can occur in the biological desulfurization process under haloalkaline conditions. The numbers correspond to the reaction equations in Table 1.2**.** SOB: sulfur oxidizing bacteria; SRB: sulfur reducing bacteria; SDB: sulfur disproportionating bacteria; T-HSOB: tetrathionate forming heterotrophic sulfur oxidizing bacteria; OM: organic matter.

Table 1.2: Overview of reaction equations of the main biological and chemical sulfur reactions that can occur in the biological desulfurization process. The numbers correspond to Figure 1.2. OM is organic matter. An overview of the main enzymes involved in the biological reactions are provided by Vavourakis et al. and Berben et al. [69, 70].

Reaction number	Reaction equation	Reaction description	References
Biological oxidation reactions			
1	$HS^- + ½\ O_2 \rightarrow S^0 + OH^-$	sulfur formation	[48, 55, 56]
2	$HS^- + 2\ O_2 \rightarrow SO_4^{2-} + H^+$	sulfate formation	[48, 55, 56]
3	$S^0 + 1½\ O_2 + H_2O \rightarrow SO_4^{2-} + 2H^+$	sulfur oxidation	[55, 71]
4	$S_x^{2-} + ½\ O_2 + H^+ \rightarrow xS^0 + OH^-$	polysulfide oxidation	[72-75]
5	$S_x^{2-} + 2\ O_2 \rightarrow SO_4^{2-} + (x\text{-}1)S^0$	polysulfide oxidation	[72-74]
6	$S_2O_3^{2-} + ½\ O_2 \rightarrow S^0 + SO_4^{2-}$	thiosulfate oxidation to sulfur	[69, 76]
7	$S_2O_3^{2-} + 4\ O_2 + H_2O \rightarrow 2\ SO_4^{2-} + 2\ H^+$	thiosulfate oxidation to sulfate	[74, 77]
8	$2\ S_2O_3^{2-} + ½\ O_2 + OM \rightarrow S_4O_6^{2-} + OH^- + HCO_3^-$	tetrathionate formation	[73, 78, 79]
Biological reduction reactions			
9	$S^0 + OM \rightarrow HS^- + H^+ + H_2O + CO_2$	sulfur reduction	[80-82]
10	$S_2O_3^{2-} + OM \rightarrow 2\ HS^- + H_2O + CO_2$	thiosulfate reduction	[80-82]
11	$SO_4^{2-} + OM \rightarrow S^{2-} + H_2O + CO_2$	sulfate reduction	[80-82]
Biological disproportionation reactions			
12	$4\ S^0 + 4\ H_2O \rightarrow SO_4^{2-} + 3\ HS^- + 5\ H^+$	sulfur disproportionation	[83-86]
13	$S_2O_3^{2-} + H_2O \rightarrow SO_4^{2-} + HS^- + H^+$	thiosulfate disproportionation	[67, 85, 86]
Chemical reactions			
14	$HS^- + (x\text{-}1)S^0 \rightleftarrows S_x^{2-} + H^+$	polysulfide equilibrium	[48, 87, 88]
15	$2\ HS^- + O_2 \rightarrow S_2O_3^{2-} + H_2O$	thiosulfate formation	[89-91]
16	$S_x^{2-} + 1\ ½\ O_2 \rightarrow S_2O_3^{2-} + (x\text{-}2)S^0$	thiosulfate formation	[48, 92, 93]
17	$S_4O_6^{2-} + HS^- \rightarrow 2\ S_2O_3^{2-} + chem\text{-}S^0 + H^+$	chemical sulfur formation	[73, 78]
18	$4\ S^0 + 4\ OH^- \rightarrow S_2O_3^{2-} + 2\ HS^- + H_2O$	Sulfur hydrolysis / disproportionation	[56, 75, 92, 94]

A smaller fraction of the microbial population in the process belongs the group of sulfur reducing bacteria (SRB) [98]. These bacteria use sulfur compounds (SO_4^{2-}, $S_2O_3^{2-}$, S^0) as electron acceptors when oxidizing organic matter [82], forming sulfide (see reactions 9-11). Moreover, some lithotrophic bacteria can derive metabolic energy from disproportionation of sulfur compounds with an intermediate valance (i.e. S^0 and $S_2O_3^{2-}$) without external electron donor [85]. Reactions 12 and 13 are catalyzed by these sulfur disproportionating bacteria (SDB).

1.5 Bioelectrochemical sulfide oxidation

In the biological gas desulfurization process, electrical energy is required for pumping in order to circulate the process solution, and for aeration of the bioreactor. The oxidation of H_2S is an exothermic reaction and thus releases energy, mostly in the form of heat. Full-scale processes therefore require energy input to cool the process solution in order to prevent too high temperatures for the bacteria (>40 °C). When this energy input can be lowered, or when energy can even be recovered from H_2S oxidation, it would improve the sustainability and economics of biological gas desulfurization. The recovery of energy from sulfide oxidation can be performed with a bioelectrochemical system (BES). A BES consist of two electrodes: an anode and a cathode, see Figure 1.3. Oxidation reactions occur at the anode, which release electrons, that flow to the cathode. At the cathode, reduction reactions take place, which consume the electrons coming from anode. In a BES, at least one of the electrode reactions is catalyzed by microorganisms. These microorganisms can either be attached to the electrode as a biofilm, be suspended in the solution, or both.

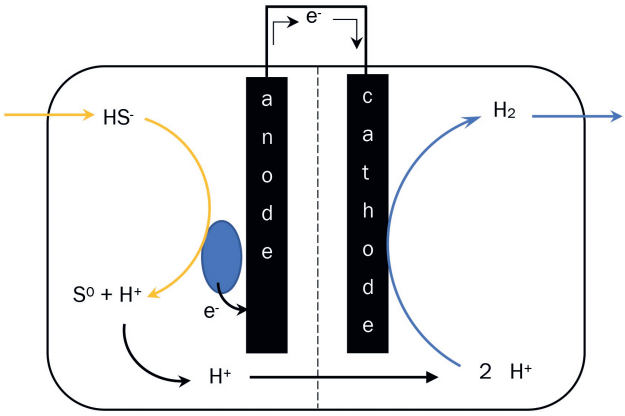

Figure 1.3: Schematic overview of a bioelectrochemical system for sulfide oxidation.

Some bacteria require the presence of redox mediators to transfer electrons to the electrode [99, 100].

The two main reactions at the anode are provided in equations 1.1 and 1.2.

$HS^- \rightarrow S^0 + 2\ e^- + H^+$ (Equation 1.1)

$HS^- + 4\ H_2O \rightarrow SO_4^{2-} + 9\ H^+ + 8\ e^-$ (Equation 1.2)

One of the applications of BES systems is the treatment of wastewater, where microorganisms degrade organic material and release the electrons to the anode to generate electric current [101]. In these systems, the anodic and cathodic compartment are separated by a membrane that is permeable for positive ions.

The main problem in current BES for sulfide removal is the deposition of elemental sulfur on the electrode as a result of electrochemical oxidation of sulfide, leading to electrode passivation and formation of the by-products sulfate and thiosulfate [102-108].

Another application of BES is to study reaction kinetics of sulfide oxidation in an electrochemical controlled environment. In previous sections, it was explained that control of the chemical and biological reactions is essential for optimal process performance. In order to study reaction kinetics, a three-electrode setup, controlled by a potentiostat is often used [99]. The potentiostat is the electronic hardware to operate a (bio)electrochemical cell. A three-electrode setup a set-up consists of a working electrode, counter electrode and a reference electrode, which are all connected to a potentiostat. Various operational modes are possible. For example, the potential of the working electrode is controlled at a certain potential (versus the reference electrode) and the current (i.e. the electron flow rate, which is a measure for the reaction rates) between the working and counter electrode is measured. It is also possible to perform dynamic experiments, in which the potential of the working electrode is changed stepwise in order to determine current production at a range of working electrode potentials.

Thus, the objective of using BES is twofold. Firstly, BES can be used to recover energy from sulfide oxidation, which would make biological gas desulfurization more energy efficient. Secondly, electrochemical methods provide opportunities to study the reactions that occur in the biological desulfurization process.

1.6 THESIS OUTLINE

The overall aim of the research described in this thesis is to increase the efficiency of the biological gas desulfurization process under haloalkaline conditions.

The experiments as described in chapters 2-4 are all performed in a pilot-scale biodesulfurization installation. In **Chapter 2** a new process line-up is investigated, containing an anaerobic bioreactor, placed in between the absorber and aerated bioreactor. It is shown that the sulfidic conditions in the anaerobic bioreactor suppress formation of sulfate and that the microbial community changes. Furthermore, biological mediated removal of sulfide from the solution in the anaerobic bioreactor takes place, leading to lower thiosulfate formation. In **Chapter 3**, this process line-up is further studied by experiments in which the sulfide concentration and hydraulic retention time (HRT) in the anaerobic bioreactor are varied. The observed removal of sulfide from the process solution in the anaerobic bioreactor suggests that bacteria may also be active in the absorber of the process. Therefore, **Chapter 4** investigates the possible role of the bacteria in the absorption of H_2S. It is shown that the bacteria enhance the absorption of H_2S.

Bioelectrochemistry is applied in chapters 5-7. **Chapter 5** describes batch experiments, in which is shown that bacteria taken from the biodesulfurization process remove sulfide from solution under anaerobic conditions. These bacteria are subsequently transferred to an electrochemical cell where they transfer electrons to the anode, producing electricity in the absence of dissolved sulfide. **Chapter 6** further investigates the principle of Chapter 5 in a continuous process. Bacteria are circulated between an 'sulfide uptake chamber', to which sulfide is continuously added, and the anode side of an electrochemical cell. This results in continuous electricity production in the absence of dissolved sulfide in the anodic chamber of the electrochemical cell.

The finding that bacteria can contain charge and this charge can be harvested in an electrochemical cell is further studied in **Chapter 7**. In this chapter, the relation between charge storage of bacteria and the redox potential in the bioreactor of the biodesulfurization process is investigated. It is shown that the bacteria contain more charge at a lower redox value and that the charge storage is related to product formation. **Chapter 8** provides a summary and general discussion of the work.

1.7 REFERENCES

[1] J. Lelieveld, K. Klingmüller, A. Pozzer, R. Burnett, A. Haines, V. Ramanathan, Effects of fossil fuel and total anthropogenic emission removal on public health and climate, Proceedings of the National Academy of Sciences, 116 (2019) 7192-7197.

[2] D.A. Burns, J. Aherne, D.A. Gay, C. Lehmann, Acid rain and its environmental effects: Recent scientific advances, Atmospheric Environment, 146 (2016) 1-4.

[3] A.P. Nascimento, J.M. Santos, J.G. Mill, T.T. de Almeida Albuquerque, N.C.R. Júnior, V.A. Reisen, É.C. Pagel, Association between the incidence of acute respiratory diseases in children and ambient concentrations of SO_2, PM_{10} and chemical elements in fine particles, Environmental Research, 188 (2020) 109619.

[4] R.E. Stoiber, S.N. Williams, B. Huebert, Annual contribution of sulfur dioxide to the atmosphere by volcanoes, Journal of Volcanology and Geothermal Research, 33 (1987) 1-8.

[5] D.A. Fike, A.S. Bradley, C.V. Rose, Rethinking the ancient sulfur cycle, Annual Review of Earth and Planetary Sciences, 43 (2015) 593-622.

[6] S.J. Smith, J.v. Aardenne, Z. Klimont, R.J. Andres, A. Volke, S. Delgado Arias, Anthropogenic sulfur dioxide emissions: 1850–2005, Atmospheric Chemistry and Physics, 11 (2011) 1101-1116.

[7] Q. Zhong, H. Shen, X. Yun, Y. Chen, Y.a. Ren, H. Xu, G. Shen, W. Du, J. Meng, W. Li, Global sulfur dioxide emissions and the driving forces, Environmental science & technology, 54 (2020) 6508-6517.

[8] I. Faloona, Sulfur processing in the marine atmospheric boundary layer: A review and critical assessment of modeling uncertainties, Atmospheric Environment, 43 (2009) 2841-2854.

[9] T.F. Berglen, T.K. Berntsen, I.S. Isaksen, J.K. Sundet, A global model of the coupled sulfur/oxidant chemistry in the troposphere: The sulfur cycle, Journal of Geophysical Research: Atmospheres, 109 (2004).

[10] H.-M. Hung, M.R. Hoffmann, Oxidation of gas-phase SO_2 on the surfaces of acidic microdroplets: Implications for sulfate and sulfate radical anion formation in the atmospheric liquid phase, Environmental science & technology, 49 (2015) 13768-13776.

[11] P. Wang, A. Richter, M. Bruns, J. Burrows, R. Scheele, W. Junkermann, K.-P. Heue, T. Wagner, U. Platt, I. Pundt, Airborne multi-axis DOAS measurements of tropospheric SO_2 plumes in the Po-valley, Italy, Atmospheric Chemistry and Physics, 6 (2006) 329-338.

[12] J. Yun, C. Zhu, Q. Wang, Q. Hu, G. Yang, Catalytic conversions of atmospheric sulfur dioxide and formation of acid rain over mineral dusts: Molecular oxygen as the oxygen source, Chemosphere, 217 (2019) 18-25.

[13] C. Nowlan, R. Martin, S. Philip, L. Lamsal, N. Krotkov, E. Marais, S. Wang, Q. Zhang, Global dry deposition of nitrogen dioxide and sulfur dioxide inferred from space-based measurements, Global Biogeochemical Cycles, 28 (2014) 1025-1043.

[14] U. Nopmongcol, R. Beardsley, N. Kumar, E. Knipping, G. Yarwood, Changes in United States deposition of nitrogen and sulfur compounds over five decades from 1970 to 2020, Atmospheric environment, 209 (2019) 144-151.

[15] M.R. Taylor, E.S. Rubin, D.A. Hounshell, Regulation as the mother of innovation: the case of SO_2 control, Law & Policy, 27 (2005) 348-378.

[16] C.T. Driscoll, K.M. Driscoll, H. Fakhraei, K. Civerolo, Long-term temporal trends and spatial patterns in the acid-base chemistry of lakes in the Adirondack region of New York in response to decreases in acidic deposition, Atmospheric Environment, 146 (2016) 5-14.

[17] S. Henschel, X. Querol, R. Atkinson, M. Pandolfi, A. Zeka, A. Le Tertre, A. Analitis, K. Katsouyanni, O. Chanel, M. Pascal, Ambient air SO_2 patterns in 6 European cities, Atmospheric environment, 79 (2013) 236-247.

[18] V. Vestreng, G. Myhre, H. Fagerli, S. Reis, L. Tarrasón, Twenty-five years of continuous sulphur dioxide emission reduction in Europe, Atmospheric chemistry and physics, 7 (2007) 3663-3681.

[19] S. Dahiya, L. Myllyvirta, Global SO_2 emission hotspot database. Ranking the world's worst sources of SO_2 pollution, in, https://www.greenpeace.org/india/en/publication/3951/global-SO2-emission-hotspots-database-ranking-the-worlds-worst-sources-of-so2-pollution-2/, 2019.

[20] S.J. Smith, H. Pitcher, T.M. Wigley, Global and regional anthropogenic sulfur dioxide emissions, Global and planetary change, 29 (2001) 99-119.

[21] C. Li, C. McLinden, V. Fioletov, N. Krotkov, S. Carn, J. Joiner, D. Streets, H. He, X. Ren, Z. Li, India is overtaking China as the world's largest emitter of anthropogenic sulfur dioxide, Scientific reports, 7 (2017) 1-7.

[22] L. Wenhui, G. Bo, Z. Zhongning, Z. Jianyong, Z. Dianwei, F. Ming, F. Xiaodong, Z. Lunju, L. Quanyou, H2S formation and enrichment mechanisms in medium to large scale natural gas fields (reservoirs) in the Sichuan Basin, Petroleum Exploration and Development, 37 (2010) 513-522.

[23] T.L. Guidotti, Hydrogen sulfide: advances in understanding human toxicity, International journal of toxicology, 29 (2010) 569-581.

[24] J. Tang, Y. Shao, J. Guo, T. Zhang, G. Meng, F. Wang, The effect of H_2S concentration on the corrosion behavior of carbon steel at 90 °C, Corrosion Science, 52 (2010) 2050-2058.

[25] R. Pahl, K. Holtappels, Explosions Limits of H_2S/CO_2/Air and H_2S/N_2/Air, Chemical Engineering & Technology: Industrial Chemistry-Plant Equipment-Process Engineering-Biotechnology, 28 (2005) 746-749.

[26] M. Gab-Allah, E.S. Goda, A. Shehata, H. Gamal, Critical review on the analytical methods for the determination of sulfur and trace elements in crude oil, Critical reviews in analytical chemistry, 50 (2020) 161-178.

[27] A. Vetere, D. Pröfrock, W. Schrader, Quantitative and qualitative analysis of three classes of sulfur compounds in crude oil, Angewandte Chemie International Edition, 56 (2017) 10933-10937.

[28] R. Shafi, G.J. Hutchings, Hydrodesulfurization of hindered dibenzothiophenes: an overview, Catalysis today, 59 (2000) 423-442.

[29] A.J. Minchener, Coal gasification for advanced power generation, Fuel, 84 (2005) 2222-2235.

[30] Q. Zhao, E. Leonhardt, C. MacConnell, C. Frear, S. Chen, Purification technologies for biogas generated by anaerobic digestion, Compressed Biomethane, CSANR, Ed, 24 (2010).

[31] L. Krayzelova, J. Bartacek, I. Díaz, D. Jeison, E.I. Volcke, P. Jenicek, Microaeration for hydrogen sulfide removal during anaerobic treatment: a review, Reviews in Environmental Science and Bio/Technology, 14 (2015) 703-725.

[32] B. Echt, D. Leppin, D. Mamrosh, D. Mirdadian, D. Seeger, B. Warren, Fundamentals of low-tonnage sulfur removal and recovery, in: Laurance Reid Gas Conditioning Conference, Norman, OK, 2017.

[33] S. Sharif Dashti, A. Shariati, M.R. Khosravi Nikou, Sensitivity analysis for selection of an optimum amine gas sweetening process with minimum cost requirement, Asia-Pacific Journal of Chemical Engineering, 10 (2015) 709-715.

[34] J.S. Eow, Recovery of sulfur from sour acid gas: A review of the technology, Environmental progress, 21 (2002) 143-162.

[35] D.A. Dalrymple, T.W. Trofe, J.M. Evans, An overview of liquid redox sulfur recovery, Chem. Eng. Prog.;(United States), 85 (1989).

[36] H.J. Wubs, A.A. Beenackers, Kinetics of the oxidation of ferrous chelates of EDTA and HEDTA in aqueous solution, Industrial & engineering chemistry research, 32 (1993) 2580-2594.

[37] H.J. Wubs, A.A. Beenackers, Kinetics of H_2S absorption into aqueous ferric solutions of EDTA and HEDTA, AIChE Journal, 40 (1994) 433-444.

[38] S. Holz, P. Köster, H. Thielert, Z. Guetta, J.-U. Repke, Investigation of the Degradation of Chelate Complexes in Liquid Redox Desulfurization Processes, Chemical Engineering & Technology, 43 (2020) 476-483.

[39] R. Steudel, Mechanism for the formation of elemental sulfur from aqueous sulfide in chemical and microbiological desulfurization processes, Industrial & Engineering Chemistry Research, 35 (1996) 1417-1423.

[40] X. Miao, Y. Ma, Z. Chen, H. Gong, Oxidative degradation stability and hydrogen sulfide removal performance of dual-ligand iron chelate of Fe-EDTA/CA, Environmental technology, 39 (2018) 3006-3012.

[41] T. Prakoso, A. Widodo, A. Indarto, R. Mariyana, A.F. Arif, T.P. Adhi, T.H. Soerawidjaja, Manganese gluconate, A greener and more degradation resistant agent for H_2S oxidation using liquid redox sulfur recovery process, Heliyon, 6 (2020) e03358.

[42] M.E. Sillanpää, T.A. Kurniawan, W.-h. Lo, Degradation of chelating agents in aqueous solution using advanced oxidation process (AOP), Chemosphere, 83 (2011) 1443-1460.

[43] I.S. Pinto, I.F. Neto, H.M. Soares, Biodegradable chelating agents for industrial, domestic, and agricultural applications—a review, Environmental Science and Pollution Research, 21 (2014) 11893-11906.

[44] A.J. Janssen, P.N. Lens, A.J. Stams, C.M. Plugge, D.Y. Sorokin, G. Muyzer, H. Dijkman, E. Van Zessen, P. Luimes, C.J. Buisman, Application of bacteria involved in the biological sulfur cycle for paper mill effluent purification, Science of the total environment, 407 (2009) 1333-1343.

[45] J.B. Klok, G. Van Heeringen, P. Shaunfield, Desulfurization of amine acid gas under turndown: performance of the biological desulfurization process, in: Laurence Reid Gas Conditioning Conference, Norman, Oklahoma USA, 2018.

[46] C. Cline, A. Hoksberg, R. Abry, A. Janssen, Biological Process for H_2S Removal from Gas Streams: The Shell-Paques/THIOPAQ™ Gas Desulfurization Process, in: Proceedings of the Laurance Reid gas conditioning conference, 2003, pp. 1-18.

[47] J. Boulegue, Solubility of elemental sulfur in water at 298 K, Phosphorus and Sulfur and the related Elements, 5 (1978) 127-128.

[48] W.E. Kleinjan, A. de Keizer, A.J. Janssen, Biologically produced sulfur, Elemental sulfur and sulfur-rich compounds I, (2003) 167-188.

[49] C. Dahl, A. Prange, Bacterial sulfur globules: occurrence, structure and metabolism, in: Inclusions in prokaryotes, Springer, 2006, pp. 21-51.

[50] A. Janssen, A. De Keizer, G. Lettinga, Colloidal properties of a microbiologically produced sulphur suspension in comparison to a LaMer sulphur sol, Colloids and surfaces B: Biointerfaces, 3 (1994) 111-117.

[51] R. Steudel, B. Eckert, Solid sulfur allotropes, Elemental sulfur and sulfur-rich compounds I, (2003) 1-80.

[52] A.P. Florentino, J. Weijma, A.J. Stams, I. Sánchez-Andrea, Sulfur reduction in acid rock drainage environments, Environmental science & technology, 49 (2015) 11746-11755.

[53] https://en.fertipaq.com/over-ons [Accessed on 23 April 2021]

[54] E. Van Zessen, A. Janssen, A. De Keizer, B. Heijne, J. Peace, R. Abry, Application of THIOPAQ™ biosulphur in agriculture, in: Proceedings of the British Sulphus Events 2004 Sulphur Conference, Barcelona, Spain, 24-27 October 2004, 2004, pp. 57-68.

[55] J.B. Klok, P.L. van den Bosch, C.J. Buisman, A.J. Stams, K.J. Keesman, A.J. Janssen, Pathways of sulfide oxidation by haloalkaliphilic bacteria in limited-oxygen gas lift bioreactors, Environmental science & technology, 46 (2012) 7581-7586.

[56] P.L. Van Den Bosch, O.C. van Beusekom, C.J. Buisman, A.J. Janssen, Sulfide oxidation at halo-alkaline conditions in a fed-batch bioreactor, Biotechnology and bioengineering, 97 (2007) 1053-1063.

[57] A. Janssen, S. Meijer, J. Bontsema, G. Lettinga, Application of the redox potential for controling a sulfide oxidizing bioreactor, Biotechnology and bioengineering, 60 (1998) 147-155.

[58] J.B. Klok, (Paqell B.V., Utrecht, the Netherlands) Personal communication (2021)

[59] A. Janssen, R. Sleyster, C. Van der Kaa, A. Jochemsen, J. Bontsema, G. Lettinga, Biological sulphide oxidation in a fed-batch reactor, Biotechnology and bioengineering, 47 (1995) 327-333.

[60] S. Alcántara, A. Velasco, A. Muñoz, J. Cid, S. Revah, E. Razo-Flores, Hydrogen sulfide oxidation by a microbial consortium in a recirculation reactor system: sulfur formation under oxygen limitation and removal of phenols, Environmental science & technology, 38 (2004) 918-923.

[61] P. Roman, R. Veltman, M.F. Bijmans, K.J. Keesman, A.J. Janssen, Effect of methanethiol concentration on sulfur production in biological desulfurization systems under haloalkaline conditions, Environmental science & technology, 49 (2015) 9212-9221.

[62] K. Kiragosyan, J.B. Klok, K.J. Keesman, P. Roman, A.J. Janssen, Development and validation of a physiologically based kinetic model for starting up and operation of the biological gas desulfurization process under haloalkaline conditions, Water research X, 4 (2019) 100035.

[63] W. Li, M. Zhang, D. Kang, W. Chen, T. Yu, D. Xu, Z. Zeng, Y. Li, P. Zheng, Mechanisms of sulfur selection and sulfur secretion in a biological sulfide removal (BISURE) system, Environment international, 137 (2020) 105549.

[64] T. Mu, M. Yang, J. Xing, Performance and characteristic of a haloalkaliphilic bio-desulfurizing system using *Thioalkalivibrio verustus* D301 for efficient removal of H_2S, Biochemical Engineering Journal, 165 (2021) 107812.

[65] J.B. Klok, M. de Graaff, P.L. van den Bosch, N.C. Boelee, K.J. Keesman, A.J. Janssen, A physiologically based kinetic model for bacterial sulfide oxidation, Water research, 47 (2013) 483-492.

[66] B.E. Jones, W.D. Grant, A.W. Duckworth, G.G. Owenson, Microbial diversity of soda lakes, Extremophiles, 2 (1998) 191-200.

[67] D.Y. Sorokin, G.J. Kuenen, G. Muyzer, The microbial sulfur cycle at extremely haloalkaline conditions of soda lakes, Frontiers in microbiology, 2 (2011) 44.

[68] D.Y. Sorokin, T. Berben, E.D. Melton, L. Overmars, C.D. Vavourakis, G. Muyzer, Microbial diversity and biogeochemical cycling in soda lakes, Extremophiles, 18 (2014) 791-809.

[69] T. Berben, L. Overmars, D.Y. Sorokin, G. Muyzer, Diversity and distribution of sulfur oxidation-related genes in *Thioalkalivibrio*, a genus of chemolithoautotrophic and haloalkaliphilic sulfur-oxidizing bacteria, Frontiers in microbiology, 10 (2019) 160.

[70] C.D. Vavourakis, M. Mehrshad, C. Balkema, R. Van Hall, A.-Ş. Andrei, R. Ghai, D.Y. Sorokin, G. Muyzer, Metagenomes and metatranscriptomes shed new light on the microbial-mediated sulfur cycle in a Siberian soda lake, BMC biology, 17 (2019) 1-20.

[71] D.P. Kelly, Thermodynamic aspects of energy conservation by chemolithotrophic sulfur bacteria in relation to the sulfur oxidation pathways, Archives of Microbiology, 171 (1999) 219-229.

[72] D.Y. Sorokin, A.M. Lysenko, L.L. Mityushina, T.P. Tourova, B.E. Jones, F.A. Rainey, L.A. Robertson, G.J. Kuenen, *Thioalkalimicrobium aerophilum* gen. nov., sp. nov. and *Thioalkalimicrobium sibericum* sp. nov., and *Thioalkalivibrio versutus* gen. nov., sp. nov., *Thioalkalivibrio nitratis* sp. nov., novel and *Thioalkalivibrio denitrificancs* sp. nov., novel obligately alkaliphilic and obligately chemolithoautotrophic sulfur-oxidizing bacteria from soda lakes, International Journal of Systematic and Evolutionary Microbiology, 51 (2001) 565-580.

[73] D.Y. Sorokin, P. Van Den Bosch, B. Abbas, A. Janssen, G. Muyzer, Microbiological analysis of the population of extremely haloalkaliphilic sulfur-oxidizing bacteria dominating in lab-scale sulfide-removing bioreactors, Applied microbiology and biotechnology, 80 (2008) 965-975.

[74] H. Banciu, D.Y. Sorokin, R. Kleerebezem, G. Muyzer, E.A. Galinski, J.G. Kuenen, Growth kinetics of haloalkaliphilic, sulfur-oxidizing bacterium *Thioalkalivibrio versutus* strain ALJ 15 in continuous culture, Extremophiles, 8 (2004) 185-192.

[75] P.L. Van den Bosch, D.Y. Sorokin, C.J. Buisman, A.J. Janssen, The effect of pH on thiosulfate formation in a biotechnological process for the removal of hydrogen sulfide from gas streams, Environmental science & technology, 42 (2008) 2637-2642.

[76] G. Muyzer, D.Y. Sorokin, K. Mavromatis, A. Lapidus, A. Clum, N. Ivanova, A. Pati, P. d'Haeseleer, T. Woyke, N.C. Kyrpides, Complete genome sequence of "*Thioalkalivibrio sulfidophilus*" HL-EbGr7, Standards in genomic sciences, 4 (2011) 23-35.

[77] V.A. Bamford, S. Bruno, T. Rasmussen, C. Appia-Ayme, M.R. Cheesman, B.C. Berks, A.M. Hemmings, Structural basis for the oxidation of thiosulfate by a sulfur cycle enzyme, The EMBO journal, 21 (2002) 5599-5610.

[78] D.Y. Sorokin, Oxidation of inorganic sulfur compounds by obligately organotrophic bacteria, Microbiology, 72 (2003) 641-653.

[79] D.Y. Sorokin, T.P. Tourova, G. Muyzer, Oxidation of thiosulfate to tetrathionate by an haloarchaeon isolated from hypersaline habitat, Extremophiles, 9 (2005) 501-504.

[80] D. Sorokin, T. Tourova, G. Muyzer, Isolation and characterization of two novel alkalitolerant sulfidogens from a Thiopaq bioreactor, *Desulfonatronum alkalitolerans* sp. nov., and *Sulfurospirillum alkalitolerans* sp. nov, Extremophiles, 17 (2013) 535-543.

[81] D.Y. Sorokin, M. Foti, B. Tindall, G. Muyzer, *Desulfurispirillum alkaliphilum* gen. nov. sp. nov., a novel obligately anaerobic sulfur-and dissimilatory nitrate-reducing bacterium from a full-scale sulfide-removing bioreactor, Extremophiles, 11 (2007) 363-370.

[82] D.Y. Sorokin, I.I. Rusanov, N.V. Pimenov, T.P. Tourova, B. Abbas, G. Muyzer, Sulfidogenesis under extremely haloalkaline conditions in soda lakes of Kulunda Steppe (Altai, Russia), FEMS microbiology ecology, 73 (2010) 278-290.

[83] A. Poser, R. Lohmayer, C. Vogt, K. Knoeller, B. Planer-Friedrich, D. Sorokin, H.-H. Richnow, K. Finster, Disproportionation of elemental sulfur by haloalkaliphilic bacteria from soda lakes, Extremophiles, 17 (2013) 1003-1012.

[84] B. Thamdrup, K. Finster, J.W. Hansen, F. Bak, Bacterial disproportionation of elemental sulfur coupled to chemical reduction of iron or manganese, Applied and environmental microbiology, 59 (1993) 101-108.

[85] A. Slobodkin, G. Slobodkina, Diversity of sulfur-disproportionating microorganisms, Microbiology, 88 (2019) 509-522.

[86] K. Finster, Microbiological disproportionation of inorganic sulfur compounds, Journal of Sulfur Chemistry, 29 (2008) 281-292.

[87] W.E. Kleinjan, A. de Keizer, A.J. Janssen, Kinetics of the reaction between dissolved sodium sulfide and biologically produced sulfur, Industrial & engineering chemistry research, 44 (2005) 309-317.

[88] P. Roman, M.F. Bijmans, A.J. Janssen, Quantification of individual polysulfides in lab-scale and full-scale desulfurisation bioreactors, Environmental Chemistry, 11 (2014) 702-708.

[89] K.Y. Chen, J.C. Morris, Kinetics of oxidation of aqueous sulfide by oxygen, Environmental science & technology, 6 (1972) 529-537.

[90] M. de Graaff, J.B. Klok, M.F. Bijmans, G. Muyzer, A.J. Janssen, Application of a 2-step process for the biological treatment of sulfidic spent caustics, Water research, 46 (2012) 723-730.

[91] D.J. O'Brien, F.B. Birkner, Kinetics of oxygenation of reduced sulfur species in aqueous solution, Environmental Science & Technology, 11 (1977) 1114-1120.

[92] W.E. Kleinjan, A. de Keizer, A.J. Janssen, Kinetics of the chemical oxidation of polysulfide anions in aqueous solution, Water Research, 39 (2005) 4093-4100.

[93] W.F. Giggenbach, Equilibriums involving polysulfide ions in aqueous sulfide solutions up to 240. deg, Inorganic Chemistry, 13 (1974) 1724-1730.

[94] R. Steudel, The chemical sulfur cycle, Environmental Technologies to Treat Sulphur Pollution: Principles and Engineering, Piet NL Lens (2020).

[95] D.Y. Sorokin, H. Banciu, L.A. Robertson, J.G. Kuenen, Haloalkaliphilic sulfur-oxidizing bacteria, The prokaryotes, 2 (2006) 969-984.

[96] U. Kappler, C. Dahl, Enzymology and molecular biology of prokaryotic sulfite oxidation, FEMS microbiology letters, 203 (2001) 1-9.

[97] D.Y. Sorokin, J.G. Kuenen, Haloalkaliphilic sulfur-oxidizing bacteria in soda lakes, FEMS microbiology reviews, 29 (2005) 685-702.

[98] D.Y. Sorokin, T. Tourova, T. Kolganova, E. Detkova, E. Galinski, G. Muyzer, Culturable diversity of lithotrophic haloalkaliphilic sulfate-reducing bacteria in soda lakes and the description of *Desulfonatronum thioautotrophicum* sp. nov., *Desulfonatronum thiosulfatophilum* sp. nov., *Desulfonatronovibrio thiodismutans* sp. nov., and *Desulfonatronovibrio magnus* sp. nov, Extremophiles, 15 (2011) 391-401.

[99] B.E. Logan, B. Hamelers, R. Rozendal, U. Schröder, J. Keller, S. Freguia, P. Aelterman, W. Verstraete, K. Rabaey, Microbial fuel cells: methodology and technology, Environmental science & technology, 40 (2006) 5181-5192.

[100] C. Picioreanu, I.M. Head, K.P. Katuri, M.C. van Loosdrecht, K. Scott, A computational model for biofilm-based microbial fuel cells, Water research, 41 (2007) 2921-2940.

[101] B.E. Logan, Simultaneous wastewater treatment and biological electricity generation, Water Science and Technology, 52 (2005) 31-37.

[102] K. Rabaey, K. Van de Sompel, L. Maignien, N. Boon, P. Aelterman, P. Clauwaert, L. De Schamphelaire, H.T. Pham, J. Vermeulen, M. Verhaege, Microbial fuel cells for sulfide removal, Environmental science & technology, 40 (2006) 5218-5224.

[103] R. Bao, S. Zhang, L. Zhao, L. Zhong, Simultaneous sulfide removal, nitrification, and electricity generation in a microbial fuel cell equipped with an oxic cathode, Environmental Science and Pollution Research, 24 (2017) 5326-5334.

[104] G. Ni, P. Harnawan, L. Seidel, A. Ter Heijne, T. Sleutels, C.J. Buisman, M. Dopson, Haloalkaliphilic microorganisms assist sulfide removal in a microbial electrolysis cell, Journal of hazardous materials, 363 (2019) 197-204.

[105] M. Sun, Z.-X. Mu, Y.-P. Chen, G.-P. Sheng, X.-W. Liu, Y.-Z. Chen, Y. Zhao, H.-L. Wang, H.-Q. Yu, L. Wei, Microbe-assisted sulfide oxidation in the anode of a microbial fuel cell, Environmental science & technology, 43 (2009) 3372-3377.

[106] F. Zhao, N. Rahunen, J.R. Varcoe, A. Chandra, C. Avignone-Rossa, A.E. Thumser, R.C. Slade, Activated carbon cloth as anode for sulfate removal in a microbial fuel cell, Environmental science & technology, 42 (2008) 4971-4976.

[107] B. Ateya, F. AlKharafi, A. Al-Azab, Electrodeposition of sulfur from sulfide contaminated brines, Electrochemical and Solid State Letters, 6 (2003) C137.

[108] P.K. Dutta, K. Rabaey, Z. Yuan, J. Keller, Spontaneous electrochemical removal of aqueous sulfide, Water research, 42 (2008) 4965-4975.

CHAPTER 2

Increasing the selectivity for sulfur formation in biological gas desulfurization

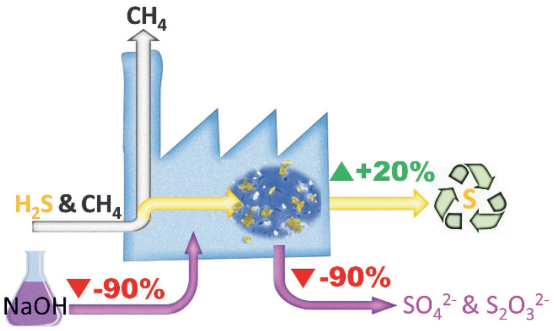

Abstract – In the biotechnological desulfurization process under haloalkaline conditions, dihydrogen sulfide (H_2S) is removed from sour gas and oxidized to elemental sulfur (S_8) by sulfide-oxidizing bacteria. Besides S_8, the by-products sulfate (SO_4^{2-}) and thiosulfate ($S_2O_3^{2-}$) are formed, which consume caustic and form a waste stream. The aim of this study was to increase selectivity towards S_8 by a new process line-up for biological gas desulfurization, applying two bioreactors with different substrate conditions (i.e., sulfidic and microaerophilic), instead of one (i.e., microaerophilic). A 111-day continuous test, mimicking full scale operation, demonstrated that S_8 formation was 96.6% on a molar H_2S supply basis; selectivity for SO_4^{2-} and $S_2O_3^{2-}$ were 1.4 and 2.0% respectively. The selectivity for S_8 formation in a control experiment with the conventional 1-bioreactor line-up was 75.6 mol%. At start-up, the new process line-up immediately achieved lower SO_4^{2-} and $S_2O_3^{2-}$ formations compared to the 1-bioreactor line-up. When the microbial community adapted over time, it was observed that SO_4^{2-} formation further decreased. In addition, the chemical formation of $S_2O_3^{2-}$ was lower due to biologically mediated removal of sulfide from the process solution in the anaerobic bioreactor. The increased selectivity for S_8 formation will result in 90% decrease in caustic consumption and waste stream formation compared to the 1-bioreactor line-up.

This chapter is published as: Rieks de Rink, Johannes B.M. Klok, Gijs J. van Heeringen, Dimitry Y. Sorokin, Annemiek ter Heijne, Remco Zeijlmaker, Yvonne M. Mos, Vinnie de Wilde, Karel J. Keesman, Cees J.N. Buisman. Increasing the selectivity for sulfur formation in biological gas desulfurization. Environmental science & technology, 53 (2019) 4519-4527.

2.1 INTRODUCTION

Since its introduction in 1993, biotechnological desulfurization under haloalkaline conditions has proven to be effective in removal and conversion of H_2S from various types of gas streams [1]. It offers several advantages over conventional physicochemical processes. Key advantages are that biotechnological desulfurization operates at ambient temperatures and pressures without the use of complex and toxic chemicals.

The first step of the biotechnological desulfurization process is the selective absorption of dihydrogen sulfide (H_2S) from a sour gas into the process solution in an absorber column. To optimally remove the H_2S from the gas stream, the sour gas and process solution are counter-currently contacted. Due to the mildly alkaline washing solution, the majority of the dissolved sulfide is chemically converted to soluble bisulfide (HS^-). To recover sulfur (S_8), the HS^--rich solution is subsequently routed to an aerated microaerophilic bioreactor. Here, chemolithoautotrophic haloalkaliphilic sulfide oxidizing bacteria (SOB) oxidize HS^- to solid S_8 particles at oxygen-limited conditions (i.e., dissolved oxygen concentration <100nM). The solid sulfur particles are harvested from the solution by gravity settling and/or centrifugation and can be reused [2]. The technology is applied on commercial scale for a wide range of different sour gases, such as biogas, natural gas and amine acid gas (>250 installations worldwide in 2017) [3, 4].

Although operating conditions can be optimized for S_8 formation, part of the HS^- is oxidized to sulfate (SO_4^{2-}) and thiosulfate ($S_2O_3^{2-}$). In current systems, a maximum of 80-90 mol% conversion to S_8 can be obtained [5-7]. SO_4^{2-} and $S_2O_3^{2-}$ formation are accompanied by proton formation and therefore require the addition of caustic soda (NaOH) (reactions 1-4; Table 2.1). Moreover, as SO_4^{2-} and $S_2O_3^{2-}$ accumulate, the salinity increases and a bleed stream is required to avoid biological failure.

Table 2.1: Major biological and chemical conversions in the biotechnological desulfurization process under haloalkaline conditions [1, 6-8]

Number	Reaction equation	Description of the reaction
1	$HS^- + ½\ O_2 \rightarrow ⅛\ S_8 + OH^-$	Biological sulfide oxidation
2	$⅛\ S_8 + 1½\ O_2 + H_2O \rightarrow SO_4^{2-} + 2\ H^+$	Biological sulfur oxidation
3	$HS^- + O_2 \rightarrow ½\ S_2O_3^{2-} + ½\ H_2O$	Chemical sulfide oxidation
4	$½\ S_2O_3^{2-} + O_2 + ½\ H_2O \rightarrow SO_4^{2-} + H^+$	Biological thiosulfate oxidation
5	$HS^- + S_{x-1} \leftrightharpoons S_x^{2-} + H^+$	Chemical polysulfide formation

When chemical consumption (caustic) and waste stream formation (bleed stream) can be lowered, the biodesulfurization process becomes more attractive. A key aspect in optimizing biological systems is the (active) microbiological community. The biological desulfurization process under haloalkaline conditions is dominated by haloalkaliphilic SOB belonging to the genus of *Thioalkalivibrio* [9, 10]. The analysis of the complete genome of *Thioalkalivibrio sulfidiphilus* [11], showed that HS^- oxidation to S_8 is catalyzed by flavocytochrome *c* sulfide dehydrogenase (Fcc). Subsequently, S_8 can be oxidized by a reversed dissimilatory sulfite reductase (rDSR) system to sulfite (SO_3^{2-}) and further to SO_4^{2-}. Hence, in current full-scale biodesulfurization systems, the formation of SO_4^{2-} is inevitable due to the dominance of SO_4^{2-} producing SOB, such as *Tv. sulfidiphilus.*

Next to the biological oxidation of HS^- to SO_4^{2-}, the efficiency of S_8 formation is hampered by the chemical oxidation of HS^-. When dissolved oxygen (O_2) and HS^- are both present in the process solution, HS^- is chemically oxidized to $S_2O_3^{2-}$ [12]. In addition, the presence of reactive polysulfides (S_x^{2-}), which are formed rapidly with S_8 and HS^- (reaction 5 in Table 2.1), also enhances the formation of $S_2O_3^{2-}$ [8]. As the HS^--rich process solution coming from the absorber is directly injected in an aerated bioreactor in the current process, formation of $S_2O_3^{2-}$ cannot be prevented.

In order to increase the selectivity for S_8 formation, production of the by-products SO_4^{2-} and $S_2O_3^{2-}$ should be minimized. Key in the enzymatic formation of SO_4^{2-} via rDSR is the oxidized electron carrier cytochrome c. The oxidation of cytochrome c occurs via reduction of oxygen by cytochrome c oxydase (CcO), which is reversibly inhibited by HS^- [13]. Hence, when exposing SOB, such as *Tv. sulfidiphilus*, to elevated HS^- levels, the oxidation route from HS^- to SO_4^{2-} is severely hampered due to suppression of CcO [14]. As a side effect of this inhibition, other enzyme systems using oxidized cytochromes, such as Fcc, are suppressed as well. When the main route of HS^- oxidation to S_8 is suppressed, it is expected that when the system is continuously operated under the CcO suppressing conditions, another HS^- oxidizing enzyme system eventually becomes dominant, which is not subjected to HS^- inhibition: sulfide-quinone reductase (SQR).

To expose SOB to elevated HS^- levels, it is suggested to include an extra bioreactor in the biodesulfurization process line-up [15]. This bioreactor, placed in between the absorber and aerated bioreactor, imposes extra retention time for the SOB in the HS^- rich process solution from the H_2S absorber. Recently, it has been shown that SOB taken from

biodesulfurization systems, are capable of HS^- uptake in the absence of oxygen [16]. Hence, it can be hypothesized that when SOB are exposed to elevated HS^- levels in the anaerobic bioreactor, HS^- concentration will be decreased and the HS^- concentration in the influent of the aerobic bioreactor is lower. As a result, chemical oxidation rates in the aerated bioreactor will decrease and $S_2O_3^{2-}$ formation will be lower. Therefore, it is hypothesized that retention time at elevated HS^- levels in the anaerobic reactor (i) imposes enzymatic suppression of SO_4^{2-} formation, (ii) imposes a change in dominating HS^- oxidation route (i.e., from Fcc to SQR) and (iii) decreases the chemical oxidation rate of HS^- to $S_2O_3^{2-}$ by stimulating HS^- uptake by SOB.

The aim of this research is to study how the addition of an anaerobic bioreactor to the process line-up will further optimize the selectivity for S_8 formation in the biological gas desulfurization process under haloalkaline conditions. The new dual bioreactor line-up was tested in continuous mode for 111 days at pilot scale (20 L), mimicking operation of full-scale conditions. During the experiment, the process performance (i.e. selectivity for sulfur (S_8), sulfate (SO_4^{2-}) and thiosulfate ($S_2O_3^{2-}$) formation) was analyzed. In addition, HS^- levels in the anaerobic reactor were monitored to test the hypothesis of biological HS^- uptake. Moreover, Next Generation Sequencing (NGS) was used to assess changes in the microbial community. The results were compared with an experiment in the same set-up without using the anaerobic bioreactor (i.e., the 1-bioreactor line-up).

2.2 MATERIALS AND METHODS

2.2.1 EXPERIMENTAL SETUP

The experiments were performed in a continuous reactor system, consisting of an H_2S absorber and two bioreactors: an anaerobic bioreactor and an aerated bioreactor (Figure 2.1). The feed gas supplied to the H_2S absorber (stream A in Figure 2.1) was a mixture of H_2S (8.9 vol% H_2S, 91.1 vol% N_2), N_2 (99.995 vol%) and CO_2 (99.995 vol%). These gases were supplied as separate streams using mass flow controllers (Profibus, Brooks instrument, Hatfield, USA) to the main feed gas line. Washing solution (stream 1) with no sulfide (“lean” solution) from the aerated bioreactor was circulated over the H_2S absorber by an eccentric screw pump (P1 in Figure 2.1).

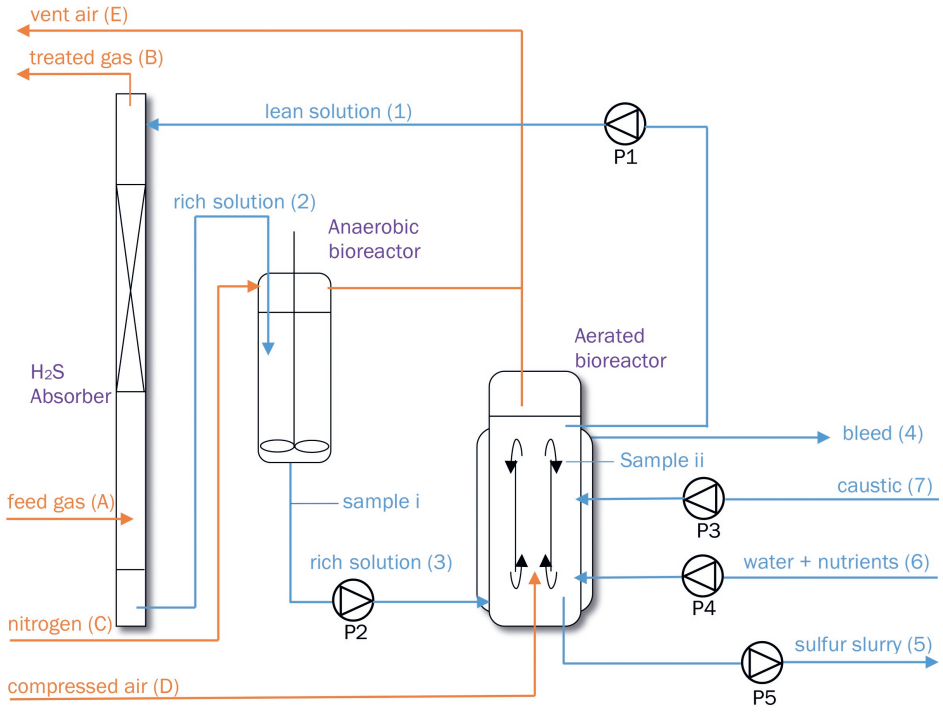

Figure 2.1: Schematic representation of the experimental setup used for the continuous experiments. The orange lines represent gaseous flows and the blue lines liquid flows. During the control experiment, the flow from the absorber bottom was routed directly to the aerated bioreactor.

The HS-containing solution ("rich" solution) was collected at the bottom of the H_2S absorber (approximately 1 L). The flow of rich solution from the bottom of the H_2S absorber to the anaerobic bioreactor (stream 2) (or to the aerated bioreactor directly in the control experiment) was driven by the pressure difference between the pressurized H_2S absorber and the atmospheric anaerobic bioreactor, and was controlled with a valve. The effluent of the anaerobic bioreactor was directed to the aerated bioreactor (stream 3) with a peristaltic pump (P2). More information about the H_2S absorber, liquid flows, pumps and pump controls is supplied in the Supporting Information (SI 1.1). The total liquid volume of the anaerobic bioreactor (5.3 L) was continuously mixed by an installed mechanical mixer (rzr2020, Heidolph Instruments, Schwabach, Germany). In both bioreactors, the pH and oxidation/reduction potential (ORP) were measured with a combined SE552/2 Inducon ORP/pH sensor, connected to a Stratos Pro Transmitter (Knick, Berlin, Germany). An

integrated Ag/AgCl electrode was used as reference for ORP and pH. To avoid air leakage into the anaerobic bioreactor, a small flow of N_2 (stream C) was supplied to its headspace.

The aerated bioreactor was a gas-lift bioreactor with a wet volume of 11.4 L with dimensions 690/150 mm (H/D). Both the anaerobic bioreactor and the aerated bioreactor were kept at a constant temperature using warm water from a thermostat bath (Kobold, Germany), which was routed through the water jackets of both reactors. The temperature in the aerated bioreactor during the experiments was 36.9 ± 1.0 °C. The temperature in the anaerobic bioreactor was 1 °C lower (35.9 ± 1.0 °C). This temperature is similar to the operating temperature of full-scale systems, which is between 30-40 °C. The ORP in the aerated bioreactor was maintained at a constant pre-set value by aeration. Compressed air (stream D) was supplied with a mass flow controller (Profibus, Brooks Instruments, Hatfield, USA). In addition, a sensor for measuring dissolved O_2 (PSt 6 Presens, Regensburg, Germany) was positioned in the aerated bioreactor. This reactor was overflowing into a bleed vessel (stream 4). The bottom of the aerated bioreactor was cone-shaped, to secure the removal of settling S_8. This S_8 slurry was removed with a pump (P5) (101 U/R, Watson Marlow, Wilmington USA) (stream 5). To compensate for the removed slurry, diluted nutrients solution via pump P3 (101 U/R, Watson Marlow, Wilmington, USA) (stream 6) and a diluted 5% (w/w) caustic solution via pump P4 (101 U/R, Watson Marlow) (stream 7) were continuously supplied. The presence of dissolved HS^- and polysulfide in the aerated bioreactor was regularly checked with lead acetate paper (H_2S-Test Paper, Tintometer GmbH, Dortmund, Germany). To determine the liquid influent and effluent streams, the vessels for storing and collecting nutrients, caustic, bleed water and sulfur slurry solutions were weighed each time a sample was taken, using a balance (PM11-K, Mettler-Toledo, Greifensee, Switzerland).

Liquid samples for analyses were taken from two sampling points located at (i) the sample port at the bottom of the anaerobic bioreactor, and (ii) the sample port of the lean solution from the aerated bioreactor.

A schematic overview of the dual reactor and the 1-bioreactor line-up is given in the Supporting Information (SI 1.2, Figure SI1.1).

2.2.2 EXPERIMENTAL OPERATION

The system (i.e. H_2S absorber bottom, anaerobic bioreactor, aerated bioreactor and tubing) was filled with a mixture of bioreactor solutions from a full-scale system, described by

Roman et al. [17]. The N_2 flow to the H_2S absorber was started at 100 NL h^{-1} (normal liter per hour) to pressurize the column to 3 bar(g). Subsequently, the lean solution flow to the top of the H_2S absorber was started at 8 kg h^{-1}. After stabilization of the solution temperature at 37 °C, the addition of carbon dioxide and hydrogen sulfide was initiated. The total H_2S load was kept constant at 4.78 mol-S day^{-1} and the CO_2 ranged from 6.43 – 53.54 mol day^{-1}. At the same time, the nutrient and caustic supply were started. The nutrients contained 2.86 mg-N L^{-1} as urea, 2 mg-K L^{-1} as KNO_3, 0.65 mg-P L^{-1} as H_2PO_4 and trace metals as described by Pfennig & Lippert [18] and were supplied together with the make-up water. The nutrients are required for growth of the bacteria and the nutrient dosing rate was used to control the biomass concentration. Caustic soda (NaOH) is required to maintain the alkalinity, which is lost by SO_4^{2-} and $S_2O_3^{2-}$ formation and by the effluent streams. After one day operation, the sulfur discharge pump (P5) was started to continuously remove the sulfur slurry from the bottom of the aerated bioreactor.

Upon introduction of H_2S, the air supply rate to the aerated bioreactor was controlled by the ORP measurement in the aerated bioreactor, using a PID controller in the PLC [19]. At start-up (i.e. first 5 days), the ORP setpoint was -325 mV. Then the setpoint was decreased to -365mV, which was maintained through the rest of the experiment. The air supply was in the range of 40-100 NL h^{-1} throughout the complete experiment. The CO_2 supply was manually set to control the pH in the aerated bioreactor; at increasing CO_2 supply rates, the pH decreased. The measured pH values in the anaerobic bioreactor were 7.5-8.7, and 8.4-9.0 in the aerated bioreactor. The pH in the aerated bioreactor during the control experiment was between 8.53 and 8.93 and the ORP setpoint was -350 mV.

2.2.3 Analysis

The reagents were of analytical grade unless stated otherwise. All analyses were performed on samples taken from the aerated bioreactor unless stated otherwise. The liquid was circulated through all sections of the system (i.e. H_2S absorber, anaerobic bioreactor and aerated bioreactor) with a flow of 8 kg h^{-1} (streams 1, 2 and 3 in Figure 2.1). Hence, the HRT's in the different sections of the process were: 4 minutes in the absorber bottom, 44 minutes in the anaerobic bioreactor and 94 minutes in the aerated bioreactor. Therefore, the alkalinity and concentrations of SO_4^{2-}, $S_2O_3^{2-}$, S_8 and bacteria were equal throughout the complete system (which was verified by measurements) and the concentrations measured in samples of the aerated bioreactor were also representative for the liquid in the H_2S absorber and anaerobic bioreactor.

The composition of the treated gas of the H_2S absorber (sampled every 3 minutes) was analyzed for H_2S, CO_2 and N_2, using a gas chromatograph (GC) (EnCal 3000, Honneywell, USA). The GC was equipped with a molsieve and a ppu column (both 10m), using helium as carrier gas. The molsieve column was operated at a pressure of 200 kPa and 100 °C. The GC was calibrated weekly.

To determine the HS^- removal in the anaerobic bioreactor, the total sulfide concentration (S^{2-}_{tot}), which is the sum of S^{2-}, HS^- and polysulfide-sulfane (S_x^{2-}), was measured in a sample of the anaerobic reactor by titration with a solution of 0.1 M $AgNO_3$, using a Titrino Plus Titrator (Metrohm, Herisau, Switzerland). Before titration, the tested sample was filtered over a 0.45 µm cellulose acetate membrane filter to remove S_8 and bacteria. 2 mL of filtered sample was added to 80 mL 4% (w/v) NaOH, with 1 mL of 30% (w/v) NH_4OH to stabilize S^{2-}_{tot}. A comparison between unfiltered and filtered samples did not show significant differences.

The specific HS^- removal efficiency in the anaerobic bioreactor (mg-S mg-N^{-1}) was calculated based on the H_2S load, the liquid flows, the measured HS^- concentration and the biomass concentration, according to Equation 2.1.

$$HS^- \ removal \ anaerobic \ bioreactor = \frac{\frac{H_2S \ load \cdot u_{H_2S}}{solution \ flow} - measured \ [S^{2-}_{tot}]}{Xb} \qquad \text{(Equation 2.1)}$$

Here, *H_2S load* is the mass loading in the H_2S absorber (mmol h^{-1}), and the *solution flow* is the liquid flow to the anaerobic reactor (L h^{-1}). u_{H_2S} is molar weight of H_2S (g mol^{-1}), *measured* $[S^{2-}_{tot}]$ is the total measured sulfide concentration (mg-S L^{-1}) and *Xb* is the biomass concentration (mg-N L^{-1}).

The biomass concentration was measured as the amount of total organic N using the Dr. Lange cuvette test LCK138 (Hach Lange, Germany). The difference between the supernatant (i.e. a sample centrifuged for 10 minutes at 14000 x g) and a non-centrifuged sample indicated the total amount of N present in the biomass. It was confirmed that the presence of biologically produced S_8 did not affect the N analyses, provided that the samples were at least 5 times diluted. Considering the generic stoichiometric chemical equation for HA-SOB, i.e. $CH_{1.8}O_{0.5}N_{0.2}$ [20], the total N amount accounts for 10 mol% of the total dry weight biomass.

The specific conductivity of the samples was monitored using an offline conductivity sensor (LF 340, WTW, Weilheim, Germany). The alkalinity was measured with titration with 0.1 M HCL to pH 4.3, using a titrator (Titralab AT1000, Hach Lange, Germany). The method was verified with an analysis in accordance with WAC/III/A/006.

After removal of cells and S_8 by centrifugation for 10 minutes at 14000 x g, the supernatant samples were analyzed for COD – in duplicate, (Lange cuvette test LCK514, Hach Lange Germany) at 605 nm, and using a spectrophotometer (Hach Lange, Germany) – to determine total dissolved $S_2O_3^{2-}$. In addition, the sample was analyzed for SO_4^{2-}, by using a Hach Lange cuvette test LCK353 and spectrophotometer at 800 nm. These methods were verified with an ion chromatography method, in accordance with ISO 10304-1.

The concentration of total suspended solids (TSS), consisting of mainly S_8, was analyzed in triplicate. A 5-15 mL sample (depending on the TSS concentration) was filtered over a pre-dried (24h, 60 °C) and pre-weighed GF/C Glass microfiber filter (Whatman). After drying (60 °C for at least 24h), the filters were weighed again. The TSS was determined as the difference between the final weight and initial weight, divided by the sample weight.

As the formed S_8 particles have a tendency to attach to the reactor wall, it was not possible to calculate the S_8 production rate from the analyses. As no products other than S_8, SO_4^{2-} and $S_2O_3^{2-}$ were measured in the reactor [7], the production rate of S_8 could be calculated from the following mass balance:

$$P_{S_8} = I_{H_2S} - P_{SO_4{}^{2-}} - P_{S_2O_3{}^{2-}} \quad \text{(Equation 2.2)}$$

Here, P_{S_8}, $P_{SO_4{}^{2-}}$ and $P_{S_2O_3{}^{2-}}$ are the production rates of S_8-S, SO_4^{2-}-S, and $S_2O_3^{2-}$-S, respectively, in mol day^{-1} and I_{H_2S} is the volumetric H_2S influent in mol day^{-1}. The production rates of both SO_4^{2-}-S and $S_2O_3^{2-}$-S (not shown) are calculated as follows:

$$P_{SO_4{}^{2-}} = \frac{effluent \cdot \overline{[SO_4{}^{2-}]} + V \cdot \Delta[SO_4{}^{2-}]}{\Delta t} \quad \text{(Equation 2.3)}$$

The selectivities were calculated according to Equation 2.4:

$$S_{SO_4{}^{2-}} = \frac{P_{SO_4{}^{2-}}}{I_{H_2S}} \quad \text{(Equation 2.4)}$$

Here, *effluent* is the total effluent of the system (L) in time interval Δt (days) (i.e. sample volumes, S_8 slurry and bleed), $\overline{[SO_4^{2-}]}$ the average concentration (mol L^{-1}) over time interval Δt, *V* the total liquid volume of the system (18,7 L) and $\Delta[SO_4^{2-}]$ the concentration changes (mol L^{-1}) over time interval Δt. The mathematical equation to determine the caustic use and bleed flow of a full scale system based on the product selectivities can be found in the Supporting Information (SI 1.3).

The samples for microbial community analysis were conserved immediately after sampling by addition of ethanol up to 50% (v/v). DNA was extracted with the Mpbio FastDNA™ SPIN Kit for Soil. Subsequently, PCR was used to amplify the V3 and V4 region of the 16S rRNA gene of bacteria giving a 400 bp product. The library prep, sequencing and data analysis was performed via the 16S BioProphyler® method [21], using the Illumina PE300 platform and MiSeq sequencer. Within the BioProphyler® method all primer sequences and low quality reads were deleted from the raw datasets. The obtained sequences were compared with the online nt database with the aid of the BLAST algorithm. Low abundance reads were not removed from the dataset and no correction on differences in library size was applied. The reported species name is the species which is most related to the detected sequence. A detailed table with NGS results, including accession numbers, can be found in Supporting Information (SI 1.4). The EMBL-EBI accession number for presented 16S rRNA sequencing set is PRJEB31478.

2.3 Results and discussion

2.3.1 Operational results

The tests in the new dual-bioreactor line-up were performed over a period of 111 days (i.e. 8.5 times HRT) and the control experiment was performed over a period of 57 days (i.e. 3 times HRT). An overview of the control experiments is shown in the Supporting Information (SI 1.5) and the performance of the new process line-up in the 111 days experimental run is shown in Figure 2.2. During the control, the liquid composition was stable from day 35-56 (i.e. the last HRT). The data during this period were used to determine the performance of the 1-bioreactor line-up.

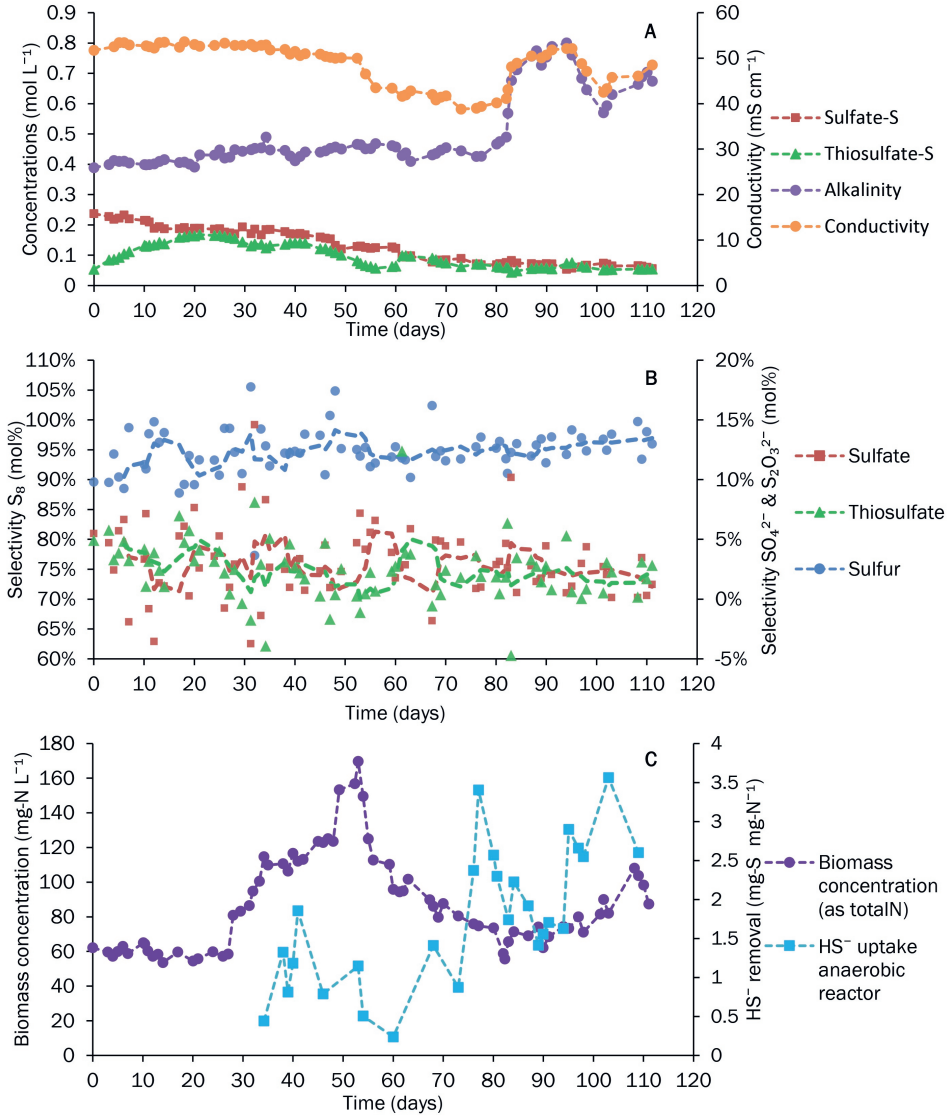

Figure 2.2: Results of the continuous experiment with anaerobic bioreactor. Figure A shows the measured concentrations of SO_4^{2-} and $S_2O_3^{2-}$, the measured conductivity (a measure for the total salinity) and the measured alkalinity in the effluent of the aerated bioreactor. In Figure B the calculated product selectivities are shown. The markers indicate the calculated daily analyses and dotted lines the moving averages (based on a 5-day period). Figure C displays the measured concentrations of biomass (as total N) and specific sulfide uptake (HS- and polysulfide) by the biomass in the anaerobic bioreactor.

The alkalinity and conductivity during this period were 0.38 ± 0.12 M and 74.0 ± 1.8 mS cm^{-1}. The SO_4^{2-}-S and $S_2O_3^{2-}$-S concentrations were 0.56 ± 0.06 M and 0.32 ± 0.02 M respectively. A comparison of the results of both experiments is given in Table 2.2. The selectivity for S_8 formation and by-products obtained in the control experiment are similar as described in literature for systems without anaerobic bioreactor [5-7].

Figure 2.2A shows the concentrations of the dominant anions in process solution of the aerated bioreactor of the new-line up experiment. After inoculation, the medium contained 0.15 mol-S as SO_4^{2-} and 0.033 mol-S as $S_2O_3^{2-}$. From the start of the run, the SO_4^{2-} levels in the process liquid decreased up to day 80, which is an indication that the rate of SO_4^{2-} formation was lower than its removal via the bleed stream. From day 80 onwards, the SO_4^{2-}-S concentration was stable at 0.07 ± 0.01 mol-S L^{-1}. For $S_2O_3^{2-}$, a different pattern was observed; during the first 24 days of operation, the levels of $S_2O_3^{2-}$ increased, indicating chemical oxidation of HS^- took place. This could be due to limited biological activity at start-up, which is often observed in biological desulfurization systems. Thereafter, up to day 60, a decrease was observed, and from day 80 onwards the $S_2O_3^{2-}$-S concentration stabilized at 0.57 ± 0.01 M.

The measured conductivity and alkalinity at the start were 51.7 mS cm^{-1} and 0.4 M respectively. The conductivity was controlled via the caustic dosing, and is dependent on the different salts in solution (Na_2SO_4, $Na_2S_2O_3$, $NaHCO_3$ and Na_2CO_3). Around day 50, both SO_4^{2-} and $S_2O_3^{2-}$ concentrations decreased quickly, which caused a decrease in conductivity as well. To restore the conductivity to ~50 mS cm^{-1}, the caustic dosing was increased. This caused a rapid increase in alkalinity from 0.45 M to 0.80 M. The alkalinity (total concentration of $NaHCO_3$ and Na_2CO_3 and expressed as concentration $NaHCO_3$) is important for efficient H_2S removal in the H_2S absorber and has to be in the range of 0.30 – 0.90 M. The main reason for the difference in conductivity between the control and the experiment with anaerobic reactor is the higher sulfate concentration in the control experiment.

The average H_2S removal efficiency in the H_2S absorber, calculated as $1-([H_2S_{out}]/[H_2S_{in}])$, was 99.75% ± 0.83%. This means that the H_2S absorber efficiently removed H_2S from the fed sour gas, i.e. only a negligible amount of H_2S was not absorbed. During the entire experimental run, no dissolved HS^- (or S_x^{2-}) was detected in the aerated bioreactor, meaning that all H_2S fed to the aerated bioreactor was converted. Furthermore, all

dissolved O_2 concentration measurements in the aerated bioreactor indicated values below detection limit of 1 ppb, meaning that the environment in the aerated bioreactor was microaerophilic.

Figure 2.2B shows the calculated selectivities for SO_4^{2-}, $S_2O_3^{2-}$ and S_8 formation from H_2S. These calculations are based on concentrations of SO_4^{2-} and $S_2O_3^{2-}$ in the effluent of the aerated bioreactor and on the bleed and sulfur slurry flows as indicated by equations 2.2, 2.3 and 2.4. As the calculated numbers are based on a sum of measurements with corresponding variance, the reported numbers show scattering up to day 60 of the experimental run. Therefore, the moving averages (dotted lines) are shown as well, which is the average value of 5 consecutive calculated selectivities.

In the first week of operation, the selectivity for S_8 formation was around 90 mol% (based on a 5-day average), with selectivity for SO_4^{2-} and $S_2O_3^{2-}$ formation around 5 mol%. In the first 60 days of operation, large fluctuations in calculated selectivity were observed. In this period, the moving average varied between 90.5 and 98.3 mol% for S_8 formation (with average 94.2 ± 4.7%); average selectivities for SO_4^{2-} and $S_2O_3^{2-}$ formation were 3.2 ± 3.7% and 2.6 ± 2.4%. While the experiment proceeded, fluctuations in the calculated selectivities decreased and a new steady state was reached. The calculated selectivity for S_8 formation (5-day average) increased to 96.9 mol% and the calculated selectivities for SO_4^{2-} and $S_2O_3^{2-}$ were 1.1% and 2.0 mol% respectively by the end of the run (day 111).

It can be noticed that the calculated product selectivities show large fluctuations at the beginning of the experiment. The fluctuations decreased as the experiment progressed. From day 70 onwards, no fluctuations were observed anymore; instead, a gradual increase was found for the selectivity for S_8 formation. An explanation can be found in the change of the microbiological community. The establishment of a new biological equilibrium is a relatively slow process and might explain the pattern in the process selectivity calculations. The microbiological composition will be discussed in the next section.

The initial biomass concentration was 60 mg-N L^{-1} (see Figure 2.2C). During operation it was found to be difficult to obtain a stable concentration of bacteria in the system. Some bacteria adhered to the produced S_8 particles and were therefore removed with the sulfur slurry and bleed. For example, it was found that a liquid sample taken from the aerated bioreactor contained 54 ± 1.0 mg-N L^{-1} (TSS = 2.0 ± 0.3 g L^{-1}) while the sulfur slurry contained around 300 ± 50 mg-N L^{-1} (TSS = 59 ± 0.5 g L^{-1}). The adhesion of biomass to S_8

fluctuated over time, which could be due to variation in pH [22, 23]. Moreover, the fluctuation in biomass concentration was related to some variation in the bleed flow. Hence, the concentration of bacteria in the system fluctuated between 55.5 and 108 mg-N L^{-1}. The biomass concentration in full-scale systems is typically in the range of 50-150 mg-N L^{-1}, dependent on the specific conditions in the system.

The total HS^- concentration in the effluent stream of the anaerobic bioreactor (stream 3) was measured on a regular basis. In the first 33 days of the experiment, the HS^- concentration was analyzed using a spectrophotometric method based on methylene blue. This method was found to be inconvenient for the HS^- concentrations in this experiment. Due to the low measurement range of this method, the measured values showed large deviations. Therefore, these results are not shown in Figure 2.2C. From day 34 onwards, a potentiometric titration with $AgNO_3$ was used to measure the HS^- concentrations, as described in the materials and methods. The measured HS^- concentration was consistently lower than the calculated values, assuming that no oxidation of dissolved total HS^- occurred in the H_2S absorber. In the anaerobic bioreactor, 9 to 54% of the total absorbed dissolved HS^- was removed. If this decrease was caused by chemical oxidation of HS^- to $S_2O_3^{2-}$, selectivity towards biological S_8 formation could not become >90%, as S_8 cannot be formed chemically under the described operational conditions, i.e. in the absence of oxygen [24]. Therefore, the SOB seem to remove HS^- in the anaerobic reactor, i.e. in the absence of oxygen. Based on the difference between calculated and measured HS^- concentrations, the specific HS^- uptake in the anaerobic bioreactor was calculated (i.e. mg-HS^- per mg-N of biomass) (see Figure 2.2C). The specific HS^- uptake in the anaerobic bioreactor was between 0.24 and 3.4 mg-S mg-N^{-1}, while ter Heijne [16] observed an HS^- uptake of 0.22 mg-S mg-N^{-1} under anaerobic conditions in a batch experiment. The HS^- uptake will be further discussed in section 3.3.

An overview of performance of the 1-bioreactor line-up and the new dual bioreactor line-up is shown in Table 2.2. Based on the results, we conclude that two main reasons can be hypothesized for the increased selectivity for sulfur formation: i) the decrease of biologically mediated formation of SO_4^{2-} ii) a decrease in concentration of HS^- in the anaerobic reactor, resulting in a less chemical formation of $S_2O_3^{2-}$ in the aerobic reactor. In the next sections, both hypotheses will be discussed in more detail.

2.3.2 DECREASE IN SULFATE FORMATION

The initial selectivity for SO_4^{2-} formation (average of first 5 days of operation) in the new process line up was 5.0 ± 1.6 mol%, which is considerably lower than in the control experiment without anaerobic reactor (14.9 ± 0.2 mol%). This short term effect cannot be explained by population dynamics or sudden changes in operation conditions of the aerated bioreactor. It is more likely that this effect is caused by instantaneous inhibition of enzymatic routes, which results in a decrease of the formation rate of SO_4^{2-}. As SO_4^{2-} formation is a biotic reaction and as such the microbial community could be influenced by this inhibition, the composition of the bacterial community was analyzed. The composition of the bacterial community was analyzed at day 3, day 19 and day 73 (see Figure 2.3).

The initial microbial community composition (day 3) showed that the population was dominated by *Tv. sulfidiphilus*, with a relative abundance of 54%, see Figure 2.3. This is in line with observations of [9, 10]. This composition mostly resembled the microbial community found at the biogas desulfurization facility in Eerbeek (Industriewater Eerbeek B.V.) [10, 17] and microbiological community of the seed SOB for the control experiment, both without anaerobic bioreactor (no NGS data were obtained throughout the control experiment). Due to the presence of Fcc, rDSR and CcO genes in the analysis of the genome of *Tv. sulfidiphilus* [10, 11], the high relative abundance presence of *Tv. sulfidiphilus* at day 3 indicates that the system has a potential for SO_4^{2-} formation.

On day 19 (after approximately 1.5 the total system's HRT), the community was similar to the community at day 3, indicating no major influence on microbial community composition of the anaerobic bioreactor in the process line-up. From day 19 to day 73 (after approximately 5.5 x HRT) a clear shift occurred in the microbiological community. The abundance of *Tv. sulfidiphilus* had decreased to less than 1% and the community became dominated by (16S rRNA gene sequences related to *Alkalilimnicola ehrlichii* MLHE-1 (relative abundance of 59%), which is a haloalkaliphilic member of the family *Ectothiorhodospiraceae* (*Gammaproteobacteria*) [25].

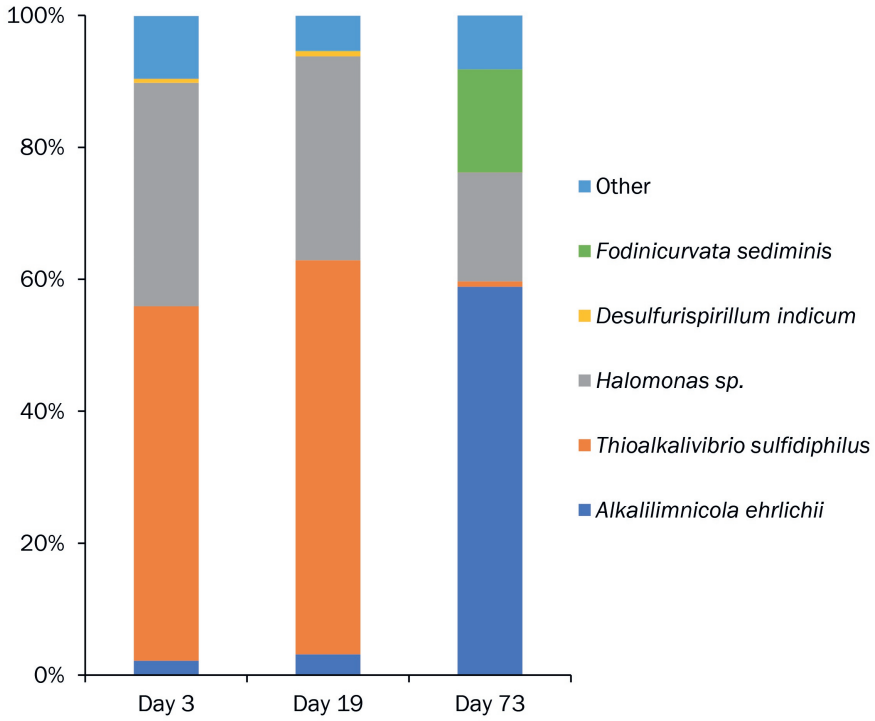

Figure 2.3: Mapping of bacterial diversity in the system by 16S rRNA gene amplicon sequencing. Samples were obtained from the aerated bioreactor. The analysis was performed with the 16S BioProphyler® method [21], using the Illumina MiSeq sequencer. The obtained sequences were compared with an online database, with the aid of the BLAST algorithm. The reported species name is the species most related to the detected sequence. The inoculum was obtained from a biodesulfurization system without anaerobic bioreactor.

The representatives of two closely related genera – *Alkalilimnicola* and *Alkalispirilum* – are haloalkaliphilic facultative chemolithoautotrophs, with the ability to grow by either aerobic or nitrate-dependent oxidation of HS^-. As the N-source was urea, growth of *Alkalilimnicola* and *Alkalispirilum* can only be explain by oxidation of HS^- using O_2 as final electron acceptor. As it was shown that these facultative SOB species oxidize HS^- exclusively to the state of elemental sulfur [26, 27], the SO_4^{2-} formation potential of the overall microbiological population present in the process solution was decreased.

In the conventional 1-bioreactor biodesulfurization process, it is expected that *Tv. sulfidiphilus* will be dominating [9]. However, for the dual bioreactor line-up we postulate that due to the suppression of the CcO by the elevated levels of HS^- in the anaerobic

bioreactor, growth of *Tv. sulfidiphilus* is suppressed. In contrast to *Tv. sulfidiphilus, Alkalilimnicola* expresses one or more genes for the membrane-bound sulfide-quinone reductase (SQR), which is another well-known enzyme associated with HS^- oxidation [26, 28]. Since HS- oxidation by SQR does not depend on the activity of CcO, *Alkalilimnicola* has a new niche to grow. This needs to be further confirmed by genomic and enzymological analyses in future work.

By day 73 the SO_4^{2-} formation was further decreased to ~2 mol%. This decrease might be explained by the shift in community composition, as the S_8-forming *Alkalilimicola* became dominant over the SO_4^{2-}-forming *Tv. sulfidiphilus*. In the dual-bioreactor process line up 90.7 ± 2.8 mol% of all fed HS^- was oxidized to S_8 on day 19. This continuously increased: 95.5 ± 1.4 mol% on day 73 and 96.9 ± 2.4% on day 111, see Figure 2.2B. While formation of S_8 increased, SO_4^{2-} formation decreased to 1.4 ± 1.3 mol% at the end of the experiment. Hence, these results support the hypothesis that introducing an anaerobic reactor in the line-up suppresses the formation of SO_4^{2-}.

From the results we conclude that there is a short-term and a long-term effect of the dual-reactor line-up on SO_4^{2-} formation. On short-term, SO_4^{2-} formation is lower compared to the 1-bioreactor line-up (5.0 ± 1.6 mol% vs 14.9 ± 0.2 mol%) due to instantaneous inhibition of the SO_4^{2-} forming enzymatic routes.

On the longer term, the microbial community showed a decrease in the potential to form SO_4^{2-} due to the dominance of *Alkaliminicola*, which is limited to S_8 formation. This resulted in a further decrease of selectivity for SO_4^{2-} formation to 1.4 ± 1.3 mol%.

2.3.3 Decrease in thiosulfate formation

While the nature of SO_4^{2-} formation is biological, $S_2O_3^{2-}$ is formed chemically when both dissolved oxygen and HS^- and/or S_x^{2-} are present in the process solution. When comparing the control experiment (1-bioreactor line-up) with the start-up of the dual bioreactor line-up, the dual-bioreactor line-up showed a lower $S_2O_3^{2-}$ formation (4.5 ± 1.0 mol%) than the 1-bioreactor line-up (9.5 ± 1.5 mol%).

From day 34 onwards, the HS^- levels in the anaerobic reactor effluent were analyzed and found to be significantly lower than expected based on the mass balance of gas and liquid flows, as discussed in section 3.1. For example, on day 34, the HS^- concentration was expected to be 19.6 mM based on the mass balance of gas and liquid flows. However, a

HS^- concentration of 18.4 mM was measured. Ter Heijne et al. [16] showed that SOB remove HS^- from solution in the absence of oxygen in a batch experiment. The results obtained in this study indicate that the SOB also remove HS^- in the anaerobic reactor (i.e. in the absence of oxygen) in a continuous reactor system. At day 34, the calculated HS^- uptake was 0.40 mg-S mg-N^{-1}, which is higher than measured by ter Heijne et al., i.e. 0.22 mg-S mg-N^{-1} [16]. Over the period of day 34 up to day 72, an average uptake rate of 1.1 mg-S mg-N^{-1} was found.

After day 72, an increase in removal efficiency of HS^- was observed (Figure 2.2C). The increase in HS^- uptake over time indicates that the bacterial population acquires the ability of (higher) HS^- uptake under anaerobic conditions. While at day 34, 9% of all the fed sulfide was removed, at day 111 54% of all fed HS^- was removed from the process solution (i.e. a HS^- concentration of 9.3 mM had been measured, while the mass balance dictates 20.6 mM). As a result of the lower HS^- levels, chemical oxidation of HS^- in the aerobic reactor decreases. While the average $S_2O_3^{2-}$ selectivity over the first five days was 4.5 ± 1.0 mol%, in the last five days of the experiment a selectivity for $S_2O_3^{2-}$ formation of 2.0 ± 1.2 mol% was found. Since the influent of the aerated bioreactor contains 50% less HS^-, also selectivity of $S_2O_3^{2-}$ formation decreased with 50%.

Yet, the mechanisms behind the HS^- uptake under anaerobic conditions are not very well understood. It has been shown that H_2S can be taken up by bacteria as it can freely diffuse over a cell membrane into the periplasm [29, 30]. In the periplasm the H_2S or HS^- can either react with internally stored sulfur particles forming polysulfide or it can undergo biological conversion [24]. For SQR enzymes, which became the dominant HS^- oxidizing enzyme system during the experiment, it has been shown that it can bind up to 4 S-atoms without the presence of oxygen [31]. Furthermore, oxidized electron carriers, such as quinones and cytochromes, might be used as (intermediate) electron acceptor, enabling conversion of (part of) the HS^- by SQR to elemental sulfur [31].

The decrease in $S_2O_3^{2-}$ formation in the dual-bioreactor line-up is the result of biological HS^- uptake in the anaerobic bioreactor. At the start of the experiment, only 10% of HS^- was taken up in the anaerobic bioreactor and the selectivity for $S_2O_3^{2-}$ was 4.5 ± 1.0 mol%. As the microbial population developed over time, HS^- uptake eventually increased to over 50% of the dosed H_2S. This resulted in a decrease in selectivity for $S_2O_3^{2-}$ formation of 2.0 ± 1.2 mol% at the end of the experiment.

2.3.4 IMPLICATIONS FOR FULL-SCALE SYSTEMS

We show in this work that incorporation of an anaerobic bioreactor in the line-up of the biological gas desulfurization process under haloalkaline conditions improves the selectivity for sulfur formation due to i) the decrease in biological SO_4^{2-} formation by suppression of SO_4^{2-} forming enzymatic route and change of the microbial community composition and ii) decrease in chemical HS^- oxidation to $S_2O_3^{2-}$, which is the result of HS^- uptake in the anaerobic reactor, thereby lowering the HS^- concentration in the rich solution to the aerated bioreactor.

Two main factors that determine the operational costs of full-scale biodesulfurization systems are consumption of caustic and production of the bleed stream. Both are associated with the production of SO_4^{2-} and $S_2O_3^{2-}$. The selectivity for S_8 formation in the 1-bioreactor line-up (H_2S absorber and aerated bioreactor) was 75.6 ± 1.3 mol%. Selectivities for SO_4^{2-} and $S_2O_3^{2-}$ formation were 14.9 ± 0.2 and 9.5 ± 1.5 mol%. The results presented in this paper show that the introduction of an anaerobic bioreactor between the H_2S absorber and the aerated bioreactor decreases the selectivity for SO_4^{2-} formation to 1.4 ± 1.3 mol% and for $S_2O_3^{2-}$ to 2.0 ± 1.2 mol%.

In full scale facilities, sulfur is usually removed by a decanter centrifuge, resulting in the formation of a sulfur cake of 60-70 weight% S. Therefore, the bleed of a full scale system is dictated by the formation of the production of SO_4^{2-} and $S_2O_3^{2-}$. Based on the product selectivities of both experiments (with and without anaerobic reactor) the specific caustic consumption and bleed formation were calculated (Table 2.2). Detailed calculation is provided in the Supporting Information (SI 1.3). The specific caustic consumption for the 1-bioreactor line-up is 1.25 kg-NaOH kg-S^{-1} and the bleed formation 24.1 L kg-S^{-1}. With the new dual bioreactor line-up, the caustic consumption and bleed formation are 0.1 kg-NaOH kg-S^{-1} and 2.4 L kg-S^{-1}. This means a decrease of 90% for both caustic use and bleed stream formation. These results show that the new dual-bioreactor line-up strongly improves the competitive edge of biological desulfurization processes. For industrial applications, there is a trade-off between cost savings for caustic consumption and bleed water production, and costs for an additional bioreactor. Especially at higher sulfur loads, the dual reactor system will become economically favorable. In addition, other site-specific conditions, such as logistics for supplies and disposal, have to be taken into account.

Table 2.2: Comparison of the conventional 1-bioreactor and the new dual-bioreactor line-up biological desulfurization processes, in terms of product selectivity, caustic use and bleed stream formation. Product selectivities are based on the average performance during the last HRT in both experiments. The caustic use and bleed stream formation have been calculated with an alkalinity 0.8 M, total sodium of 1.3 M and 40% water content in the sulfur cake. Details of the calculations to determine caustic use and bleed formation can be found in the Supporting Information (SI 1.5).

	Conventional biological desulfurization process (1-bioreactor line-up)	**New biological desulfurization process (dual bioreactor line-up)**	**Decrease**
Selectivity for S_8 formation (%)	75.6	96.6	
Selectivity for SO_4^{2-} formation (%)	14.9	1.4	
Selectivity for $S_2O_3^{2-}$ formation (%)	9.5	2.0	
Caustic use (kg-NaOH kg-S^{-1})	1.25	0.12	90%
Bleed (L kg-S^{-1})	24.1	2.4	90%

2.4 Acknowledgements

This research was financed by Paqell B.V. We thank Harry Darmeveil and Angelo Fornerino (DNV-GL) for their support in the experiment work, Cees Molenaar and Jurgen Kramer (Paques) for their support in the engineering of the test plant, Rob Elzinga (Bioclear) for the NGS analyses and prof. A.J.H. Janssen and prof. G. Muyzer for the fruitful discussions. D.Y. Sorokin was supported by the Gravitation-SIAM program of the Dutch Ministry of Education and Science (24002002).

2.5 REFERENCES

[1] A.J. Janssen, P.N. Lens, A.J. Stams, C.M. Plugge, D.Y. Sorokin, G. Muyzer, H. Dijkman, E. Van Zessen, P. Luimes, C.J. Buisman, Application of bacteria involved in the biological sulfur cycle for paper mill effluent purification, Sci Total Environ, 407 (2009) 1333-1343.

[2] E. Van Zessen, A. Janssen, A. De Keizer, B. Heijne, J. Peace, R. Abry, Application of THIOPAQ™ biosulphur in agriculture, in: Proceedings of the British Sulphus Events 2004 Sulphur Conference, Barcelona, Spain, 24-27 October 2004, 2004, pp. 57-68.

[3] J.B. Klok, G. van Heeringen, R. de Rink, H. Wijnbelt, G. Bowerbank, Techno-economic impact of the next generation Thiopaq O&G process for sulfur removal, in: GPA-GCC, Muscat, Oman, 2018.

[4] J.B. Klok, G. van Heeringen, R. De Rink, H. Wijnbelt, Introducing the next generation of the THIOPAQ O&G process for biotechnological gas desulphurization: THIOPAQ-SQ, in: Sulphur, 2017.

[5] S. Alcantara, A. Velasco, A. Munoz, J. Cid, S. Revah, E. Razo-Flores, Hydrogen sulfide oxidation by a microbial consortium in a recirculation reactor system: sulfur formation under oxygen limitation and removal of phenols, Environ Sci Technol, 38 (2004) 918-923.

[6] J.B. Klok, P.L. van den Bosch, C.J. Buisman, A.J. Stams, K.J. Keesman, A.J. Janssen, Pathways of sulfide oxidation by haloalkaliphilic bacteria in limited-oxygen gas lift bioreactors, Environmental science & technology, 46 (2012) 7581-7586.

[7] P.L. Van Den Bosch, O.C. van Beusekom, C.J. Buisman, A.J. Janssen, Sulfide oxidation at halo-alkaline conditions in a fed-batch bioreactor, Biotechnology and bioengineering, 97 (2007) 1053-1063.

[8] W.E. Kleinjan, A. de Keizer, A.J. Janssen, Kinetics of the chemical oxidation of polysulfide anions in aqueous solution, Water research, 39 (2005) 4093-4100.

[9] D.Y. Sorokin, P.L. van den Bosch, B. Abbas, A.J. Janssen, G. Muyzer, Microbiological analysis of the population of extremely haloalkaliphilic sulfur-oxidizing bacteria dominating in lab-scale sulfide-removing bioreactors, Appl Microbiol Biotechnol, 80 (2008) 965-975.

[10] D.Y. Sorokin, M.S. Muntyan, A.N. Panteleeva, G. Muyzer, *Thioalkalivibrio sulfidiphilus* sp. nov., a haloalkaliphilic, sulfur-oxidizing gammaproteobacterium from alkaline habitats, Int J Syst Evol Microbiol, 62 (2012) 1884-1889.

[11] G. Muyzer, D.Y. Sorokin, K. Mavromatis, A. Lapidus, A. Clum, N. Ivanova, A. Pati, P. d'Haeseleer, T. Woyke, N.C. Kyrpides, Complete genome sequence of "*Thioalkalivibrio sulfidophilus*" HL-EbGr7, Stand Genomic Sci, 4 (2011) 23-35.

[12] D.J. O'Brien, F.B. Birkner, Kinetics of oxygenation of reduced sulfur species in aqueous solution, Environmental Science & Technology, 11 (1977) 1114-1120.

[13] J.P. Collman, S. Ghosh, A. Dey, R.A. Decreau, Using a functional enzyme model to understand the chemistry behind hydrogen sulfide induced hibernation, Proc Natl Acad Sci U S A, 106 (2009) 22090-22095.

[14] J.M. Visser, L.A. Robertson, H.W. Van Verseveld, J.G. Kuenen, Sulfur production by obligately chemolithoautotrophic *Thiobacillus* species, Applied and Environmental Microbiology, 63 (1997) 2300-2305.

[15] J. Klok, A.J.H. Janssen, G. Van Heeringen, J.H. Van Dijk, Process for the biological conversion of bisulphide into elemental sulphur, in: P. BV (Ed.), 2017.

[16] A. ter Heijne, R. de Rink, D. Liu, J.B.M. Klok, C.J.N. Buisman, Bacteria as an Electron Shuttle for Sulfide Oxidation, Environmental Science & Technology Letters, 5 (2018) 495-499.

[17] P. Roman, J.B. Klok, J.A. Sousa, E. Broman, M. Dopson, E. Van Zessen, M.F. Bijmans, D.Y. Sorokin, A.J. Janssen, Selection and Application of Sulfide Oxidizing Microorganisms Able to Withstand Thiols in Gas Biodesulfurization Systems, Environ Sci Technol, 50 (2016) 12808-12815.

[18] N. Pfennig, K.D. Lippert, Über das vitamin B 12-bedürfnis phototropher Schwefelbakterien, Archives of microbiology, 55 (1966) 245-256.

[19] A.J. Janssen, S. Meijer, J. Bontsema, G. Lettinga, Application of the redox potential for controling a sulfide oxidizing bioreactor, Biotechnol Bioeng, 60 (1998) 147-155.

[20] H. Banciu, D.Y. Sorokin, R. Kleerebezem, G. Muyzer, E.A. Galinski, J.G. Kuenen, Growth kinetics of haloalkaliphilic, sulfur-oxidizing bacterium *Thioalkalivibrio versutus* strain ALJ 15 in continuous culture, Extremophiles, 8 (2004) 185-192.

[21] B. Geurkink, S. Doddema, H. de Vries, G.J. Euverink, E. Croese, Value of Next Generation Sequencing as Monitoring Tool For Microbial Corrosion-A Practical Case from Bioprophyling to Tailor made MMM Analysis, in: CORROSION 2016, NACE International, 2016.

[22] S. Takakuwa, T. Fujimori, H. Iwasaki, Some properties of cell-sulfur adhesion in *Thiobacillus thiooxidans*, The Journal of General and Applied Microbiology, 25 (1979) 21-29.

[23] T.L. Takeuchi, I. Suzuki, Cell Hydrophobicity and Sulfur Adhesion of *Thiobacillus thiooxidans*, Appl Environ Microbiol, 63 (1997) 2058-2061.

[24] K.Y. Chen, J.C. Morris, Kinetics of oxidation of aqueous sulfide by oxygen, Environmental science & technology, 6 (1972) 529-537.

[25] S.E. Hoeft, J.S. Blum, J.F. Stolz, F.R. Tabita, B. Witte, G.M. King, J.M. Santini, R.S. Oremland, *Alkalilimnicola ehrlichii* sp. nov., a novel, arsenite-oxidizing haloalkaliphilic gammaproteobacterium capable of chemoautotrophic or heterotrophic growth with nitrate or oxygen as the electron acceptor, Int J Syst Evol Microbiol, 57 (2007) 504-512.

[26] D.Y. Sorokin, T.P. Tourova, O.L. Kovaleva, J.G. Kuenen, G. Muyzer, Aerobic carboxydotrophy under extremely haloalkaline conditions in *Alkalispirillum/Alkalilimnicola* strains isolated from soda lakes, Microbiology, 156 (2010) 819-827.

[27] D.Y. Sorokin, T.N. Zhilina, A.M. Lysenko, T.P. Tourova, E.M. Spiridonova, Metabolic versatility of haloalkaliphilic bacteria from soda lakes belonging to the *Alkalispirillum-Alkalilimnicola* group, Extremophiles, 10 (2006) 213-220.

[28] C. Griesbeck, G. Hauska, M. Schütz, Biological sulfide oxidation: sulfide-quinone reductase (SQR), the primary reaction, Recent research developments in microbiology, 4 (2000) 179-203.

[29] E. Cuevasanta, A. Denicola, B. Alvarez, M.N. Moller, Solubility and permeation of hydrogen sulfide in lipid membranes, PLoS One, 7 (2012) e34562.

[30] J.C. Mathai, A. Missner, P. Kugler, S.M. Saparov, M.L. Zeidel, J.K. Lee, P. Pohl, No facilitator required for membrane transport of hydrogen sulfide, Proc Natl Acad Sci U S A, 106 (2009) 16633-16638.

[31] M. Marcia, J.D. Langer, D. Parcej, V. Vogel, G. Peng, H. Michel, Characterizing a monotopic membrane enzyme. Biochemical, enzymatic and crystallization studies on *Aquifex aeolicus* sulfide:quinone oxidoreductase, Biochim Biophys Acta, 1798 (2010) 2114-2123.

CHAPTER 3

Effect of process conditions on the performance of a dual-reactor biodesulfurization process

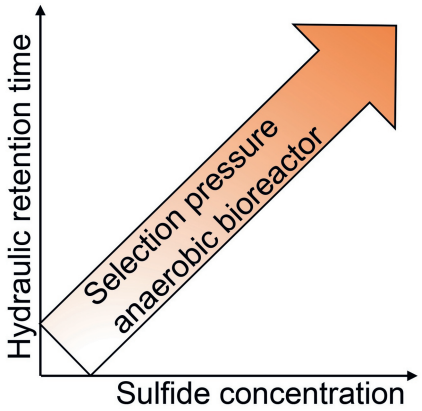

Abstract – The biotechnological gas desulfurization process under haloalkaline conditions is widely applied for removal of toxic H_2S from sour gas streams. Recently, the process has been extended with an anaerobic process step (dual-reactor line-up), increasing the selectivity for elemental sulfur (S_8) from ~85% to 97% and decreasing the formation of (thio)sulfate. It was also found that biological sulfide uptake took place in the anaerobic bioreactor. In order to apply this process in industry, more insight is needed of the effect of the process conditions on the process performance. The effect of the process conditions HRT and sulfide concentration in the anaerobic bioreactor and pH on the overall product selectivities and on biological sulfide uptake in the anaerobic bioreactor were investigated. 7 experiments were performed in a pilot-scale biodesulfurization set-up. In all experiments, high selectivities (>95%) for S_8 formation were obtained, except when the pH was increased from 8.5 to 9.1 (selectivity of 88%). Furthermore, a higher sulfide uptake in the anaerobic bioreactor was observed with increasing sulfide concentration and at higher pH. We hypothesize the biological sulfide uptake under anaerobic conditions is related to polysulfide. Our results increase the understanding how to control biological sulfide conversion in the dual-reactor biodesulfurization process.

Rieks de Rink, Suyash Gupta, Flavia Piccioli de Carolis, Dandan Liu, Annemiek ter Heijne, Johannes B.M. Klok, Cees J.N. Buisman. Effect of process conditions on the performance of a dual-reactor biodesulfurization process (submitted)

3.1 INTRODUCTION

In the 1990s, a biological gas desulfurization process was developed for the removal and conversion of toxic hydrogen sulfide gas (H_2S) from biogas [1, 2]. In this process, 'sour' gas is counter-currently contacted with process solution in an absorber column, whereby H_2S is removed from the gas stream and absorbed into the process solution. For optimal and biocompatible removal of H_2S, the process solution is a haloalkaline (bi)carbonate solution. When absorbed, H_2S is converted into both soluble bisulfide (HS^-) and, due to the presence of elemental sulfur, into soluble polysulfide (S_x^{2-}). This 'sulfide rich' solution from the absorber is directed to an aerated bioreactor where the dissolved sulfide (i.e. HS^- and S_x^{2-}) are oxidized by haloalkaliphilic sulfide oxidizing bacteria (SOB) into predominantly elemental sulfur (S_8). S_8 is harvested from the process solution by gravity settling and/or centrifugation and can be used for e.g. agricultural purposes [3, 4]. Nowadays, the technology is applied globally for desulfurization of various types of sour gas streams, such as natural gas and several refinery gases [5, 6].

In general, about 10-20% of the incoming H_2S is oxidized into the byproducts sulfate (SO_4^{2-}) and thiosulfate ($S_2O_3^{2-}$) [7, 8]. SO_4^{2-} formation occurs biologically when too much O_2 is supplied. In addition, $S_2O_3^{2-}$ is formed due to a chemical reaction between sulfide and O_2. Therefore, levels of O_2 and H_2S are minimized in the aerated bioreactor. The formation of the afore mentioned side products is unwanted as its formation i) requires NaOH addition to compensate proton formation, ii) requires removal via a bleed stream to maintain salinity levels, iii) decreases the recovery of elemental sulfur, and iv) requires more O_2 and therefore more energy [9]. Thus, lowering the side product formation will decrease the operational costs and carbon footprint of the process.

Recently, the process has been extended with an anaerobic bioreactor, placed in between the absorber and aerated bioreactor (dual reactor line-up) [9]. With the incorporation of this anaerobic bioreactor, a selectivity for S_8 of 97% was achieved. Selectivities for SO_4^{2-} and $S_2O_3^{2-}$ were 2% and 1% respectively. The sulfidic conditions in the anaerobic reactor suppressed biological SO_4^{2-} formation, because sulfide reversibly blocks enzymes in the pathway for SO_4^{2-} formation [9]. In addition, a change in the microbial community was observed. It was hypothesized that the adopted population had a lower tendency for SO_4^{2-} formation as it was suggested that the bacteria that became dominant (*Alkalilimnicola*) were unable to form SO_4^{2-}, i.e. could only oxidize sulfide to S_8 [10, 11]. Furthermore, it was found that the measured sulfide concentration in the anaerobic bioreactor was lower than the sulfide concentration as calculated based on the mass balance of H_2S and liquid

circulation flow rate. This indicates sulfide was biologically removed from solution in the anaerobic bioreactor. Since a lower sulfide concentration in the rich solution leads to lower chemical formation rates of $S_2O_3^{2-}$, sulfide uptake in the anaerobic bioreactor also contributed to the increased selectivity for S_8 formation.

In the previous study by de Rink et al., [9] the performance of the dual reactor process was assessed at fixed process conditions. Therefore, it is unknown how different process conditions affect the process performance of the dual reactor desulfurization process. In full scale application, several process factors, such as the sulfide concentration in the rich solution and the pH of the process solution, are dependent by the specification of the gas stream that needs to be treated. Furthermore, the hydraulic retention time (HRT) in the anaerobic bioreactor is determined by its designed size.

The aim of this study is to investigate the effect of the process factors sulfide concentration and HRT in the anaerobic bioreactor and pH on product formation and biological sulfide uptake. We hypothesize that a higher sulfide concentration and a longer retention time in the anaerobic bioreactor increase the inhibitory effect on SO_4^{2-} formation. Furthermore, we want to gain better understanding of biological sulfide uptake in the anaerobic bioreactor, since this may influence the selectivity as well. To investigate the effect of the sulfide concentration and HRT in the anaerobic bioreactor and the pH, we operated a pilot-scale dual-reactor biodesulfurization installation under different conditions, i.e. varying the gas flow rates of H_2S and CO_2, liquid circulation rate and volume in the anaerobic reactor. We analyzed product selectivity of the process and sulfide uptake in the anaerobic bioreactor as the main process performance parameters.

3.2 MATERIALS AND METHODS

3.2.1 EXPERIMENTAL SET-UP

Experiments were performed in a pilot-scale biodesulfurization installation, consisting of an absorber column, anaerobic bioreactor and aerated bioreactor, as described elsewhere [9]. The details of the experimental set-up can be found in the Supporting Information (SI 2.1).

3.2.2 EXPERIMENTAL OPERATION

To study the effect of the sulfide concentration and HRT in the anaerobic bioreactor and pH, 7 experiments were performed in which the conditions were varied (see Table 3.1). The

operational conditions were set by varying the H_2S flow rate (i.e. the S-load), the CO_2 flow rate (this determines the pH), the solution circulation flow rate (flow from aerated bioreactor to absorber to anaerobic bioreactor to aerated bioreactor) and the volume of the anaerobic bioreactor (this determines the HRT). A large stock of inoculum was prepared by mixing effluent from a full-scale desulfurization installation treating amine acid gas [12] and effluent from previous experiments in the same installation [9] in ratio of approximately 1:1. The inoculum was stored at 4 °C, and each experiment was started with the inoculum from this inoculum stock. For each experiment, the system was filled with a 50/50 mixture of a 0.8M $NaHCO_3$ solution and inoculum.

After filling the system, the flow of N_2 (100 NL h^{-1}, i.e. 100 L h^{-1} under standard pressure and temperature) and CO_2 was started to pressurize the absorber to 3 bar(g). Then the solution circulation was started, see Table 3.1 for the circulation flow rates in each experiment. When the temperature had increased to 37 °C, the flow of H_2S was initiated. When the ORP in the aerated bioreactor reached -370 mV, the air flow was started in manual mode. After the ORP stabilized, the air flow was controlled at -370 mV automatically by a PI controller. At the same time, the caustic and nutrient dosing were started. The caustic was a 5% (w/w) NaOH solution and was dosed to maintain the alkalinity of the process solution, which is lost due to formation of SO_4^{2-} and $S_2O_3^{2-}$ and via the bleed. The nutrients are required for growth/maintenance of the bacteria. Nutrients solution consisted of macro nutrient as described by de Rink et al. [9] and 1 mL L^{-1} trace element mix as described by Pfennig and Lippert [13]. The nutrient dosing rate was set in such way that the total residual nitrogen concentration in the supernatant was <15 mg-N L^{-1}. In this way, overdosing of nutrients is prevented and the bacteria consume all nutrients. The decanter was started after several days of operation to remove elemental sulfur from the process solution in order to maintain the TSS around 5 g L^{-1}.

Each experiment was performed for at least 1 system HRT, which was typically around 30 days. The system HRT is calculated as the total system volume divided by the bleed flow. Experiment 5 was performed for 2.9 HRT. Experiment 7 was performed for 4.1 system HRT. In this experiment, the highest S-load (170 g day^{-1}) was applied and therefore required a longer startup time in order to grow enough bacteria to handle the high amount of sulfide.

3.2.3 ANALYSES

All analyses were performed on samples of the aerobic bioreactor, which were taken every weekday. Samples to analyze the sulfide concentration were taken 2-3 times per week from the anaerobic bioreactor. The alkalinity and concentrations of SO_4^{2-}, $S_2O_3^{2-}$, S_8 and bacteria were assumed homogenous throughout all process sections, due to the solution circulation through the process sections (absorber, anaerobic- and aerated bioreactor) [9]. pH and conductivity were analyzed offline using a HQ440d multi analyzer (Hach, Germany). Alkalinity, expressed as the concentration HCO_3^-, was measured with an automated TitrinoPlus titrator (Metrohm) by titrating to pH 4.3 using a 0.1M HCl solution. SO_4^{2-} and $S_2O_3^{2-}$ concentrations were determined on the samples supernatant (after centrifuging for 10 min at 14000 g) using a Dionex ICS-2100 Ion Chromatograph (ThermoScientific) with a Thermo Fisher Scientific IonPac AG17 Guard (Thermo Fisher Scientific, Waltham, MA, USA) and Thermo Fisher Scientific IonPac AS17 column (Thermo Fisher Scientific) at 30 °C. The eluent was KOH at a flowrate of 1.0 mL min^{-1}. The sample injection volume was 10 µl. The biomass concentration was measured as the amount of total nitrogen based on the absorbance of nitrophenol, using the Dr. Lange cuvette test LCK138 (Hach Lange, Germany), as described by de Rink et al. [9]. The difference between the supernatant (i.e., a sample centrifuged for 10 min at 14000 g) and a non-centrifuged sample indicated the total amount of N present in the (suspended) biomass. To exclude interference by salts and biologically produced S_8, the samples were diluted at least 5 times. N accounts for approximately 10% of the dry weight biomass [14].

To determine the sulfide uptake in the anaerobic bioreactor, the total sulfide concentration (S_{tot}^{2-}), which is the sum of S^{2-}, HS^- and polysulfide-sulfane (S_x^{2-}), was measured in a sample of the anaerobic reactor by titration with a solution of 0.1 M $AgNO_3$, using a Titrino Plus Titrator (Metrohm, Switzerland). Before titration, the sample was filtered over a 0.45 µm cellulose acetate membrane filter to remove S_8 and bacteria. The filtered sample was added to 80 mL 4% (w/v) NaOH, with 1 mL of 30% (w/v) NH_4OH to stabilize S_{tot}^{2-}.

The microbial community of the inoculum and the process solution at the end of each experiment (taken from the aerated bioreactor) was analyzed using 16S rRNA gene based amplicon sequencing. Details of the analysis can be found in the Supporting Information (SI 2.2). The EMBL-EBI accession number for the presented 16S rRNA sequencing set is PRJEB44162.

3.2.4 CALCULATIONS

As the formed S_8 particles tend to attach to the reactor wall, it was not possible to calculate the S_8 production rate from the analyses. As no products other than S_8, SO_4^{2-} and $S_2O_3^{2-}$ were measured in the reactor [8], the production rate of S_8 was calculated from the mass balance as shown in equation 3.1:

$$P_{S_8-S} = I_{H_2S} - P_{SO_4{}^{2-}-S} - P_{S_2O_3{}^{2-}-S} \quad \text{(Equation 3.1)}$$

Here, P_{S_8-S}, $P_{SO_4{}^{2-}-S}$ and $P_{S_2O_3{}^{2-}-S}$ are the production rates of S_8, SO_4^{2-}, and $S_2O_3^{2-}$, respectively, in mol-S day^{-1} and I_{H_2S} is the volumetric H_2S influent in mol day^{-1}. The production rates of both SO_4^{2-}-S (equation 3.2) and $S_2O_3^{2-}$-S (equation 3.3) were calculated as follows:

$$P_{SO_4{}^{2-}-S} = \frac{effluent \cdot \overline{[SO_4{}^{2-}-S]} + V \cdot \Delta[SO_4{}^{2-}-S]}{\Delta t} \quad \text{(Equation 3.2)}$$

$$P_{S_2O_3{}^{2-}-S} = \frac{effluent \cdot \overline{[S_2O_3{}^{2-}-S]} + V \cdot \Delta[S_2O_3{}^{2-}-S]}{\Delta t} \quad \text{(Equation 3.3)}$$

Here, *effluent* is the total effluent of the system (L) in time interval Δt (days) (i.e. sample volumes and bleed), $\overline{[SO_4{}^{2-}-S]}$ and $\overline{[S_2O_3{}^{2-}-S]}$ the average concentration (mol-S L^{-1}) over time interval Δt, V the total liquid volume of the system and $[SO_4{}^{2-}-S]$ and $[S_2O_3{}^{2-}-S]$ the concentration changes (mol-S L^{-1}) over time interval Δt.

The selectivities were calculated according to equations 3.4, 3.5 and 3.6:

$$S_{SO_4{}^{2-}} = \frac{P_{SO_4{}^{2-}-S}}{I_{H_2S}} \quad \text{(Equation 3.4)}$$

$$S_{S_2O_3{}^{2-}} = \frac{P_{S_2O_3{}^{2-}-S}}{I_{H_2S}} \quad \text{(Equation 3.5)}$$

$$S_{S_8} = 1 - \frac{P_{SO_4{}^{2-}-S} - P_{S_2O_3{}^{2-}-S}}{I_{H_2S}} \quad \text{(Equation 3.6)}$$

Since these values are calculated from the measured concentrations of SO_4^{2-} and $S_2O_3^{2-}$ and the measured bleed rate, there is some scatter on the daily data points. Therefore, the results also show the moving average (average over 5 consecutive days).

The specific sulfide uptake efficiency in the anaerobic bioreactor was calculated based on the H_2S load, the liquid flows and the measured sulfide concentration, according to Equation 3.7.

$$sulfide\ uptake\ anaerobic\ bioreactor = \frac{H_2S\ load}{solution\ flow} - measured\ [S_{tot}^{2-}] \quad \text{(Equation 3.7)}$$

The specific sulfide uptake is calculated by dividing the sulfide uptake by the biomass concentration. Since the biomass concentration was measured as the total organic N [8, 9], the specific sulfide uptake is expressed as mg-S mg-N^{-1}.

3.3 Results and discussion

3.3.1 Representative experiment

The performance of the dual-reactor desulfurization process in a representative experimental run (experiment 2) is shown in Figure 3.1. Figure 3.1A shows the measured concentrations of SO_4^{2-}-S, $S_2O_3^{2-}$-S, alkalinity and conductivity of the process solution. At start-up (day 0), the concentration of SO_4^{2-}-S was 0.10 M, $S_2O_3^{2-}$-S was 0.01 M, alkalinity was 0.65 M and the conductivity was 45.3 mS cm^{-1}. Throughout the experiment, the conductivity, which is a measure for the salinity, was constant (49.1 ± 1.5 mS cm^{-1} on average). The measured SO_4^{2-} and $S_2O_3^{2-}$ concentrations changed based on their net rate of formation and the bleed rate. The SO_4^{2-}-S concentration increased from 0.10 M to 0.17 M during the experiment. This means that, overall, the formation rate of SO_4^{2-} was higher than its removal rate via the bleed stream. The $S_2O_3^{2-}$-S concentration initially increased and reached its highest value at day 13 (0.03 M). This means that, until day 13, the formation rate of $S_2O_3^{2-}$ was higher than its removal rate via the bleed stream. After day 13, the concentration started to decrease, reaching 0 (i.e. below the detection limit of 0.2 mM) at day 22 and remained 0 until the end of the experiment (day 29). The alkalinity of the process solution decreases because of the formation of SO_4^{2-} and $S_2O_3^{2-}$ (both resulting in proton production) and loss via the bleed. Alkalinity was controlled by the caustic dosing rate, as caustic addition increases the alkalinity. During the experiment, the caustic dosing rate was adjusted in order the maintain the alkalinity as constant as possible. During the experiment, the alkalinity decreased from 0.65 M to 0.48 M and was 0.58 ± 0.05 M on average.

Figure 3.1B shows the product selectivities (daily values and 5-day moving average). In the initial 7 days of operation, the average selectivity for S_8 formation was 97.6 ± 7.1% and selectivities for SO_4^{2-} and $S_2O_3^{2-}$ were 0.7 ± 6.2 and 1.7 ± 2.1%. During the experiment, the selectivity for S_8 formation decreased gradually and was 91.5 ± 4.3% and the end of the experiment (day 29). This was mainly the result from an increase in the selectivity for SO_4^{2-} during the experiment, to 8.5 ± 4.3% (average of the last 5 days). The selectivity for $S_2O_3^{2-}$ formation (moving average) was around 2% up to day 13, then started to decrease, and from day 20 onwards, the moving average was <0%. This means that the formation rate of $S_2O_3^{2-}$ was lower than the conversion rate of $S_2O_3^{2-}$. The $S_2O_3^{2-}$-S concentration from day 25 onwards was 0 (i.e. below the detection limit of 0.2mM), meaning that all $S_2O_3^{2-}$ which was formed, was converted. $S_2O_3^{2-}$ can be used by SOB as substrate [15, 16].

Figure 3.1C shows the concentration of biomass-N in the process solution and the sulfide uptake in the anaerobic bioreactor, which is the difference between the calculated sulfide concentration and the measured concentration. The initial biomass concentration was 32 mg-N L^{-1} and, due to growth of the bacteria, increased to 62 mg-N L^{-1} at the end of the experiment. The biomass concentration depends on the nutrient dosing rate, biomass growth rate and the removal of biomass via the bleed stream and sulfur cake. The increase in biomass concentration during the experiment indicates the growth rate of the bacteria was higher than removal via bleed and sulfur cake. The sulfide concentration in the rich solution (i.e. the solution in the anaerobic bioreactor) in case no biological removal would take place, was 220 mg-S L^{-1}, which is calculated based on the mass balance of the H_2S dosing rate and the liquid circulation flow rate. The measurement of the sulfide concentration in the anaerobic bioreactor, however, showed that the actual sulfide concentration was lower than calculated, due to the sulfide uptake by bacteria [9, 17, 18]. On the 2nd day of operation, the measured sulfide concentration was 158 mg-S L^{-1}, i.e. the sulfide uptake was 62 mg-S L^{-1}. On day 20, the sulfide uptake had increased to 98 mg-S L^{-1}. In this period, the increase in sulfide uptake was proportional to the increase in biomass concentration, and the specific uptake was 1.5 – 2.0 mg-S mg-N^{-1}. From day 20 to 39, the sulfide uptake decreased, although biomass concentration further increased, and on day 29, the specific uptake was 1.1 mg-S mg-N^{-1}. The average sulfide uptake during the whole experiment was 75.5 ± 13.5 mg-S L^{-1} and the average specific uptake was 1.86 ± 0.52 mg-S mg-N^{-1}.

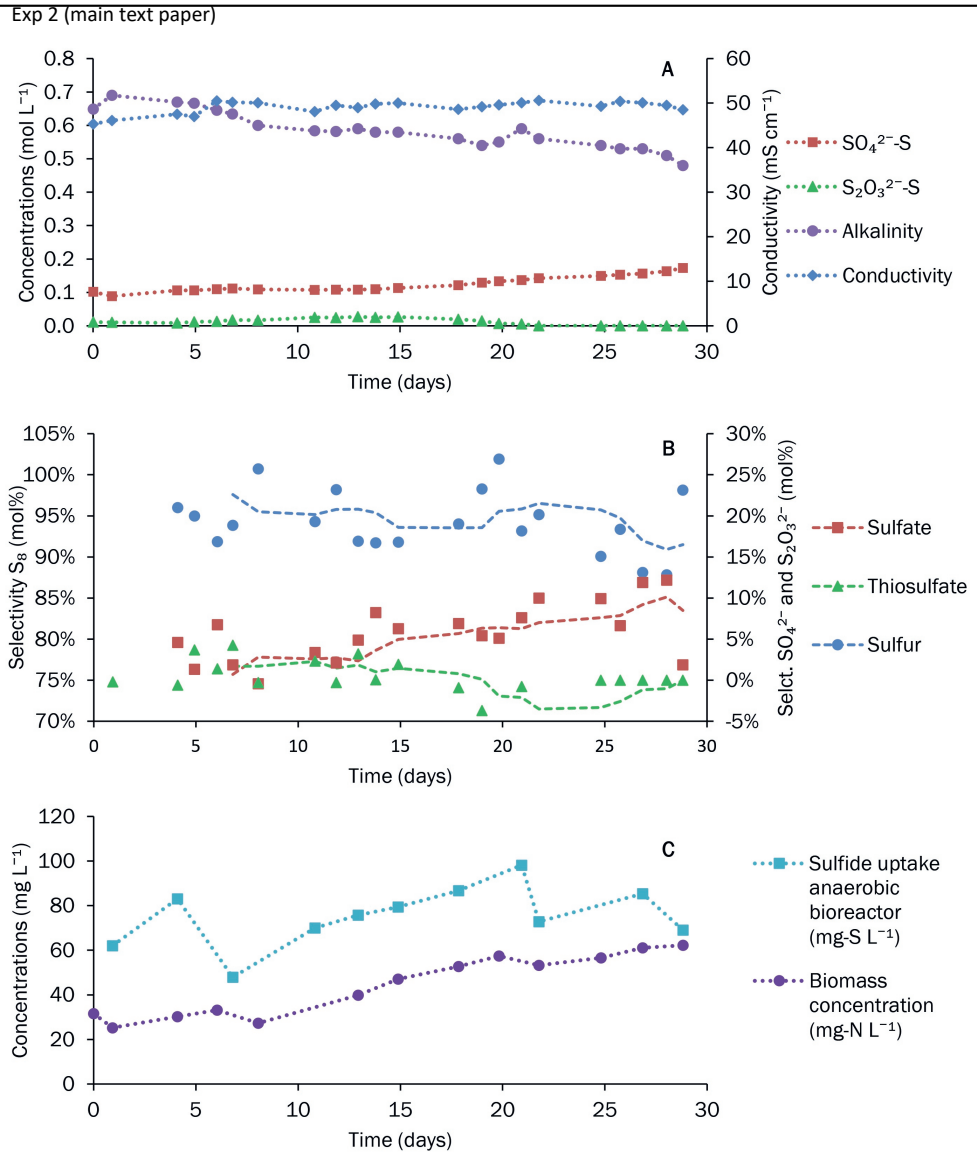

Figure 3.1: Experimental results of experiment 2. Figure A shows the concentrations of the SO_4^{2-}, $S_2O_3^{2-}$, the alkalinity and the conductivity. Figure B shows the calculated product selectivities. The dots are the daily measurements, and the dashed line indicates the moving average (average value of 5 consecutive measurements). Figure C shows the biomass concentration in the process solution and the sulfide uptake by the bacteria in the anaerobic bioreactor.

3.3.2 EFFECT OF PROCESS CONDITIONS

To study the effect of the conditions in the anaerobic reactor on the process performance, 7 long-term experiments were performed in which the conditions of the anaerobic bioreactor (i.e. HRT and sulfide concentration) were varied. Furthermore, the effect of pH was investigated. An overview of the experimental settings, conditions and results is provided in Table 3.1. Graphs with results of all experimental runs can be found in the Supporting Information (SI 2.3).

In none of the experiments, free sulfide was detected in the aerated bioreactor (except during process upsets), meaning that during normal operation all sulfide was converted. Based on the volume of the aerated bioreactor, the sulfide conversion rates were 5.7 g L^{-1} day^{-1} for experiments 1-3, 10.5 g L^{-1} day^{-1} for experiments 4-6 and 14.9 g L^{-1} day^{-1} for experiment 7. To the best of our knowledge, 14.9 g L^{-1} day^{-1} is the highest sulfide conversion rate described in literature.

Statistical analysis with the One-way ANOVA test showed that the pH had a significant effect on the selectivity for S_8 formation (p-value <0.01) in our experiments. Experiments 5 and 6 had the same sulfide concentration and HRT in anaerobic bioreactor (0.48 g L^{-1} and 20 min), but the pH in the aerated bioreactor in experiment 5 was 8.5 and in experiment 6 9.1. The selectivity for S_8 formation decreases from 94.6 ± 3.5% in experiment 5 to 88.4 ± 6.3% in experiment 6. The decreased selectivity for S_8 formation in experiment 6 was the result of a higher selectivity for SO_4^{2-} formation: 4.7 ± 3.2% in experiment 5 and 12.1 ± 6.3% in experiment 6. The selectivities for $S_2O_3^{2-}$ formation were similar (0.8 ± 2.1% in experiment 5 and -0.5 ± 4.7% in experiment 6). Previous research in a system without anaerobic bioreactor showed that the selectivity for S_8 formation decreased at higher pH and that $S_2O_3^{2-}$ formation increased at higher pH [19]. Based on our experiment it can be concluded that also in the dual reactor line-up, increasing pH results in lower selectivity for S_8.

Table 3.1: Overview of experimental settings and results. Each experiment was started with the same inoculum, except for experiment 6, which was a continuation of experiment 5.

	Exp 1	Exp 2	Exp 3	Exp 4	Exp 5	Exp 6	Exp 7
S-load (g-S day^{-1})	65	65	65	120	120	120	170
CO_2 flow rate (NL h^{-1})	50	50	50	50	50	5	50
Circulation flow rate (L h^{-1})	12.4	12.4	12.4	10.5	10.5	10.5	8.4
Volume anaerobic reactor (L)	2.2	4.3	6.0	1.7	3.5	3.5	1.5
Theoretical sulfide concentration anaerobic reactor (g L^{-1})	0.22	0.22	0.22	0.48	0.48	0.48	0.85
HRT anaerobic reactor (min)	10	20	30	10	20	20	10
Duration (days)	30	29	31	28	43	17	47
Number of system HRTs	1.5	1.0	1.4	1.5	2.9	1.2	4.1
pH anaerobic reactor (-)	7.6 ± 0.1	7.7 ± 0.1	7.7 ± 0.1	7.7 ± 0.2	7.5 ± 0.1	8.8 ± 0.3	7.8 ± 0.1
Average ORP anaerobic reactor (mV)	-420 ± 3	-423 ± 3	-421 ± 2	-428 ± 4	-431 ± 4	-463 ± 5	-441 ± 7
Average pH aerated reactor (-)	8.4 ± 0.1	8.4 ± 0.1	8.4 ± 0.1	8.5 ± 0.1	8.5 ± 0.1	9.1 ± 0.2	8.7 ± 0.2
Average conductivity (mS cm^{-1})	51.8 ± 3.7	49.1 ± 1.5	61.1 ± 2.1	49.0 ± 2.3	51.0 ± 3.2	60.0 ± 2.7	48.5 ± 3.9
Average alkalinity (M)	0.55 ± 0.10	0.58 ± 0.06	0.67 ± 0.06	0.58 ± 0.08	0.63 ± 0.04	0.48 ± 0.06	0.61 ± 0.11
Average biomass concentration (start – end concentration) (mg-N L^{-1})	45 (20 – 89)	44 (32 – 62)	43 (26 – 74)	51 (24 – 82)	48 (29 – 57)	74 (57 – 104)	62 (22 – 114)
Sulfide conversion rate aerated bioreactor (g L^{-1} day^{-1})	5.7	5.7	5.7	10.5	10.5	10.5	14.9
Average selectivity S_8 (%)	91.5 ± 8.4	95.1 ± 5.2	94.2 ± 4.5	96.5 ± 6.6	94.6 ± 3.5	88.4 ± 6.3	94.9 ± 3.5
Average selectivity SO_4^{2-} (%)	7.5 ± 9.3	5.0 ± 5.0	5.6 ± 5.5	3.0 ± 3.4	4.7 ± 3.2	12.1 ± 9.0	3.9 ± 3.2
Average selectivity $S_2O_3^{2-}$ (%)	1.1 ± 3.6	-0.1 ± 5.0	0.2 ± 2.7	0.5 ± 6.5	0.8 ± 2.1	-0.5 ± 4.7	1.2 ± 1.4
Absolute sulfide uptake (mg L^{-1})	54 ± 18	76 ± 14	57 ± 12	113 ± 36	60 ± 43	237 ± 9	377 ± 6
Specific sulfide uptake (mg- S mg-N^{-1})	1.18 ± 0.51	1.86 ± 0.52	1.37 ± 0.55	2.27 ± 0.69	1.25 ± 1.07	4.11 ± 0.46	3.99 ± 0.82

To assess the effect of sulfide concentration and HRT in the anaerobic bioreactor, experiments 1-5 and 7 were compared. The original hypothesis was that a higher sulfide concentration and a higher HRT in the anaerobic bioreactor increase the inhibition of SO_4^{2-} formation and thus lead to a higher selectivity for S_8 formation. Significant differences were found between experiment 1 and 4 (p-value of 0.043) and experiments 1 and 7 (p-value 0.048). In experiments 1, 4 and 7, the HRT in the anaerobic bioreactor was 10 min and sulfide concentrations were 0.22, 0.48 and 0.85 g L^{-1} respectively. In experiment 1, the average selectivity for S_8 formation was 91.5 ± 8.4%. In experiment 4 and 7, selectivities for S_8 formation of 96.5 ± 6.6% and 94.9 ± 3.5% were obtained. This means that with an HRT of 10 min, the selectivity for S_8 was lower at a sulfide concentration of 0.22 g L^{-1} compared to sulfide concentrations of 0.48 and 0.85 g L^{-1}.

Except for experiments 1 and 6, in all experiments, a very high selectivity for S_8 was achieved (>94%). To achieve a selectivity for S_8 formation >94% in the dual reactor line-up, a certain combination of sulfide concentration and HRT in the anaerobic bioreactor should be met. When the sulfide concentration in the rich solution is 0.22 g L^{-1}, the HRT in the anaerobic reactor should be at least 20 min. When the sulfide concentration is 0.48 g L^{-1} or higher, an HRT of 10 min in the anaerobic bioreactor is sufficient. The highest average selectivity for S_8 formation was achieved in experiment 4 (96.5 ± 6.6%). In a previous study in the same set-up, a selectivity for S_8 formation of 96.9 ± 2.4% was achieved (average over the last 5 days of the experimental run) [9]. In this experiment, the sulfide concentration and HRT in the anaerobic bioreactor were 0.45 g L^{-1} and 20 minutes, and the pH in the aerated bioreactor was 8.3, i.e., the conditions were most similar to experiment 5 in this study.

The most dominant by-product in all experiments, was SO_4^{2-}, with selectivities ranging from 3.0 ± 3.4% in experiment 4, to 12.1 ± 9.0% in experiment 6. The highest average selectivity for $S_2O_3^{2-}$ formation was observed in experiment 7, which had the highest sulfide loading rate (1.2 ± 1.4%). The lowest average selectivity for $S_2O_3^{2-}$ formation was observed in experiment 6 (the experiment with higher pH): -0.5 ± 4.7%. The average selectivities for $S_2O_3^{2-}$ formation for all experiments were lower than the average selectivities for SO_4^{2-} formation, meaning that SO_4^{2-} was the main by-product. For experiments 2 and 6, the average selectivity for $S_2O_3^{2-}$ formation was <0%. As it is known that at least some $S_2O_3^{2-}$ is being produced, and the formation rate increases at higher pH [19], we conclude that

the biological oxidation of $S_2O_3^{2-}$ to SO_4^{2-} plays an important role in the process. This should be further confirmed by biological respiration tests.

The rates of the biological reactions in the biological gas desulfurization process (i.e. formation of S_8 and SO_4^{2-}) are dependent on the O_2/H_2S supply ratio [7, 8, 19, 20]. At higher O_2/H_2S supply ratios, the selectivity for SO_4^{2-} will increase, whereas selectivity for S_8 formation will increase at lower O_2/H_2S supply ratios. In our set-up, the redox potential, which is a measure for the O_2/H_2S supply ratio [8, 21, 22], was used to control the air flow to the aerated bioreactor. The O_2/H_2S ratio itself was not measured here. In all experiments, the ORP in the aerated bioreactor was controlled at -370mV by automatic adjustment of the airflow rate, except for a small period in experiment 7, where it was controlled at -380mV. -370mV was found to be a convenient ORP [9], meaning that high selectivity for S_8 was achieved with stable operation (i.e. no sulfide in the bulk of the solution in the aerated bioreactor). In case the ORP is too high (i.e. more O_2 dosed), more SO_4^{2-} is formed; in case ORP is too low, sulfide may accumulate, leading to process failure [8]. Furthermore, previous studies found that limitations in the biological activity (e.g. by addition of toxic organo-sulfur compounds), selectivity for $S_2O_3^{2-}$ formation increases whilst selectivity of SO_4^{2-} decreases [15, 23]. Potentially, higher selectivities for S_8 formation (i.e. lower selectivities for SO_4^{2-} formation) could have been achieved with a lower ORP set-point and lower biomass concentrations [23], although the drawback is that this will result in a less stable process.

The average pH value's, conductivity, alkalinity and redox potential in the anaerobic reactor are shown in Table 3.1 as well. The average conductivity (a measure for total salinity) and alkalinity (buffer capacity) values in all experiments were in the range of 48-61 mS cm^{-1} and 0.48-0.67 M. In addition, the average pH in the aerated bioreactor in experiments 1-3, all with an S-load of 65 g day^{-1}, was 8.4. The pH in the biological desulfurization process is mainly determined by the absorption of CO_2 in the absorber and the stripping of CO_2 in the aerated bioreactor. Due to the high buffer capacity (alkalinity), fluctuations in pH were limited. In experiments 4 and 5, the pH was 8.5. Since the S-load in these experiments was higher (120 g day^{-1}), more air was required for the conversion of sulfide. Hence, more CO_2 is stripped, leading to a slightly higher pH. In experiment 7, the pH was 8.7 because the S-load was 170 g day^{-1}. The average pH values of the rich solution, measured in the anaerobic bioreactor, were 7.6 – 7.8. In experiment 6, however, the pH values in both aerated and anaerobic bioreactor were 9.1 and 8.8 respectively due to the lower partial pressure CO_2

in the feed gas. In the anaerobic reactor, the ORP is mainly dependent on the sulfide concentration, with more negative ORP at higher sulfide concentrations. For experiments 1-3 (theoretical sulfide concentration of 0.22 g L^{-1}), the average ORP was -420 to -423mV. In experiments 4 and 5 (0.48 g L^{-1} sulfide), the average ORP was -429 to -431mV and in experiment 7 (0.85 g L^{-1} sulfide) -437 mV. In experiment 6 (0.48 g L^{-1} sulfide) and a higher pH, the ORP in the anaerobic reactor was -463 mV.

3.3.3 Microbial community analysis

Microbial community analysis based on 16S rRNA gene sequencing shows various known and potential sulfur-oxidizing bacteria (SOB) from the class *Gammaproteobacteria*, such as *Alkalilimnicola*, *Thioalkalivibrio*, *Thioalkalimicrobium* and *Thioalkalispirila* (Figure 3.2). Members of the genera *Alkalilimnicola* (relative abundance of 13 to 67%) and *Thioalkalivibrio* (7 to 27%) were in particular highly abundant in all experimental runs.

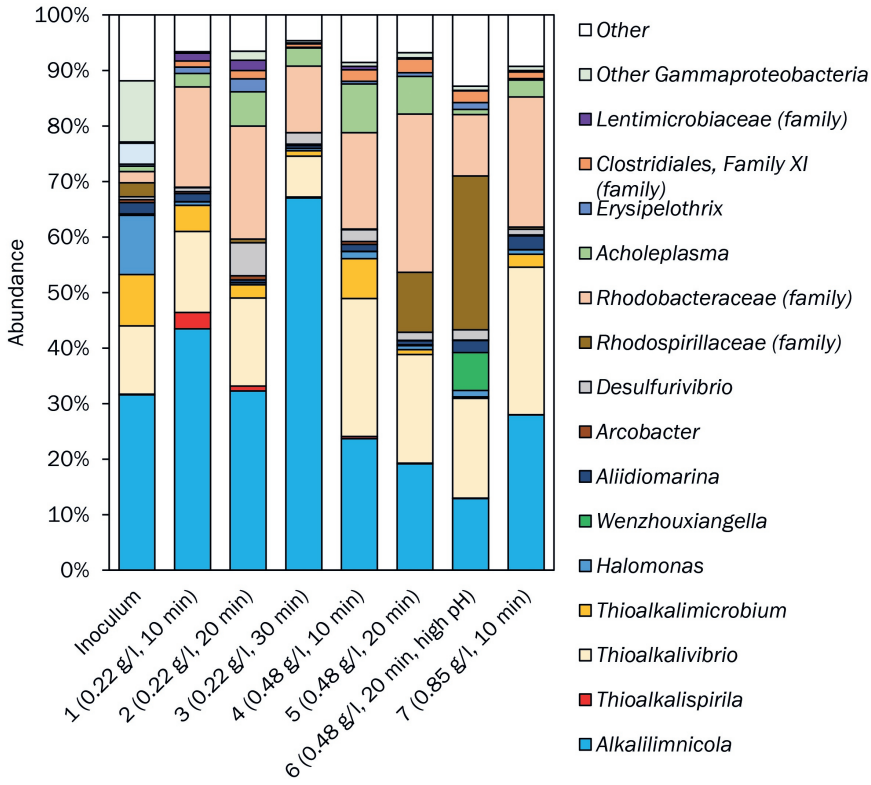

Figure 3.2: Taxa bar plot showing the relative abundances of microbial taxa in the aerated bioreactor at the end of the experiments. All species (or families) with a relative abundance of at least 5% in one of the samples are shown.

These results are comparable to the results obtained in previous experiments in a set-up with an incorporated anaerobic bioreactor, in which *Thioalkalivibrio* appeared as the most abundant genus at the start of the reactor run and was outnumbered by *Alkalilimnicola* by the end of the experiment [9]. *Alkalilimnicola* can grow chemo-autotrophically under anaerobic conditions and therefore has an advantage over *Thioalkalivibrio* which can only grow aerobically [24, 25]. The highest relative abundance of *Alkalilimnicola* was observed in experiment 3 (67%), which had the highest HRT in the anaerobic bioreactor. In experiment 7, with the highest sulfide concentration (0.85 g L^{-1}) and low HRT (10 min), the relative abundances of *Alkalilimnicola* and *Thioalkalivibrio* were similar (around 27%), suggesting less competition between these two bacteria species due to availability of more substrate. The other SOB *Thioalkalimicrobium* and *Thioalkalispira* were less abundant (<10%) at the end of all the experiments. Apart from the above-mentioned SOB, members of family *Rhodobacteracea* were found to be highly abundant in all the experiments (11 to 29%), but not in the inoculum (2%). Known members of this family are *Roseinatronbacter* and *Rhodobaca*, which can oxidize sulfide during organotrophic growth [26-29]. Hence, the high relative abundance of members of the *Rhodobacteracea* can be explained by their anoxygenic growth. Another family member is *Stappia*, which has potential to oxidize $S_2O_3^{2-}$ to SO_4^{2-} and has been detected in sulfide removing bioreactors [30-32]. Both *Alkalilimnicola* and *Thioalkalivibrio* were less abundant at the end of experiments 5 and 6. Members of the family *Rhodospirillacaea* were abundant in these runs and were more relatively abundant at a high pH. The members of *Rhodospirillacaea*, *Rhodospira* and *Rhodopseudomonas sulfidophila* can actively oxidize sulfide at microaerophilic conditions, while using organic compounds as substrates [33, 34]. As no organic carbon is added in the system, the potential source of organic compounds could be the dead biomass. The abundance of proteolytic bacteria *Wenzhouxiangella* also indicates the presence of dead biomass**.** The lowest selectivity for S_8 formation in experiments 6 can therefore be associated with a decrease in the number of chemoautotrophs and increase in heterotrophic bacteria.

The microbial composition analysis showed the presence of both autotrophic and heterotrophic SOB. However, to better understand their role, it is essential to know which of them were potentially active. Additionally, to have more insights into the biological processes occurring in the system, it is relevant to understand if other process parameters could influence microbial community composition or vice versa.

3.3.4 BIOLOGICAL SULFIDE UPTAKE IN THE ANAEROBIC BIOREACTOR

To investigate the effect of the sulfide concentration in the anaerobic bioreactor on the specific sulfide uptake, experiments 1, 4 and 7 were compared. In all these experiments, the HRT in the anaerobic reactor was 10 min. The results are shown in Figure 3.3A. For experiments 1 and 4, the average specific uptake over the entire run is shown. For experiment 7, the average uptake for days 36-46 is shown, as in this period the sulfide concentration in the anaerobic reactor (i.e. S-load) was at the anticipated level. It was found that an increasing sulfide concentration resulted in a higher specific sulfide uptake.

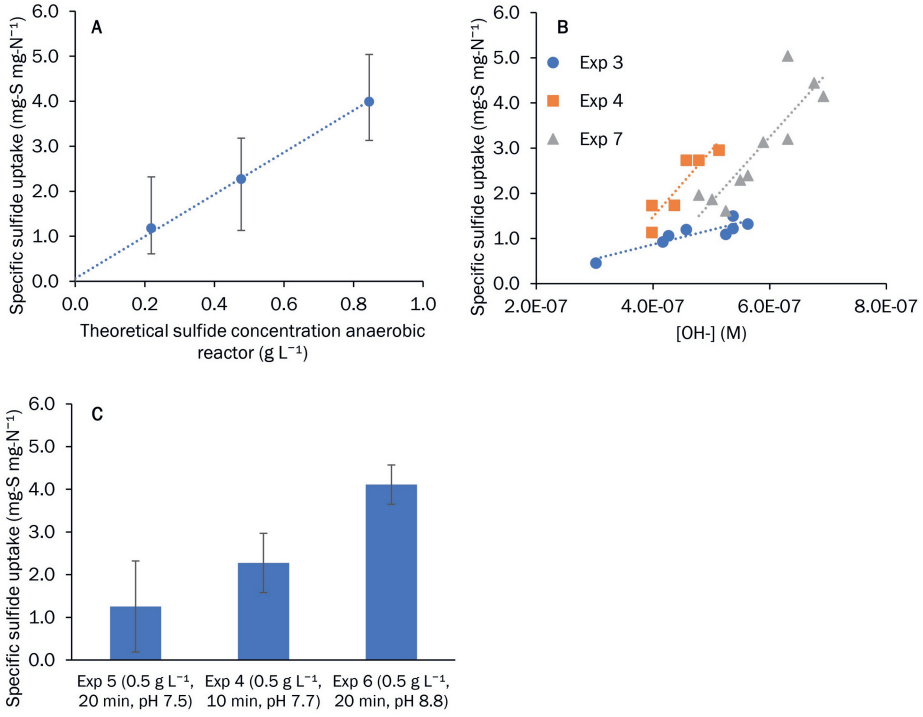

Figure 3.3: Effect of process conditions on the specific sulfide uptake in the anaerobic bioreactor. Figure A shows the effect of sulfide concentration in the anaerobic reactor. The specific sulfide uptake increases with sulfide concentration. Average values with the minimum and maximum measured values are shown. Figures B and C show the effect of pH on specific sulfide uptake. Figure B shows the daily measurements of specific sulfide uptake plotted against the calculated OH^- concentration for several experiments (3, 4 and 7). Figure C shows the average specific sulfide uptake for the experiments with a theoretical sulfide concentration in the anaerobic bioreactor of 0.48 g L^{-1}.

Secondly, it was noticed that small variations of the pH in the anaerobic bioreactor within a run had effect on the specific sulfide uptake. In Figure 3.3B the specific sulfide uptake in experiments 3, 4 and 7 is plotted against the calculated [OH^-]. This shows that pH and specific sulfide uptake are positively correlated. The specific sulfide uptake for experiments 4, 5 and 6 was also compared, see Figure 3.3C. In these experiments, the theoretical sulfide concentration in the anaerobic reactor was 0.48 g L^{-1}. It was found that the average specific sulfide uptake increased with increasing pH. In experiment 6, the experiment with increased pH, the highest specific sulfide uptake was found.

Our results show that more sulfide uptake from the process solution in the anaerobic bioreactor takes place when: i) the sulfide concentration is higher, and ii) the pH is higher. Whereas H_2S can freely pass the cell membrane [35-37], most ions require active transport [38]. At higher pH, more sulfide is present in the ionic form (i.e. as HS^-). The fact that H_2S can freely pass the cell membrane whilst HS^- probably requires active transport seems contradictory with the observation that more sulfide is removed from solution at higher pH. However, it is also known that at higher pH, more sulfide is present as polysulfides (S_x^{2-}), which is formed due to an equilibrium reaction between HS^- and elemental sulfur (S_8), see equation 3.8 [39, 40]. As S_8 is present in excess, the concentration of S_x^{2-} in the experiments increases with higher HS^- concentration (i.e. higher S-load) and at higher pH [41].

$$HS^- (aq) + \frac{x-1}{8} S_8 (s) \leftrightharpoons S_x^{2-} (aq) + H^+ (aq) \qquad \text{(Equation 3.8)}$$

The permeability of membranes for solutes depends on their partition coefficient, i.e. the ratio in solubility in the membranes and water [42], which suggests that S_x^{2-} is easier to transport than HS^-. Hence, we hypothesize that mainly S_x^{2-} is removed from solution in the anaerobic bioreactor. The method we have used measured the sum of all forms of sulfide (i.e. S^{2-}, HS^- and polysulfide-sulfane (S_x^{2-})). We haven't experimentally quantified the concentration of S_x^{2-} separate from the concentration of HS^-. Further experimental work dedicated on S_x^{2-} is required to confirm the role of S_x^{2-} in the observed biological sulfide removal in the anaerobic bioreactor.

Based on this observation we hypothesize the following sulfide conversion routes in the biodesulfurization process are taking place (see Figure 3.4). In the 'sulfidic zone', consisting of the absorber and anaerobic bioreactor, H_2S is initially chemically absorbed from the gas phase to the liquid phase. In the alkaline solution it is deprotonated into

bisulfide (HS^-). Due to the equilibrium reaction with elemental sulfur (see equation 3.8), polysulfide (S_x^{2-}) is formed. Based on our results, we hypothesize that S_x^{2-} is taken up by the bacteria. Part of it is stored in the cell ("bound-S_x^{2-}") and part is converted to S_8, e.g. by reducing electron carriers, which stores electrons ("e^--shuttling") [9, 17, 18]. This means that the bacteria are becoming reduced in the sulfidic zone. In the 'microaerophilic zone', i.e. the aerated bioreactor, dissolved O_2 from the compressed air is used as final electron acceptor. In this zone the bacteria are transferred into the oxidized form. Since there is no free sulfide in the effluent of the aerated bioreactor, all residual sulfide is converted. The suppression of enzymes in the pathway for SO_4^{2-} formation, by sulfide in the sulfidic zone, results in an increased overall system performance in terms of selectivity for S_8 formation.

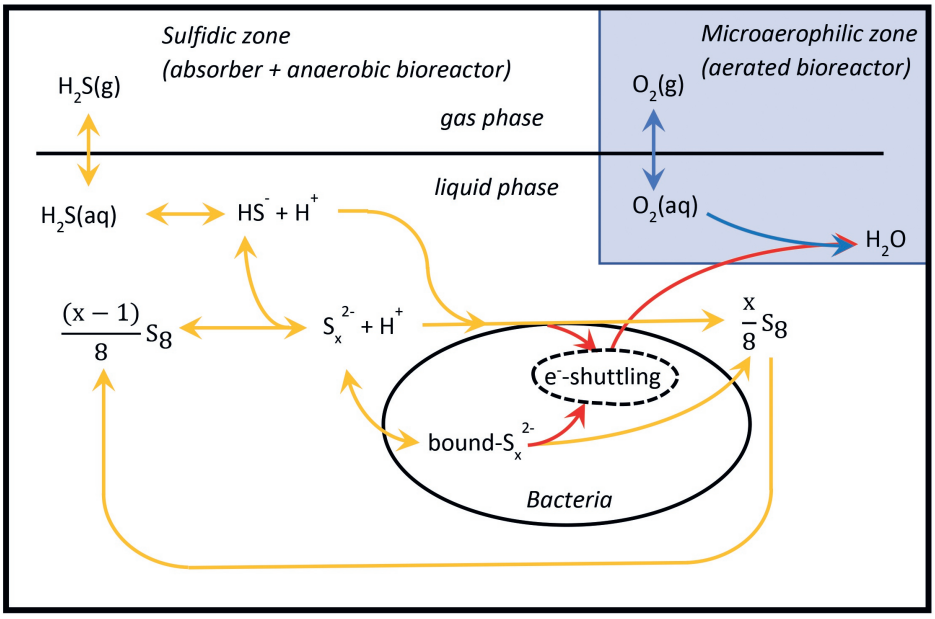

Figure 3.4: Schematic overview of hypothesized sulfide conversion route in the biological gas desulfurization process. The process is separated in the 'sulfidic zone' (in white), consisting of the absorber and anaerobic bioreactor, and the microaerophilic zone (in blue), consisting of the aerated bioreactor. In the sulfidic zone, sulfide is present and O_2 is absent; in the microaerophilic zone, O_2 is available. In the sulfide zone, polysulfide is taken up from the solution by the bacteria and is either stored (bound-S_x^{2-}), or converted to S_8 and the electrons are being stored. In the microaerophilic zone O_2 is used as final electron acceptor and all sulfide is converted. Conversion of sulfur compounds is indicated with yellow arrows; electron shuttling is indicated with red arrows and reactions with O_2 are indicated with blue arrows.

3.4 Conclusion

We investigated the effect of the process factors sulfide concentration and HRT in the anaerobic bioreactor and pH on product formation and biological sulfide uptake in the dual reactor biodesulfurization process. For the experiments with a pH of 8.4 – 8.7 in the aerated bioreactor, the selectivities for S_8 were 94 – 96 mol% (average over an experiment), provided the HRT in the anaerobic bioreactor was higher than 10 min or the sulfide concentration in the anaerobic bioreactor was higher than 0.2 g L^{-1}. An increase in pH to 9.1 resulted in higher SO_4^{2-} formation and therefore lead to a lower selectivity for S_8 formation (88 mol%). Furthermore, the biological removal of sulfide uptake in the anaerobic reactor increased at higher sulfide concentration in the anaerobic reactor and higher pH, suggesting the biological uptake of sulfide in the anaerobic bioreactor is related to polysulfide. Although higher pH results in higher sulfide uptake, this leads to a lower selectivity for S_8 formation.

3.5 Acknowledgements

This research was financed by Paqell B.V.

3.6 REFERENCES

[1] A. Janssen, R. Sleyster, C. Van der Kaa, A. Jochemsen, J. Bontsema, G. Lettinga, Biological sulphide oxidation in a fed-batch reactor, Biotechnology and bioengineering, 47 (1995) 327-333.

[2] A.J. Janssen, P.N. Lens, A.J. Stams, C.M. Plugge, D.Y. Sorokin, G. Muyzer, H. Dijkman, E. Van Zessen, P. Luimes, C.J. Buisman, Application of bacteria involved in the biological sulfur cycle for paper mill effluent purification, Science of the total environment, 407 (2009) 1333-1343.

[3] E. Van Zessen, A. Janssen, A. De Keizer, B. Heijne, J. Peace, R. Abry, Application of THIOPAQ™ biosulphur in agriculture, in: Proceedings of the British Sulphus Events 2004 Sulphur Conference, Barcelona, Spain, 24-27 October 2004, 2004, pp. 57-68.

[4] A.R. Mol, R.D. van der Weijden, J. Klok, C.J. Buisman, Properties of sulfur particles formed in biodesulfurization of biogas, Minerals, 10 (2020) 433.

[5] A. Janssen, C. Buisman, W. Kijlstra, P. van Grinsven, The Shell–Paques desulfurisation process for H_2S removal from high pressure natural gas, synthesis gas and Claus tail gas, in: Proceedings Ninth Gas Research Institute Sulfur Recovery Conference, 1999.

[6] J.B. Klok, G. van Heeringen, R. de Rink, H. Wijnbelt, G. Bowerbank, Techno-economic impact of the next generation Thiopaq O&G process for sulfur removal, in: GPA-GCC, Muscat, Oman, 2018.

[7] J.B. Klok, P.L. van den Bosch, C.J. Buisman, A.J. Stams, K.J. Keesman, A.J. Janssen, Pathways of sulfide oxidation by haloalkaliphilic bacteria in limited-oxygen gas lift bioreactors, Environmental science & technology, 46 (2012) 7581-7586.

[8] P.L. Van Den Bosch, O.C. van Beusekom, C.J. Buisman, A.J. Janssen, Sulfide oxidation at halo-alkaline conditions in a fed-batch bioreactor, Biotechnology and bioengineering, 97 (2007) 1053-1063.

[9] R. De Rink, J.B. Klok, G.J. Van Heeringen, D.Y. Sorokin, A. Ter Heijne, R. Zeijlmaker, Y.M. Mos, V. De Wilde, K.J. Keesman, C.J. Buisman, Increasing the selectivity for sulfur formation in biological gas desulfurization, Environmental science & technology, 53 (2019) 4519-4527.

[10] D.Y. Sorokin, T.P. Tourova, O.L. Kovaleva, J.G. Kuenen, G. Muyzer, Aerobic carboxydotrophy under extremely haloalkaline conditions in *Alkalispirillum/Alkalilimnicola* strains isolated from soda lakes, Microbiology, 156 (2010) 819-827.

[11] D.Y. Sorokin, T.N. Zhilina, A.M. Lysenko, T.P. Tourova, E.M. Spiridonova, Metabolic versatility of haloalkaliphilic bacteria from soda lakes belonging to the *Alkalispirillum–Alkalilimnicola* group, Extremophiles, 10 (2006) 213-220.

[12] J.B. Klok, G. Van Heeringen, P. Shaunfield, Desulfurization of amine acid gas under turndown: performance of the biological desulfurization process, in: Laurence Reid Gas Conditioning Conference, Norman, Oklahoma USA, 2018.

[13] N. Pfennig, K.D. Lippert, Über das vitamin B 12-bedürfnis phototropher Schwefelbakterien, Archiv für Mikrobiologie, 55 (1966) 245-256.

[14] H. Banciu, D.Y. Sorokin, R. Kleerebezem, G. Muyzer, E.A. Galinski, J.G. Kuenen, Growth kinetics of haloalkaliphilic, sulfur-oxidizing bacterium *Thioalkalivibrio versutus* strain ALJ 15 in continuous culture, Extremophiles, 8 (2004) 185-192.

[15] K. Kiragosyan, M. Picard, D.Y. Sorokin, J. Dijkstra, J.B. Klok, P. Roman, A.J. Janssen, Effect of dimethyl disulfide on the sulfur formation and microbial community composition during the biological H2S removal from sour gas streams, Journal of Hazardous Materials, 386 (2020) 121916.

[16] D.Y. Sorokin, The microbial sulfur cycle at extremely haloalkaline conditions of soda lakes, Frontiers in microbiology, 2 (2011) 44.

[17] R. de Rink, J.B. Klok, G.J. van Heeringen, K.J. Keesman, A.J. Janssen, A. ter Heijne, C.J. Buisman, Biologically enhanced hydrogen sulfide absorption from sour gas under haloalkaline conditions, Journal of hazardous materials, 383 (2020) 121104.

[18] A. ter Heijne, R. de Rink, D. Liu, J.B. Klok, C.J. Buisman, Bacteria as an electron shuttle for sulfide oxidation, Environmental science & technology letters, 5 (2018) 495-499.

[19] P.L. Van den Bosch, D.Y. Sorokin, C.J. Buisman, A.J. Janssen, The effect of pH on thiosulfate formation in a biotechnological process for the removal of hydrogen sulfide from gas streams, Environmental science & technology, 42 (2008) 2637-2642.

[20] J.M. Visser, L.A. Robertson, H.W. Van Verseveld, J.G. Kuenen, Sulfur production by obligately chemolithoautotrophic *Thiobacillus* species, Applied and Environmental Microbiology, 63 (1997) 2300-2305.

[21] J.B.M. Klok, Modelling of full-scale haloalkaline biodesulfurization systems, in: Modeling studies of biological gas desulfurization under haloalkaline conditions - PhD thesis Wageningen University, 2015.

[22] P. Roman, M.F. Bijmans, A.J. Janssen, Influence of methanethiol on biological sulphide oxidation in gas treatment system, Environmental technology, 37 (2016) 1693-1703.

[23] K. Kiragosyan, J.B. Klok, K.J. Keesman, P. Roman, A.J. Janssen, Development and validation of a physiologically based kinetic model for starting up and operation of the biological gas desulfurization process under haloalkaline conditions, Water research X, 4 (2019) 100035.

[24] S.E. Hoeft, J.S. Blum, J.F. Stolz, F.R. Tabita, B. Witte, G.M. King, J.M. Santini, R.S. Oremland, *Alkalilimnicola ehrlichii* sp. nov., a novel, arsenite-oxidizing haloalkaliphilic gammaproteobacterium capable of chemoautotrophic or heterotrophic growth with nitrate or oxygen as the electron acceptor, International journal of systematic and evolutionary microbiology, 57 (2007) 504-512.

[25] D.Y. Sorokin, M.S. Muntyan, A.N. Panteleeva, G. Muyzer, *Thioalkalivibrio sulfidiphilus* sp. nov., a haloalkaliphilic, sulfur-oxidizing gammaproteobacterium from alkaline habitats, International journal of systematic and evolutionary microbiology, 62 (2012) 1884-1889.

[26] E. Boldareva, I. Bryantseva, A. Tsapin, K. Nelson, D.Y. Sorokin, T. Tourova, V. Boichenko, I. Stadnichuk, V. Gorlenko, The new alkaliphilic bacteriochlorophyll a-containing bacterium

Roseinatronobacter monicus sp. nov. from the hypersaline Soda Mono Lake (California, United States), Microbiology, 76 (2007) 82-92.

[27] V. Gorlenko, S. Buryukhaev, E. Matyugina, S. Borzenko, Z. Namsaraev, I. Bryantseva, E. Boldareva, D.Y. Sorokin, B. Namsaraev, Microbial communities of the stratified soda Lake Doroninskoe (Transbaikal region), Microbiology, 79 (2010) 390-401.

[28] A.D. Milford, L.A. Achenbach, D.O. Jung, M.T. Madigan, *Rhodobaca bogoriensis* gen. nov. and sp. nov., an alkaliphilic purple nonsulfur bacterium from African Rift Valley soda lakes, Archives of microbiology, 174 (2000) 18-27.

[29] D.Y. Sorokin, T. Tourova, B. Kuznetsov, I. Bryantseva, V. Gorlenko, *Roseinatronobacter thiooxidans* gen. nov., sp. nov., a new alkaliphilic aerobic bacteriochlorophyll a—containing bacterium isolated from a soda lake, Microbiology, 69 (2000) 75-82.

[30] C. Huang, Z.-l. Li, F. Chen, Q. Liu, Y.-k. Zhao, J.-z. Zhou, A.-j. Wang, Microbial community structure and function in response to the shift of sulfide/nitrate loading ratio during the denitrifying sulfide removal process, Bioresource technology, 197 (2015) 227-234.

[31] C. Huang, Y. Zhao, Z. Li, Y. Yuan, C. Chen, W. Tan, S. Gao, L. Gao, J. Zhou, A. Wang, Enhanced elementary sulfur recovery with sequential sulfate-reducing, denitrifying sulfide-oxidizing processes in a cylindrical-type anaerobic baffled reactor, Bioresource Technology, 192 (2015) 478-485.

[32] P. San-Valero, J.M. Penya-Roja, F.J. Álvarez-Hornos, G. Buitrón, C. Gabaldón, G. Quijano, Fully aerobic bioscrubber for the desulfurization of H2S-rich biogas, Fuel, 241 (2019) 884-891.

[33] T. Hansen, Sulfide als electrondonor voor *Rhodospirilphila* nov. spec, a new species of the purple non-sulfur bacteria, Archiv für Mikrobiologie, 92 (1974) 45-48.

[34] N. Pfennig, H. Lünsdorf, J. Süling, J.F. Imhoff, *Rhodospira trueperi* gen. nov., spec. nov., a new phototrophic Proteobacterium of the alpha group, Archives of microbiology, 168 (1997) 39-45.

[35] E. Cuevasanta, A. Denicola, B. Alvarez, M.N. Möller, Solubility and permeation of hydrogen sulfide in lipid membranes, PloS one, 7 (2012) e34562.

[36] J.C. Mathai, A. Missner, P. Kügler, S.M. Saparov, M.L. Zeidel, J.K. Lee, P. Pohl, No facilitator required for membrane transport of hydrogen sulfide, Proceedings of the National Academy of Sciences, 106 (2009) 16633-16638.

[37] S. Riahi, C.N. Rowley, Why can hydrogen sulfide permeate cell membranes?, Journal of the American Chemical Society, 136 (2014) 15111-15113.

[38] E. Gouaux, R. MacKinnon, Principles of selective ion transport in channels and pumps, science, 310 (2005) 1461-1465.

[39] W.E. Kleinjan, A. de Keizer, A.J. Janssen, Kinetics of the reaction between dissolved sodium sulfide and biologically produced sulfur, Industrial & engineering chemistry research, 44 (2005) 309-317.

[40] P. Roman, M.F. Bijmans, A.J. Janssen, Quantification of individual polysulfides in lab-scale and full-scale desulfurisation bioreactors, Environmental Chemistry, 11 (2014) 702-708.

[41] W.E. Kleinjan, A. de Keizer, A.J. Janssen, Equilibrium of the reaction between dissolved sodium sulfide and biologically produced sulfur, Colloids and Surfaces B: Biointerfaces, 43 (2005) 228-237.

[42] E. Cuevasanta, M.N. Möller, B. Alvarez, Biological chemistry of hydrogen sulfide and persulfides, Archives of biochemistry and biophysics, 617 (2017) 9-25.

CHAPTER 4

Biologically enhanced hydrogen sulfide absorption from sour gas under haloalkaline conditions

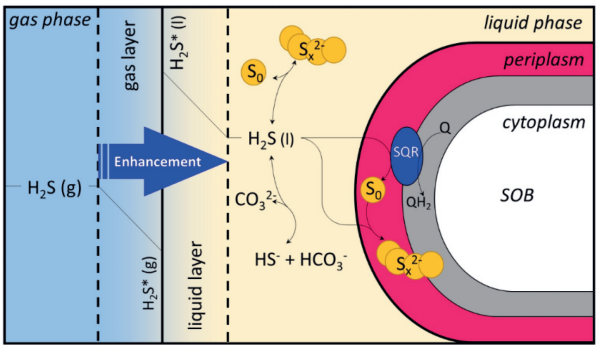

Abstract – We studied a biotechnological desulfurization process for removal of toxic hydrogen sulfide (H_2S) from sour gas. The process consists of two steps: i) Selective absorption of H_2S into a (bi)carbonate solution in the absorber column and ii) conversion of sulfide to sulfur by sulfide oxidizing bacteria (SOB) in the aerated bioreactor. In previous studies, several physico-chemical factors were assessed to explain the observed enhancement of H_2S absorption in the absorber, but a full explanation was not provided. We investigated the relation between the metabolic activity of SOB and the enhancement factor. Two continuous experiments on pilot-scale were performed to determine H_2S absorption efficiencies at different temperatures and biomass concentrations. The absorption efficiency improved at increasing temperatures, i.e. H_2S concentration in the treated gas decreased from 715 ± 265 ppmv at 25.4 °C to 69 ± 25 ppmv at 39.4 °C. The opposite trend is expected when H_2S absorption is solely determined by physico-chemical factors. Furthermore, increasing biomass concentrations to the absorber also resulted in decreased H_2S concentrations in the treated gas, from approximately 6000 ppmv without biomass to 1664 ± 126 ppmv at 44 mg-N L^{-1}. From our studies it can be concluded that SOB activity enhances H_2S absorption and leads to increased H_2S removal efficiencies in biotechnological gas desulfurization.

This chapter is published as: Rieks de Rink, Johannes B.M. Klok, Gijs J. van Heeringen, Karel J. Keesman, Albert J.A. Janssen, Annemiek Ter Heijne, Cees J.N. Buisman. Biologically enhanced hydrogen sulfide absorption from sour gas under haloalkaline conditions. Journal of hazardous materials, (2020) 383, 121104.

4.1 INTRODUCTION

Gas streams, such as natural gas, biogas and several refinery gases arising from processing crude oil and gas, may contain toxic and corrosive hydrogen sulfide gas (H_2S). Therefore, these sour gas streams require treatment before combustion. In the 1990's, a biotechnological gas desulfurization process has been developed as an environmentally friendly and cost effective alternative to conventionally applied chemical-physical desulfurization processes, such amine-Claus, scavengers and liquid iron based technologies [1]. Advantages of the biological process are (i) operation at ambient temperatures and pressures, (ii) no requirement of toxic and expensive chemicals and (iii) formation of re-usable sulfur [2]. The process is widely applied in industry with over 250 installation worldwide in 2017 [3]. To further develop the process, a better understanding of the absorption step is required.

Removal of H_2S gas is achieved in an absorber column by counter-current contact with process solution, see Figure 4.1. For effective removal of H_2S, the process solution is a haloalkaline (high salt, high pH) sodium (bi)carbonate solution of approximately 1 M Na^+ and a pH of 7.5-9.0. In the absorber, H_2S gas is dissolved in the solution as bisulfide (HS^-) and polysulfide (S_x^{2-}). The sulfide-rich solution is then routed to a bioreactor. By the controlled addition of air to this bioreactor, all dissolved sulfide is oxidized, mainly to elemental sulfur by sulfide oxidizing bacteria (SOB). The biological produced sulfur has an oxidation state of zero and therefore it is denoted as S^0. In the bulk of the solution, the elemental sulfur mainly exists in the form of rings of 8 S-atoms (S_8) [4]. S^0 formation is preferred over sulfate and thiosulfate formation to minimize caustic use and bleed stream formation. Process solution from the bioreactor, which is recycled to the absorber, contains sodium (bi)carbonate, sulfur particles, SOB and sodium (thio)sulfate. A small stream of the bioreactor solution is routed to the sulfur separation section, which typically consists of a settler and/or decanter centrifuge.

The biological and chemical conversion reactions under haloalkaline, microaerophilic conditions (i.e. the processes occurring in the bioreactor) have been studied extensively to optimize the conversion efficiency towards S_8 formation [5-13]. The role of microbial activity on the absorption step of the process has never been elucidated, because it is unlikely that SOB, using O_2 as final electron acceptor for sulfide oxidation, are active under the strictly anaerobic conditions that prevail in the absorber column. However, a recent study shows that in a batch experiment SOB are capable of removing HS^- (6.9 µmol mg-N^{-1}) from solution

in the absence of oxygen in approximately 5 minutes [14]. The removal of sulfide by SOB under anaerobic conditions was also observed in a continuously operated biodesulfurization system [8]. If SOB would remove HS^- from the solution in the absorber, this would increase the mass transfer rate of H_2S and thus SOB would contribute to the absorption of H_2S.

In general, the transfer of a compound from the gaseous to the liquid phase occurs when a driving force exists, i.e. an activity difference at the interphase of the gas and liquid phase. According to Fick's law of diffusion, a components mass transfer rate depends on its concentration gradient in the liquid film of the gas-liquid interface, which is often the rate limiting step. A chemical reaction of the respective component in the liquid film, such as protonation, dissociation or conversion, increases the overall mass transfer rate. The increase of mass transfer by a chemical reaction is called 'enhancement' and is quantified by the enhancement factor *E*. Quantification of enhancement factors is not straightforward as it requires knowledge of the reaction paths and rates, which in turn depend on e.g. temperature, irreversible and reversible kinetics, stoichiometry and product diffusion coefficients and concentrations [15].

A number of mechanisms that enhance H_2S absorption (i.e. increase the rate of mass transfer) in biological gas desulfurization are known. After the H_2S has dissolved in the liquid (Equation 4.1), the first enhancement mechanism is the reaction of H_2S with the alkaline process solution, forming HS^- (Equation 4.2) [16]. Under the conditions in the process (i.e. pH in the range of 7.5-9.0 and alkalinity in the range of 0.4-0.9 M), the main alkaline component is bicarbonate (HCO_3^-), which is in equilibrium with carbonate (CO_3^{2-}) and hydroxide (OH^-) ions, according to Equation 4.3. Due to the buffer system, the pH is relatively constant. At higher CO_2 and H_2S pressures in the sour gas, a higher buffer capacity (i.e. alkalinity) may be required.

$$H_2S\ (g) \leftrightharpoons H_2S\ (aq) \qquad \text{(Equation 4.1)}$$

$$H_2S\ (aq) + OH^- \leftrightharpoons HS^- + H^+\ (aq) \qquad \text{(Equation 4.2)}$$

$$CO_3^{2-} + H_2O \leftrightharpoons HCO_3^- + OH^- \qquad \text{(Equation 4.3)}$$

Equation 4.2 is referred to as the 'homogeneous reaction'. Hence, the enhancement of H_2S absorption can be increased by increasing the (bi)carbonate concentration (the alkalinity) and the pH of the process solution.

A second mechanism is the autocatalytic reaction of dissolved sulfides with S^0 particles, forming a range of polysulfide species (S_x^{2-}, where $2 \leq x \leq 9$), according to Equation 4.4 [16, 17]. This reaction is referred to as a 'heterogeneous reaction' [16].

$$HS^- (aq) + (x-1)\ S^0 (s) \leftrightharpoons S_x^{2-} (aq) + H^+ (aq) \qquad \text{(Equation 4.4)}$$

As for the homogeneous reaction, a higher S^0 concentration results in a higher enhancement factor. However, S^0 is in excess at relatively low concentrations (i.e. 0.03 g L^{-1} at an HS^- concentration of 1 mM). At excess S^0 concentrations, the maximum enhancement is reached [16]. Kleinjan et al. concluded that enhancement of H_2S however cannot be explained by heterogeneous reaction alone and their findings suggest the existence of an additional factor contributing to the enhanced H_2S absorption [16]. Since it was shown that SOB can remove sulfide from solution under anaerobic conditions [8, 14], our hypothesis is that the metabolic activity of SOB is involved in the absorption of H_2S from sour gas.

In this study, we investigated the relation between the activity of SOB and H_2S absorption efficiencies from the gas phase into the liquid phase in the absorber column of the biological desulfurization process under haloalkaline conditions. As microbial respiration depends on temperature, and the process operates at mesophilic conditions, firstly the relation between temperature (25 °C – 60 °C) and microbial activity of the SOB was investigated. Secondly, the effect of the SOB activity on H_2S absorption was assessed in a pilot-scale biodesulfurization plant, via (i) varying the temperature of the solution (containing SOB) to the absorber column, and (ii) varying biomass concentration to the solution of the absorber column.

4.2 MATERIALS AND METHODS

4.2.1 BIOMASS RESPIRATION TESTS

To determine the effect of temperature on the respiration activity of SOB, dedicated respiration tests were performed as described by Klok et al. [10, 18]. In these tests, the SOB activity was measured as the oxygen consumption rate upon injection of sulfide. The experiments were performed in 20 mL temperature-controlled glass reactors, equipped with magnetic stirrer. The reactors were closed and supplied with a dissolved oxygen (DO) sensor (PSt3, PreSens Precision Sensing GmbH, Regensburg, Germany). First, SOB taken from a lab-scale biodesulfurization reactor [18] were suspended in a buffer solution

(containing 0.66 M $NaHCO_3$ and 1.34 M $KHCO_3$) to a biomass concentration of 2.5 mg-N L^{-1}. The SOB suspension was aerated for at least 5 minutes until the solution was saturated with oxygen. Subsequently, 20 µL of sulfide stock solution (Na_2S) was injected, resulting in a sulfide concentration of 0.2 mM. Previous research demonstrated that SOB show the highest activity at this sulfide concentration [10]. The decrease in DO concentration was measured with time intervals of 5 seconds. The slope of the oxygen concentration of the first minute after the injection of sulfide, was used as a measure of the oxidation rate. Sulfide oxidation rates were determined for temperatures between 25 °C and 60 °C, in at least triplicate for each temperature. The time between the addition of SOB and sulfide to the temperature-controlled buffer solution varied (ranging from 5 to 30 minutes). Measurements without SOB were performed in the same buffer solution to determine the chemical oxidation rate of sulfide.

4.2.2 H_2S ABSORPTION EXPERIMENTS

To investigate how SOB activity influences H_2S absorption in the absorber of the biological desulfurization process, experiments in a pilot-scale biodesulfurization installation were performed. In this continuously operated installation, the efficiency of the conversion of sulfide to S^0 was studied [8]. For that study, the pilot was in stable operation for 111 days. Directly after this period, experiments were conducted to assess the effect of SOB activity on H_2S absorption efficiency. This was done by: (i) by varying the temperature of the solution to the absorber, and (ii) by varying the biomass concentration in the solution to the absorber.

4.2.2.1 Experimental set-up

The pilot-scale biodesulfurization installation consisted of an H_2S absorber, an anaerobic bioreactor (volume of 5.3 L) and an aerated bioreactor (volume 11.4 L) (Figure 4.1). The H_2S absorber was built of a stainless-steel column with an inner diameter of 5 cm and a height of 4 m, containing 2 meter of packed bed. In the column gas and liquid were contacted in counter current mode. The packed bed consisted of glass spheres with a diameter of 1.2 cm, resulting in a bed porosity of 43% [19]. Hence, the free volume in the packed bed was 1.7 L. Each meter of bed was supported by a perforated stainless-steel plate, which acted as liquid redistribution plate in order to minimize wall effects. A synthetic sour gas (stream A in Figure 4.1), consisting of 4.45 vol % H_2S, 50.00 vol % CO_2 and 45.55 vol % N_2, was fed to the absorber column with a flow rate of 100 NL h^{-1}, using mass flow controllers (Profibus, Brooks instrument, Hatfield, USA). Hence, the total H_2S load was 4.8

mol day^{-1} and the CO_2 load was 53.5 mol day^{-1}. The synthetic sour gas mostly resembles amine acid gas, but its H_2S/CO_2 ratio is also representative for a biogas or natural gas stream.

During the temperature experiment, the excess liquid from the aerobic bioreactor was directed to a bleed vessel (stream 5) via an overflow weir. For the biomass experiment, the auxiliary vessel (5 L) was included in the set-up (see section 2.2.3). The temperature of the process solution was controlled by warm water from a thermostat bath (Kobold, Germany), which was routed through the water jackets of the anaerobic bioreactor, the aerated bioreactor and the auxiliary vessel (during the biomass experiment). The temperature of the solution was measured in the aerated bioreactor (T 1 in Figure 4.1) and at the inlet of the absorber (T 2). The lean solution line and the absorber column were covered with insulating material to maintain a constant temperature. Further details of the set-up are provided in the Supporting Information (SI 3.1).

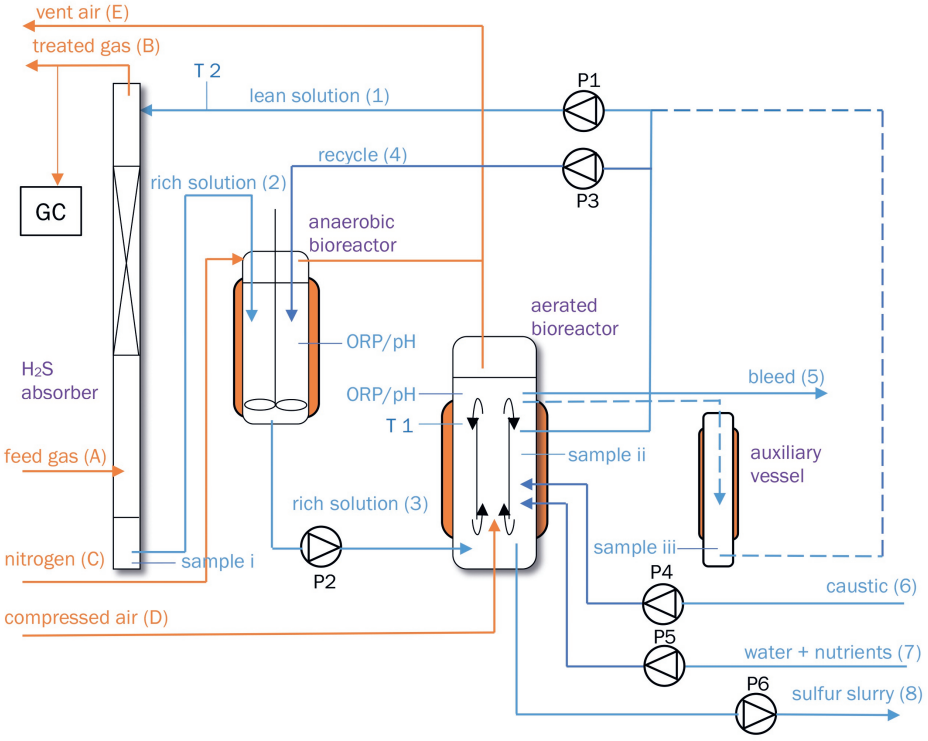

Figure 4.1: Flow scheme of the experimental set-up. The dashed lines apply to the biomass experiment. During the temperature experiment the auxiliary vessel was not part of the set-up.

4.2.2.2 Effect of temperature

The effect of temperature on the H_2S absorption efficiency was assessed during continuous operation of the system by varying the temperature stepwise. In this experiment, the lean solution, ((bi)carbonate solution, containing SOB and sulfur particles) to the absorber was taken from the aerated bioreactor and the auxiliary vessel was bypassed. The feed gas flow was started after stabilization of the lean solution flow (stream 1) (10 kg h^{-1}), temperature (41.2°C in the aerated bioreactor and 37.9 °C at the absorber inlet), and pressure (3.1 bar(g) in the absorber). Then, the temperature (measured at the absorber inlet) was decreased from 38.1 to 25.4°C in four steps of 2-4 °C, by decreasing the temperature setpoint of the water bath. Each temperature setting was maintained for at least 2.5 hours. The treated gas composition was analyzed every 4 minutes, meaning that at least 37 measurements of the treated gas composition were taken during each temperature step. In the last step, the temperature was increased from 25.4 to 39.4°C to determine whether the effect on H_2S absorption is reversible in this temperature range. The standard deviation on the temperature measurement in each temperature step was max 0.3 °C.

During the three days of the experiment, the process solution composition was measured daily by analysis of a sample from the aerated bioreactor (sample ii in Figure 4.1). The liquid circulated through all sections of the system (i.e. absorber, anaerobic bioreactor and aerated bioreactor) at a relatively high flow rate (i.e. 9.1 L h^{-1}). Therefore, the HRT in the various process sections was low (7 minutes in the absorber, 17 minutes in the anaerobic bioreactor and 36 minutes in the aerated bioreactor) compared to the HRT of the integrated system (8.9 days). As a result, concentrations of SO_4^{2-}, $S_2O_3^{2-}$, S^0 and bacteria are assumed to be equal throughout the system. On average, the reactor solution contained 0.67 ± 0.01 M $NaHCO_3$, 0.068 ± 0.008 M SO_4^{2-} and 0.031 ± 0.001 M $S_2O_3^{2-}$. The average specific conductivity, a measure for the dissolved salt concentration, was 48.7 ± 0.6 mS cm^{-1}. The biomass concentration was 70.7 ± 9.0 mg-N L^{-1} and the TSS (concentration of suspended solids, mainly S^0) was 1.75 g L^{-1}. The pH was 7.74 ± 0.06 in the anaerobic bioreactor and 8.24 ± 0.05 in the aerated bioreactor (average over the complete experiment). The average pressure during the experiment was 3.12 ± 0.02 bar(g). Furthermore, the presence of sulfide in the aerated bioreactor was assessed daily using lead-acetate paper (H_2S-Test Paper, Tintometer GmbH, Dortmund, Germany). During the complete experiment, no sulfide was detected.

4.2.2.3 Effect of biomass on H_2S absorption

The effect of biomass concentration on the H_2S absorption process was determined in a dynamic experiment, in which the biomass concentration in the solution to the absorber was increased from 0 to approximately 40 mg-N L^{-1} within the course of 3.5 hours. This experiment was performed 2 days after completion of the temperature experiments. Therefore, we assume that the microbial community composition present in the system during the temperature experiments, is similar. To start with a solution without SOB, the auxiliary vessel was filled with a freshly prepared 0.7 M $NaHCO_3$ solution. The solution from the auxiliary vessel was directed to the absorber (see dashed lines in Figure 4.1). When solution flow from auxiliary vessel to absorber was started, the aerated bioreactor (containing the process solution with SOB and S^0) immediately started to overflow into the auxiliary vessel. Hence, the biomass concentration in the flow to the absorber started to increase as soon as the solution flow was initiated. The biomass concentration was measured in the bottom section of the auxiliary vessel (sample iii in Figure 4.1) after 0 h, 0.5 h, 1 h and 1.5 h after starting the liquid circulation. The time constant of the changing biomass concentration in the flow to the absorber was preliminary determined by HRT of the auxiliary vessel. The HRT of the auxiliary vessel was 55 minutes and each run lasted for 3.5 hours (i.e. >3 x HRT of the auxiliary vessel). To describe the change in biomass concentration in the flow to the absorber, a dynamical model was developed to calculate the biomass concentration in the auxiliary vessel. The model was validated against the measured biomass concentrations.

The chemical composition of the solution in the absorber bottom, anaerobic bioreactor, aerated bioreactor, auxiliary vessel and tubing, was measured immediately before the start of the experiment by taking a sample taken from the aerated bioreactor (sample ii). The alkalinity was 0.69 M; SO_4^{2-} was 0.053 M, and $S_2O_3^{2-}$ was 0.044 M. The conductivity was 48.6 mS cm^{-1} and the biomass concentration was 56.6 mg-N L^{-1}. The temperature in the reactors (including auxiliary vessel) was controlled at a temperature of 43.1°C, (measured in the aerated bioreactor). Subsequently, the lean solution flow to the top of the H_2S absorber was started at 6 kg h^{-1}. Immediately hereafter, the feed gas flow was started.

The experiment was performed in duplicate. Therefore, after 3.5 hours, the auxiliary vessel was drained and refilled with a 0.70 M $NaHCO_3$ solution where after the experiment was repeated. The solution's temperature at the inlet of the absorber was 38.5 ± 2.0 °C in the first experiment and 38.4 ± 0.4 °C in the second experiment. The average pressure in the

absorber during both runs was 3.12 ± 0.003 bar(g). During the complete experiment, no sulfide was detected in the solution to the absorber.

4.2.3 ANALYSES

The concentrations of H_2S, CO_2 and N_2 in the treated gas of the absorber were analyzed every four minutes using a gas chromatograph (Elster Encal 3000, Honeywell, USA). CO_2 and N_2 were analyzed using a mol sieve capillary column (10m) coupled to a thermal conductivity detector (TCD), operated at 100°C and 200 kPa. H_2S was analyzed on a PPU column (10m) and another TCD, operated at 60°C and 200 kPa. Carrier gas was helium (flow 472 mL min^{-1}). The injector temperature was 100°C and the GC was calibrated weekly.

The alkalinity, total concentration of HCO_3^- and CO_3^{2-}, expressed as concentration HCO_3^-, was measured by titrating with 0.1 M HCl, using a titrator (Titralab AT1000, Hach Lange, Germany).

The biomass concentration was measured as the amount of total organic N using the Hach Lange cuvette test LCK138 (Hach Lange, Germany). The difference between the culture's supernatant (centrifuged sample for 10 minutes at 14000 rcf) and non-centrifuged sample indicates the total amount of N present in the biomass. Therefore, the biomass concentration is expressed as mg-N L^{-1}. Presence of biologically produced sulfur particles did not affect the results, provided that the samples were diluted at least 5 times. Considering the stoichiometric equation of HA-SOB, i.e. $CH_{1.8}O_{0.5}N_{0.2}$ [20], the total N accounts for 10-11 mol% of the total dry weight biomass.

The composition of the microbial community was analyzed once during the experiments by 16S rRNA gene Amplicon Sequencing. The materials and methods and results of this analysis can be found in the Supporting Information SI 3.2. Experiments were performed on 9 consecutive days and the sample for the microbial community analysis was taken on day 5. The dilution rate of the system (based on the effluent streams) was 0.09 day^{-1}, so we assume that the microbial community throughout all experiments was similar.

The conductivity of the samples was monitored with an offline conductivity sensor (LF 340, WTW, Weilheim, Germany).

Sulfate and COD (a measure for thiosulfate) concentrations were analyzed in duplicate using Hach Lange cuvette tests LCK353 and LCK514 (Hach Lange, Germany) in the sample's supernatant. Cells and S_8 were removed from the solution by centrifugation for 10 minutes at 14000 x g. Sulfate was measured at 800nm and COD at 605nm using a spectrophotometer (Hach Lange, Germany).

The total suspended solids concentration (TSS), mainly consisting of S^0 particles, was analyzed in triplicate. 15 mL sample was filtered over a pre-dried and pre-weighed GF/C Glass microfiber filter (Whatman). After (pre)drying (60 °C for at least 24 h), the filters were weighed again. The TSS was determined as the difference between the final weight and initial weight, divided by the sample weight.

To determine the sulfide removal from solution by SOB in the absorber, the total sulfide concentration (S_{tot}^{2-}), which is the sum of S^{2-}, HS^- and polysulfide-sulfane (S_x^{2-}), was measured in a sample of the absorber bottom by titration with a solution of 0.1 M $AgNO_3$, using a Titrino Plus Titrator (Metrohm, Herisau, Switzerland). Before titration, the tested sample was filtered over a 0.45 µm cellulose acetate membrane filter to remove S_8 and bacteria. 2 mL of filtered sample was added to 80 mL 4% (w/v) NaOH, with 1 mL of 30% (w/v) NH_4OH to stabilize S_{tot}^{2-}. A comparison between unfiltered and filtered samples did not show significant differences.

4.2.4 CALCULATIONS AND MODELS

The specific HS^- removal efficiency in the anaerobic bioreactor (γ, in mg-S mg-N^{-1}) was calculated based on the H_2S load, the liquid flows, the measured HS^- concentration and the biomass concentration, according to Equation 4.4.

$$\gamma = \frac{\frac{H_2S\ load}{Q_{lean}} - [S_{tot}^{2-}]_{meas}}{Xb} \qquad \text{(Equation 4.5)}$$

Here, *H_2S load* is the mass loading in the H_2S absorber (mg-S h^{-1}), and the Q_{lean} is the lean liquid flow to the absorber (L h^{-1}). $[S_{tot}^{2-}]_{meas}$ is the total measured sulfide concentration (mg-S L^{-1}) and *Xb* is the biomass concentration (mg-N L^{-1}) in the absorber.

A differential equation model was developed in Excel to describe the biomass concentration in the lean solution over time. A detailed description of this model can be found in the Supporting Information (SI 3.3).

4.3 Results and discussion

4.3.1 Effect of temperature on SOB activity

To study the effect of temperature on the rate of biological sulfide oxidation, respiration tests were performed with SOB from a lab-scale biodesulfurization reactor [18], between 25 °C and 60 °C, see Figure 4.2.

As can be seen in Figure 4.2A, the chemical oxidation rates that were obtained in the absence of SOB, are negligible compared to the combined biological and chemical rates. For temperatures up to 45 °C, the replicates show little deviation and an exponential increase in activity is found with increasing temperatures (see solid line in Figure 4.2A).

However, at temperatures higher than 45 °C, the deviation between the replicates increases and the majority of the measurements are well below the exponential curve. The decreased SOB activity at temperatures above 45 °C is the result of thermal inactivation of the bacterial population, while the relatively large differences in activity between the replicates is caused by the wide range of incubation times of SOB at the respective

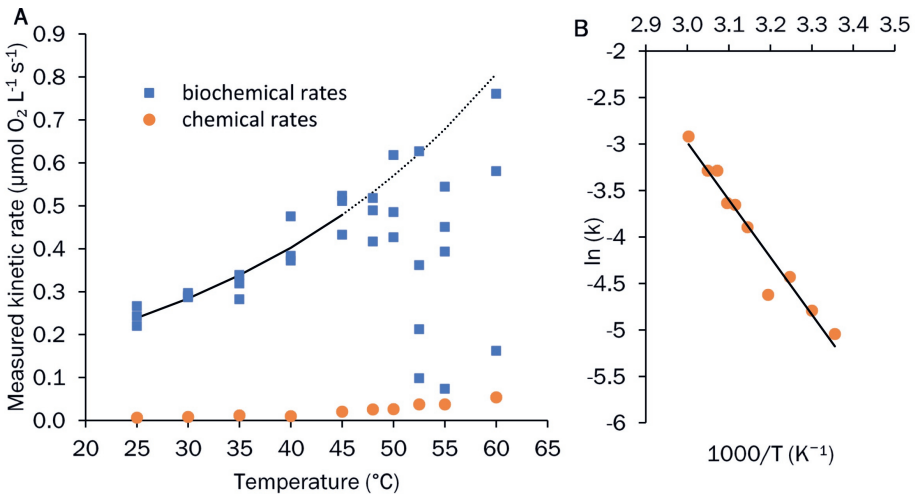

Figure 4.2: A) Results of the respiration tests. The orange dots represent the chemical sulfide oxidation rates (without SOB) and the blue squares the combined biological and chemical rates (with SOB). Between 25 °C and 45 °C SOB activity increases exponentially with temperature (indicated by the solid line); at higher temperatures, thermal inactivation of SOB takes place and the majority of the measurements are below the theoretical curve (dashed line). B) Arrhenius plot, constructed using the chemical sulfide oxidation rates of Figure 4.2A.

temperature. The activity decline in time of SOB at temperatures of 52.5, 55 and 60 °C is described by Klok [18]. Biological oxidation of sulfide is thus strongly influenced by temperature. Between 25 and 45 °C, biological activity increased with temperature; at temperatures above 45°C, biological activity decreased due to thermal inactivation of SOB. Hence, the temperature window of 25-45°C was chosen for the temperature dependency studies on H_2S absorption in the absorber of the pilot-scale biodesulfurization process.

The experimental data of the chemical oxidation rates were used to estimate parameters in Arrhenius' law (see Figure 4.2B). The observed chemical oxidation rates show a good fit, with E_A = 50.0 kJ mol^{-1}, A = 3.49 mol L^{-1} s^{-1} and T_r 35 °C [18]. The calculated activation energy (E_A) of sulfide oxidation is comparable to the activation energy reported for sulfide oxidation in seawater; E_A = 51 kJ mol^{-1} [21].

4.3.2 Effect of temperature on H_2S absorption

Next, the effect of the temperature on the absorption of H_2S in the pilot-scale biodesulfurization system was investigated. The results are shown in Figure 4.3. At the lowest temperature (25.4 °C), the H_2S concentration in the treated gas was 714 ± 265 ppmv. At increasing temperatures, the H_2S concentration in the treated gas showed a linear decrease to 69 ± 25 ppmv at 39.4°C. Thus, at higher temperatures, more H_2S was removed from the gas, indicating that the absorption efficiency was higher. The H_2S concentrations in the treated gas at the higher temperatures are comparable to the normal performance of the pilot-system during continuous operation before the temperature experiment. For example, the average H_2S concentration in the treated gas during a typical day with the same feed gas was 150 ± 68 ppmv. At this day, the temperature at the absorber inlet was 35.2 °C, the pressure was 3.2 bar(g) and the alkalinity 0.68 M. The liquid flow was also 10 kg h^{-1} (same as during the temperature experiment). The coefficient of variation (CV) of the H_2S concentration measurements (i.e. standard deviation divided by the average) during each temperature step is high, but fairly constant. Four of the temperature levels have a CV of 37%. At temperature 31°C, the CV is 25% and at 38°C it is 48%.

In general, the mass transfer rates of H_2S and CO_2 depend on a combination of temperature effects on reaction kinetics, diffusivities and solubilities. It is known that a lower temperature leads to lower equilibrium partial pressures of H_2S and CO_2 [22, 23] (see also Supporting Information SI 3.4), which results in an increased H_2S and CO_2

absorption efficiency. Another effect of a lower temperature is the decrease of reaction rates of CO_2 with the (bi)carbonate buffer system. Because dissociation of H_2S is faster than hydrolysis of CO_2 [24, 25], more buffer capacity is available for H_2S absorption. Thus, if the H_2S absorption in the biodesulfurization process would be solely based on these physico-chemical laws, at lower temperatures a lower H_2S concentration in the treated gas would be expected [26]. Our results show the opposite trend. We therefore speculate that the increased absorption efficiency at higher temperatures is likely to be caused by the effect of temperature on the SOB activity in the lean solution to the absorber, as will be discussed in more detail below.

In a batch experiment, Ter Heijne et al. found that SOB are able to remove sulfide from a solution under anaerobic conditions and in the absence of external electron acceptors [14]. It was hypothesized that bacteria can oxidize sulfide to sulfur under anaerobic conditions and store the released electrons in the form of reduced electron carriers, such as cytochromes and quinones. In our continuously operated reactor experiments, we observed the same phenomenon. The calculated sulfide concentration in the sulfide rich

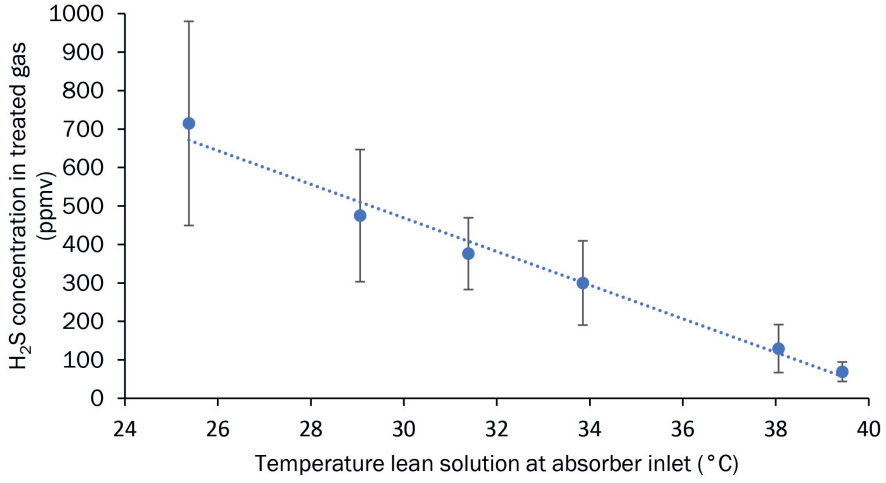

Figure 4.3: Results of the temperature experiment. The average H_2S concentration in the treated gas at each temperature setting, with standard deviation, is indicated with a blue dot and error bar. The inlet H_2S concentration was constant at 4.45 v% (44500 ppmv). When the lean solution (containing SOB) to the absorber has a higher temperature, the H_2S concentration in the treated gas is lower, which means more H_2S is absorbed from the gas.

solution from the absorber would be 21.9 mM based upon the mass balance (i.e. all sulfide levels in gas streams and liquid streams coming into and leaving the absorber column). However, the measured sulfide concentration (the sum of S^{2-}, HS^- and polysulfide-sulfane) in the bottom section of the absorber was 18.0 ± 0.8 mM, indicating that part of the sulfide was removed from the solution by SOB in the absorber. The removal of dissolved sulfide cannot be explained by the presence of external electron acceptors, such as nitrate or dissolved oxygen. Nitrate is not present in the process solution, as it is not supplied to the process and the dissolved oxygen concentration in the aerated bioreactor is below the detection limit of 100 nM.

4.3.3 Effect of biomass concentration on H_2S absorption

To further assess the effect of SOB on H_2S absorption, the biomass concentration in the lean solution to the top of the absorber was varied. The results of this experiment, which was performed in duplicate, are shown in Figure 4.4.

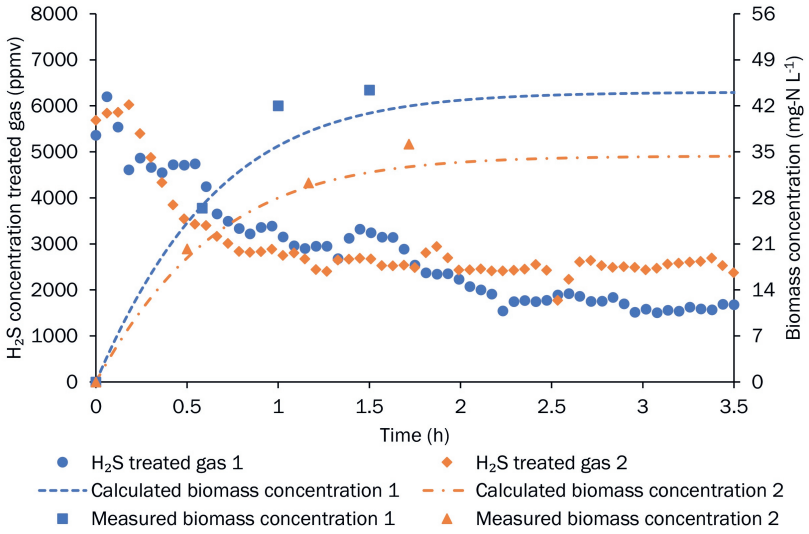

Figure 4.4: Results of the experiment in which the biomass concentration in the flow to the absorber is increased in time. The H_2S concentration in the treated gas is represented by the blue dots (run 1) and orange diamonds (run 2). The dashed lines represent the modelled biomass concentration (in mg-N L^{-1}) in the solution to the absorber. The actual biomass concentration was measured several times (blue squares for run 1 and orange triangles for run 2) to verify the model. The inlet H_2S concentration was constant at 4.45 vol % (44500 ppmv). The results show that the H_2S concentration in the treated gas decreases with increasing biomass concentrations, indicating that SOB increase the H_2S absorption rate.

In the first run, which is depicted in blue, the biomass concentration in the lean solution to the absorber increased from 0 to 43 mg-N L^{-1}. The calculated biomass concentrations (see Supporting Information SI 2) were in good agreement with laboratory measurements. The initial H_2S concentration in the treated gas was 6200 ppm. During the initial stage of the run, no SOB were present in the lean solution to the absorber and the obtained H_2S concentration is the result of physical-chemical absorption only. As the biomass concentration in the lean solution increased, the H_2S concentration in the treated gas decreased and stabilized after 2-2.5 hours of operation. The average H_2S concentration in the last hour (2.5–3.5h) of the experiment was 1664 ± 126 ppmv. This is higher than in the above described temperature experiment, because the solution flow rate to the absorber in the biomass experiment was lower (6 kg h^{-1} instead of 10 kg h^{-1}).

In the second run, the biomass concentration reached a maximum value of 35 mg-N L^{-1}. A similar trend in H_2S concentration was observed compared to run 1: the H_2S concentration in the treated gas was 6024 ppmv at the start of the run (without SOB in the lean solution), and with increasing biomass concentration, the H_2S concentration in the treated gas decreased. The H_2S concentration in the treated gas stabilized at 2509 ± 104 ppmv, which is higher than in the first experimental run. This is as expected, since the biomass concentration in run 2 was lower, which is the result of 20% biomass removal after replacing the bicarbonate solution in the auxiliary vessel. Based on the work of Kleinjan et al., S^0 is present in excess amounts compared to HS^- [16]. Therefore, it is unlikely that the decreased absorption efficiency of H_2S in run 2 compared to run 1 can be explained by decreased enhancement of polysulfide formation, i.e. the heterogeneous reaction. Hence, this experiment also indicates that SOB increase the absorption efficiency of H_2S.

4.3.4 BIOLOGICALLY ENHANCED H_2S ABSORPTION

In previous research by Kleinjan et al., two different enhancement factors for H_2S mass transfer were identified: (i) reaction with (bi)carbonate (homogenous reaction) and (ii) reaction with S^0 particles (e.g. the heterogeneous reaction) [16]. The enhancement factor for the homogeneous reaction (at an alkalinity of 0.15 M and pH 8.5) varied from 41-51 and the enhancement factor due to sulfur particles reached values up to 2.5 [16]. However, these two mechanisms could not fully explain the total enhancement of H_2S absorption found by measurements. It was hypothesized by Kleinjan et al. that the remaining enhancement could be caused by a shuttle mechanism of large hydrophobic sulfur

particles that H_2S can bind to [16]. Such a shuttle mechanism of particles was for example shown for activated carbon particles enhancing CO_2 absorption [27]. However, this hypothesis hasn't been investigated for the biological desulfurization process described in this paper.

The objective of this study was to determine the effect of the SOB activity under oxygen-free conditions, i.e. in the absorber column, on the enhancement of H_2S absorption. The results presented in this paper show that the activity of SOB enhance H_2S absorption by removing sulfide from the process solution. The kinetics of the removal of sulfide by SOB depends on the SOB activity (i.e. temperature) and the SOB concentration. To obtain insight in possible biological mechanisms of the enhanced H_2S absorption, the composition of the microbial community was analyzed using 16S rRNA gene Amplicon Sequencing (Supporting Information SI 3.2). The two most abundant SOB species in the system were *Thioalkalivibrio sulfidiphilius* HL-EbGr7 (53.5%) and *Alkalilimnicola ehrlichi* MLHE-1 (25.7%). Both strains are members of the family *Ectothiorhodospiraceae* (*Gammaproteobacteria*), which are gram-negative bacteria. These bacteria, and especially *Tv. sulfidiphilus,* are often the dominant species in these biodesulfurization installations, both lab-scale and full-scale [12, 28-31]. However, when an anaerobic reactor was added to the line-up of the biodesulfurization process to suppress biological formation of sulfate, it was found that *Alkalilimnicola ehrlichii* became dominant over *Tv. sulfidiphilus* [8]. At the same time, the selectivity for sulfur formation increased from approximately 90 to 97%. The analysis of the complete genome of *Tv. sulfidiphilus* [32], a dominant SOB species found in the full scale facility of Industriewater Eerbeek, the Netherlands [28], showed the presence of genes encoding an FCC type of sulfide dehydrogenase, which converts HS^- to S^0. Flavocytochrome c/sulfide dehydrogenase is a membrane-bound enzyme in alkaliphilic autotrophic bacteria and transfers electrons to cytochromes c [33]. Cytochromes *c* are oxidized by cytochrome c oxidase (CcO), using O_2 as final electron acceptor.

Alkalilimnicola ehrlichii MLHE-1 is a facultative chemolithoautotroph [34]. *Alkalilimnicola* most probably oxidizes HS^- by use of the membrane-bound sulfide-quinone reductase (SQR), which is another well-known enzyme associated with HS^- oxidation. SQR uses quinones as electron carriers. Reduced quinones, i.e. quinol, can be oxidized by either quinol oxidase (QO), using O_2 as electron acceptor, or by NADH dehydrogenase (DH), forming NADH from NAD^+ [10, 35-38]. Several studies have proposed mechanisms for sulfide oxidation by SQR and the product of SQR is, most probably, (soluble) polysulfide

[35, 37, 39, 40]. Due to absence of external electron acceptors (i.e. oxygen or nitrate), no oxidation of the electron carriers can occur in the absorber.

Several biological mechanisms could contribute to anaerobic sulfide removal by SOB in the absorber in the absence of external electron acceptors. Upon absorption of H_2S in the process liquid, HS^- and S_x^{2-} are transferred over the outer cell membrane to the periplasm of the gram-negative SOB. We assume that here the sulfide is converted, as the total periplasmic volume would be too small to account for the total amount of sulfide removed. Sulfide could be converted either by (i) forming cell-bound polysulfides upon reaction with internal stored S^0 [20], (ii) oxidation by sulfide oxidizing enzymes (SQR and FCC), thereby reducing its associated electron carriers (quinones, cytochromes and NAD^+) [10], and/or (iii) binding to the active sites of SQR to form a polysulfide chain of 3 or 4 S atoms [40]. As a result of these conversion reactions, reduction of oxidized molecules takes place in the SOB, i.e. the SOB will reach a lower oxidation state, which is represented by Equation 4.6. Subsequent oxidation of SOB occurs via reduction of oxygen (Equation 4.7), in the aerated bioreactor. As the process solution containing the SOB is continuously circulated between absorber and bioreactor, bacteria can shuttle electrons obtained from sulfide oxidation and intracellular binding in the absorber to the bioreactor. We hypothesize that this shuttle mechanisms results in so-called biologically enhanced H_2S absorption.

$$H_2S + SOB^+ \longrightarrow SOB^- + \tfrac{1}{8} S_8 + 2\ H^+ \qquad \text{(Equation 4.6)}$$

$$SOB^- + 2\ H^+ + \tfrac{1}{2}\ O_2 \longrightarrow SOB^+ + H_2O \qquad \text{(Equation 4.7)}$$

4.3.5 CONSIDERATIONS

This paper shows that SOB in the process solution presumably enhance H_2S absorption and comprise (part of) the remaining enhancement factor. Although some potential mechanisms for biological H_2S enhancement have been discussed, still more research is required to fully understand underlying mechanisms. Biologically enhanced H_2S absorption differs from conventional physico-chemical factors (i.e. the homogeneous and heterogeneous reaction), because it depends on several physiologically based parameters, such as the composition of the microbial community and gene expression levels. These physiological parameters depend mainly on the process conditions. For example, the pilot-scale system, which was used in the experiments described in this paper, has an additional anaerobic bioreactor (dual-reactor system). It was found by Ter Heijne et al. that SOB taken from a dual-reactor system removed more sulfide from the solution than SOB from a system

that consisted of a single aerated bioreactor [14]. An increased sulfide removal capacity of SOB can be the result of the anaerobic reactor, as this increases the contact time of SOB with dissolved sulfide in the absence of oxygen [8]. Therefore, the biological enhancement factor is expected to be different for different microbiomes and operational conditions. As the mechanism of anaerobic sulfide removal is not yet fully understood, it is not possible to quantify the biological enhancement factor based on our experimental data. Further research is required to understand underlying kinetics and reaction pathways. Since the H_2S concentration in the gas phase decreases along the height of the absorber column, i.e. from bottom to top, the conventional driving force for H_2S transfer based on Fick's Law is lowest in the top section. Therefore, we hypothesize that the effect of the biological enhancement factor is most pronounced in the top section of the absorber column. For efficient H_2S absorption, it is important to obtain the required and very low H_2S concentrations in the treated gas whilst minimizing liquid recirculation and column height. Since the absorption step is limited by the rate of mass transfer of H_2S, maximizing biological enhancement by operation at optimal microbial metabolism rates, e.g. temperature and biomass concentration, will contribute to more efficient H_2S removal. Furthermore, when it would be possible to quantify the biological enhancement factor, design and operation of full-scale facilities can be improved.

4.4 Acknowledgements

This research was financed by Paqell B.V. We thank Remco Zeijlmaker, Harry Darmeveil and Angelo Fornerino (DNV-GL) for their support in the experiment work, Jan-Henk van Dijk (Paqell B.V.), Cees Molenaar and Jurgen Kramer (Paques B.V.) for their support in the engineering of the test plant and prof. Alfons J. Stams for stimulating discussions.

4.5 REFERENCES

[1] J.B. Klok, G. van Heeringen, R. de Rink, H. Wijnbelt, G. Bowerbank, Techno-economic impact of the next generation Thiopaq O&G process for sulfur removal, in: GPA-GCC, Muscat, Oman, 2018.

[2] A.J. Janssen, R. Ruitenberg, C.J. Buisman, Industrial applications of new sulphur biotechnology, Water Sci Technol, 44 (2001) 85-90.

[3] J.B. Klok, G. van Heeringen, R. De Rink, H. Wijnbelt, Introducing the next generation of the THIOPAQ O&G process for biotechnological gas desulphurization: THIOPAQ-SQ, in: Sulphur, 2017.

[4] W.E. Kleinjan, A. de Keizer, A.J. Janssen, Biologically produced sulfur, in: Elemental sulfur and sulfur-rich compounds I, Springer, 2003, pp. 167-188.

[5] S. Alcántara, A. Velasco, A. Muñoz, J. Cid, S. Revah, E. Razo-Flores, Hydrogen sulfide oxidation by a microbial consortium in a recirculation reactor system: sulfur formation under oxygen limitation and removal of phenols, Environmental science & technology, 38 (2004) 918-923.

[6] C.J. Buisman, B.G. Geraats, P. Ijspeert, G. Lettinga, Optimization of sulphur production in a biotechnological sulphide-removing reactor, Biotechnology and Bioengineering, 35 (1990) 50-56.

[7] C.J. Buisman, P. IJspeert, A. Hof, A.J. Janssen, R.T. Hagen, G. Lettinga, Kinetic parameters of a mixed culture oxidizing sulfide and sulfur with oxygen, Biotechnology and bioengineering, 38 (1991) 813-820.

[8] R. de Rink, J.B.M. Klok, G.J. van Heeringen, D.Y. Sorokin, A. Ter Heijne, R. Zeijlmaker, Y.M. Mos, V. de Wilde, K.J. Keesman, C.J.N. Buisman, Increasing the selectivity for sulfur formation in biological gas desulfurization, Environmental Science & Technology, (2019).

[9] A. Janssen, R. Sleyster, C. Van der Kaa, A. Jochemsen, J. Bontsema, G. Lettinga, Biological sulphide oxidation in a fed-batch reactor, Biotechnology and bioengineering, 47 (1995) 327-333.

[10] J.B.M. Klok, M. de Graaff, P.L.F. van den Bosch, N.C. Boelee, K.J. Keesman, A.J.H. Janssen, A physiologically based kinetic model for bacterial sulfide oxidation, Water Research, 47 (2013) 483-492.

[11] J.B. Klok, P.L. van den Bosch, C.J. Buisman, A.J. Stams, K.J. Keesman, A.J. Janssen, Pathways of sulfide oxidation by haloalkaliphilic bacteria in limited-oxygen gas lift bioreactors, Environmental science & technology, 46 (2012) 7581-7586.

[12] P. Roman, J. Lipinska, M.F.M. Bijmans, D.Y. Sorokin, K.J. Keesman, A.J.H. Janssen, Inhibition of a biological sulfide oxidation under haloalkaline conditions by thiols and diorgano polysulfanes, Water Res, 101 (2016) 448-456.

[13] P.L. van den Bosch, O.C. van Beusekom, C.J. Buisman, A.J. Janssen, Sulfide oxidation at halo-alkaline conditions in a fed-batch bioreactor, Biotechnology and bioengineering, 97 (2007) 1053-1063.

[14] A. Ter Heijne, R. de Rink, D. Liu, J.B.M. Klok, C.J.N. Buisman, Bacteria as an Electron Shuttle for Sulfide Oxidation, Environ Sci Technol Lett, 5 (2018) 495-499.

[15] P.-F. Biard, A. Couvert, M. Ben Amor, Simulation of hydrogen sulphide absorption in alkaline solution using a packed column AU - Azizi, Mohamed, Environmental Technology, 35 (2014) 3105-3115.

[16] W.E. Kleinjan, J.N. Lammers, A. de Keizer, A.J. Janssen, Effect of biologically produced sulfur on gas absorption in a biotechnological hydrogen sulfide removal process, Biotechnol Bioeng, 94 (2006) 633-644.

[17] P. Roman, M.F.M. Bijmans, A.J.H. Janssen, Quantification of individual polysulfides in lab-scale and full-scale desulfurisation bioreactors, Environmental Chemistry, 11 (2014) 702-708.

[18] J.B.M. Klok, Temperature effects on the biological desulfurization process, in: Modeling studies of biological gas desulfurization under haloalkaline conditions - PhD thesis Wageningen University, 2015.

[19] A.S. Pushnov, Calculation of average bed porosity, Chemical and Petroleum Engineering, 42 (2006) 14-17.

[20] H. Banciu, D.Y. Sorokin, R. Kleerebezem, G. Muyzer, E.A. Galinski, J.G. Kuenen, Growth kinetics of haloalkaliphilic, sulfur-oxidizing bacterium *Thioalkalivibrio versutus* strain ALJ 15 in continuous culture, Extremophiles, 8 (2004) 185-192.

[21] F.J. Millero, A. LeFerriere, M. Fernandez, S. Hubinger, J.P. Hershey, Oxidation of hydrogen sulfide with hydrogen peroxide in natural waters, Environmental science & technology, 23 (1989) 209-213.

[22] F. Lucile, P. Cézac, F.o. Contamine, J.-P. Serin, D. Houssin, P. Arpentinier, Solubility of carbon dioxide in water and aqueous solution containing sodium hydroxide at temperatures from (293.15 to 393.15) K and pressure up to 5 MPa: experimental measurements, Journal of Chemical & Engineering Data, 57 (2012) 784-789.

[23] J. Xia, Á.P.-S. Kamps, B. Rumpf, G. Maurer, Solubility of hydrogen sulfide in aqueous solutions of single strong electrolytes sodium nitrate, ammonium nitrate, and sodium hydroxide at temperatures from 313 to 393 K and total pressures up to 10 MPa, Fluid phase equilibria, 167 (2000) 263-284.

[24] A.J. Kidnay, W.R. Parrish, D.G. McCartney, Fundamentals of natural gas processing, CRC press, 2011.

[25] A.H. England, A.M. Duffin, C.P. Schwartz, J.S. Uejio, D. Prendergast, R.J. Saykally, On the hydration and hydrolysis of carbon dioxide, Chemical Physics Letters, 514 (2011) 187-195.

[26] O. Maile, H. Tesfagiorgis, E. Muzenda, Factors influencing chemical absorption of CO_2 and H_2S in biogas: a review, (2015).

[27] G. Quicker, E. Alper, W. Deckwer, Effect of fine activated carbon particles on the rate of CO_2 absorption, AI Ch. EJ;(United States), 33 (1987).

[28] D.Y. Sorokin, M.S. Muntyan, A.N. Panteleeva, G. Muyzer, *Thioalkalivibrio sulfidiphilus* sp. nov., a haloalkaliphilic, sulfur-oxidizing gammaproteobacterium from alkaline habitats, Int J Syst Evol Microbiol, 62 (2012) 1884-1889.

[29] P. Roman, Biotechnological removal of H_2S and thiols from sour gas streams under haloalkaline conditions, in, Wageningen University, 2016.

[30] D.Y. Sorokin, P. Van Den Bosch, B. Abbas, A. Janssen, G. Muyzer, Microbiological analysis of the population of extremely haloalkaliphilic sulfur-oxidizing bacteria dominating in lab-scale sulfide-removing bioreactors, Applied microbiology and biotechnology, 80 (2008) 965-975.

[31] K. Kiragosyan, J.B. Klok, K.J. Keesman, P. Roman, A.J. Janssen, Development and validation of a physiologically based kinetic model for starting up and operation of the biological gas desulfurization process under haloalkaline conditions, Water Research X, (2019) 100035.

[32] G. Muyzer, D.Y. Sorokin, K. Mavromatis, A. Lapidus, A. Clum, N. Ivanova, A. Pati, P. d'Haeseleer, T. Woyke, N.C. Kyrpides, Complete genome sequence of "*Thioalkalivibrio sulfidophilus*" HL-EbGr7, Stand Genomic Sci, 4 (2011) 23-35.

[33] D.Y. Sorokin, G.A.H. de Jong, L.A. Robertson, G.J. Kuenen, Purification and characterization of sulfide dehydrogenase from alkaliphilic chemolithoautotrophic sulfur-oxidizing bacteria, FEBS Letters, 427 (1998) 11-14.

[34] S.E. Hoeft, J.S. Blum, J.F. Stolz, F.R. Tabita, B. Witte, G.M. King, J.M. Santini, R.S. Oremland, *Alkalilimnicola ehrlichii* sp. nov., a novel, arsenite-oxidizing haloalkaliphilic gammaproteobacterium capable of chemoautotrophic or heterotrophic growth with nitrate or oxygen as the electron acceptor, Int J Syst Evol Microbiol, 57 (2007) 504-512.

[35] C. Griesbeck, G. Hauska, M. Schütz, Biological sulfide oxidation: sulfide-quinone reductase (SQR), the primary reaction, Recent research developments in microbiology, 4 (2000) 179-203.

[36] D.Y. Sorokin, T.P. Tourova, O.L. Kovaleva, J.G. Kuenen, G. Muyzer, Aerobic carboxydotrophy under extremely haloalkaline conditions in *Alkalispirillum/Alkalilimnicola* strains isolated from soda lakes, Microbiology, 156 (2010) 819-827.

[37] C. Griesbeck, M. Schütz, T. Schödl, S. Bathe, L. Nausch, N. Mederer, M. Vielreicher, G. Hauska, Mechanism of Sulfide-Quinone Reductase Investigated Using Site-Directed Mutagenesis and Sulfur Analysis, Biochemistry, 41 (2002) 11552-11565.

[38] J.B.M. Klok, P.L.F. van den Bosch, C.J.N. Buisman, A.J.M. Stams, K.J. Keesman, A.J.H. Janssen, Pathways of Sulfide Oxidation by Haloalkaliphilic Bacteria in Limited-Oxygen Gas Lift Bioreactors, Environmental Science & Technology, 46 (2012) 7581-7586.

[39] J.A. Brito, F.L. Sousa, M. Stelter, T.M. Bandeiras, C. Vonrhein, M. Teixeira, M.M. Pereira, M. Archer, Structural and Functional Insights into Sulfide:Quinone Oxidoreductase, Biochemistry, 48 (2009) 5613-5622.

[40] M. Marcia, J.D. Langer, D. Parcej, V. Vogel, G. Peng, H. Michel, Characterizing a monotopic membrane enzyme. Biochemical, enzymatic and crystallization studies on *Aquifex aeolicus* sulfide:quinone oxidoreductase, Biochim Biophys Acta, 1798 (2010) 2114-2123.

CHAPTER 5

Bacteria as electron shuttle for sulfide oxidation

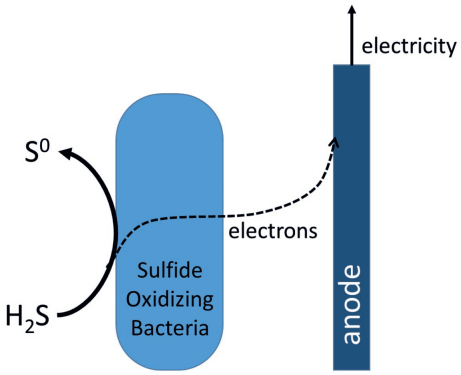

Abstract – Biological desulfurization under haloalkaliphilic conditions is a widely applied process, in which haloalkalophilic sulfide oxidizing bacteria (SOB) oxidize dissolved sulfide with oxygen as final electron acceptor. We show that these SOB can shuttle electrons from sulfide to an electrode, producing electricity. Reactor solutions from two different biodesulfurization installations were used, containing different SOB communities. 0.2 mM sulfide was added to the reactor solutions with SOB in absence of oxygen, and sulfide was removed from solution. Subsequently, the reactor solutions with SOB, and the centrifuged reactor solutions without SOB, were transferred to an electrochemical cell, where they were contacted with an anode. Charge recovery was studied at different anode potentials. At an anode potential of +0.1 V vs Ag/AgCl, average current densities of 0.48 A m^{-2} and 0.24 A m^{-2} were measured for the two reactor solutions with SOB. Current was negligible for reactor solutions without SOB. We postulate that these differences in current are related to differences in microbial community composition. Potential mechanisms for charge storage in SOB are proposed. The ability of SOB to shuttle electrons from sulfide to an electrode offers new opportunities for developing a more sustainable desulfurization process.

This chapter is published as: Annemiek ter Heijne, Rieks de Rink, Dandan Liu, Johannes B. M. Klok, Cees J. N. Buisman. Bacteria as electron shuttle for sulfide oxidation. Environmental science & technology letters (2018), 5, 495−499

5.1 INTRODUCTION

Dihydrogen sulfide (H_2S) is a toxic, odorous and corrosive component present in, for example, natural gas and biogas. If present in gas streams, it oxidizes into SO_2 upon combustion, with air pollution, acid rain and smog as a result. Therefore, sour gas stream desulfurization is required before use. The biological desulfurization process under haloalkaline conditions is one of the processes to remove H_2S from gas streams [1]. In this process, halkaliphilic sulfide oxidizing bacteria (SOB) convert dissolved bisulfide (HS^-) and dissolved oxygen (O_2) into elemental sulfur crystals (S_8), described by the overall reaction:

$$HS^- + ½\ O_2 \rightarrow ⅛\ S_8 + OH^- \qquad \text{(Equation 5.1)}$$

The traditional process consists of two steps: absorption of H_2S in an absorber column, and oxidation into S_8 in an aerated bioreactor. Operating the process at high salt concentrations (halophilic) and alkaline conditions leads to enhanced H_2S absorption and therefore a robust absorption process [1]. The haloalkaliphilic biodesulfurization process is widely applied in the food, paper, mining, and oil and gas industry [2].

Sulfide oxidation is a process also occurring in sediments. It has been shown that cable bacteria present in sediments can oxidize sulfide in anaerobic layers and transport electrons over distances of several centimeters [3]. They thus act as electron shuttle between anaerobic sediment and higher aerobic layers. Sulfide has also been studied as electron donor in the field of bioelectrochemical systems (BESs), where electrodes are used for treatment of sulfide and sulfate containing wastewater. Typically, two processes occur in the anode compartment of such microbial fuel cells: 1) sulfate is reduced into sulfide by sulfate-reducing bacteria, and 2) sulfide is oxidized into elemental sulfur at the anode of microbial fuel cells, either electrochemically or bioelectrochemically, resulting in electricity production [4-7]. Major challenges observed in these sulfide oxidizing BESs are (i) formation of sulfur depositions at the surface of the electrode, leading to inactivation of electrodes and affecting process stability, and (ii) formation of different products besides S_8, like thiosulfate and sulfate, as a result of both chemical and biological reactions.

In this work, we show that SOB remove sulfide from a haloalkaline solution in the absence of oxygen. Subsequently, when the planktonic SOB are transferred to an electrochemical cell, they release electrons at an anode. We demonstrate that SOB can act as electron shuttle between two systems, enabling electricity recovery in an electrochemical cell.

5.2 MATERIALS & METHODS

5.2.1 MICROORGANISMS AND SOLUTION COMPOSITION

Two types of sludges (reactor solutions containing SOB) from different biodesulfurization installations were used: (i) sludge of the full-scale installation in Eerbeek (Industriewater Eerbeek BV, The Netherlands), consisting of an absorber column and an aerated bioreactor, fed with H_2S containing biogas, and (ii) sludge of a pilot-scale installation, consisting of an absorber column, anaerobic and aerated bioreactor [8], fed with a synthetic gas containing H_2S, CO_2 and N_2. Sludge of the full-scale installation in Eerbeek will be referred to as Single Reactor (SR) solution, and sludge of the pilot-scale installation will be referred to as Dual Reactor (DR) solution.

Reactor solutions were harvested from the aerated bioreactor, operated at primarily S_8 forming conditions, for both installations. The DR solution had an alkalinity (expressed as concentration HCO_3^-) of 0.68 M, pH was 8.22, and conductivity was 43.2 mS cm^{-1}. SR solution had an alkalinity of 0.88 M, pH was 8.5, and conductivity was 56 mS cm^{-1}. The alkalinity was determined by titration with 0.1 M HCl with the Titrino plus (Metrohm, Herisau, Switzerland). pH and conductivity were measured with HQ440d multi (Hach Lange, Germany). In addition to sodium carbonate/bicarbonate, the reactor solutions contained a mixed culture of mainly SOB, elemental S_8 crystals, and sodium sulfate and thiosulfate. The concentration of bacteria in the reactor solution was 72.4 mg-N L^{-1} for the SR-SOB, and 29.2 mg-N L^{-1} for the DR-SOB, measured as the difference between total N and dissolved N (supernatant of a sample centrifuged for 10 minutes at 10000rpm) with LCK138 (Hach Lange, Germany).

5.2.2 SOLUTION PRE-TREATMENT

To test the ability of SOB to remove sulfide from solution under anaerobic conditions, a three step pre-treatment procedure was followed.

First, the reactor solution with SOB was aerated overnight to allow complete oxidation of the SOB. Oxidation was assumed complete when the solution remained saturated with oxygen, as measured with a DO sensor (ProSense, Oosterhout, the Netherlands).
Second, the reactor solution was flushed with N_2 until all oxygen was removed (i.e. DO was below detection limit of 26 nmol L^{-1}). After flushing, the pH had increased to 9.61 for the DR solution and 9.43 for the SR solution due to CO_2 stripping. Furthermore, 6-8% of water

was evaporated, leading to slightly higher conductivity and alkalinity at the start of the sulfide uptake and discharge experiments. From this step onwards, pH, conductivity and alkalinity stayed constant during all experiments.
Third, 0.2 mM sulfide was added as $Na_2S.{\sim}3H_2O$ (Analar NORMAPUR, VWR, analytical grade).

5.2.3 DISCHARGE EXPERIMENTS

The pre-treated reactor solution was transferred to an electrochemical cell with a total liquid volume of 50 mL (See SI 4, Figure SI4.1) and a headspace of 30 mL. The anode was a graphite rod electrode (3x3x80mm) with a submerged external surface area of 3.1 cm^2. The cathode was a Pt foil (2.8 cm^2) connected to the outside of the cell via a Pt wire. The reference electrode (Ag/AgCl, 3 M KCl (+0.205 V vs. SHE)) was inserted in the solution via a capillary. The solution was stirred with a magnetic stirrer. Before each experiment, the electrochemical cell was cleaned with demineralized water, and the anode was cleaned using sandpaper (Silicon Carbine 1200/4000, P2000 grit, Gauss Union Company, China). Before injection of the sample into the electrochemical cell, the cell was flushed with N_2 to remove oxygen. Experiments were performed with (i) pre-treated reactor solution with SOB, and (ii) pre-treated reactor solution without SOB. To obtain reactor solution without SOB, the solution was centrifuged after the sulfide uptake experiment (10 minutes, 10000 rpm) and the supernatant was transferred to the electrochemical cell. Reactor solutions with and without SOB were tested at least twice; replicates were performed with new reactor solutions after pre-treatment. The number of replicates is indicated with n, and averages and standard errors are reported. Experiments were performed in a temperature controlled cabinet at 25°C.

5.2.4 SULFIDE UPTAKE MEASUREMENTS

To verify whether sulfide was removed from solution, sulfide uptake experiments were performed. Reactor solutions with and without SOB were subjected to the pre-treatment described in section 5.2.2 and tested in duplicate. Five minutes after 0.2 mM sulfide was added, the final sulfide concentration was measured using Hach Lange kit LCK-635, after filtering over a 0.45 µm filter. In case no free sulfide was measured, an additional test was performed with lead(II)acetate paper (Merck, Darmstadt, Germany). This lead(II)acetate paper shows color when trace sulfide levels (<ppb) are present.

5.2.5 ELECTROCHEMICAL CONTROL AND MEASUREMENTS

A potentiostat (Ivium n-stat with IviumSoft v.2.594, Eindhoven, the Netherlands) was used to control the anode potential in a three electrode setup, with the anode as working electrode, Ag/AgCl as the reference electrode, and the cathode as counter electrode. Two methods were used: chronoamperometry and linear sweep. During chronoamperometry, the anode potential was controlled at -0.1 V, 0 V, and +0.1 V versus the reference electrode for a defined time period (usually 600 seconds). During linear sweep, the anode potential was changed from -0.6 to +0.4 V vs Ag/AgCl with a scan rate of 1 mV s^{-1} (performed once for each solution).

5.2.6 CHEMICAL ANALYSIS AND CALCULATIONS

Sulfide was added from an anaerobic stock solution, of which the concentration was verified by titration with a solution of 0.1 M AgNO3, using a Titrino Plus Titrator (Metrohm, Herisau, Switzerland). 1 mL of the stock solution was added to 80 mL 4% (w/v) NaOH, with 1 mL of 30% (w/v) NH_4OH to stabilize sulfide. The sulfide concentration (0.2 mM) was very low compared to the concentrations of sulfur, sulfate and thiosulfate. Hence, it was impossible to accurately determine the end-product of sulfide conversion, which is required to set-up sulfur mass balances in these experiments.

Anode coulombic efficiency η_C (%) was calculated according to: $\eta_C = \frac{\int_0^t I dt}{[S^{2-}]_0 \cdot V \cdot 2 \cdot F} \cdot 100\%$

Where I=current (A), t=time (s), $[S^{2-}]_0$=sulfide concentration at start of the experiment, V=liquid volume (50 mL), 2 is the amount of electrons transferred (assuming 2-electron oxidation of sulfide to S_8 as the installation were operated at primarily S_8 forming conditions) and F=Faraday constant (96485 C mol^{-1}).

5.3. RESULTS AND DISCUSSION

5.3.1 ELECTRICITY WAS RECOVERED FROM SULFIDE OXIDIZING BACTERIA

After pre-treatment of reactor solutions (overnight aeration, flushing with N_2, and addition of 0.2 mM sulfide, SOB were tested for their ability to use the electrode as electron acceptor. Current was measured in the electrochemical cell at an anode potential of +0.1 V vs Ag/AgCl. The total charge recovered in the first 10 minutes from reactor solutions with and without SOB is shown in Figure 5.1 (based on current profiles as shown in SI 4, Figure SI4.2). Total charge recovered was 68 ± 12 mC for DR-SOB (n=4) and 34 ± 2 mC

for SR-SOB (n=2), while charge recovery from centrifuged reactor solution without bacteria was negligible (2 ± 0.6 and 1 ± 0.7 mC). This shows that that electrons were extracted from suspended SOB and not from other components present in the reactor solution, e.g. traces of sulfide. DR-SOB produced an average current density of 0.48 A m^{-2} (averaged over 600 s), whereas SR-SOB produced an average current density of 0.24 A m^{-2}. SOB in both types of installations are thus able to use the anode as electron acceptor.

The higher charge for DR-SOB compared to SR-SOB could be result of the nature of the process in which the SOB were grown. In the single reactor process, oxidation of sulfide and reduction of oxygen can take place simultaneously. In the dual reactor, SOB are exposed to a regime of alternating reducing conditions (anaerobic reactor, abundance of sulfide) and oxidizing conditions (aerobic reactor, low sulfide). As a result, DR-SOB are exposed to a regime where oxidation of sulfide and reduction of oxygen are taking place in successive steps. We hypothesize that this intermittent exposure to sulfide and oxygen may stimulate electron storage; potential mechanisms will be discussed later.

Additional experiments were performed at different anode potentials of -0.1 V, 0 V and +0.1 V vs Ag/AgCl, for both types of SOB, to study the effect of anode potential on charge recovery. The charge was normalized to biomass concentration and expressed as mC $mg\text{-}N^{-1}$ (Figure 5.2).

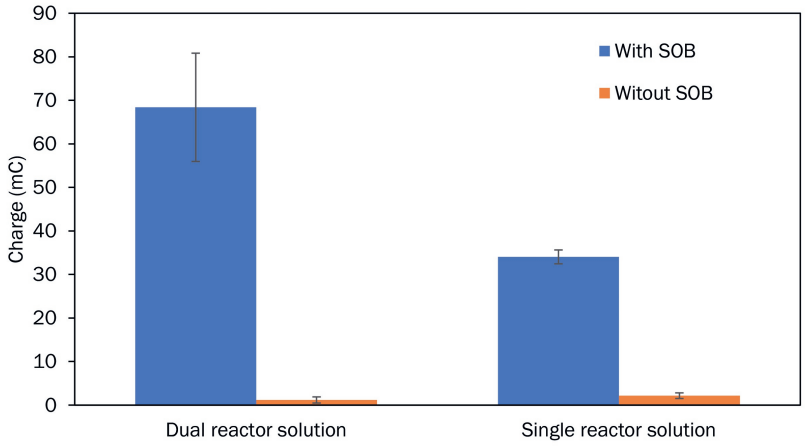

Figure 5.1: Charge was recovered from SOB for dual reactor (n=4) and single reactor (n=2) solutions, including standard error. Reactor solutions without SOB resulted in negligible charge. Total charge was higher for DR-SOB compared to SR-SOB, even though biomass concentration was lower (29.2 mg-N L^{-1}) than for the SR-SOB (72.4 mg-N L^{-1}). Total charge was measured during the first 600 seconds at anode potential of +0.1 V vs Ag/AgCl.

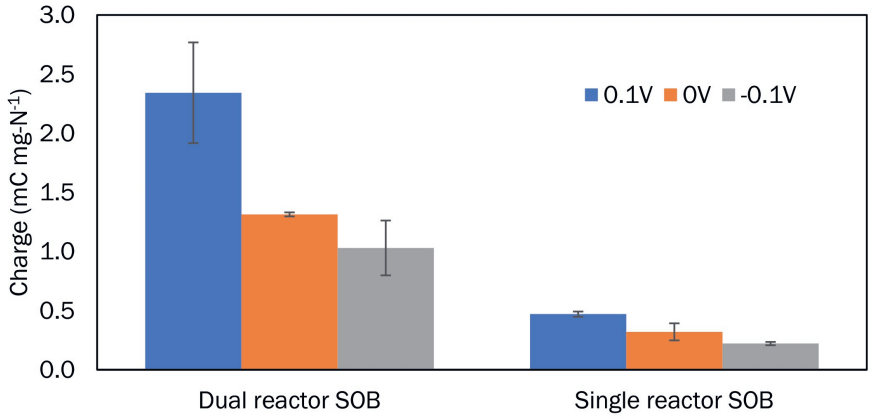

Figure 5.2: Charge, normalized to the amount of biomass (mC mg-N^{-1}) was highest at +0.1 V anode potential, and decreased for lower anode potentials. DR-SOB showed higher current densities than SR-SOB. All experiments were at least 2 replicates, and standard error is shown.

At +0.1 V anode potential, the highest current and total charge was measured, as +0.1 V as this is the situation with the highest overpotential (driving force). Current and total charge decreased with more negative anode potential.

To exclude that the produced current originated from the H_2 gas formed in the single chamber electrochemical cell, an additional experiment was performed in which the cathode was placed in a separate bottle, connected to the anode chamber via a 3 M KCl salt bridge. Similar currents were observed, showing that the effect of H_2 on current production was negligible.

The 10 minute discharge period did not allow for complete discharge of SOB. To determine the coulombic efficiency, which represents the part of the electrons from sulfide that end up as electric current, the experiments were also performed for a longer time period of 24 hours with DR-SOB. Assuming S_8 as product (as observed in the DR installation), 13-35% of the charge in sulfide was recovered as electricity. These values are in the same range as reported for sulfide oxidation at bio-anodes [4].

5.3.2 Sulfide was removed by SOB under anaerobic conditions

Sulfide uptake experiments were performed in duplicate to confirm that sulfide was removed from solution by SOB under anaerobic conditions. Reactor solutions with and without SOB were exposed to 0.2 mM sulfide. For the DR-SOB, no free sulfide was detected after 5 minutes of exposure, which was further confirmed with lead acetate paper. For the

SR-SOB, sulfide concentrations decreased. Control tests on centrifuged reactor solution without SOB also showed a decrease in sulfide concentrations (see SI4, Table SI4.1). To prove that sulfide removal by SOB was significant, an unpaired one-sided equal variance t-test based on the two measured replicates for each situation was done. This t-test showed that sulfide levels for both DR-SOB and SR-SOB were lower ($p<0.001$ for DR-SOB and $p=0.023$ for SR-SOB) than sulfide levels for the centrifuged solutions without SOB. The specific sulfide uptake in these experiments was 0.22 ± 0 mg-S/mg-N for DR-SOB and 0.063 ± 0.002 mg-S/mg-N for SR-SOB.

5.3.3 LINEAR SWEEP

Linear sweep measurements were performed for both types of SOB to study the dynamic response of SOB and reactor solution to a change in anode potential (Figure 5.3). At more positive anode potentials, higher current was measured for the DR-SOB than for the SR-SOB, even though biomass concentration was 2.5x lower. To analyse background effects, both reactor solutions were tested without SOB. Minor current production was observed, presumably related to the capacitance of the electrode and to oxidation of trace concentrations of sulfide. An additional measurement was done on the centrifuged reactor solution without SOB amended with 0.2 mM sulfide, showing that sulfide is electrochemically oxidized in a similar potential range as SOB.

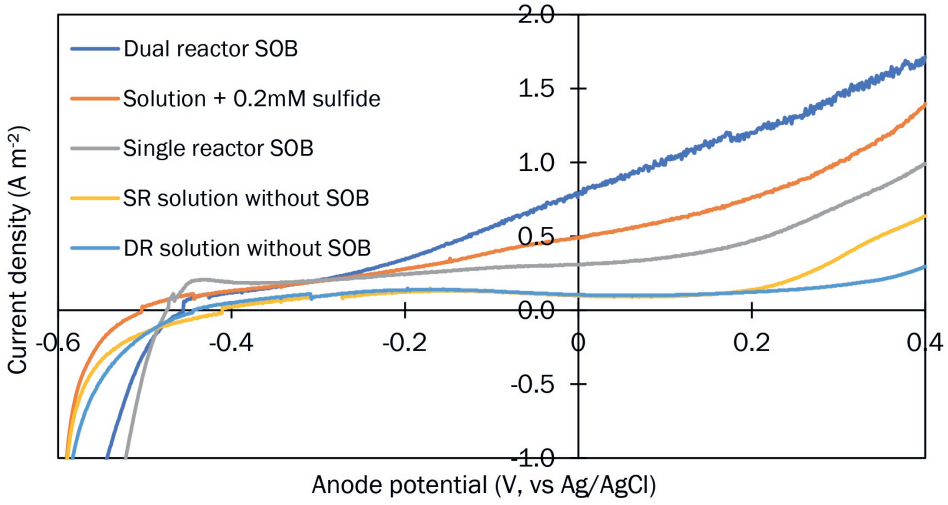

Figure 5.3: Linear sweep reveal current profiles for SOB from both reactors that increase with increasing anode potential. Current in presence of SOB is higher than in absence of SOB.

5.3.4 STORAGE MECHANISMS

Analysis of the microbial communities revealed bacteria from the genus *Thioalkalivibrio* as the dominant SOB in the single reactor plant, whereas bacteria from the genus *Alkalilimnicola* were the dominant SOB in the dual reactor plant (see SI 4, Figure SI4.3). Two types of enzymatic routes for biological sulfide oxidation to elemental sulfur are known: flavocytochrome c sulfide dehydrogenase (FCC) and sulfide quinone reductase (SQR) [9]. In *Thioalkalivibrio sulfidophilus*, the electrons from sulfide oxidation enter the respiration chain via FCC [10]. These electrons are transferred to cytochromes c, and are finally transferred to oxygen by cytochrome c oxidase. For *Alkalilimnicola ehrlichii,* it has been reported that sulfide is oxidized using the SQR enzyme bound to the plasma membrane [9, 11], thereby reducing the electron carrier quinone to its reduced equivalent quinol. Quinol can be oxidized in several ways, for example by oxygen using quinol oxidase. Because both oxidation routes are a cascade of electron transfer reactions, sulfide and oxygen are not simultaneously converted. Based on this knowledge on sulfide conversion mechanisms of SOB in haloalkaliphilic systems and electron transfer mechanisms in electro-active biofilms [12, 13], we postulate that SOB can store electrons in their electron carriers, such as cytochromes and quinones. Electrodes, in combination with other techniques, will offer new opportunities to study the role of cytochromes, quinones and storage mechanisms in the electron transport chain of sulfide oxidizing bacteria.

5.3.5 OUTLOOK

Whereas sulfide oxidation at a bioanode has been described before [4-7], the novelty of this study lies in the charge shuttling capacity of SOB. In this two-stage process, planktonic SOB from biodesulfurization systems take up sulfide under anaerobic conditions, and produce current using an anode as electrode acceptor.

Compared to the established sulfide removal processes, electrodes have the advantage that sulfide can be used as energy source. If combined with an oxygen reducing cathode, the main product would be electricity, or, when coupled to a hydrogen producing cathode, electricity can be converted into hydrogen. Both processes result in a more positive energy balance compared to electricity use for aeration of the bioreactor. In addition, the absence of oxygen might lead to higher selectivity towards S_8, as the use of electrodes provides a way to decouple sulfide oxidation from mixing, which is coupled to aeration in the traditional process.

Compared to MFCs for sulfide removal, sulfur deposition on the anode may be prevented, leading to a more stable process, as the SOB take up sulfide outside the electrochemical cell. In addition, the high bicarbonate concentration results in low risk of anode acidification, a problem commonly encountered in MFCs [14], and it results in low ohmic losses due to the high ionic conductivity of the reactor solutions, being 45-55 mS cm^{-1}, about 10 times higher than conductivity in wastewaters used in MFCs.

The use of electrodes in the biological desulfurization process is a new application and still many questions remain unanswered. Aspects that need to be addresses are, amongst others, to study the mechanisms for charge storage in SOB, to determine under which conditions SOB can sustain growth using the electrode as electron acceptor, to assess product formation, the effect of free sulfide in interaction with the electrode, and to optimize the system and process conditions. Insights in all these factors may result in a new process in which electrodes are integrated in the biodesulfurization process, further increasing its sustainability.

5.4 REFERENCES

[1] A.J. Janssen, P.N. Lens, A.J. Stams, C.M. Plugge, D.Y. Sorokin, G. Muyzer, H. Dijkman, E. Van Zessen, P. Luimes, C.J. Buisman, Application of bacteria involved in the biological sulfur cycle for paper mill effluent purification, Science of the total environment, 407 (2009) 1333-1343.

[2] B. Echt, D. Leppin, D. Mamrosh, D. Mirdadian, D. Seeger, B. Warren, Fundamentals of low-tonnage sulfur removal and recovery, in: Laurance Reid Gas Conditioning Conference, Norman, OK, 2017.

[3] S. Larsen, L.P. Nielsen, A. Schramm, Cable bacteria associated with long-distance electron transport in N ew E ngland salt marsh sediment, Environmental microbiology reports, 7 (2015) 175-179.

[4] R. Bao, S. Zhang, L. Zhao, L. Zhong, Simultaneous sulfide removal, nitrification, and electricity generation in a microbial fuel cell equipped with an oxic cathode, Environmental Science and Pollution Research, 24 (2017) 5326-5334.

[5] K. Rabaey, K. Van de Sompel, L. Maignien, N. Boon, P. Aelterman, P. Clauwaert, L. De Schamphelaire, H.T. Pham, J. Vermeulen, M. Verhaege, Microbial fuel cells for sulfide removal, Environmental science & technology, 40 (2006) 5218-5224.

[6] M. Sun, Z.-X. Mu, Y.-P. Chen, G.-P. Sheng, X.-W. Liu, Y.-Z. Chen, Y. Zhao, H.-L. Wang, H.-Q. Yu, L. Wei, Microbe-assisted sulfide oxidation in the anode of a microbial fuel cell, Environmental science & technology, 43 (2009) 3372-3377.

[7] F. Zhao, N. Rahunen, J.R. Varcoe, A. Chandra, C. Avignone-Rossa, A.E. Thumser, R.C. Slade, Activated carbon cloth as anode for sulfate removal in a microbial fuel cell, Environmental science & technology, 42 (2008) 4971-4976.

[8] J. Klok, G. Van Heeringen, R. De Rink, H. Wijnbelt, G. Bowerbank, Techno-Economic Impact of the Next Generation Thiopaq O&G Process for Sulfur Removal, Proceedings of the GPA-GCC, Muscat, Oman, (2018) 6-8.

[9] C. Griesbeck, G. Hauska, M. Schütz, Biological sulfide oxidation: sulfide-quinone reductase (SQR), the primary reaction, Recent research developments in microbiology, 4 (2000) 179-203.

[10] G. Muyzer, D.Y. Sorokin, K. Mavromatis, A. Lapidus, A. Clum, N. Ivanova, A. Pati, P. d'Haeseleer, T. Woyke, N.C. Kyrpides, Complete genome sequence of "*Thioalkalivibrio sulfidophilus*" HL-EbGr7, Standards in genomic sciences, 4 (2011) 23-35.

[11] D.Y. Sorokin, T.P. Tourova, O.L. Kovaleva, J.G. Kuenen, G. Muyzer, Aerobic carboxydotrophy under extremely haloalkaline conditions in *Alkalispirillum/Alkalilimnicola* strains isolated from soda lakes, Microbiology, 156 (2010) 819-827.

[12] S. Freguia, K. Rabaey, Z. Yuan, J. Keller, Electron and carbon balances in microbial fuel cells reveal temporary bacterial storage behavior during electricity generation, Environmental science & technology, 41 (2007) 2915-2921.

[13] Y. Liu, D.R. Bond, Long-distance electron transfer by *G. sulfurreducens* biofilms results in accumulation of reduced c-type cytochromes, ChemSusChem, 5 (2012) 1047.

[14] C.I. Torres, A. Kato Marcus, B.E. Rittmann, Proton transport inside the biofilm limits electrical current generation by anode-respiring bacteria, Biotechnology and bioengineering, 100 (2008) 872-881.

CHAPTER 6

Continuous electron shuttling by sulfide oxidizing bacteria as a novel strategy to produce electric current

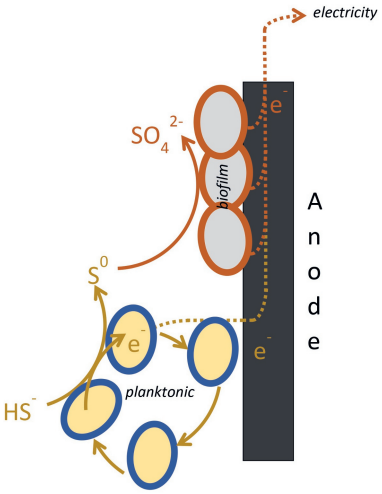

Abstract – Sulfide oxidizing bacteria (SOB) are widely applied in industry to convert toxic H_2S into elemental sulfur. Haloalkaliphilic planktonic SOB can remove sulfide from solution under anaerobic conditions (SOB are 'charged'), and release electrons at an electrode (discharge of SOB). The effect of this electron shuttling on product formation and biomass growth is not known. Here, we study and demonstrate a continuous process in which SOB remove sulfide from solution in an anaerobic 'uptake chamber', and shuttle these electrons to the anode of an electrochemical cell, in the absence of dissolved sulfide. Two experiments over 31 and 41 days were performed. At a sulfide loading rate of 1.1 mmol-S day^{-1}, electricity was produced continuously (3A m^{-2}) without dissolved sulfide in the anolyte. The main end product was sulfate (56% in experiment 1 and 78% in experiment 2), and 87% and 77% of the electrons in sulfide were recovered as electricity. It was found that the current density was dependent on the sulfide loading rate and not on the anode potential. Biological growth occurred, mainly at the anode as biofilm, in which the deltaproteobacterial genus *Desulfurivibrio* was dominating. Our results demonstrate a novel strategy to produce electricity from sulfide in an electrochemical system.

Rieks de Rink, Micaela B. Lavender, Dandan Liu, Johannes B.M. Klok, Dimitry Y. Sorokin, Annemiek ter Heijne, Cees J.N. Buisman. Continuous electron shuttling by sulfide oxidizing bacteria as a novel strategy to produce electric current (submitted)

6.1. INTRODUCTION

Hydrogen sulfide (H_2S) is a toxic and corrosive compound which can be present in several types of gas streams, such as natural gas and biogas [1, 2]. Combustion of H_2S leads to the formation of sulfur dioxide, causing acid rain [3]. For sustainable control of sulfur emissions, a biotechnological gas desulfurization process has been developed, which recovers biologically formed elemental sulfur (S^0) [4, 5]. This process has been applied on commercial scale since the early nineties [6, 7].

The process solution consists of a sodium carbonate/bicarbonate buffer of ~1 M Na^+ and the pH varies from 7.5 – 9.5. Sulfide is oxidized to (predominantly) S^0 by haloalkaliphilic sulfide-oxidizing bacteria (SOB), with O_2 as final electron acceptor. Several sustainable aspects of this process are: i) operation under ambient pressure and temperature; ii) no requirement of toxic chemicals, and iii) S^0 can easily be harvested from the process solution for reuse, for example as fertilizer [8]. Besides S^0, sulfate (SO_4^{2-}) and thiosulfate ($S_2O_3^{2-}$) are formed, which are unwanted because it requires the addition of NaOH and, as a consequence, the formation of a bleed stream [9-11]. The formation of SO_4^{2-} and $S_2O_3^{2-}$ is stimulated at elevated O_2 concentrations and therefore the O_2 is controlled at very low concentrations.

To make the process more sustainable, recent studies focused on decreasing the chemical consumption [9, 11, 12]. Another important aspect of the sustainability of biological gas desulfurization is the energy consumption, which is the focus of this study. In the current process, most of the energy consumption is related to the aeration of the bioreactor for O_2 supply. In addition, the process solution has to be cooled due to the heat released by the exothermic oxidation of sulfide. Therefore, the enthalpy of the oxidation of sulfide is lost.

Recently, it has been found that the SOB taken from the biodesulfurization process are electroactive. These planktonic bacteria can use an electrode as final electron acceptor, instead of O_2 [13]. Furthermore, it was demonstrated that these SOB can remove dissolved sulfide from solution under anaerobic conditions [9, 13, 14]. If this principle can be applied in a continuous electrochemical process for the removal of sulfide, this would have several benefits: i) no energy is required for aeration (O_2 supply), and ii) electrons are harvested from sulfide oxidation, which can be used to recover energy (e.g. in the form of H_2, which can be formed at the cathode). Bioelectrochemical sulfide removal has been studied extensively [15-18]. However, one of the major drawbacks is the deposition of sulfur on the anode when the anode is contacted with dissolved sulfide directly. This deposition occurs due to an electrochemical reaction and will eventually lead to electrode passivation [19-

21]. Thus, the challenge is to prevent direct contact between dissolved sulfide and the anode, which can be achieved by utilizing the shuttling capacity of SOB, as shown in batch experiments by by ter Heijne et al. [13]. This electron shuttling capacity of SOB is still poorly understood. In the batch experiments, the product formation and biomass growth could not be monitored [13].

In this paper we demonstrate a continuous bioelectrochemical process for the removal and conversion of sulfide using the sulfide shuttling capacity of SOB in the absence of O_2. This is achieved by circulating SOB between an 'anolyte recirculation reactor', to which sulfide was continuously added and where SOB removed the dissolved sulfide from solution anaerobically, and the anode of an electrochemical cell, where no dissolved sulfide was present and electrons were released. By shuttling SOB between this reactor and the electrochemical cell, the sulfide removal and release of electrons was thus spatially separated. Product formation, biomass growth and composition were studied to understand the underlying mechanisms of the overall process.

6.2 Materials and methods

6.2.1 Experimental set-up

Experiments were performed in a system consisting of an electrochemical cell, an anolyte recirculation reactor (connected to the anode side of the electrochemical cell) and a catholyte recirculation reactor (connected to the cathode side), see Figure 6.1. The liquid volume of the anolyte recirculation reactor and catholyte recirculation reactor were 400 mL each. The working electrode (anode) was a graphite plate and the counter electrode a titanium plate coated with Pt/IrO_2 (Magneto, special anodes, Schiedam, the Netherlands), both with an effective surface area of 22 cm^2. A cation exchange membrane (FumaTech GmbH, Germany) was used to separate anode and cathode compartments, both with a volume of 33 mL. The anode compartment was filled with graphite granules (approximately 27 g) with a size of 2-4 mm (enViro-gran typ 514, enViro-cell, Oberursel, Germany) and the cathode compartment was filled with approximately 100 glass beads of 6-7 mm. An Ag/AgCl, 3M KCl reference electrode (ProSense/QIS, the Netherlands) was connected to the anode chamber via a capillary. A potentiostat (nStat, multichannel, Ivium, Eindhoven, the Netherlands) was used to control the anode potential and record the current.

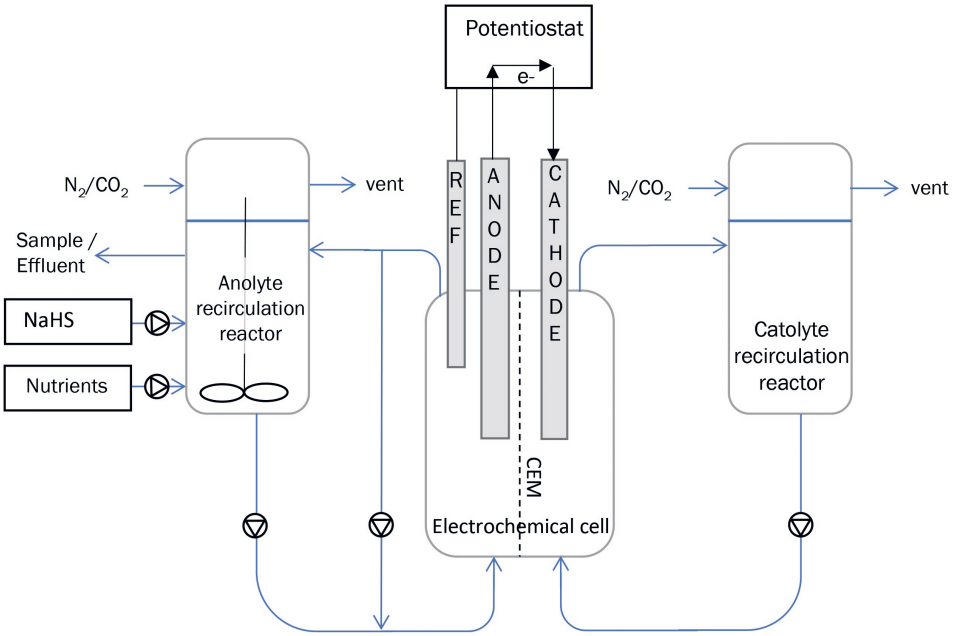

Figure 6.1: Schematic drawing of experimental set-up. Sulfide was continuously added to the anolyte recirculation reactor where SOB removed the sulfide from solution. The solution was circulated over the anode side of the electrochemical cell, where electricity was produced

First, the anode and cathode, including the recirculation reactors, were filled with an $NaHCO_3$ solution of approximately 1 M and liquid circulation was started. 1 M is a typical Na^+ concentration of the (full-scale) biodesulfurization process. To ensure anaerobic conditions in the system, the headspaces of recirculation reactors were continuously purged with a N_2/CO_2 gas stream of 4 L h^{-1}, dosed via Mass Flow controllers (Brooks). The pH was controlled by adjusting the ratio between the N_2 and CO_2 flow rates, which was approximately 4:1. After the O_2 concentration was below the detection limit (15 ppb), SOB biomass from an operating biodesulfurization installation was added to the anolyte recirculation reactor. This installation is described by de Rink et al. [9] and operated under similar conditions when the SOB were harvested. Approximately 10 mL inoculum was prepared by washing the biomass with 1 M $NaHCO_3$ solution using several centrifugation steps, to remove sulfur particles and (thio)sulfate.

Due to the anolyte liquid circulation, the planktonic SOB were continuously transferred from the anolyte recirculation reactor to the anode side of the electrochemical cell and back.

After about 1 hour of liquid circulation, the dosing of NaHS and nutrients was initiated and the potentiostat was started. Gas bags filled with N_2 gas were connected to the headspaces of the NaHS and nutrient stock bottles in order to keep these anaerobic. NaHS was prepared by dissolving NaHS.xH_2O (hydrosulfide hydrate pure flakes, Acros Organics) in demineralized water, which was extensively flushed with N_2. The sulfide concentration was verified by potentiometric titration with 0.1 M $AgNO_3$ using a TitrinoPlus titrator (Metrohm).

6.2.2 Operation of the continuous set-up

Two biotic experiments (experiments 1 and 2) and one abiotic experiment (experiment 3) were performed. In each experiment, the anode potential was changed stepwise and each potential was maintained for at least 4 days. All anode potentials are reported versus Ag/AgCl, 3 M KCl. The applied anode potentials were: -0.1, -0.2, -0.3, -0.35 and -0.4 V in experiment 1; -0.1, -0.2, -0.3, and -0.4 V in experiment 2; -0.1 and -0.4 V in experiment 3. Experiment 1 had a total duration of 31 days. The NaHS concentration in the stock solution was 20.45 g-S L^{-1} and was continuously dosed into the anolyte recirculation reactor with a flow rate of 1.66 g/day, resulting in a constant sulfide loading rate of 1.06 mmol-S day^{-1}. The circulation flow rate over the anolyte recirculation reactor was 0.6 L h^{-1}, which resulted in an HRT of 40 minutes in the anolyte recirculation reactor. An overview of the flow rates, volumes and HRT's in the different parts of the system is provided in the supplementary material (SI 5.1). Nutrients solution consisted of macro nutrient as described by de Rink et al. [9] and 1 mL L^{-1} trace element mix as described by Pfennig and Lippert [22]. The nutrient dosing rate was set in such way that the total residual nitrogen concentration in the supernatant was <10 mg-N L^{-1}. In this way, overdosing of nutrients is prevented and the bacteria consume all nutrients. This dosing strategy is similar to full-scale biodesulfurization installations.

In experiment 1, $[Fe(CN)_6]^{3-}$ was added to the catholyte recirculation reactor on day 15 in order to change the cathode reaction from H_2 formation to the reduction of $[Fe(CN)_6]^{3-}$. The cathode potential changed, but the current didn't change. However, from day 16 onwards, it was noticed that total and dissolved N concentrations increased, even after nutrient dosing was stopped at day 21. Probably some $[Fe(CN)_6]^{3-}$ leaked through the membrane into the anode compartment. From day 16 onwards, the difference between total-N and dissolved-N concentrations still represents the concentration of planktonic bacteria, but an accurate N-balance, including calculation of the amount of biofilm, could not be made.

Experiment 2 had a total duration of 41 days. The NaHS concentration in the stock solution was lowered to 8.90 g-S L^{-1} in order to have a higher inflow rate. Furthermore, the nutrients were diluted 2x and the dosing rate was doubled compared to experiment 1. The sulfide loading rate in experiment 2 varied in order to find the maximal sulfide uptake capacity of the bacteria. Initial loading rate was 0.79 mmol-S day^{-1}. From day 12-29, the loading rate was increased to 1.16 mmol-S day^{-1}; from day 30-42, the sulfide loading rate was again 0.79 mmol-S day^{-1}. The recirculation flow rate over the anolyte recirculation vessel was decreased to 0.42 L h^{-1}, resulting in an HRT of 58 minutes.

Experiment 3 was an abiotic experiment, performed after experiment 2. Despite thorough cleaning of the system and replacement of the graphite granules, some biological activity was observed in this abiotic experiment. Therefore, approximately 0.1 M sodium azide (NaN_3) was added to the system, after which the system was considered abiotic. The effect of NaN_3 on the current production was verified with cyclic voltammetry in a separate electrochemical cell and no effect on the current was observed in the potential range of our experiments. The abiotic experiment was performed for 10 days. The sulfide loading rate was 0.99 mmol-S day^{-1} and no nutrients were dosed. The liquid circulation rate in experiment 3 was also 0.42 L h^{-1}, corresponding to an HRT in the anolyte recirculation vessel of 58 minutes.

During the experiments, the pH was controlled around 8.3 by adjusting the CO_2 flow rate to the headspaces of the recirculation reactors. The initial alkalinity (i.e. bicarbonate concentration) was 1.0 M and conductivity was 52 mS cm^{-1}. Due to acidification and dilution, the alkalinity and conductivity decreased during the experiments. For example, at the end of the experiment 1, the alkalinity and conductivity were 0.37 M and 31 mS cm^{-1}. Under the applied pH (~8.3), practically all sulfide is present as HS^-. Based on the measured current and the product formation, the electron balance is reasonable, which confirms that release of gaseous H_2S is negligible.

The thermodynamics of any (bio)electrochemical system is determined by both anode and cathode reactions and their corresponding potentials. In our experiments, the cathode potential was approximately -0.8 V to form H_2. This consumed electricity, but energy is recovered in the form of hydrogen gas.

6.2.3 ANALYSES

Daily samples were taken from the anolyte recirculation reactor. A sample from the catholyte recirculation reactor was taken at the end of the experiments. pH and conductivity were analyzed offline using a HQ440d multi analyzer (Hach, Germany). Alkalinity, expressed as [HCO_3^-] was measured with an automated TitrinoPlus titrator (Metrohm) by titrating to pH 4.3 using a 0.1 M HCl solution. SO_4^{2-} and $S_2O_3^{2-}$ concentrations were determined on the samples supernatant (after centrifuging for 10 min at 14000 g) using a Dionex ICS-2100 Ion Chromatograph (ThermoScientific) with a Thermo Fisher Scientific IonPac AG17 Guard (Thermo Fisher Scientific, Waltham, MA, USA) and Thermo Fisher Scientific IonPac AS17 column (Thermo Fisher Scientific) at 30 °C. The eluent was KOH at a flowrate of 1.0 mL min^{-1}. The sample injection volume was 10 µL. The biomass concentration was measured as the amount of total organic N using the Dr. Lange cuvette test LCK138 (Hach Lange, Germany), as described by de Rink et al. [9]. The difference between the supernatant (i.e., a sample centrifuged for 10 min at 14000 g) and a non-centrifuged sample indicated the total amount of N present in the (planktonic) biomass. To exclude interference by salts and biologically produced S^0, the samples were diluted at least 5 times. Based on the amount of N added with the nutrients and the measured N concentrations, an N-balance was made in order to calculate the amount of biomass attached to the electrode (biofilm), see Equation 6.4. The dissolved sulfide concentration in the anolyte recirculation reactor was measured using the Hach Lange cuvette test LCK635 (Hach Lange, Germany). Furthermore, lead acetate paper (Merck) was used to check presence/absence of dissolved sulfide. The O_2 concentration in the headspaces of the anode and cathode chambers was measured with oxygen sensor spots and Fibox 4 trace meter (PreSens, Regensburg Germany).

During each run, the experiment was occasionally interrupted to make polarization curves (determine current production at a range of anode potentials). The applied potentials were -0.5, -0.45, -0.4, -0.35, -0.3, -0.2 and -0.1 V (vs Ag/AgCl) and current was measured each second. Each potential was maintained for 5 minutes and the last measurement for each potential was taken as the current production at the respective anode potential. During the polarization curves, the sulfide dosing was maintained.

The microbial communities of the planktonic bacteria and biofilm were analyzed using 16S amplicon sequencing. Samples were taken from the liquid and the graphite granules at the end of each run. Also a sample of the inoculum (planktonic biomass) was analyzed. Details

of the analysis can be found in the Supporting Information (SI 5.2). The EMBL-EBI accession number for the presented 16S rRNA sequencing set is PRJEB44164.

At the end of the experiments, presence of elemental sulfur on the electrode was verified using XRD analysis. Details can be found in the Supporting Information (SI 5.3).

6.2.4 CALCULATIONS

The production of SO_4^{2-}-S (Equation 6.1) and $S_2O_3^{2-}$-S (Equation 6.2) were calculated as follows:

$$P_{SO_4^{2-}-S}(mol) = effluent \cdot \overline{[SO_4^{2-} - S]} + V \cdot \Delta[SO_4^{2-} - S] \quad \text{(Equation 6.1)}$$

$$P_{S_2O_3^{2-}-S}(mol) = effluent \cdot \overline{[S_2O_3^{2-} - S]} + V \cdot \Delta[S_2O_3^{2-} - S] \quad \text{(Equation 6.2)}$$

Here, *effluent* is the effluent of the system (i.e. the sample volume from the anolyte recirculation reactor) (L), $\overline{[SO_4^{2-} - S]}$ and $\overline{[S_2O_3^{2-} - S]}$ are the average concentrations (mol-S L^{-1}) of two consecutive samples, *V* is the total liquid volume of the system and $\Delta[SO_4^{2-} - S]$ and $\Delta[S_2O_3^{2-} - S]$ are the concentration changes (mol-S L^{-1}) between the samples. At the end of the experiments, some SO_4^{2-} was detected in the catholyte (<5% of the concentration in the anolyte). Hence this was not taken into account in the calculation for the SO_4^{2-} production.

As no products other than S_8, SO_4^{2-} and $S_2O_3^{2-}$ were measured in the reactor [11], and it was not possible to quantify the amount of S_8, production of S_8 was calculated from the mass balance:

$$P_{S_8-S}(mol) = I_{H_2S} - P_{SO_4^{2-}-S} - P_{S_2O_3^{2-}-S} \quad \text{(Equation 6.3)}$$

Here, P_{S_8-S}, $P_{SO_4^{2-}-S}$ and $P_{S_2O_3^{2-}-S}$ are the productions of S^0, SO_4^{2-}, and $S_2O_3^{2-}$, respectively, in mol S-product and I_{HS^-} is the volumetric HS^- influent in mol S.

Overall product selectivities were calculated as:

$$Overall\ S_{SO_4^{2-}-S}(\%) = \frac{Total\ P_{SO_4^{2-}-S}\,(mol-S)}{Total\ I_{HS^-}(mol\ S)} \quad \text{(Equation 6.4)}$$

$$Overall\ S_{S_2O_3^{2-}-S}(\%) = \frac{Total\ P_{S_2O_3^{2-}-S}\,(mol-S)}{Total\ I_{HS^-}(mol\ S)} \quad \text{(Equation 6.5)}$$

$$Overall\ S_{S_8-S}(\%) = \frac{Total\ P_{S_8-S}\ (mol-S)}{Total\ I_{HS^-(mol-S)}} \quad \text{(Equation 6.6)}$$

The amount of biofilm, expresses as mg-N per liter of the total system volume, was calculated as the difference between the measured total-N concentration and the theoretical total N concentration. The theoretical total-N concentration (N_T) was calculated according to Equation 6.7:

$$N_{T\ day\ x}\ \left(\frac{mg-N}{L}\right) = N_{T\ day\ x-1} + \left(\frac{N\ added\ with\ nutrients - measured\ totalN}{V}\right) \quad \text{(Equation 6.7)}$$

Based on the formed products, the total amount of released electrons was calculated. The amount of e^- released per S^0 formed, is 2; for each mol of SO_4^{2-} produced, an addition amount of 6 mol e^- is released. The amount of electrons harvested at the anode was determined based sum of the current (as logged by the potentiostat). Based on the SO_4^{2-} formation, the amount of e^- used for biomass growth was calculated based on the work of Klok et al. [10]. The coulombic efficiency (CE) was calculated according to Equation 6.8.

$$CE\ (\%) = \frac{e^-\ harvested\ at\ anode + e^-\ to\ biomass\ growth}{e^-\ released\ by\ S^0\ production + e^-\ released\ by\ SO_4^{2-}\ production} \quad \text{(Equation 6.8)}$$

6.3 Results and discussion

Two experiments were performed, in which planktonic bacteria continuously removed the supplied sulfide from solution in the anolyte recirculation reactor and subsequently released electrons at the anode of the (bio)electrochemical cell. The results of these two experiments are shown in Figures 6.2 (experiment 1) and 6.3 (experiment 2), and the performance of the reactors will be described and discussed in the following chapters.

6.3.1 Continuous electricity production

Figures 6.2A and 6.3A show the sulfide loading rate, the applied anode potential and the resulting current density. In both experiments, current density increased during the first days of the experiment and reached a peak at day 5. Thereafter, current decreased and stabilized.

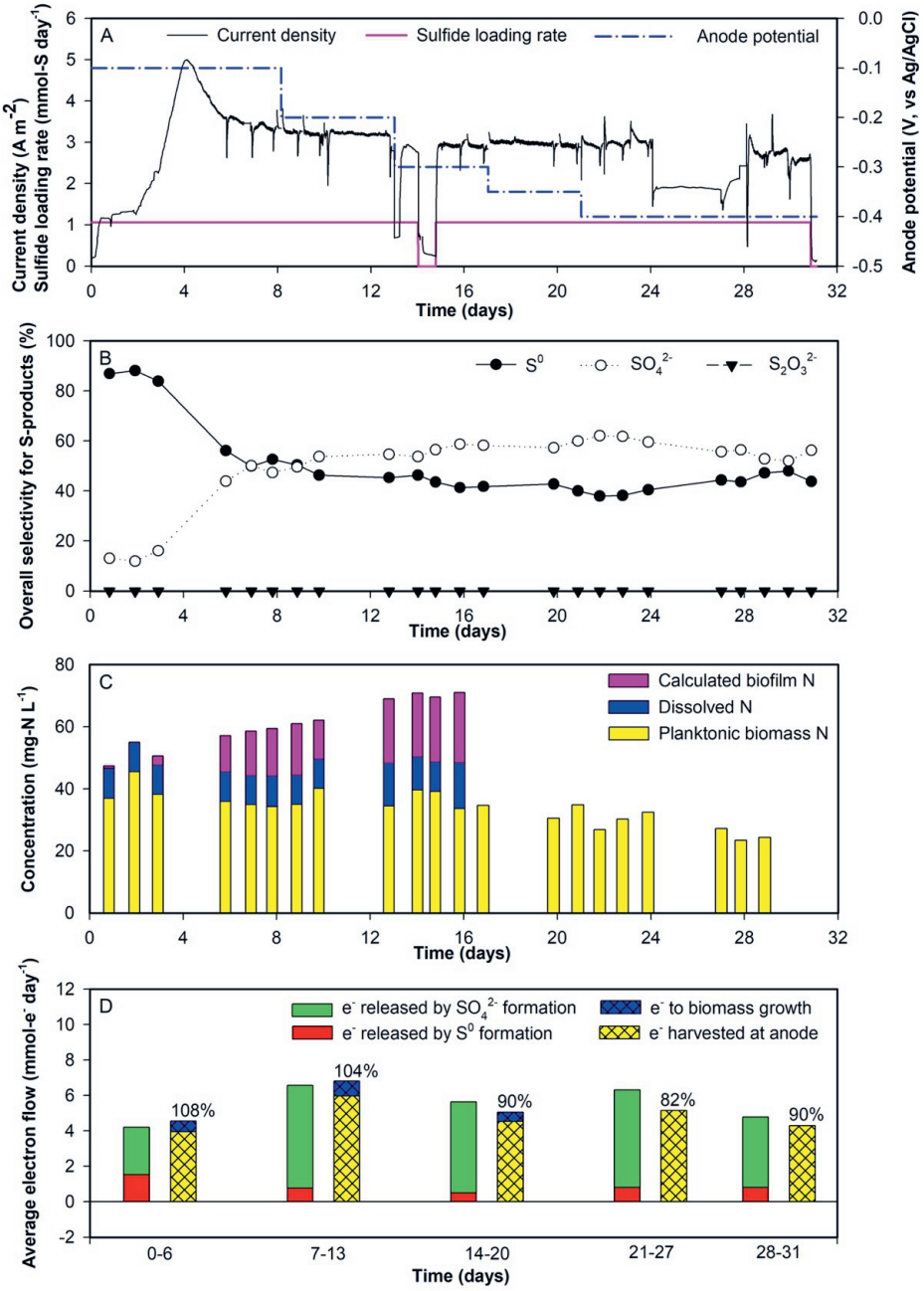

Figure 6.2: Results of experiment 1. A shows the sulfide dosing rate, applied anode potential and current production; in B the overall selectivities for the S-products is shown; C shows the measured planktonic biomass concentration and the calculated concentration of biofilm (based on the total system's volume); in D the electron balance is shown.

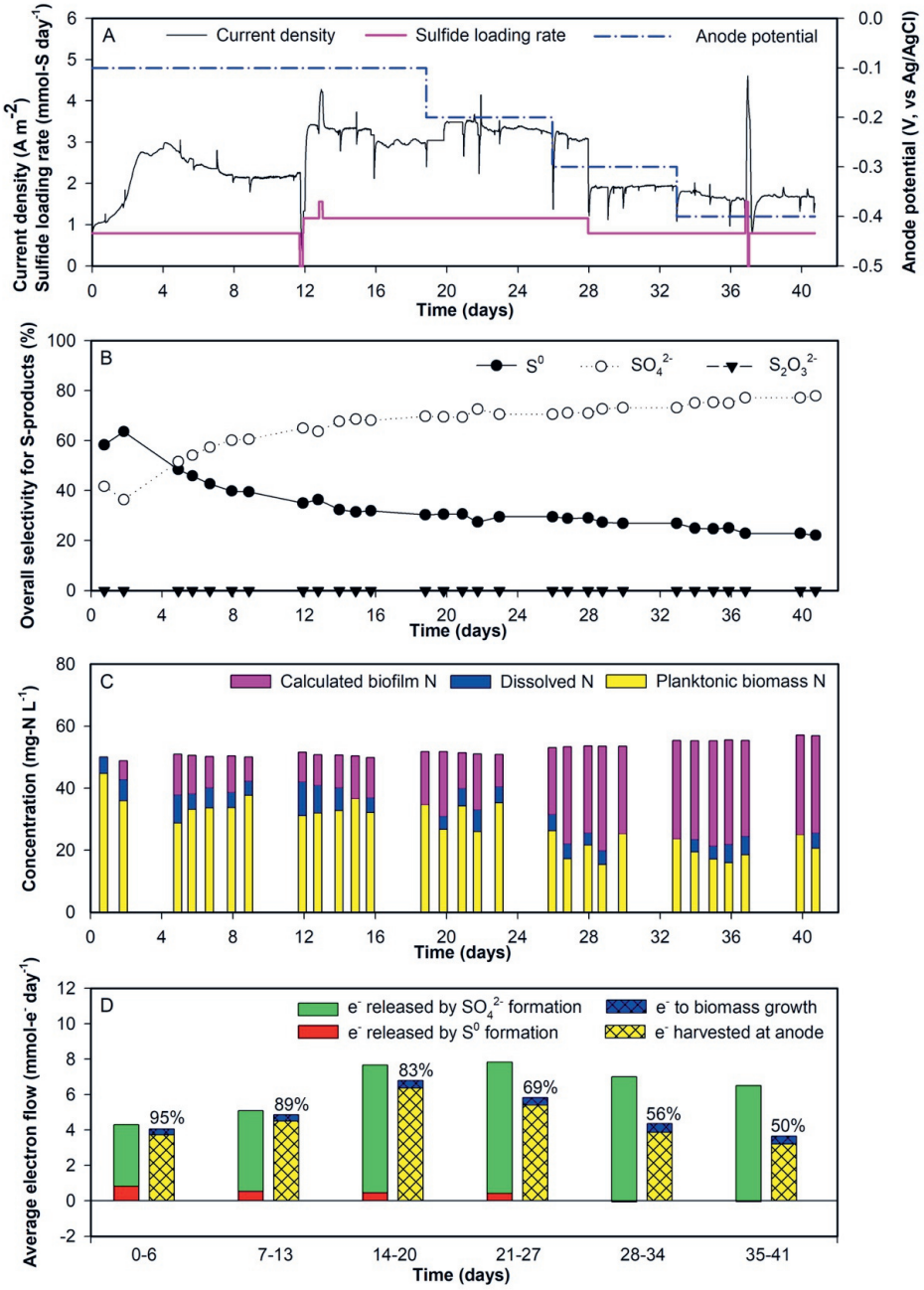

Figure 6.3: Results of experiment 2. A shows the sulfide dosing rate, applied anode potential and current production; in B the overall selectivities for the S-products is shown; C shows the measured planktonic biomass concentration and the calculated concentration of biofilm (based on the total system's volume); in D the electron balance is shown.

In experiment 1, the sulfide load was constant at 1.06 mmol day^{-1} (see Figure 6.2A). Throughout the experiment, all supplied sulfide was converted. In the first 3 days, the current density was approximately 1 A m^{-2}. In this period, sulfide was converted into predominantly S^0 (see Figure 6.2B). After the third day, the current density increased and eventually stabilized around 3 A m^{-2} at day 6. On day 3-6, the selectivity for SO_4^{2-} increased and consequently, the selectivity for S^0 decreased. Since SO_4^{2-} formation releases more electrons than S^0 formation, the increase in the current density was related to the increase in SO_4^{2-} formation. The product formation is discussed in more detail in section 6.3.2. The theoretical dissolved sulfide concentration in the anolyte recirculation reactor was 0.07 mM, based on sulfide loading and recirculation flow rate. However, no dissolved sulfide was detected in the anolyte during the entire run, except for days 3 and 14 where some dissolved sulfide was detected (see SI 5.4). Thus, sulfide was removed by SOB in the anolyte recirculation reactor, and the average sulfide uptake was 2.06 µmol mg-N^{-1}, based on an average biomass concentration of 34 mg-N L^{-1}. At day 14, an unstable current was measured, and dissolved sulfide was detected in the anolyte. Therefore, the sulfide dosing was stopped overnight and the cable connections between the potentiostat and the three electrodes were verified. The following day, the sulfide dosing was restarted and no more dissolved sulfide was detected in the anolyte. In addition, the current density stabilized at previously obtained value of 3 A m^{-2}. From day 24-27 the measured current density was lower, due to an offset of the reference electrode. After replacement of the reference electrode, the measured current density returned to 3 A m^{-2}. In this period, sulfide uptake in the anolyte recirculation reactor continued, and no dissolved sulfide was detected in the anolyte recirculation reactor.

Also throughout experiment 2, all supplied sulfide was converted. Experiment 2 was started with a sulfide loading rate of 0.79 mmol-S day^{-1}. The initial current density was 1 A m^{-2}, which stabilized around 2 A m^{-2} at day 8 (see Figure 6.3A). In the first days of experiment 2, the same pattern as in experiment 1 was observed: Initially, the selectivity for S^0 formation was high. When SO_4^{2-} formation increased, the current density became higher. No dissolved sulfide was detected in the anolyte recirculation reactor until day 12. Therefore, at day 13 the sulfide load was increased to 1.16 mmol-S day^{-1}, which resulted in an increase in the current density, and still no dissolved sulfide was detected in the anolyte. Hence, the sulfide uptake was 3.5 µmol mg-N^{-1} during this period, which was 32% higher than in experiment 1. After a second increase to 1.56 mmol-S day^{-1}, the current density reached a value of 3.84 A m^{-2}. However, after the second increase, dissolved

sulfide was detected with lead acetate paper (not quantified) and the sulfide load was reduced to 1.16 mmol-S day^{-1}. At this dosing rate, the measured current density was around 3 A m^{-2}, similar to the current density measured in experiment 1. From day 20 onwards, detectable quantities of dissolved sulfide were present in the anolyte. However, the majority of sulfide was still being removed (SI 5). At day 28, the sulfide loading rate was decreased to the initial value of 0.79 mmol-S day^{-1}, resulting in a current of 1.8 A m^{-2}.

In both runs, the initial applied anode potential was -0.1 V vs Ag/AgCl. From previous batch experiments, this anode potential was found to be sufficiently high to recover electrons from 'charged' SOB [13]. During the experiment, polarization curves were recorded (results discussed in section 6.3.5). From these curves, it appears that current production is possible at anode potentials <-0.1 V vs Ag/AgCl. Theoretically, a lower anode potential results in a lower driving force for electron transfer. When the driving force is too low, no current can be generated. To study the effect of anode potential, the applied anode potential was stepwise decreased to -0.4 V in both experiments. Surprisingly, this decrease did not have an effect on the current density. In our experiments, decreasing the anode potential from -0.1 V to -0.4 V did not result in an increase in the selectivity for S^0 formation. Since the current density at constant sulfide loading rate is dependent on the product formation (i.e. S^0 and SO_4^{2-}), the current density did not change when the anode potential was changed. The current density did change when the sulfide loading rate was changed (in experiment 2). Thus, in addition to the product selectivity, also the substrate supply determined the measured current density.

6.3.2 PRODUCT FORMATION

Figures 6.2B and 6.3B show the overall product selectivities in experiments 1 and 2. In both experiments, no thiosulfate ($S_2O_3^{2-}$) was detected. As $S_2O_3^{2-}$ is a reaction product of chemical oxidation of dissolved sulfide with oxygen [23, 24], its absence can be explained by the absence of dissolved sulfide and/or the absence of O_2 in the anolyte. At the start of both experiments, the selectivity for S^0 formation was higher than for SO_4^{2-} formation. However, after a few days of operation, SO_4^{2-} rather than S^0 became the main end product of sulfide oxidation. Bacteria prefer SO_4^{2-} formation over S^0 formation due to the higher Gibbs free energy. In the conventional biological desulfurization process, SO_4^{2-} formation is minimized by limiting the O_2 supply [10, 11]. The product formation also depends on the microbial community, which is discussed in section 6.3.6. In this section, the mechanisms of SO_4^{2-} formation are further discussed.

For experiment 1, the overall selectivity for SO_4^{2-} formation was 56% and the selectivity for S^0 formation 44%. For experiment 2, the selectivity for SO_4^{2-} was 78% and selectivity for S^0 22%. From day 28 onwards, all HS^- dosed was converted into SO_4^{2-}. In none of the experiments, S_8-sulfur was detected on the granules or graphite plate, as confirmed with XRD analysis. The overall obtained selectivities for S^0 formation are similar to the results of Ni et al. [15] who obtained a selectivity for S^0 formation of 40% in a fed-batch reactor set-up with a similar electrochemical cell. In the conventional biological desulfurization process a selectivity for sulfur formation of 97% has been achieved [9].

6.3.3 BIOMASS GROWTH

The amount of biomass in the system is shown in Figures 6.2C (experiment 1) and 6.3C (experiment 2). The yellow bars represent the biomass of planktonic cells. The blue bars show the measured dissolved N concentration, which is most likely resulting from non-consumed nutrients in the form of urea and/or ammonium. The concentration of planktonic biomass decreased over the course of both experiments (i.e. the yellow bars in Figures 6.2C and 6.3C). This means that the loss of planktonic bacteria via the effluent was higher than the increase of planktonic bacteria via bacterial growth. Based on the nutrient dosing rate, a higher total nitrogen concentration in the effluent was expected. For example, at the end of run 2, the measured biomass was about 50% lower than expected based on the supply of nutrients. Thus, there is another nitrogen sink, which is most likely the formation of a biofilm on the anode. The amount of biofilm could be calculated based on the addition of nutrients and the measurement of the nitrogen concentration in the anolyte. This amount, expressed as mg-N L^{-1} of the total system, is represented by the purple bars in the Figures 6.2C and 6.3C. Hence, the height of the bars represents the total amount of N in the system, which consist of biofilm, planktonic bacteria and non-consumed nutrients.

From figures 6.2C and 6.3C it appears that growth of sulfur metabolizing bacteria occurred, i.e. the bulk of the dosed nutrients were consumed. The majority of the growth occurred at the anode in the form of biofilm. At the end of experiment 2, the amount of biofilm-N on the electrode was determined by measuring the total N concentration of the granules, and was found to be 10.85 mg-N. This translates to 31.46 mg-N L^{-1} based on the total volume of the system and is in agreement with the amount of biofilm calculated based on the N-balance (31.28 mg-N L^{-1}).

6.3.4 ELECTRON BALANCE

Based on the average values for produced current, product formation and biomass growth, electron balances were made for periods of a week of operation. Results are shown in Figures 6.2D and 6.3D.

For experiment 1 (Figure 6.2D), during day 0-6, the average rate of electrons released was 4.2 mmol e^- day^{-1}, of which 37% was coming from oxidation of HS^- to S^0 and 63% from the oxidation of HS^- to SO_4^{2-}. In this period, the rate of harvesting electrons at the anode was 4.0 mmol e^- day^{-1}, which was 94% of the e^- released from HS^-. When taking into account the calculated e^- used for biomass growth (0.16 mmol e^- day^{-1}), the coulombic efficiency was 108%. The coulombic efficiencies varied over the time periods. The overall coulombic efficiency during experiment 1 was 87%.

During experiment 2, the coulombic efficiencies were around 90% (up to day 20). Towards the end of the experiment the coulombic efficiency decreased for unknown reasons and was 56% in the period of day 35-41. In this period, it was noticed that the formation of SO_4^{2-} was slightly higher than the amount of HS^- supplied. This can be explained by SO_4^{2-} production from S^0 which has been formed in the initial stage of the experiment. As a result, from day 28-41, the net production of S^0 formation is negative. Hence, the e^- released by S^0 formation (the red bar in Figure 6.3D) in this period is expressed as a negative number. The overall coulombic efficiency during experiment 2 was 77%. The coulombic efficiencies obtained in the experiments are higher than reported by Ni et al. (48.4%), who used a similar medium, but higher sulfide concentrations [15].

6.3.5 BIOTIC VS ABIOTIC OPERATION

To study the effect of the presence of SOB on HS^- removal, an abiotic control experiment was performed at anode potentials of -0.1 V and -0.4 V. Despite thorough cleaning of the system and replacement of the graphite granules, an exponential increase in current density and SO_4^{2-} production was observed after a few days, which was likely due to some remaining biological activity. Therefore, sodium azide (NaN_3) was added to the system. Azide is a general agent to block growth of aerobic bacteria by the inhibition of the terminal cytochrome c oxidases of their respiratory chain [25, 26]. Addition of NaN_3 had a direct effect on the current density. After each addition, the current density dropped. After the first addition (1.7 g L^{-1}), the current density dropped, but started to increase after several hours. Therefore, more NaN_3 was added (total 6.8 g L^{-1}) until no direct effect on current

density was observed anymore; at this moment the current was almost zero. After the 4th addition, the experiment was considered abiotic. It was confirmed in a separate batch test that azide did not react with the electrode under the applied process conditions.

Under the abiotic conditions, dissolved sulfide was always present in the anolyte recirculation reactor. For the abiotic experiment the system was operated at an anode potential of -0.1 V for 4 days. During this period, a current density of 0.46 A m^{-2} was obtained at a sulfide dosing rate of 0.99 mmol-S day^{-1}. This is lower than the 3 A m^{-2} that was measured in the presence of bacteria. At the same time, sulfide levels increased in the anolyte during the abiotic experiment, indicating that sulfide uptake in the anolyte recirculation reactor only occurred with planktonic bacteria. Both SO_4^{2-} and $S_2O_3^{2-}$ were produced at rates of 0.14 mmol day^{-1} and 0.08 mmol-S day^{-1}. Interestingly, $S_2O_3^{2-}$ was not detected in the biotic experiments because no dissolved sulfide was present. At an anode potential of -0.4 V, the current density was negative (-0.1 A m^{-2}). This means that electrons flowed in reverse direction, i.e. from counter electrode to working electrode. Biotic and abiotic polarization curves are shown in Figure 6.4.

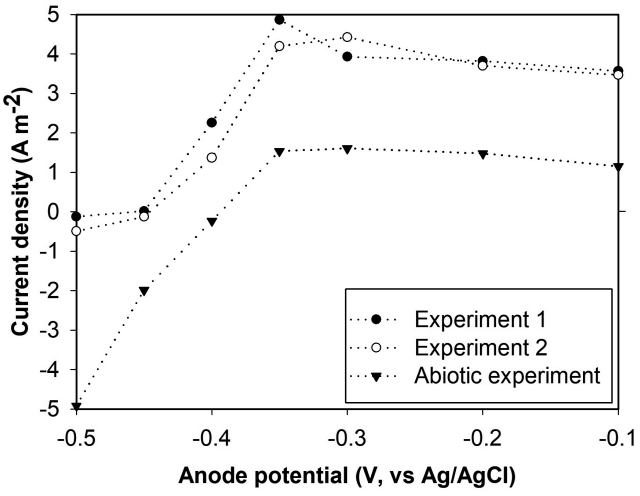

Figure 6.4: Typical polarization curves for the biological runs 1 and 2 and the abiotic control experiment. Polarization curves were made by stepwise increasing the anode potential (from -0.5V to -0.1V) and measuring the current. Each potential was maintained for 5 minutes to obtain a stable current at the applied potential. The plotted values are the last measured value.

For the biotic experiments, a negative current was observed at anode potentials of -0.5 and -0.45 V. For higher anode potentials, current density was positive. Under abiotic conditions, the current density was still negative at an anode potential of -0.4 V and positive at potentials of -0.35 V and higher. A further increase in anode potential did not result in higher current density. Between -0.35 and -0.1 V the anode potential did not influence the current. Under these conditions, the current density was determined by sulfide dosing and not by the anode potential.

6.3.6 MICROBIAL COMMUNITY

The microbial community of the planktonic bacteria and the biofilm was analyzed at the end of each run. The inoculum, obtained from a pilot-scale biodesulfurization plant, was also analyzed. Results are shown in Table 6.1. The inoculum contains *Thioalkalivibrio* (relative abundance 32%) and *Alkalilimnicola* (18%). Both are haloalkaliphilic SOB. *Thioalkalivibrio sulfidiphilus* has previously been found to be the dominant SOB in both full-scale and lab scale biodesulfurization installations [27, 28]. Genome analysis indicates that it oxidizes HS^- to S^0 via flavocytochome *c* (Fcc) sulfide dehydrogenase and S^0 to SO_4^{2-} via the reversed DSR pathway [29]. *Alkalilimnicola* species are facultatively autotrophic and facultatively anaerobic SOB [30, 31]. It has been suggested that some *Alkalilimnicola* members are limited to partial sulfide oxidation to S^0 [9].

At the end of each experiment, the microbial community of both the planktonic and the biofilm biomass had changed compared to the inoculum. In both experiments, the biofilm was dominated by bacteria belonging to the genus of *Desulfurivibrio*, with a relative abundance of 37.0% in experiment 1 and 43.3% in experiment 2. *Desulfurivibrio* is also present in the planktonic biomass (21.6 and 11.1 %), while the relative abundance of *Desulfurivibrio* in the inoculum was only 1.3%. The genus includes a single species: *Desulfurivibrio alkaliphilus* [32]. Until now, *Desulfurivibrio alkaliphilus* was only found in soda lakes [32, 33]. It is an obligately anaerobic deltaproteobacterium originally described as sulfur-thiosulfate reducer. However, more recently it was found that *Desulfurivibrio alkaliphilus* is a chemolithoautotrophic sulfur disproportionator [34]. This means it is using S^0 as both electron acceptor and donor, dismutating it to 1 mol SO_4^{2-} and 3 mol HS^-. Furthermore, it can also couple the oxidation of sulfide to sulfate to the reduction of nitrate/nitrite to ammonium [35, 36]. In our experiments, the N-source was urea and NO_3^{2-} and NO_2^{2-} were not supplied. Therefore, *Desulfurivibrio alkaliphilus* could have been responsible for the formation of SO_4^{2-}, but it is not clear whether it was contributing to the

Table 6.1: Overview of the key bacterial species in the solution (planktonic biomass) and attached to the electrode (biofilm) as analyzed via 16S rRNA amplicon sequencing. An extensive table of the present species is provided in the Supporting Information (SI 5.3; Table 5.2).

	Relative abundances						
	Inoculum	End of exp 1 (planktonic)	End of exp 1 (biofilm)	End of exp 2 (planktonic)	End of exp 1 (biofilm)	**Key physiology**	**Occurrence**
Sulfide oxidizing bacteria (SOB)							
Alkalilimnicola	18.48%	18.58%	4.02%	6.36%	1.94%	facultatively autotrophic and facultatively denitrifying SOB	Soda lakes and biodesulfurization plants
Thioalkalispirila	0.22%	1.21%	0.12%	3.34%	0.23%	microaerophilic lithoautotrophic SOB	Soda lakes
Thioalkalivibrio	31.88%	2.54%	0.75%	16.40%	9.93%	Lithoautotrophic SOB	Soda lakes and Thiopaq reactors
Thioalkalimicrobium	3.00%	2.90%	0.34%	0.73%	0.99%	Lithoautotrophic SOB	Soda lakes and Thiopaq reactors
Rhodobacteraceae / other	28.75%	2.59%	0.42%	9.38%	2.43%	Might be photoheterotrophic anaerobic SOB	Might be in soda lakes
Arcobacter	0.06%	3.08%	0.08%	14.30%	0.86%	Microaerophilic sulfide oxidation	Marine
Anaerobic sulfur bacteria							
Desulfurivibrio	1.28%	21.59%	36.97%	11.11%	43.31%	Elemental sulfur disproportionation or sulfur reduction with H_2	Biodesulfurization plants
Desulfurispirillum	0.35%	1.10%	6.03%	0.35%	1.38%	Sulfur reduction; dissimilatory ammonification	Soda lakes
Fermentative bacteria							
Acholeplasma	0.58%	6.10%	0.67%	3.44%	1.99%	Fermentative	Found in soda lake metagenomes
Anoxynatronum	0.83%	0.92%	1.30%	0.28%	2.73%	Fermentative	Soda lakes
Tindallia	0.40%	0.14%	1.89%	0.16%	1.51%	Acetogenic, can use H_2 and reduce thiosulfate	Soda lakes
Uncultured (*cloacimonetes*)	0.00%	2.12%	2.84%	0.10%	0.40%	Fermentative	Found in soda lake metagenomes
Hydrolytic bacteria							
Lentimicrobiaceae / uncultured	0.24%	15.69%	3.69%	16.13%	8.02%	Polysaccharidolytic	Soda lakes
Natronoflexus	0.00%	0.03%	7.31%	0.01%	0.45%	sugar fermentation	Soda lakes

observed bioelectrochemical HS^- oxidation to S^0. *Desulfurivibrio alkaliphilus* is related to the long-distance electron transferring cable bacteria [35, 36]. Furthermore, it possess genes for the expression of conductive pili, which are used for external electron transfer [37]. The dominance of *Desulfurivibrio alkaliphilus* in the biofilm was also observed by Ni et al. [15]. It must be noted that electricity was produced immediately from the start of the experiment, i.e. with only planktonic bacteria. Since the relative abundance of *Desulfurivibrio* in the inoculum was only 1.28%, *Desulfurivibrio* is not the only species that can exchange electrons with the electrode and that a biofilm is not required for the electricity production. This is in agreement with the experiments of ter Heijne et al., in which no biofilm was present [13].

At the end of run 1, the relative abundance of *Alkalilimnicola* in the solution was still 18%, while the relative abundance of *Thioalkalivibrio* decreased to 2.5%. In run 2, relative abundances of both *Alkalilimnicola* (6%) and *Thioalkalivibrio* (10%) in the solution had decreased.

6.3.7 CONSIDERATIONS

The aim of this study was to investigate a continuous electrochemical process to recover electrons from sulfide in a 2-step process to spatially separate the removal of sulfide and release of electrons. This was done by applying the electron shuttling capacity of SOB. Our results show that i) continuous release of electrons by SOB takes place in absence of dissolved sulfide at the anode, ii) biomass growth occurs and iii) no S^0 deposition on the electrode took place.

However, there is still room for improvement, e.g. with respect to product formation. In both experiments, the main product was sulfate. Sulfate formation is unwanted, because it requires NaOH addition to prevent acidification of the process solution. In experiment 1, the overall selectivity for sulfur formation was 44% and in experiment 2, the selectivity for sulfur formation was 22%.

Even though the aim was to growth planktonic biomass, which can be recirculated between anolyte recirculation reactor and the anode compartment, it was found that biomass was accumulating on the electrode, while the amount of planktonic biomass slightly decreased during the experiments. This suggests that most of the metabolic energy was obtained by the biofilm, even without dissolved sulfide in the solution to the anode compartment. Probably, the sulfate was formed by bacteria in the biofilm (e.g. *Desulfurivibrio*, which was

the dominant species in the biofilm). Furthermore, at the first days of each experiment, while no biofilm was present yet, the selectivity for sulfur was much higher (see Figure 6.2 and 6.3). Therefore it is hypothesized that the planktonic bacteria oxidize sulfide to sulfur and that the biofilm oxidizes sulfur to sulfate. Hence, it remains a challenge to be able to control the product formation towards sulfur (without dissolved sulfide in solution). Preventing the formation of a biofilm might be an important step to obtain a higher selectivity for sulfur formation.

We have demonstrated that bacteria can take up sulfide in the anolyte recirculation reactor and subsequently discharge electrons to the anode of an electrochemical cell without dissolved sulfide present in the electrochemical cell. This lowers the risk of electrode passivation resulting from sulfur deposition on the anode via electrochemical oxidation. This electrode passivation is problematic in (bio)electrochemical systems for direct sulfide removal. We have used XRD to determine the presence of elemental sulfur on the electrode and no elemental sulfur was detected. Future research should focus on the sulfur deposition to confirm that the electron shuttling approach prevents electrodeposition of elemental sulfur.

Another advantage is that, due to the application of haloalkaliphilic bacteria, the system can be operated at high salt concentrations (1 M Na^+) and alkaline conditions (pH 8 – 9). This decreases ohmic resistances, resulting in a higher energy efficiency of the bioelectrochemical system compared to systems operated at neutrophilic conditions and low salt concentrations. Compared to conventional biodesulfurization processes, no energy is required for e.g. aeration of the bioreactor and energy from the oxidation of sulfide is recovered. This will improve the energy efficiency of biological gas desulfurization under haloalkaline conditions.

6.4 Acknowledgements

This research was financed by Paqell B.V. We thank Ilse Gerrits for help with the XRD analysis and Marion Meima and Sven Warris for help with the DNA extractions and bioinformatics.

6.5 REFERENCES

[1] L. Krayzelova, J. Bartacek, I. Díaz, D. Jeison, E.I. Volcke, P. Jenicek, Microaeration for hydrogen sulfide removal during anaerobic treatment: a review, Reviews in Environmental Science and Bio/Technology, 14 (2015) 703-725.

[2] L. Wenhui, G. Bo, Z. Zhongning, Z. Jianyong, Z. Dianwei, F. Ming, F. Xiaodong, Z. Lunju, L. Quanyou, H_2S formation and enrichment mechanisms in medium to large scale natural gas fields (reservoirs) in the Sichuan Basin, Petroleum Exploration and Development, 37 (2010) 513-522.

[3] D.A. Burns, J. Aherne, D.A. Gay, C. Lehmann, Acid rain and its environmental effects: Recent scientific advances, Atmospheric Environment, 146 (2016) 1-4.

[4] C. Buisman, R. Post, P. Ijspeert, G. Geraats, G. Lettinga, Biotechnological process for sulphide removal with sulphur reclamation, Acta biotechnologica, 9 (1989) 255-267.

[5] A. Janssen, R. Sleyster, C. Van der Kaa, A. Jochemsen, J. Bontsema, G. Lettinga, Biological sulphide oxidation in a fed-batch reactor, Biotechnology and bioengineering, 47 (1995) 327-333.

[6] J.B. Klok, G. van Heeringen, R. De Rink, H. Wijnbelt, Introducing the next generation of the THIOPAQ O&G process for biotechnological gas desulphurization: THIOPAQ-SQ, in: Sulphur, 2017.

[7] A.J. Janssen, P.N. Lens, A.J. Stams, C.M. Plugge, D.Y. Sorokin, G. Muyzer, H. Dijkman, E. Van Zessen, P. Luimes, C.J. Buisman, Application of bacteria involved in the biological sulfur cycle for paper mill effluent purification, Science of the total environment, 407 (2009) 1333-1343.

[8] E. Van Zessen, A. Janssen, A. De Keizer, B. Heijne, J. Peace, R. Abry, Application of THIOPAQ™ biosulphur in agriculture, in: Proceedings of the British Sulphus Events 2004 Sulphur Conference, Barcelona, Spain, 24-27 October 2004, 2004, pp. 57-68.

[9] R. De Rink, J.B. Klok, G.J. Van Heeringen, D.Y. Sorokin, A. Ter Heijne, R. Zeijlmaker, Y.M. Mos, V. De Wilde, K.J. Keesman, C.J. Buisman, Increasing the selectivity for sulfur formation in biological gas desulfurization, Environmental science & technology, 53 (2019) 4519-4527.

[10] J.B. Klok, P.L. van den Bosch, C.J. Buisman, A.J. Stams, K.J. Keesman, A.J. Janssen, Pathways of sulfide oxidation by haloalkaliphilic bacteria in limited-oxygen gas lift bioreactors, Environmental science & technology, 46 (2012) 7581-7586.

[11] P.L. Van Den Bosch, O.C. van Beusekom, C.J. Buisman, A.J. Janssen, Sulfide oxidation at halo-alkaline conditions in a fed-batch bioreactor, Biotechnology and bioengineering, 97 (2007) 1053-1063.

[12] K. Kiragosyan, P. Roman, K.J. Keesman, A.J. Janssen, J.B. Klok, Stoichiometry-driven heuristic feedforward control for oxygen supply in a biological gas desulfurization process, Journal of Process Control, 94 (2020) 36-45.

[13] A. ter Heijne, R. de Rink, D. Liu, J.B. Klok, C.J. Buisman, Bacteria as an electron shuttle for sulfide oxidation, Environmental science & technology letters, 5 (2018) 495-499.

[14] R. de Rink, J.B. Klok, G.J. van Heeringen, K.J. Keesman, A.J. Janssen, A. ter Heijne, C.J. Buisman, Biologically enhanced hydrogen sulfide absorption from sour gas under haloalkaline conditions, Journal of hazardous materials, 383 (2020) 121104.

[15] G. Ni, P. Harnawan, L. Seidel, A. Ter Heijne, T. Sleutels, C.J. Buisman, M. Dopson, Haloalkaliphilic microorganisms assist sulfide removal in a microbial electrolysis cell, Journal of hazardous materials, 363 (2019) 197-204.

[16] K. Rabaey, K. Van de Sompel, L. Maignien, N. Boon, P. Aelterman, P. Clauwaert, L. De Schamphelaire, H.T. Pham, J. Vermeulen, M. Verhaege, Microbial fuel cells for sulfide removal, Environmental science & technology, 40 (2006) 5218-5224.

[17] M. Sun, Z.-X. Mu, Y.-P. Chen, G.-P. Sheng, X.-W. Liu, Y.-Z. Chen, Y. Zhao, H.-L. Wang, H.-Q. Yu, L. Wei, Microbe-assisted sulfide oxidation in the anode of a microbial fuel cell, Environmental science & technology, 43 (2009) 3372-3377.

[18] B. Zhang, H. Zhao, C. Shi, S. Zhou, J. Ni, Simultaneous removal of sulfide and organics with vanadium (V) reduction in microbial fuel cells, Journal of Chemical Technology & Biotechnology, 84 (2009) 1780-1786.

[19] B. Ateya, F. AlKharafi, A. Al-Azab, Electrodeposition of sulfur from sulfide contaminated brines, Electrochemical and solid-state letters, 6 (2003) C137-C140.

[20] P.K. Dutta, K. Rabaey, Z. Yuan, J. Keller, Spontaneous electrochemical removal of aqueous sulfide, Water research, 42 (2008) 4965-4975.

[21] E. Vaiopoulou, T. Provijn, A. Prévoteau, I. Pikaar, K. Rabaey, Electrochemical sulfide removal and caustic recovery from spent caustic streams, Water research, 92 (2016) 38-43.

[22] N. Pfennig, K.D. Lippert, Über das vitamin B 12-bedürfnis phototropher Schwefelbakterien, Archiv für Mikrobiologie, 55 (1966) 245-256.

[23] D.J. O'Brien, F.B. Birkner, Kinetics of oxygenation of reduced sulfur species in aqueous solution, Environmental Science & Technology, 11 (1977) 1114-1120.

[24] P.L. Van den Bosch, D.Y. Sorokin, C.J. Buisman, A.J. Janssen, The effect of pH on thiosulfate formation in a biotechnological process for the removal of hydrogen sulfide from gas streams, Environmental science & technology, 42 (2008) 2637-2642.

[25] H.C. Lichstein, M.H. Soule, Studies of the effect of sodium azide on microbic growth and respiration: I. The action of sodium azide on microbic growth, Journal of bacteriology, 47 (1944) 221.

[26] M. Solioz, E. Carafoli, B. Ludwig, The cytochrome c oxidase of Paracoccus denitrificans pumps protons in a reconstituted system, Journal of Biological Chemistry, 257 (1982) 1579-1582.

[27] D.Y. Sorokin, M.S. Muntyan, A.N. Panteleeva, G. Muyzer, *Thioalkalivibrio sulfidiphilus* sp. nov., a haloalkaliphilic, sulfur-oxidizing gammaproteobacterium from alkaline habitats, International journal of systematic and evolutionary microbiology, 62 (2012) 1884-1889.

[28] D.Y. Sorokin, P. Van Den Bosch, B. Abbas, A. Janssen, G. Muyzer, Microbiological analysis of the population of extremely haloalkaliphilic sulfur-oxidizing bacteria dominating in lab-scale sulfide-removing bioreactors, Applied microbiology and biotechnology, 80 (2008) 965-975.

[29] G. Muyzer, D.Y. Sorokin, K. Mavromatis, A. Lapidus, A. Clum, N. Ivanova, A. Pati, P. d'Haeseleer, T. Woyke, N.C. Kyrpides, Complete genome sequence of "*Thioalkalivibrio sulfidophilus*" HL-EbGr7, Standards in genomic sciences, 4 (2011) 23-35.

[30] S.E. Hoeft, J.S. Blum, J.F. Stolz, F.R. Tabita, B. Witte, G.M. King, J.M. Santini, R.S. Oremland, *Alkalilimnicola ehrlichii* sp. nov., a novel, arsenite-oxidizing haloalkaliphilic gammaproteobacterium capable of chemoautotrophic or heterotrophic growth with nitrate or oxygen as the electron acceptor, International journal of systematic and evolutionary microbiology, 57 (2007) 504-512.

[31] D.Y. Sorokin, T.N. Zhilina, A.M. Lysenko, T.P. Tourova, E.M. Spiridonova, Metabolic versatility of haloalkaliphilic bacteria from soda lakes belonging to the *Alkalispirillum–Alkalilimnicola* group, Extremophiles, 10 (2006) 213-220.

[32] D.Y. Sorokin, A.Y. Merkel, Desulfurivibrio, in: W.B. Whitman (Ed.) Bergey's Manual of Systematics of Archaea and Bacteria, John Wiley & Sons, 2020.

[33] D.Y. Sorokin, T. Tourova, M. Mußmann, G. Muyzer, *Dethiobacter alkaliphilus* gen. nov. sp. nov., and *Desulfurivibrio alkaliphilus* gen. nov. sp. nov.: two novel representatives of reductive sulfur cycle from soda lakes, Extremophiles, 12 (2008) 431-439.

[34] A. Poser, R. Lohmayer, C. Vogt, K. Knoeller, B. Planer-Friedrich, D. Sorokin, H.-H. Richnow, K. Finster, Disproportionation of elemental sulfur by haloalkaliphilic bacteria from soda lakes, Extremophiles, 17 (2013) 1003-1012.

[35] C. Thorup, A. Schramm, A.J. Findlay, K.W. Finster, L. Schreiber, Disguised as a sulfate reducer: growth of the deltaproteobacterium *Desulfurivibrio alkaliphilus* by sulfide oxidation with nitrate, MBio, 8 (2017).

[36] H. Müller, J. Bosch, C. Griebler, L.R. Damgaard, L.P. Nielsen, T. Lueders, R.U. Meckenstock, Long-distance electron transfer by cable bacteria in aquifer sediments, The ISME journal, 10 (2016) 2010-2019.

[37] D.J. Walker, R.Y. Adhikari, D.E. Holmes, J.E. Ward, T.L. Woodard, K.P. Nevin, D.R. Lovley, Electrically conductive pili from pilin genes of phylogenetically diverse microorganisms, The ISME journal, 12 (2018) 48-58.

CHAPTER 7

Bacteria determine the measured oxidation reduction potential in the biological gas desulfurization process

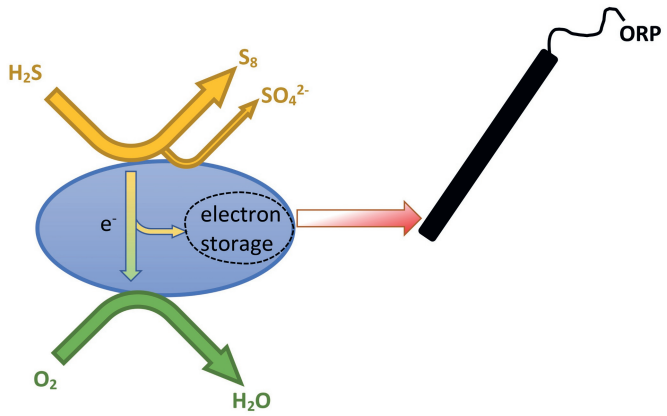

Abstract – In the biotechnological gas desulfurization process, dissolved sulfide is oxidized into predominantly elemental sulfur (S_8) by sulfide oxidizing bacteria (SOB) under strict oxygen limited conditions. Online measurement of the oxygen reduction potential (ORP) is used to control the O_2 supply to the bioreactor to maximize the selectivity for S_8 formation and minimize unwanted sulfate formation. While ORP in the bioreactor is considered to be a measure of mainly the sulfide and oxygen concentrations, in practice, none of these components are detectable. Recently, it was shown that SOB can shuttle electrons from sulfide to an electrode. In this study, we investigated the sensitivity of stored charge in SOB towards ORP. In batch experiments under anaerobic conditions, the step change in measured ORP was -275 mV after the addition of 0.2 mM sulfide without SOB, whilst ORP decreased only with a step of -180 mV when SOB were present. Furthermore, stored charge in SOB was measured in an electrochemical cell. These SOB were harvested from a pilot-scale desulfurization installation, which was operated at different ORP setpoints (-250 to -390 mV vs Ag/AgCl) in the aerated bioreactor, in which sulfide was not detectable. It was found that more charge was recovered from SOB when ORP in the aerated bioreactor was lower. These measurements were used to calibrate a model to describe the ORP based on charge storage in SOB, which showed that sulfate formation decreases when SOB contain more charge. Our results can be used to further optimize efficiency of the biological desulfurization process.

Rieks de Rink, Dandan Liu, Annemiek ter Heijne, Cees J.N. Buisman, Johannes B.M. Klok. Bacteria determine the measured oxidation reduction potential in the biological gas desulfurization process (submitted)

7.1. INTRODUCTION

In the 1990's a biological desulfurization process was developed for the removal and conversion of toxic H_2S from sour gas streams [1-3]. In this process, H_2S is absorbed in an haloalkaline process solution (i.e. >1 M Na^+ with (bi)carbonate buffer and pH 8-10) and subsequently oxidized into predominantly elemental sulfur (S_8) by haloalkaliphilic sulfide oxidizing bacteria (SOB). S_8 is harvested from the process solution by gravity settling and/or centrifugation and can be reused, for example as agricultural fertilizer [4, 5]. The main reaction equations are shown in Table 7.1.

Besides formation of S_8 (Table 7.1, reaction 4), the by-products sulfate (SO_4^{2-}) and thiosulfate ($S_2O_3^{2-}$) are formed (Table 7.1, reactions 5 and 6). SO_4^{2-} is produced biologically at excess oxygen supply [6-10], whereas formation of $S_2O_3^{2-}$ is due to a chemical reaction between sulfide and oxygen [6, 11-13]. SO_4^{2-} and $S_2O_3^{2-}$ production are unwanted because of the corresponding proton formation. This requires addition of NaOH to maintain the alkalinity of the process solution. Furthermore, formation of a bleed stream is required to prevent accumulation of the sodium salts SO_4^{2-} and $S_2O_3^{2-}$.

To obtain a high selectivity for S_8 formation, the O_2 should be supplied in optimal proportion to the supplied H_2S and should be controlled at very low concentrations. The term selectivity is generally applied in chemical engineering to describe the mole fractions of

Table 7.1: Main reactions in the biological desulfurization process under haloalkaline conditions *[7, 8, 14].*

Number	Reaction equation	Description of the reaction
1	H_2S (aq) ⇋ HS^- + H^+	H_2S deprotonation (absorber, chemical)
2	HS^- + $\frac{x-1}{8}$ S_8 (s) ⇋ S_x^{2-} + H^+	Polysulfide formation (absorber, chemical)
3	CO_2 + H_2O ⇋ HCO_3^- + H^+	CO_2 dissociation (absorber, chemical)
4	HS^- + ½ O_2 ⟶ ⅛ S_8 (s) + OH^-	Sulfur formation (aerated bioreactor, biological)
5	HS^- + 2 O_2 ⟶ SO_4^{2-} + 2 H^+	Sulfate formation (aerated bioreactor, biological)
6	HS^- + O_2 ⟶ ½ $S_2O_3^{2-}$ + ½ H_2O	Thiosulfate formation (aerated bioreactor, chemical)

substrate converted into the end-product. In full-scale systems, the O_2 supply is controlled via the online measurement of the ORP (oxidation/reduction potential) in the bioreactor [2]. A PI controller is applied to adjust the air flow rate to the bioreactor to maintain a pre-set ORP value. In the biodesulfurization process, the ORP is typically controlled in the range of -250 to -450 mV vs Ag/AgCl [15]. The ORP is an overall parameter and can be described thermodynamically by the Nernst equation when the solution is in equilibrium (Equation 7.1).

$$E_H = E_H^0 + \frac{RT}{nF} \cdot \ln\left(\frac{\prod Ox}{\prod Red}\right) \quad \text{(Equation 7.1)}$$

Here, E_H is the ORP potential (in equilibrium), E_H^0 is the reference potential, R is the gas constant, T is the temperature, n is the number of electrons involved in the redox reaction, F is the faraday constant, $\prod$ox is the sum of oxidation species in the solution and $\prod$Red is the sum of reducing species in the solution. The ORP is mainly dependent on components that can accept or donate electrons, but other parameters, like pH, temperature and dissolved salts will influence the ORP as well [2].

In previous research, the ORP in the biodesulfurization process was assumed to be mainly dependent on the electron donor sulfide (which decreases the ORP) and the electron acceptor dissolved oxygen (which increases the ORP) [2, 16]. To describe the dependency of ORP on the sulfide and dissolved O_2 concentration, Klok et al. proposed the following equation, which is based on the Nernst equation (Equation 7.2) [16]:

$$ORP = \xi 1 + \xi 2 \log(\gamma_{O_2}) + \xi 3 \log(\gamma_{HS^-}) \quad \text{(Equation 7.2)}$$

In Equation 7.2, $\xi 1, \xi 2$ and $\xi 3$ are empiric parameters and γ_{O_2} and γ_{HS^-} the activity coefficients of O_2 and HS^- (see also appendix A of Kiragosyan et al. [17]). The calibrated model was used to describe the operation a full-scale biological desulfurization system [16]. This model was validated based on real dynamic data of the same full scale plant and was able to accurately predict the ORP behaviour of the system and its end-product formation rates [16]. Since the solution in the bioreactor of the biodesulfurization process is not in equilibrium, the measured ORP is mainly determined by the component with the highest electron exchange density with the ORP electrode [2]. Despite an accurately predicted ORP, a striking discrepancy between the model of Klok et al. and the actual

operation was found: The model predicted concentrations of dissolved oxygen and sulfide in the detectable range [16], while in practice, these are below the detection limit [10].

Recently, it was shown that SOB taken from the biodesulfurization process are able to store charge from sulfide oxidation and can be discharged at the anode of an electrochemical cell [18]. Sulfide uptake was also observed in the anaerobic bioreactor in a continuously operated system [19, 20]. Thus, bacteria are 'charged' in the anaerobic reactor and 'discharged' in the aerated reactor. We hypothesize that, since SOB can also exchange electrons with an electrode, the charge stored in SOB also contributes to the measured ORP of the process solution. The aim of this study is to elucidate the relation between ORP and charge storage in SOB and how this affects product formation.

7.2 Materials and Methods

7.2.1 Batch experiments

Batch experiments were performed in 20 mL glass reactors in a water bath that was controlled at 35 °C. Reactors were equipped with a magnetic stirrer. The reactors were closed and supplied with a dissolved oxygen (DO) sensor (PSt3, PreSens Precision Sensing GmbH, Regensburg, Germany) and a redox sensor (ProSense, Ag/AgCl reference electrode, Oosterhout, the Netherlands). Measurements were done with either a 1.0 M $NaHCO_3$ / Na_2CO_3 solution (pH 8.5) or a bioreactor solution taken from a full-scale biodesulfurization plant as described by Klok et al. [21]. Solutions were flushed for 5 min with compressed air through a small hole in the cap of the reactors, after which the ORP was measured. Thereafter, the solutions were flushed with N_2 until the measured DO was below detection limit (i.e. <15 ppb). ORP was measured again. Subsequently, 64 µL of either an HS^- or S_x^{2-} stock solution was added. In both cases, the initial sulfide concentration in the reactor was 0.2 mM. An HS^- stock was prepared by dissolving Na_2S flocks $Na_2S.3H_2O$ (Analar NORMAPUR, VWR, analytical grade) in anaerobic demineralized water. A polysulfide (S_x^{2-}) stock solution was prepared by dissolving Na_2S in demineralized water with an excess of biologically produced sulfur particles, which were obtained from the sulfur cake produced in a full-scale plant. After injection of sulfide, a small N_2 purge was applied on the headspace of the reactors to prevent ingress of O_2, while ORP was measured and recorded every minute.

7.2.2 SET-UP OF THE PILOT-SCALE BIODESULFURIZATION INSTALLATION

The pilot-scale biodesulfurization installation ('pilot plant') consisted of an absorber, an anaerobic bioreactor and an aerated bioreactor (see Figure 7.1). N_2, CO_2 and H_2S were supplied via mass-flow controllers (Brooks instruments, USA) to the absorber column. The absorber column was a 4 m stainless steel column with a diameter of 5 cm and contained 2 m packing where counter-current gas/liquid contact took place. The packing consisted of glass spheres with a diameter of 1 cm. Process solution from the aerated bioreactor without sulfide ('lean solution') was pumped to the top of the absorber column. The solution flowed downwards, absorbing practically all H_2S and some CO_2. The treated gas was leaving the absorber at the top. The 'rich solution' was collected at the bottom of the absorber and pumped to an anaerobic bioreactor.

The anaerobic bioreactor was a glass vessel with a liquid volume of 3.4 L, which was mixed with a mechanical mixer. A small stream of N_2 was supplied to the headspace of the reactor to ensure anaerobic conditions. The pH and ORP were measured online by a combined SE552/2 Inducon ORP/pH sensor, connected to a Stratos Pro Transmitter (Knick, Germany). An integrated Ag/AgCl electrode was used as a reference for the ORP and pH measurement. The flow of rich solution from the anaerobic bioreactor to the aerated bioreactor was driven by a peristaltic pump (Watson and Marlow).

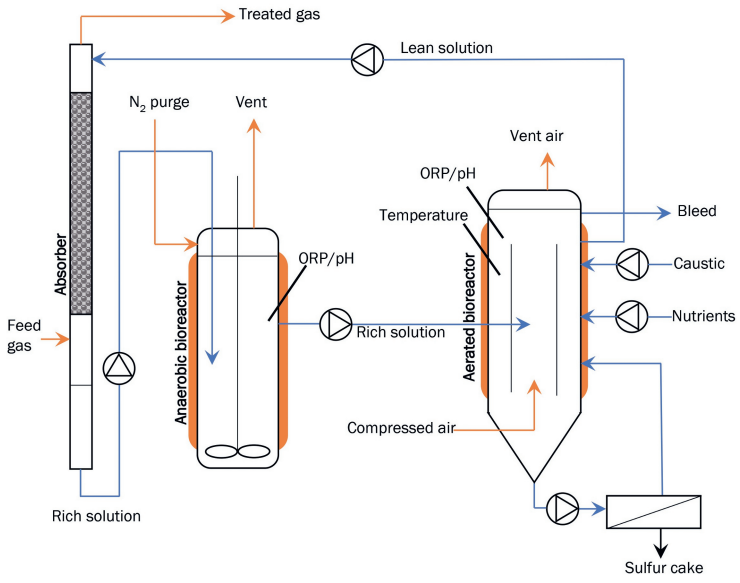

Figure 7.1: Set-up of the pilot plant. Blue lines represent liquid flow; orange lines represent gaseous flows. The bioreactors were temperature controlled with a water jacket (indicated in orange)

The aerated bioreactor was a glass vessel with a volume of 11.4 L, with dimensions 690/150 mm (H/D). This was a gas lift reactor with riser / downer system. A combined ORP/pH probe was used to measure the pH and ORP value in the bioreactor. The ORP in the aerated bioreactor was maintained at a constant pre-set value by automatic adjustment of the air flow rate of compressed air, using a programmable logic controller (PLC). Compressed air was supplied with a mass flow controller (Brooks Instruments, USA) via an air sparger, and was injected at the bottom of an internal cylinder, just above the inlet of the rich solution from the anaerobic bioreactor.

Caustic and nutrients were dosed to the aerated bioreactor via a pulse/pause timer. An effluent stream (bleed) was overflowing from the aerated bioreactor to maintain a constant liquid level. Warm water from a thermostatic bath was routed through the water jackets of the aerated and anaerobic bioreactor. The temperature in the aerated bioreactor was maintained at 37-38 °C. The aerated bioreactor had a conical bottom where elemental sulfur settled. The underflow of the conical bottom was routed to a decanter centrifuge via a pump. The centrate from the decanter was routed back into the aerated bioreactor. Elemental sulfur was recovered as a sulfur cake. Liquid samples for analyses were taken from the sample port of the lean solution from the aerated bioreactor.

7.2.3 MEASUREMENT OF CHARGE STORAGE IN SOB AT DIFFERENT ORP VALUES

7.2.3.1 Operation of the pilot plant

To study the relation between ORP and charge storage in SOB, biomass from the aerated bioreactor of the pilot was collected to perform discharge measurements. The pilot plant was operated at 2 different conditions. Under condition 1, the feed gas flow rate to the absorber was 103.5 NL h^{-1} (normal liter per hour) and consisted of 3.38% H_2S, 48.31% CO_2 and 48.31 % N_2. The sulfur load was 120.2 g-S day^{-1} and the lean solution flow to the absorber was 11 kg h^{-1} (10.5 L h^{-1}). After ORP experiments for condition 1, the CO_2 flow rate was decreased in order to increase the pH of the process solution. Under condition 2, the feed gas flow rate was 102.5 NL h^{-1} and consisted of 2.44 % H_2S, 4.88 % CO_2 and 92.68 % N_2. The sulfur load was 85.9 g-S day^{-1}, which has to be decreased due to an apparent lower biological activity. During discharge experiments under conditions 1, the biomass concentration was 53 mg-N L^{-1} and the pH was 8.5. During discharge experiments under condition 2, the biomass concentration was 104 mg-N L^{-1} and the pH was 9.2. During normal operation under both operational conditions, the redox setpoint in the aerated

bioreactor was maintained at -370 mV. For both conditions, the ORP setpoint was changed step-wise. The initial measurement was done at the original redox setpoint of -370 mV. Thereafter, the redox setpoint was changed to -390 mV and subsequently -330 mV and -250 mV (condition 1) and -350 mV and -330 mV (condition 2). Each ORP setpoint was maintained for 1-2 hours; the biomass samples were taken from the aerated bioreactor at least 30 minutes after the redox setpoint was changed. -390 mV was the lowest ORP setpoint applied, as sulfide started to accumulate in the process solution at an ORP of ≤ -400mV.

During experiment 1, after the measurement at -250 mV, the airflow was further increased from 50 to 200 NL h^{-1}. However, the redox potential did not increase and remained fluctuating between -250 and -200 mV.

The ORP experiment for condition 1 was performed when the pilot plant had been in operation for 37 days. For condition 2, the pilot plant had been in operation for 16 days. In the supporting information, details can be found of the bioreactor solution composition in the pilot during ORP experiments (SI 6.1) and composition of the microbial community (SI 6.2).

7.2.3.2 Discharge measurements in an electrochemical cell

The electrochemical system was of a 2-compartment reactor, consisting of 2 180 mL glass bottles, separated by a cation exchange membrane of 8 cm^2 (Fumatech, Germany). Graphite rod electrodes (Müller & Rössner GmbH, Germany), with a diameter of 5 mm and a submerged area of 6.8 cm^2, were used as working and counter electrodes. The reference electrode was an Ag/AgCl, 3 M KCl electrode (+0.21 V vs SHE) (Prosense, the Netherlands), connected to the anode chamber via a capillary. The anode chamber was flushed with N_2 gas for 5 min before the bioreactor solution from the pilot was injected and was stirred with a magnetic stirrer. The catholyte was a 1 M $NaHCO_3$ solution. The electrodes were connected to a potentiostat (nStat, multichannel, Ivium, the Netherlands). The discharge measurements were conducted for 10 minutes at an anode potential of 0.1 V vs Ag/AgCl, as applied before [18]. Before each experiment, the anode chamber was cleaned with demineralized water and the anode was cleaned using sandpaper. When the redox potential in the aerated bioreactor of the biodesulfurization system had stabilized at the required potential, a sample of 120 mL from the aerated bioreactor of the pilot-scale biodesulfurization set-up was transferred (anaerobically) to the anodic chamber of this

electrochemical system. For each redox potential, at least 2 discharge measurements were performed. Furthermore, 1 discharge test was performed on the sample's supernatant (i.e. without SOB) after centrifugation for 10 min at 10000 rpm to determine charge in the medium.

7.2.4 ANALYSIS

The biomass concentration was measured as the amount of total organic N using the Dr. Lange cuvette test LCK138 (Hach Lange, Germany), as described by [20]. The difference between the supernatant (i.e., a sample centrifuged for 10 min at 14000 g) and a non-centrifuged sample indicated the total amount of N present in the (suspended) biomass. To exclude interference by salts and biologically produced S^0, the samples were diluted at least 5 times. Sulfide concentration in the batch experiments was analyzed using a modified methylene blue method as described elsewhere [8]. During the discharge experiments, the presence of dissolved HS^- and polysulfide in the aerated bioreactor was checked at each ORP setpoint with lead acetate paper (Merck, Germany).

7.2.5 MODELLING CHARGE STORAGE IN SOB

In Equation 7.2 (proposed by Klok et. al.), the ORP is a function of sulfide and O_2. Our hypothesis is that ORP is also dependent on charge stored by SOB. To relate ORP to stored charge in SOB, we propose the following empiric model:

$$ORP = p1 + p2 \cdot \log(\Upsilon) \qquad \text{(Equation 7.3)}$$

In Equation 7.3, Υ represents the charge harvested from SOB during 10 minutes in the discharge measurements (mC), $p1$ (mV) and $p2$ (mV/log(mC)) are empiric parameters which were estimated via a non-linear least square parameter routine, as described in the Supporting Information (SI 6.3). As some charge was harvested from the supernatant of the bioreactor solution (i.e. without SOB), Υ was determined according to Equation 7.4.

$$\Upsilon = \Upsilon_{sol} - \Upsilon_{sup} \qquad \text{(Equation 7.4)}$$

Where the indices *sol* represents the bioreactor solution and *sup* represents the supernatant of the bioreactor solution.

7.2.6 Relation between charge storage in SOB and product formation

In another study [22], 7 long-term experiments were performed in the pilot plant with the aim to investigate the effect of different process conditions on the product selectivities. In these long-term experiments, product selectivities and biomass concentration were regularly measured. Data from these long-term experiments were used to determine the relation between charge storage in SOB and product formation.

The developed model (i.e. Equation 7.3) was used to calculate the average specific charge in the SOB (χ, mC L mg-N^{-1}) from the measured ORP and biomass concentration, and the determined values of p1 and p2, according to Equation 7.5.

$$\chi(ORP) = \frac{1}{Xb} \cdot 10^{\left(\frac{ORP-p1}{p2}\right)} \quad \text{(Equation 7.5)}$$

Where Xb the measured biomass concentration (mg-N L^{-1}).

7.3 Results and discussion

7.3.1 Batch experiments

To obtain insight in the effect of SOB and sulfide (in absence of O_2) on the ORP of the process solution, batch tests were performed with SOB (bioreactor solution with a biomass concentration of 41 mg-N L^{-1}) and without SOB ((bi)carbonate buffer solution). The results are shown in Figure 7.2.

The initial ORP values of the (bi)carbonate buffer solution and bioreactor solution after aeration and flushing with N_2 were similar (around -150 mV). After addition of 2 mM HS^- or S_x^{2-}, the ORP of the solution with SOB decreased to -340 mV after 1 min, while the ORP of the solution without SOB decreased to -417 mV (for HS^-) and -419 mV for (S_x^{2-}). Within two minutes after the addition of sulfide, the measured ORP for the solution with SOB started to increase and stabilized at -328 mV (HS^-) and -325 mV (S_x^{2-}). The ORP of the solution without SOB did not increase and stabilized at -431 mV (HS^-) and -423 mV (S_x^{2-}). After 20 min, no residual sulfide was detected in the solution with SOB, indicating the sulfide had been removed from solution by SOB under anaerobic conditions. No removal of sulfide from the (bi)carbonate buffer solution was observed. The biological uptake of sulfide under anaerobic condition has been observed before both in batch tests [18] as in previous experiments in the pilot biodesulfurization installation [19, 20]. These results indicate that,

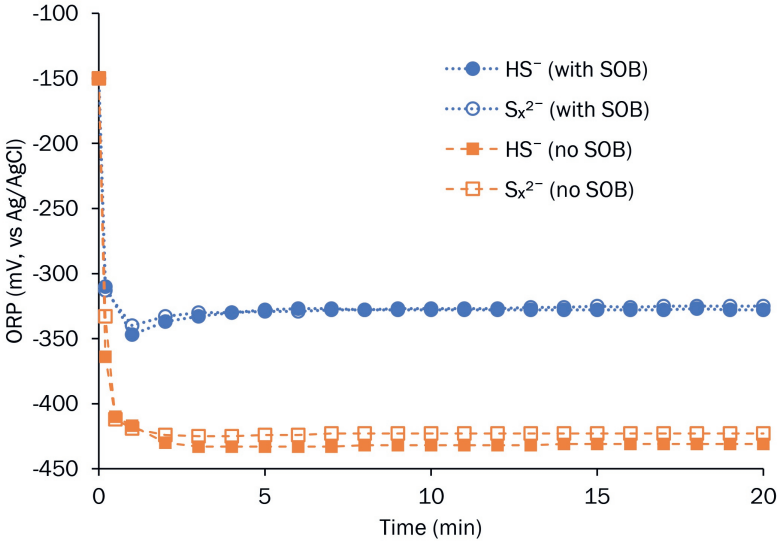

Figure 7.2: Results of effect on ORP with addition of sulfide and in polysulfide as obtained in the batch tests. The blue dots are analysis with SOB and orange squares without SOB. The closed symbols represent analysis with addition of HS^- and open symbols with S_x^{2-}.

besides O_2 and sulfide, the ORP is influenced by SOB. Since the ORP is expressed on a logarithmic scale, a difference between -325 mV (with SOB) and -425 mV (without SOB) is a considerable difference.

In previous research, it has been shown that different microbial communities have a different charge storing capacity. Furthermore, the community with a lower charge storing capacity produced less electricity in an electrochemical cell [18]. This might suggest that different microbial communities have a different effect on the ORP.

7.3.2 DISCHARGE EXPERIMENTS

Results of the discharge experiments are shown in Figure 7.3. The bar graphs represent the absolute amount of recovered charge in the electrochemical cell after 600 sec at an applied anode potential of 0.1 V vs Ag/AgCl. At none of the measurements, free sulfide was present in the solution. In experiment 1 (fig 2A), for ORP setpoints of -390 to -330mV, more charge was recovered from the sample taken from the aerated bioreactor at a lower (more negative) ORP in the aerated bioreactor. At an ORP setpoint of -390 mV, the recovered charge was 28.8 ± 5.14 mC and at -330 mV 2.0 ± 0.12 mC. At -250 mV, the recovered

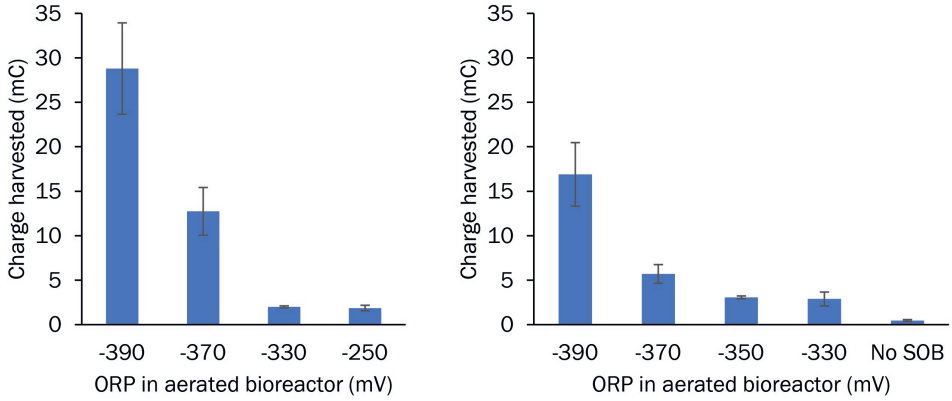

Figure 7.3: Results of the discharge experiments. The bar graphs indicate the charge harvested from the solution of the aerated bioreactor at different ORP's. The recovered charge is obtained by discharge for 600 sec at an applied anode potential of 0.1 V vs Ag/AgCl. The left plot shows results of experiment 1, the right plot shows results of experiment 2. Average values are shown for two or three replicates; the error bar indicates the standard deviation.

charge was 1.9 ± 0.31 mC. Thus, increasing the ORP from -330 mV to -250 mV did not lead to more recovered charge.

Afterwards, the redox potential was restored at -370 mV, and charge recovery was 8.4 ± 1.6 mC, which was lower than the first measurement at -370 mV (12.7 ± 12.1 mC) (data not shown). Online data of ORP and air flow rate in the aerated bioreactor during experiment 1 can be found in the Supporting Information (SI 6.4).

During experiment 2, the same trend as in experiment 1 was observed for redox potentials between -390 mV and -350 mV. Charge recovery at ORP setpoints of -350 mV and -330 mV was similar. During experiment 2, a discharge experiment was performed in which the SOB were removed from the bioreactor solution by centrifugation prior to injection into the electrochemical cell to quantify the charge recovered from the solution without SOB. In this experiment, the recovered charge was 0.46 ± 0.1 mC, showing that the contribution of reactor solution to total charge was negligible (in accordance with Ter Heijne et al., 2018). At the time this sample was taken, the aerated bioreactor was operated at -370 mV.

For both experiments, the total charge was higher at a lower (more negative) ORP values, indicating that SOB contain more charge when the bioreactor is operated at a lower ORP. Furthermore, for ORP values of -370 mV and -390 mV, the recovered charge in experiment

2 was lower than in experiment 1, i.e. less charge was recovered from the SOB in experiment 2. This could be due to differences in the H_2S-load, pH and biomass concentration. These results show that a lower ORP of the process solution results in a higher amount of stored charge in the SOB for ORP values between -390 mV – -350 mV.

7.3.3 Modelling charge storage in SOB

Based on the discharge measurements, the proposed empirical model for ORP (Equation 7.3) was calibrated. The empirical values of $p1$ and $p2$ were found to be -322.5 ± 7.1 mV and -49.9 ± 7.9 mV. The model fit on the experimental data is shown in Figure 7.4. The calibrated model is not a generic model as the characteristics of the electrochemical cell which was used to recover charge, highly influences the total recovered charge (e.g. electrode surface area and cell volume). However, for our experiments the empirical model describes the measured data well for the ORP range of -390 mV to -330 mV vs Ag/AgCl, which is the typical operation window for the biological gas desulfurization process [8, 15, 20, 23]. The recovered charge at an ORP of -250 mV in experiment 1 was not considered in the model fit, as this value is outside the trend of the other measurements (see Figure 7.4). Note that the value of $p2$ is negative, which indicates that the stored charge in the bacteria shows similar behavior as a reductant as described with the Nernst equation. Hence, an increased stored charge will result in a decreasing ORP value.

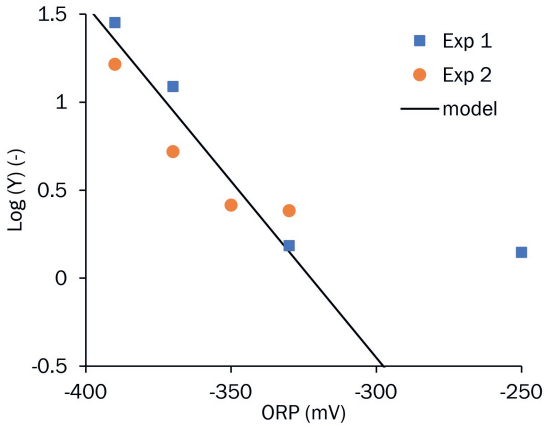

Figure 7.4: Model results for the relation between ORP and charge storage (Y) in SOB based on the discharge measurements.

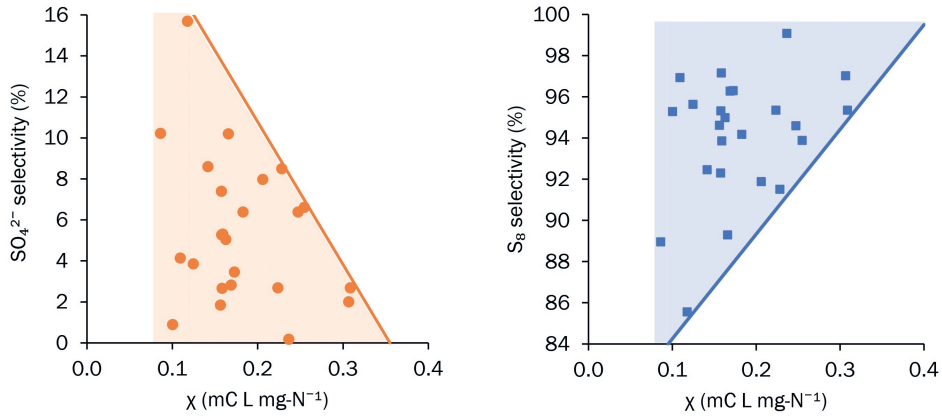

Figure 7.5: Relationship between calculated specific charge in SOB (according to the model as described in section 3.3) and the product selectivities in 7 long-term experiments in the pilot-scale desulfurization installation operated under varying conditions. selectivity for SO_4^{2-} formation (orange dots) and selectivity for S_8 formation (blue squares). The orange dots represent the measured selectivities for SO_4^{2-} formation and blue squares the measured selectivities for S_8 formation. The solid lines represent the linear relation between the specific stored charge in the bacteria and the maximum selectivity for SO_4^{2-} formation / minimum selectivity for S_8 formation that can be obtained.

7.3.4 Product formation in SOB

Data of 7 long-term experiments in the pilot plant were used to assess the relation between the calculated average specific charge in SOB (χ) and the measured selectivities for SO_4^{2-} and S_8 formation. The results are shown in Figure 7.5. The data points show scattering. For example, for values of χ between 0.1-0.2 mC L mg-N^{-1}, selectivities for SO_4^{2-} formation are in the range of 0-15 mol% and selectivities for S_8 formation are in the range of 84-97 mol%. Besides SO_4^{2-} and S_8, also $S_2O_3^{2-}$ is formed and therefore the selectivities of SO_4^{2-} and S_8 formation do not always sum up to 100%. Thus, there doesn't seem to be a clear relationship between χ and product formation. However, for higher values of χ, the maximum selectivity for SO_4^{2-} that is obtained, decreases and the minimum selectivity for S_8 formation increases. The high(er) selectivities for SO_4^{2-} formation and lower selectivities for S_8 formation were related to lower specific charge (i.e. < 0.2 mC L mg-N^{-1}). We found linear relations between χ and the boundaries of the selectivies for SO_4^{2-} and S_8 formation. The relation between χ and the maximum selectivity for SO_4^{2-} formation that can be obtained is indicated with the orange solid line in Figure 7.4; the relation between χ and the minimum selectivity for S_8 formation that is obtained is indicated with the blue solid

line. These lines thus show the maximum selectivity for SO_4^{2-} and minimum selectivity for S_8 formation in relation to specific stored charge. The scattering could be explained by the fact that, besides χ, more factors are affecting product formation, such as the composition of the microbial community. NGS analysis revealed that the microbial composition in the process fluctuates [22]. SO_4^{2-} formation only occurs when bacteria are present that can form SO_4^{2-}. Thus, even when the specific charge of the SOB is below <0.3 mC L mg-N^{-1} the selectivity for SO_4^{2-} formation can still be low when the bacterial population is dominated by SOB that are limited to the formation of S_8 [20, 24, 25]. Another aspect of the microbial composition is that a fraction of the bacteria in the system does not belong to the class of SOB. This fraction is also measured as part of the overall biomass concentration, and therefore influences χ.

Since the ORP setpoint during these 7 long term experiments was always controlled at -370 mV or -380 mV, χ was predominantly sensitive for the biomass concentration, which varied between 25 – 115 mg-N L^{-1}. In general, at higher H_2S loading rates, a higher biomass concentration is required to oxidize all sulfide. On the other hand, at constant ORP, χ becomes lower when the biomass concentration increases (see Equation 7.5).

In previous work with neutrophilic *Thiobacillus* species by Visser et al. [9], it has been shown that biological product formation is determined by the reduction degree of the cytochrome pool, which depends on the O_2/H_2S supply ratio. When the O_2 supply is constant, an increase in the sulfide loading rate results in an increase in S_8 formation and a decrease in SO_4^{2-} formation. This coincided with an increasing reduction degree of the cytochrome pool. When the reduction degree approached 100%, no SO_4^{2-} was formed anymore. The reduction degree of the cytochrome pool is the fraction of cytochromes that are in the reduced form [10].

Our work shows that selectivity for sulfate and sulfur formation is related to the specific stored charge. When the specific stored charge in the bacteria increased, less SO_4^{2-} was formed and more S_8. Therefore, we hypothesize that the charge storage in the bacteria is proportional to the reduction degree of the cytochrome pool. At lower specific charge in SOB, the reduction degree of the bacteria is lower and therefore, more SO_4^{2-} is formed [9, 10], (Figure 7.4). The total amount of charge stored in SOB is determined by the ORP, but the average specific charge is also determined by the biomass concentration. Therefore, the interplay between ORP setpoint and biomass concentration influences the product

selectivities in the biological gas desulfurization process. Thus, at higher biomass concentration, the ORP setpoint should be decreased to obtain high selectivity for S_8 formation.

7.3.5 CONSIDERATIONS

In this paper we show that the ORP of the process solution in the biodesulfurization process is also determined by the SOB. The behavior of the ORP upon addition of sulfide is different in the presence of SOB than without SOB. Furthermore, SOB in the aerated bioreactor contain charge; this charge can be measured in an electrochemical system. The amount of charge in the SOB is dependent on the applied ORP in the aerated bioreactor. Hence, the ORP setpoint determines electrons stored in SOB. A lower ORP results in higher charge storage. Moreover, the amount of charge in SOB at a certain ORP is also related to process conditions. For example, in the discharge experiments (experiment 1), 2 discharge measurements were performed at an ORP of -370mV (before and after the ORP setpoint was increased to -250mV). The amount of harvested charge was higher before the ORP setpoint was increased to -250 mV than after.

We hypothesize that the amount of harvested charge is proportional to the reduction degree (of the cytochrome pool) of the bacteria. In the biological desulfurization process this reduction degree of the bacteria is determined by the O_2/H_2S supply ratio. In the biodesulfurization process, the ORP is used to control O_2 supply. However, a link between reduction degree and ORP has not been studied yet. By lowering the ORP setpoint, the reduction degree of bacteria increases, and thus the bacterial end-product formation shifts from SO_4^{2-} formation to S_8 formation [9, 16].

Our results also show the limitations of an ORP based control strategy, because it is an indirect measurement and ORP is dependent on several parameters, which are influenced by process fluctuations. Kiragosyan et al. investigated a feedforward control strategy based on the O_2/H_2S supply [17]. In this control strategy, the O_2 supply was adjusted based on the H_2S supply in order to maintain a constant O_2/H_2S supply. It was shown that this control strategy resulted in higher selectivities for S_8 formation than a feedback control strategy based on the measurement of ORP, especially when the H_2S-supply fluctuated. However, the disadvantage of this feedforward control strategy is the need of more (complex) instrumentation to accurately determine the H_2S supply and O_2 consumption. This requires

measurements of the feed gas flow rate, its H_2S concentration and the O_2 concentration in the vent air of the bioreactor.

The model that we have developed is an empiric model, and the total charge obtained only applies for the discharge conditions in the electrochemical cell that was used in our experiments. However, the principles that are outlined here, can be used to develop a more generic model to describe the relation between ORP, charge storage in SOB and product formation. That would also require measurement of the reduction degree of the SOB, for example via an electrochemical measurement. Online measurement of the reduction degree of the bacteria would allow for an advanced control strategy to maximize S_8 formation in biological gas desulfurization systems.

ORP-based control strategies are applied in many biological processes, both aerobic and anaerobic processes. Examples are nitrification/denitrification, nutrient removal, perchlorate reduction and anaerobic digestion [26-31]. In these other types of biological processes, the presence of (certain types of) microorganisms may also have an effect on the measured ORP. For these processes, the ORP based control may thus also be further improved by better understanding the relation between microorganisms and the ORP.

7.4 Conclusions

The ORP in the bioreactor of the biological desulfurization process was always considered to be dependent on the sulfide and oxygen concentration. However, both are undetectable in the bioreactor. We demonstrate that the SOB in the bioreactor also determine the measured ORP. The SOB contain charge and this charge can be measured at the anode of an electrochemical cell. The charge of the bacteria in the bioreactor is dependent on the ORP setpoint in the bioreactor: At a lower ORP, SOB contain more charge. Furthermore, the charge storage could be linked to the product formation. When the calculated specific stored charge in the bacteria is higher, the maximum selectivity for SO_4^{2-} formation decreases. At the same time, the minimum selectivity for S_8 formation increases. Thus, a higher specific charge leads to a better process performance in terms of product formation. These results reveal the limitations of the ORP based control strategy that is applied in all full-scale biodesulfurization plants. Furthermore, our results may provide useful insights for other biological processes with an ORP-based control strategy.

7.5 REFERENCES

[1] C. Buisman, R. Post, P. Ijspeert, G. Geraats, G. Lettinga, Biotechnological process for sulphide removal with sulphur reclamation, Acta biotechnologica, 9 (1989) 255-267.

[2] A. Janssen, S. Meijer, J. Bontsema, G. Lettinga, Application of the redox potential for controling a sulfide oxidizing bioreactor, Biotechnology and bioengineering, 60 (1998) 147-155.

[3] A.J. Janssen, P.N. Lens, A.J. Stams, C.M. Plugge, D.Y. Sorokin, G. Muyzer, H. Dijkman, E. Van Zessen, P. Luimes, C.J. Buisman, Application of bacteria involved in the biological sulfur cycle for paper mill effluent purification, Science of the total environment, 407 (2009) 1333-1343.

[4] E. Van Zessen, A. Janssen, A. De Keizer, B. Heijne, J. Peace, R. Abry, Application of THIOPAQ™ biosulphur in agriculture, in: Proceedings of the British Sulphus Events 2004 Sulphur Conference, Barcelona, Spain, 24-27 October 2004, 2004, pp. 57-68.

[5] A.R. Mol, R.D. van der Weijden, J. Klok, C.J. Buisman, Properties of sulfur particles formed in biodesulfurization of biogas, Minerals, 10 (2020) 433.

[6] A. Janssen, R. Sleyster, C. Van der Kaa, A. Jochemsen, J. Bontsema, G. Lettinga, Biological sulphide oxidation in a fed-batch reactor, Biotechnology and bioengineering, 47 (1995) 327-333.

[7] J.B. Klok, P.L. van den Bosch, C.J. Buisman, A.J. Stams, K.J. Keesman, A.J. Janssen, Pathways of sulfide oxidation by haloalkaliphilic bacteria in limited-oxygen gas lift bioreactors, Environmental science & technology, 46 (2012) 7581-7586.

[8] P.L. Van Den Bosch, O.C. van Beusekom, C.J. Buisman, A.J. Janssen, Sulfide oxidation at halo-alkaline conditions in a fed-batch bioreactor, Biotechnology and bioengineering, 97 (2007) 1053-1063.

[9] J.M. Visser, L.A. Robertson, H.W. Van Verseveld, J.G. Kuenen, Sulfur production by obligately chemolithoautotrophic *thiobacillus* species, Applied and Environmental Microbiology, 63 (1997) 2300-2305.

[10] J.B. Klok, M. de Graaff, P.L. van den Bosch, N.C. Boelee, K.J. Keesman, A.J. Janssen, A physiologically based kinetic model for bacterial sulfide oxidation, Water research, 47 (2013) 483-492.

[11] D.J. O'Brien, F.B. Birkner, Kinetics of oxygenation of reduced sulfur species in aqueous solution, Environmental Science & Technology, 11 (1977) 1114-1120.

[12] K.Y. Chen, J.C. Morris, Kinetics of oxidation of aqueous sulfide by oxygen, Environmental science & technology, 6 (1972) 529-537.

[13] M. de Graaff, J.B. Klok, M.F. Bijmans, G. Muyzer, A.J. Janssen, Application of a 2-step process for the biological treatment of sulfidic spent caustics, Water research, 46 (2012) 723-730.

[14] W.E. Kleinjan, A. de Keizer, A.J. Janssen, Kinetics of the reaction between dissolved sodium sulfide and biologically produced sulfur, Industrial & engineering chemistry research, 44 (2005) 309-317.

[15] P. Roman, M.F. Bijmans, A.J. Janssen, Quantification of individual polysulfides in lab-scale and full-scale desulfurisation bioreactors, Environmental Chemistry, 11 (2014) 702-708.

[16] J.B. Klok, K.J. Keesman, A. Janssen, Modelling of full-scale haloalkaline biodesulfurization systems, in: Modelling studies of biological gas desulfurization under haloalkaline conditions, PhD thesis, Wageningen University, 2015.

[17] K. Kiragosyan, P. Roman, K.J. Keesman, A.J. Janssen, J.B. Klok, Stoichiometry-driven heuristic feedforward control for oxygen supply in a biological gas desulfurization process, Journal of Process Control, 94 (2020) 36-45.

[18] A. ter Heijne, R. de Rink, D. Liu, J.B. Klok, C.J. Buisman, Bacteria as an electron shuttle for sulfide oxidation, Environmental science & technology letters, 5 (2018) 495-499.

[19] R. de Rink, J.B. Klok, G.J. van Heeringen, K.J. Keesman, A.J. Janssen, A. ter Heijne, C.J. Buisman, Biologically enhanced hydrogen sulfide absorption from sour gas under haloalkaline conditions, Journal of hazardous materials, 383 (2020) 121104.

[20] R. De Rink, J.B. Klok, G.J. Van Heeringen, D.Y. Sorokin, A. Ter Heijne, R. Zeijlmaker, Y.M. Mos, V. De Wilde, K.J. Keesman, C.J. Buisman, Increasing the selectivity for sulfur formation in biological gas desulfurization, Environmental science & technology, 53 (2019) 4519-4527.

[21] J.B. Klok, G. Van Heeringen, P. Shaunfield, Desulfurization of amine acid gas under turndown: performance of the biological desulfurization process, in: Laurence Reid Gas Conditioning Conference, Norman, Oklahoma USA, 2018.

[22] R. de Rink, S. Gupta, F. Piccioli de Carolis, D. Liu, A. Ter Heijne, J.B. Klok, C.J. Buisman, Effect of process conditions on the performance of a dual-reactor biodesulfurization process [unpublished manuscript, chapter 3 of this thesis] (2021).

[23] A. Janssen, R. Ruitenberg, C. Buisman, Industrial applications of new sulphur biotechnology, Water Science and Technology, 44 (2001) 85-90.

[24] D.Y. Sorokin, T.P. Tourova, O.L. Kovaleva, J.G. Kuenen, G. Muyzer, Aerobic carboxydotrophy under extremely haloalkaline conditions in *Alkalispirillum/Alkalilimnicola* strains isolated from soda lakes, Microbiology, 156 (2010) 819-827.

[25] D.Y. Sorokin, T.N. Zhilina, A.M. Lysenko, T.P. Tourova, E.M. Spiridonova, Metabolic versatility of haloalkaliphilic bacteria from soda lakes belonging to the *Alkalispirillum–Alkalilimnicola* group, Extremophiles, 10 (2006) 213-220.

[26] M.V. Ruano, J. Ribes, A. Seco, J. Ferrer, An advanced control strategy for biological nutrient removal in continuous systems based on pH and ORP sensors, Chemical Engineering Journal, 183 (2012) 212-221.

[27] P.M. de la Vega, E.M. de Salazar, M. Jaramillo, J. Cros, New contributions to the ORP & DO time profile characterization to improve biological nutrient removal, Bioresource technology, 114 (2012) 160-167.

[28] P.M. Ndegwa, L. Wang, V.K. Vaddella, Potential strategies for process control and monitoring of stabilization of dairy wastewaters in batch aerobic treatment systems, Process Biochemistry, 42 (2007) 1272-1278.

[29] C. Vongvichiankul, J. Deebao, W. Khongnakorn, Relationship between pH, oxidation reduction potential (ORP) and biogas production in mesophilic screw anaerobic digester, Energy Procedia, 138 (2017) 877-882.

[30] C. Zhang, J. Guo, J. Lian, Y. Song, C. Lu, H. Li, Bio-mixotrophic perchlorate reduction to control sulfate production in a step-feed sulfur-based reactor: A study of kinetics, ORP and bacterial community structure, Bioresource technology, 269 (2018) 40-49.

[31] S. Li, J. Mu, Y. Du, Z. Wu, Study and application of real-time control strategy based on DO and ORP in nitritation–denitrification SBR start-up, Environmental technology, (2019) 1-12.

Chapter 8

General discussion

8.1. INTRODUCTION

In the biological gas desulfurization process under haloalkaline conditions, sulfide oxidizing bacteria (SOB) convert toxic H_2S from sour gas streams into reusable elemental sulfur (S^0). The process is applied on commercial scale for several types of sour gas streams, such as natural gas, biogas and several gas streams arising from processing crude oil or gas, with over 250 full-scale plants worldwide in 2016 [1]. A challenge of the current process is to control the biological and chemical reactions in the process in order to minimize the formation of the by-products sulfate (SO_4^{2-}) and thiosulfate ($S_2O_3^{2-}$). In contrast to S^0 formation, the formation of SO_4^{2-} and $S_2O_3^{2-}$ results in the production of protons, which require the addition of NaOH and the formation of a bleed stream in order to maintain the required alkalinity and salt concentration of the process solution. The formation rate of SO_4^{2-} increases at higher oxygen supply, whilst SO_4^{2-} formation is suppressed at elevated sulfide concentrations [2, 3]. $S_2O_3^{2-}$ is formed when dissolved sulfide and oxygen are contacted. Hence, its formation rate increases at higher oxygen and/or sulfide concentrations. Thus, although operation at excess sulfide concentration would eliminate sulfate formation, it would result in excessive thiosulfate formation. Furthermore, when sulfide is present in the bioreactor, the H_2S absorption efficiency in the absorber decreases.

To minimize by-product formation, the aerated bioreactor is operated without detectable concentrations of oxygen and sulfide. This is controlled via online measurement of the oxidation / reduction potential (ORP). The air supply to the bioreactor is adjusted to maintain a pre-set ORP value. The optimal ORP window is between -390 and -350 mV vs Ag/AgCl [2]. However, even though the ORP is controlled within this optimal window, formation of SO_4^{2-} and $S_2O_3^{2-}$ is inevitable in the current process. The selectivity for S^0 formation is typically 80-90%.

The main goals of the thesis were:

1. To increase the selectivity for S^0 formation by extending the process line-up with an anaerobic bioreactor
2. To apply bioelectrochemistry to recovery energy from sulfide oxidation and to study its reaction kinetics

8.2 NEW PROCESS LINE-UP

8.2.1 INCORPORATION OF ANAEROBIC REACTOR IMPROVES SELECTIVITY FOR SULFUR FORMATION

To increase the selectivity for S^0 formation, the process line-up was extended with an anaerobic, sulfidic bioreactor, placed in between the absorber and the aerated bioreactor: the dual-reactor line up (Chapters 2 and 3). The hypothesis was that the sulfidic conditions in the this bioreactor suppress SO_4^{2-} formation. Immediately at start-up of the dual-reactor line up, a lower SO_4^{2-} formation compared to a traditional 1-bioreactor line-up was observed. Furthermore, the microbial community changed during months of operation. In the experiments as described in Chapter 2, the initial microbial community was dominated by bacteria belonging to the genus of *Thioalkalivibrio*. One of the members, *Thioalkalivibrio sulfidiphilus,* has been found to be dominant in full-scale and lab-scale biodesulfurization bioreactors [4-6]. Analysis of the genome showed that these bacteria possess genes encoding for enzymes that can oxidize S^0 to SO_4^{2-}. In the dual-reactor line up, bacteria belonging to the genus of *Alkalilimnicola* became dominant. It has been suggested that these bacteria are limited to S^0 formation and cannot form SO_4^{2-} [7, 8]. Therefore, this change in the microbial community was suggested to result in a lower tendency for SO_4^{2-} formation on the longer term. As described in Chapter 2, average selectivities for S^0, SO_4^{2-} and $S_2O_3^{2-}$ of 97%, 2% and 1% were achieved after 111 days of operation. These results show that the anaerobic bioreactor imposes a selection pressure on the system, which was hypothesized to be dependent on the HRT and the sulfide concentration in the anaerobic bioreactor. In Chapter 3 this hypothesis was tested. It was shown that either the HRT in the anaerobic bioreactor should be at least 20 minutes, or the sulfide concentration should be at least 0.5 g L^{-1} to achieve a high selectivity for S^0 formation (>95%). This finding is important for the design of full-scale systems. Next to these observations, the pH affected the process performance. The selectivity for S^0 formation was 96% at pH 8.5 and 88% at pH 9.1 (with the same sulfide concentration and HRT in the anaerobic bioreactor). The lower selectivity for S^0 formation at higher pH was also reported in studies on the traditional 1-bioreactor line-up [6].

Throughout this thesis, the bioreactor that was added to the process line-up has been called ‘anaerobic bioreactor’, because no O_2 is supplied to this reactor. However, the reason for the incorporation of this bioreactor is to expose bacteria to sulfidic conditions. Therefore, ‘sulfidic bioreactor’ is a more adequate term for this bioreactor.

8.2.2 BACTERIA REMOVED SULFIDE FROM SOLUTION UNDER ANAEROBIC CONDITIONS

An additional finding was the fact that bacteria removed sulfide from solution in the sulfidic bioreactor. The measured sulfide concentration was lower than expected based on the supply of H_2S and the liquid circulation flow rate. Furthermore, it was observed that the removal of sulfide by bacteria, i.e. the specific sulfide uptake, increased with time (Chapter 2). This increase indicated that the capacity of the bacteria to remove sulfide under anaerobic conditions increased over the course of the experiment. A direct effect of sulfide uptake in the anaerobic bioreactor is that the sulfide concentration of the solution into the aerated bioreactor is lower. This leads to lower formation of $S_2O_3^{2-}$. Furthermore, it was found that the biological sulfide uptake increased at higher sulfide concentrations and at higher pH (Chapter 3). The concentration of polysulfides (S_x^{2-}), which are formed due to an equilibrium reaction between HS- and S^0, increases at higher sulfide concentrations and at higher pH. Possibly, biological sulfide uptake under anaerobic conditions is related to polysulfides. Anaerobic sulfide removal is further discussed in section 8.4.

8.2.3 MECHANISMS OF INCREASED SELECTIVITY FOR S^0 FORMATION BY INCORPORATION OF THE ANAEROBIC BIOREACTOR

Although we have shown that the incorporation of a sulfidic bioreactor increases the selectivity for sulfur formation, the underlying mechanisms are not yet fully understood. The oxidation of sulfide to elemental sulfur in SOB can proceed via two enzymes: Flavocytochrome c/sulfide dehydrogenase (FCC) or sulfide/quinone oxidoreductase (SQR) [9]. FCC donates electrons from sulfide oxidation to cytochromes c; SQR donated electrons to quinones. The oxidation of these electron carriers occurs via cytochrome c oxidase (CcO) and quinol oxidase (QO) respectively, using O_2 as final electron acceptor. The oxidation of the electron carriers creates a membrane potential, which is used to generate energy (e.g. in the form of ATP). Because the midpoint potential of quinones is more negative than that of cytochromes, sulfide oxidation via SQR for provides more energy compared to FCC [9].

Thioalkalivibrio sulfidiphilus most likely uses FCC to oxidize sulfide to S^0 and it can further oxidize S^0 to SO_4^{2-} [10, 11]. Since sulfide reversibly inhibits CcO [12-14], the sulfidic conditions in the anaerobic bioreactor suppress the cytochrome system, which favors the oxidation of sulfide via SQR. In Chapter 2 it has been hypothesized that *Alkalilimnicola* uses SQR [7] and therefore was able to become dominant.

Besides SO_4^{2-} formation via S^0, SOB can also form SO_4^{2-} by the oxidation of $S_2O_3^{2-}$ via the SOX system [10, 15]. In Chapter 3 it was shown that the $S_2O_3^{2-}$ concentration of the solution was zero, whilst it is known that always some $S_2O_3^{2-}$ is formed. This indicated that the oxidation rate of $S_2O_3^{2-}$ (to SO_4^{2-}) was higher than its chemical formation rate, suggesting that SO_4^{2-} was formed from $S_2O_3^{2-}$. Furthermore, SO_4^{2-} can also be formed via reduction and disproportion of S^0 and $S_2O_3^{2-}$ [16]. In our experiments, we only determined the end-products and therefore it is not known to which extent these 3 different routes contributed to SO_4^{2-} formation, i.e. the dominant route for SO_4^{2-} formation was not identified.

Another effect of the sulfidic conditions in the sulfidic bioreactor is that the electron carriers (cytochrome and quinone) become reduced. A study by Visser showed that the formation of S^0 and SO_4^{2-} were dependent on the reduction degree of the cytochrome pool, which was dependent on the O_2/H_2S supply. The reduction degree is defined as the fraction of reduced electron carriers vs total amount of electron carriers. A higher reduction degree resulted in less SO_4^{2-} formation [14, 17]. Electrons can be transferred between the quinone pool and the cytochrome pool, thus the reduction degrees of these electron carriers are coupled [9]. The increased reduction degree of the electron carriers due to the sulfidic conditions could be another mechanism by which the sulfidic bioreactor contributed to lower SO_4^{2-} formation.

In this thesis we have used 16S amplicon sequencing (NGS) to determine the composition of the microbial community in the system. However, to fully understand the mechanisms behind the anaerobic reactor, other methods are required. For example, when the dominant strains could be isolated, experiments with these isolates can provide information on the metabolisms, such as the (dis)ability to form SO_4^{2-} or to oxidize $S_2O_3^{2-}$. Furthermore, genome and transcriptome analysis could indicate which enzymes are present and active to provide insights in the dominant route for SO_4^{2-} formation. This could help to further improve the selectivity for S^0 formation.

8.2.4 Other items for future research

In Chapter 3 it was shown that a higher pH resulted in a lower selectivity for S^0 formation. The pH of the process solution is mainly dependent on the H_2S/CO_2 ratio of the feed gas that is being treated. The benefit of a higher pH is that the H_2S absorption in the absorber is better and therefore a lower alkalinity and liquid circulation flow rate to the top of the absorber are required to remove all H_2S. However, a high pH results in a lower selectivity

for S^0 formation and therefore a higher NaOH consumption and bleed stream formation. Thus, it remains a challenge to obtain a high (>95%) selectivity for sulfur formation when the pH of the process solution is high, i.e. due to a gas stream with a high H_2S/CO_2 ratio.

The inoculum used for the experiments as described in Chapter 3 was a combination of bioreactor reactor solution from previous pilot experiments (i.e. Chapter 2) and a full-scale plant. It consisted for approximately 30% of bacteria belonging to the genus of *Alkalilimnicola*. In Chapter 2, the increase of the relative abundance of *Alkalilimnicola* was linked to the increased selectivity for S^0 formation. Another study also indicated that the biomass composition affected the product selectivities [4]. When the population already has a low tendency for SO_4^{2-} formation, the effect of the incorporation of a sulfidic bioreactor is less pronounced. Hence, also the microbial composition of the used inoculum partly determined the obtained product selectivities as described in Chapter 3. Furthermore, in the experiments, stable feed gas flow rates and compositions are applied. However, in full-scale applications, the feed gas may vary in flow and composition, which can impact the product selectivities [18].

Another aspect that was not studied is the HRT in the aerated bioreactor. This parameter could also be of importance to control product selectivities in the dual-reactor line up. Since the bacteria are continuously circulated between the sulfidic and aerated bioreactor, the ratio between two HRT's could have an impact on the process performance. Hence, more research is required to better understand and optimize the operation of the dual-reactor line-up.

8.2.5 Bacteria enhance H_2S absorption

The fact that SOB remove sulfide from solution under anaerobic conditions in the anaerobic bioreactor also led to the hypothesis that bacteria may play a role in the absorption of H_2S from the gas stream in the absorber column. In Chapter 4 it was shown that the bacteria enhance the absorption of H_2S from the gas stream. In previous work, 2 enhancement factors were described for H_2S absorption in the process solution of the biological gas desulfurization process: i) the homogeneous reaction, which is the reaction of H_2S with the alkaline process solution to form HS^-, and ii) the heterogeneous reaction, which is the reaction of H_2S (and HS^-) with sulfur particles to form polysulfide (S_x^{2-}). However, it was concluded that these 2 factors could not fully describe the observed enhancement [19]. Taking into account the results as described in Chapter 4 of this thesis, the third

enhancement factor is the activity (i.e. sulfide uptake) of the SOB under anaerobic conditions.

Unfortunately, we could not quantify this biological enhancement factor. In order to do this, more dedicated experiments need to be performed. A challenge will be to distinguish between the heterogeneous enhancement factor (i.e. the reaction of sulfide with sulfur particles, forming polysulfide) and the biological enhancement factor. For this, experiments with bacteria and without sulfur particles, and experiments with sulfur particles and without bacteria should be conducted. Another challenge is that the biological enhancement factor is probably dependent on the anaerobic sulfide uptake capacity of the bacteria, which may vary with the composition of the microbial community and process conditions, as indicated in Chapters 2 and 3. As the incorporation of a sulfidic bioreactor results in a higher anaerobic sulfide uptake capacity, the incorporation of a sulfidic bioreactor may result in a higher biological enhancement factor and thus a more efficient H_2S absorption. When the biological enhancement factor could be quantified and / or predicted, this could improve the performance of full-scale absorber columns.

8.3 Bioelectrochemical sulfide oxidation

8.3.1 Recovering electrons from SOB in the absence of dissolved sulfide

In the biological desulfurization process, SOB use oxygen as electron acceptor for sulfide oxidation. We found that SOB are electroactive and can also use the anode of an electrochemical cell as electron acceptor (Chapters 5-7). By applying the ability of SOB to remove sulfide from solution under anaerobic conditions, current could be produced in the absence of dissolved sulfide in the electrochemical cell.

In batch experiments, it was shown that planktonic SOB produced current at anode potentials of 0.1, 0 and -0.1 V (vs Ag/AgCl, 3 M KCl) (Chapter 5). To avoid precipitation of elemental sulfur on the anode, SOB were exposed to sulfide, i.e. “charged”, before being transferred to the BES. Hence, electric current was produced in the absence of dissolved sulfide. The production of electrical current increased at higher anode potentials due to a higher driving force for electron transfer. Furthermore, current production was affected by the microbial community; bacteria harvested from the dual-reactor line up removed more sulfide from solution and produced a higher current than bacteria taken from a full-scale system using the traditional 1-bioreactor line-up.

Due to the very low amount of sulfide, it was not possible to determine product formation and biomass growth in the batch experiments. To study this, continuous experiments were performed (Chapter 6), using the electron shuttling capacity of SOB as shown of Chapter 5. It was found that biomass growth occurred, mainly in the form of a biofilm. The main end-product, especially after longer time of operation, was SO_4^{2-} and not S^0. Although SO_4^{2-} formation releases more electrons and therefore produces more current, its formation is unwanted due to the corresponding proton formation and a lower recovery of reusable elemental sulfur.

During the experiments, the anode potential was stepwise decreased from -0.1 V to -0.4 V. However, this did not influence product formation and, as a consequence, the current production. Thus, at constant sulfide loading rate, the current production was not dependent on the anode potential. This differed from the batch experiment, where a lower anode potential resulted in lower current production. Whereas the community of the planktonic bacteria was dominated by *Thioalkalivibrio* and *Alkalilimnicola* (which are also the main genera in the biodesulfurization process, Chapters 2 and 3), the biofilm was dominated by bacteria belonging to the genus of *Desulfurivibrio*, which has been described as a sulfur disproportionator [20]. It is using S^0 as electron donor and acceptor (Equation 8.1):

$$4\ S^0 + 4\ H_2O \rightarrow SO_4^{2-} + 3\ HS^- + 5\ H^+ \qquad \text{(Equation 8.1)}$$

However, in the BES, the electrode acts as electron acceptor and therefore a more likely reaction is:

$$S^0 + 4\ H_2O \rightarrow SO_4^{2-} + 8\ H^+ + 6\ e^- \qquad \text{(Equation 8.2)}$$

Desulfurivibrio has been detected in the biological desulfurization process, but its abundance was very low. Another study on BES for sulfide removal also found *Desulfurivibrio* to be dominant in the biofilm [21]. Apparently, these bacteria grow by oxidizing sulfur (compounds) and donating electrons to an electrode.

From the results in Chapter 6 it appeared very likely that the planktonic bacteria oxidized HS^- to S^0 and the biofilm further oxidized S^0 to SO_4^{2-}. However, future research is required to determine the exact mechanisms behind product formation in a continuous BES.

In Chapter 7 it was found that the SOB in the aerated bioreactor of the biological desulfurization process contain electrons, which can be harvested in an electrochemical cell. It was shown that: i) next to sulfide and oxygen, the ORP in the aerated bioreactor is also determined by SOB, ii) the amount of recovered electrons / charge from the SOB increases when the ORP setpoint was decreased (between ORP values of -390 – -330mV), and iii) a higher specific stored charge resulted in higher selectivity for S^0 formation and lower selectivity for SO_4^{2-} formation. These results showed the limitations of the ORP based control strategy, which is further discussed in section 8.6.

In general, electron transfer from bacteria to an electrode can occur via either direct electron transfer or mediated electron transfer [22]. In our experiments it is most likely that electric current was produced via direct electron transport, because i) electric current was produced instantaneously when the electrochemical measurement was started, and ii) current production also occurred after washing the bacteria which removed possible redox mediators from the solution. Direct electron transfer can occur via outer membrane cytochromes, conductive pili or nanowires [22]. Which of these mechanisms is used by SOB is unknown.

In order to have driving force for electron transfer from the bacteria to the anode, i.e. produce electric current in a BES, the potential of the charged bacteria should be lower (more negative) than the anode potential. In the continuous BES experiments (Chapter 6), the anode potential was controlled at values of -100 to -400 mV (vs Ag/AgCl). At -400 mV, the current density was similar as at an anode potential of -100 mV, showing that the system was not limited by the anode potential. However, this was after a biofilm had been formed on the anode. Once a biofilm is present that oxidizes S^0 to SO_4^{2-}, decreasing the anode potential does not result in a decrease of the SO_4^{2-} formation. In the continuous BES experiments, the sulfide dosing rate was set based on the maximum uptake capacity of the planktonic bacteria in anolyte uptake chamber. This uptake capacity is probably dependent on the discharge in the electrochemical cell. If more electrons are released in the electrochemical cell (for example by extending the HRT in the electrochemical cell), more sulfide can be taken-up in the anolyte uptake chamber and a higher current production could be reached.

BES systems are often compared based on current density (the normalized current production based on the anode surface area). For a sulfide removing BES it is more

important to prevent S^0 deposition on the anode (electrode passivation) and to minimize SO_4^{2-} production (proton formation). S^0 formation releases less electrons than SO_4^{2-} formation, resulting in lower current production. Furthermore, S^0 deposition can be prevented by using the sulfide shuttling capacity of the SOB although this limits the sulfide loading rate and thus current production.

8.3.2 APPLICATIONS OF BES IN BIOLOGICAL SULFIDE OXIDATION

Our results show that BES have 2 possible applications in biological gas desulfurization: i) recovery of energy, and ii) use as a process control mechanism.

Energy production with a BES depends on the anode and cathode reactions and their corresponding potentials. The cell voltage (E_{cell}) is defined as Equation 8.3:

$$E_{cell} = E_{cathode} - E_{anode} \qquad \text{(Equation 8.3)}$$

When E_{cell} is positive ($E_{cathode} > E_{anode}$) electrical energy is produced; when E_{cell} is negative ($E_{cathode} < E_{anode}$) electrical energy is required to drive the reactions. The power production or consumption is proportional to E_{cell}. The two most used cathode reactions are reduction of oxygen to water or reduction of water to hydrogen gas and hydroxide. The standard potential (the thermodynamic equilibrium potential at a pH of 7) for O_2 reduction is +0.6 V (vs Ag/AgCl), whereas H_2 formation occurs at -0.6 V [23]. Taken into account the anode potential for sulfide oxidation (-0.1 V to -0.4 V), O_2 reduction results in the production of electrical energy. H_2 formation requires input of electrical energy, but part of this energy is recovered in the form of H_2. In both cases, the energy efficiency becomes higher when the anode potential is lower (more negative). However, the actual electrode potential required for a certain reaction to occur deviates from the theoretical potential, i.e. a certain overpotential is required for the reaction to take place. The overpotential is for example dependent on the cathode material. The overpotential results in a voltage loss in the system. O_2 reduction would either require an 'open air' cathode or air must be blown into the cathode compartment, which requires energy. O_2 cross-over to the anode would decrease the coulombic efficiency of the anode. Therefore, H_2 formation seems to be the most feasible way to recover energy from sulfide oxidation.

BES can possibly also be used for process control in the biodesulfurization process. As shown in Chapter 7, the amount of charge that could be harvested from the bacteria in the aerated bioreactor could be measured, and the amount of charge was shown to be linked

to product formation. Higher selectivity for S^0 formation occurs when the specific stored charge is higher. Thus, measurement of the stored charge in SOB could be used to improve the O_2 supply control strategy, for example by adjusting the ORP setpoint to maintain an optimal amount of charge storage in the SOB.

Preventing the formation of a biofilm seems to be essential for successful implementation of BES for biological desulfurization, since this would be a strategy to prevent sulfate formation. As shown in Chapter 6, the microbial community of the bacteria in the biofilm is different from the bacteria that are normally present in the bioreactor. The bacteria in the biofilm seem to be responsible for SO_4^{2-} formation. Although this results in more current production and thus higher energy recovery, more NaOH is required to compensate for the formed protons. A biofilm is also unwanted when a BES is used for process control, as this disturbs the measurement of the planktonic bacteria. In many BES systems, carbon based electrodes are used because they are cheap and have a high conductivity and biocompatibility [24]. To prevent formation of a biofilm, application of other electrode materials therefore may be useful.

8.4 Electron shuttling by haloalkaliphilic SOB

Throughout the work of this PhD thesis, it has been shown that the SOB in the biological desulfurization process take-up sulfide from the process solution in the absence of an electron acceptor. The sulfide is stored and electrons are released when an electron acceptor (i.e. O_2 or an anode) is present. This phenomenon is referred to as 'electron shuttling'. The uptake of sulfide under anaerobic conditions has been shown in various ways:

- Sulfide (probably HS^- and S_x^{2-}) was removed from solution in the absorber and sulfidic bioreactor of the dual-reactor biodesulfurization process (Chapters 2, 3 and 4)
- More H_2S was removed from the gas stream in the absorber when the biological activity was higher (Chapter 4)
- HS^- and S_x^{2-} were removed from solution in anaerobic batch experiments (Chapters 5 and 7)
- HS^- was taken up in the anolyte uptake chamber in continuous electrochemical experiments (Chapter 6)
- Electrons were recovered from SOB in an electrochemical cell in the absence of dissolved sulfide and O_2 (Chapters 5, 6 and 7)

An overview of the sulfide shuttling by SOB, with corresponding chapter numbers, is depicted in Figure 8.1.

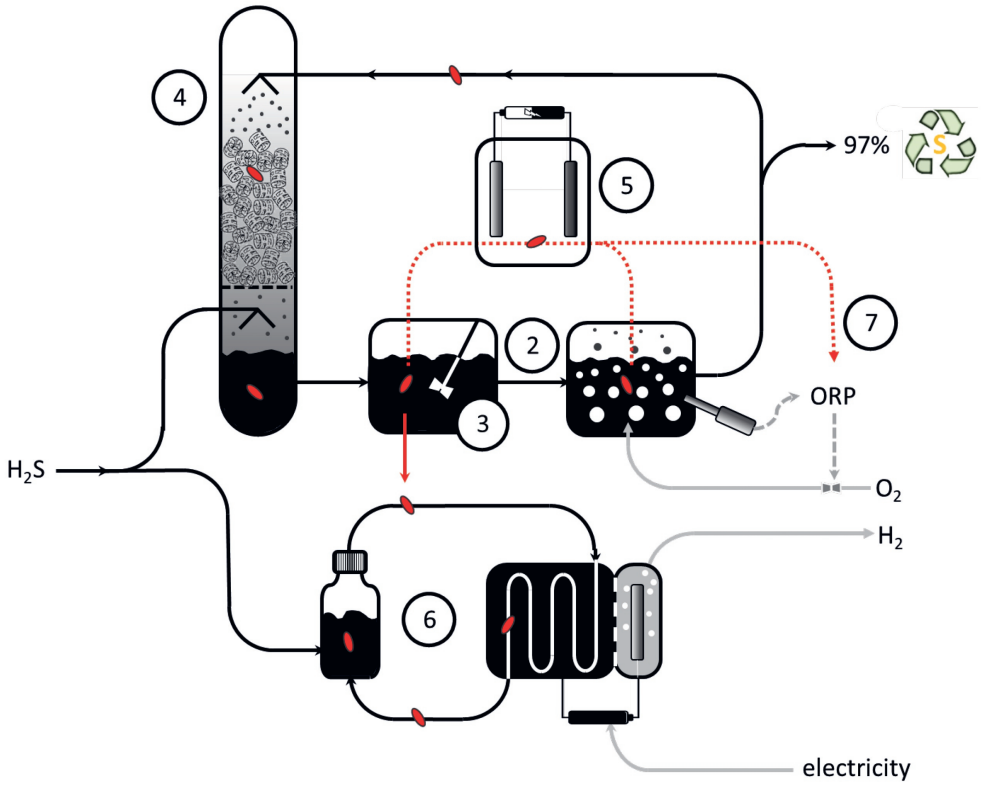

Figure 8.1: Sulfide shuttling in haloalkaliphilic SOB (indicated in red) as shown in the various chapters of this thesis. The numbers in the figure corresponds to the thesis chapters. In Chapters 2 and 3, bacteria shuttle sulfide from the anaerobic / sulfidic bioreactor to the aerated bioreactor. The incorporation of the sulfidic bioreactor results in a very high selectivity for elemental sulfur formation (~97%) In Chapter 4, bacteria 'enhance' the H_2S absorption in the absorber, shuttling sulfide from the absorber to the aerated bioreactor. In Chapter 5, bacteria taken from the biodesulfurization installation are charged with sulfide and subsequently discharged at the anode of an electrochemical cell in absence of dissolved sulfide. In Chapter 6, bacteria are used in a continuous process for sulfide removal and electric current production, which can be used to form H_2. In Chapter 7, bacteria from the aerated bioreactor are shown to contain electrons, which is dependent on the ORP of the aerated bioreactor.

In the pilot experiments, sulfide (and / or electrons from sulfide) was shuttled from the anaerobic sulfidic zone (the absorber and sulfidic bioreactor) to the microaerophilic zone (the aerated bioreactor). Furthermore, the bacteria from the aerated bioreactor can be discharged at the anode of an electrochemical cell. In chapters 5 and 6 it is shown that bacteria can remove sulfide from solution and subsequently release electrons to an electrode in the absence of dissolved sulfide. Thus, the bacteria act as a shuttle: they are charged with sulfide and discharged with oxygen or at an electrode.

An overview of the amount of sulfide uptake in the various experiments, is provided in Table 8.1. In the pilot biodesulfurization installation, the total sulfide concentration was measured in the sulfide rich solution in the sump of the absorber column and in the sulfidic bioreactor. In the experiments as described in Chapter 2, the maximum uptake in the sump of the absorber reached 0.15 g L^{-1}, i.e. the theoretical sulfide concentration based on the H_2S feed rate and liquid flow rate was 0.78 g L^{-1}, and the measured concentration was 0.63 g L^{-1}. Since the biomass concentration was 56 mg-N L^{-1}, the specific uptake was 2.7 mg-S mg-N^{-1}. In the sulfidic bioreactor, the specific uptake was 3.4 mg-S mg-N^{-1}.

Table 8.1: Overview of the amount of sulfide uptake in the various experiments.

Chapter	Location	Theoretical sulfide concentration (mg-S L^{-1})	Measured sulfide concentration (mg-S L^{-1})	Sulfide uptake (mg-S L^{-1})	Specific uptake (mg-S mg-N^{-1})
2	Absorber bottom	780	631	149	2.66
2	Sulfidic bioreactor	780	591	191	3.41
3	Sulfidic bioreactor	478	248	231	4.44
4	Absorber bottom	700	576	124	1.77
5	Batch bottle	6.4	0	6.4	0.22
6	Anolyte uptake chamber	3.8	0	3.8	0.12
7	Batch bottle	6.4	0	6.4	0.22

In Chapter 3 the maximum measured uptake in the sulfidic bioreactor was even higher: 4.4 mg-S mg-N^{-1}. In the experiments in Chapter 4, the specific uptake measured in the rich solution coming from the absorber (absorber bottom) was 1.8 mg-S mg-N^{-1}. The generic elemental composition of haloalkaliphilic bacteria is $CH_{1.8}O_{0.5}N_{0.2}$ [15]. Assuming the SOB biomass in our experiments also consisted of 10% nitrogen, a sulfide uptake of 4.4 mg-S mg-N^{-1} is equal to 0.44 mg-S per mg SOB.

In batch tests as described in chapters 5 and 7, the specific sulfide uptake under anaerobic conditions was 0.22 mg-S mg-N^{-1}. This is a much lower uptake than observed in the pilot desulfurization installation. An important difference is that in the batch tests no dissolved sulfide was detectable anymore, i.e. all sulfide was removed, whereas in the absorber bottom and sulfidic bioreactor only part of the sulfide was removed. The full removal of sulfide in the BES experiments was important to ensure no dissolved sulfide was present in the electrochemical cell. This full removal was observed for bacteria taken from the dual-reactor installation. For bacteria taken from a traditional 1-bioreactor installation, only part of the sulfide was removed. In the continuous experiments as described in Chapter 6, also complete uptake was observed, with a maximum of 0.12 mg-S mg-N^{-1}. However, in the batch experiments, bacteria were first fully 'discharged' with oxygen and in the continuous electrochemical measurement, bacteria were not fully discharged in the electrochemical cell.

Although sulfide uptake under anaerobic conditions has been shown in various experiments, the mechanisms are not known yet. In chapters 2, 3, 4 and 5 several mechanisms for anaerobic sulfide removal have been postulated. It is not sure whether sulfide is only taken up and stored, or if also conversion takes place, for example by reduction of the electron carriers. However, the concentration of these carriers is not high enough to explain the observed sulfide uptake. Many bacteria store zero-valent sulfur in the form of sulfur globules, either inside or outside the cell. Various forms of sulfur have been detected in these globules, such as S_8 and polythionates ($S_x(SO_3)_2$) [25]. It has been shown that more sulfide is taken-up at higher / excess sulfide concentrations. Furthermore, more sulfide uptake was observed at higher pH. This suggests that polysulfide may play a role in the anaerobic sulfide uptake. Maybe sulfide is stored as cell-bound polysulfide. In our experiments, we determined the sulfide uptake by measuring the total dissolved sulfide concentration (the sum of H_2S, HS^-, S^{2-} and S_x^{2-}) and the uptake was calculated based on the sulfide mass balance. The role of polysulfides in the biological gas desulfurization

process and specifically on the anaerobic sulfide uptake by bacteria, should therefore be further investigated. This could be done by separately determining HS^- and S_x^{2-} concentration in the sulfidic bioreactor. Furthermore, future research should focus on isolating cells before and after sulfide uptake to measure how much and in what form sulfide and electrons are stored in these cells.

8.5 SULFIDE OXIDATION WITH O_2 VS SULFIDE OXIDATION WITH AN ELECTRODE

In this section a comparison is made between sulfide oxidation using oxygen as final electron acceptor (the bioreactor process) and bioelectrochemical sulfide oxidation (BES process), in which bacteria use the electrode as final electron acceptor. In both cases, product formation is determined by analyzing the end products of the conversion of sulfide, which are elemental sulfur, sulfate and thiosulfate.

For the bioreactor process, the conversions of sulfide to the end products elemental sulfur, sulfate and thiosulfate are described by the reaction equations as shown in Table 8.2. One of the first to describe these reactions, was Gijs Kuenen in 1975 [26] and many researchers used the same set of equations. These are overall reaction equations based on reaction stoichiometry. For example, 0.5 mol O_2 is required to oxidize 1 mol of sulfide to elemental sulfur (see reactions 3 and 4) and 2 mol O_2 is required to fully oxidize 1 mol of sulfide to sulfate (see reaction 5). In Chapter 6 of this thesis it was shown that sulfide can also be oxidized in a bioelectrochemical system without O_2, using the anode as terminal electron acceptor for sulfide oxidation. For the BES, the reactions are denoted as half reactions, see Table 8.3.

Table 8.2: Reaction equations to describe sulfide oxidation in the biological desulfurization process using O_2 as final electron acceptor.

Number	Reaction equation	Description	Bio/ chem
1	$HS^- + ½\ O_2 \rightarrow S^0 + OH^-$	Sulfide oxidation to elemental sulfur	Bio
2	$S_x^{2-} + ½\ O_2 + H^+ \rightarrow xS^0 + OH^-$	Polysulfide oxidation	Bio
3	$HS^- + 2\ O_2 \rightarrow SO_4^{2-} + H^+$	Sulfide oxidation to sulfate	Bio
4	$S^0 + 1½\ O_2 + H_2O \rightarrow SO_4^{2-} + 2\ H^+$	Elemental sulfur oxidation to sulfate	Bio
5	$HS^- + O_2 \rightarrow ½\ S_2O_3^{2-} + ½\ H_2O$	Sulfide oxidation to thiosulfate	Chem
6	$½\ S_2O_3^{2-} + ½\ H_2O + O_2 \rightarrow SO_4^{2-} + H^+$	Thiosulfate oxidation to sulfate	Bio

Table 8.3: Reaction equations to describe sulfide oxidation in bioelectrochemical sulfide oxidation, using an anode as final electron acceptor. In electrochemical sulfide oxidation (reaction 3), S^0 is deposited on the electrode.

Number	Reaction equation	Description	Bio/ chem
1	$HS^- \rightarrow S^0 + 2\ e^- + H^+$	Sulfide oxidation to elemental sulfur	Bio
2	$S_x^{2-} \rightarrow xS^0 + 2\ e^-$	Polysulfide oxidation	Bio
3	$HS^- \rightarrow S^0 + 2\ e^- + H^+$	Electrochemical sulfide oxidation	Chem
4	$HS^- + 4\ H_2O \rightarrow SO_4^{2-} + 9\ H^+ + 8\ e^-$	Sulfide oxidation to sulfate	Bio
5	$S^0 + 4\ H_2O \rightarrow SO_4^{2-} + 8\ H^+ + 6\ e^-$	Elemental sulfur oxidation to sulfate	Bio

In the BES process, elemental sulfur can be formed biologically (according to reactions 1 and 2 in Table 8.3), but it can also be formed electrochemically when sulfide is directly contacted with the electrode (reaction 3). This reaction is unwanted as electrodeposition of elemental sulfur results in electrode passivation [27]. In our BES, planktonic bacteria transfer electrons to the electrode via direct electron transport (see section 3). The electron transport in the bioreactor and BES process are schematically shown in Figure 8.2.

From reaction 4 and 5 in Table 8.3, it can be seen that water is used for the formation of sulfate. Also in the bioreactor process, the oxygen in SO_4^{2-} originates from H_2O, but this is not reflected by the overall reaction equations. Experiments by van den Bosch et al. and

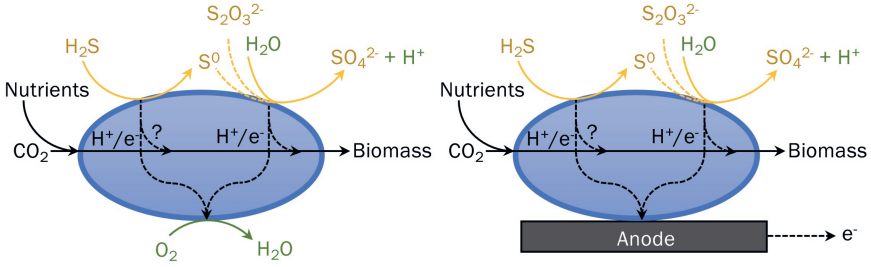

Figure 8.2: Simplified schematic representation of sulfide oxidation routes bioreactor process (left) and BES process (right). Sulfate can be formed by oxidation of S^0 and by oxidation of $S_2O_3^{2-}$ (indicated by dashed lines). Due to the electron shuttling capacity of the bacteria, the oxidation of sulfide (providing electrons) and the release of electrons to either O_2 or an anode do not need to take place simultaneously. The generic elemental biomass composition of haloalkaliphilic bacteria is $CH_{1.8}O_{0.5}N_{0.2}$ [15]. Furthermore, bacteria may form osmolytes to cope with hypersaline conditions [11, 28]

Klok et al. in a traditional 1-bioreactor line-up showed the existence of an electron gap: more S-compounds were produced than calculated based on the consumed amount of O_2 [3, 28]. The reason is that electrons are also required for assimilation reactions, i.e. CO_2/HCO_3^- fixation to form biomass. It was shown that sulfide could be fully oxidized to sulfate at an O_2/H_2S supply ratio of 1.5. This was called the limited oxygen route (LOR) [28]. In the LOR, electrons from the electron carriers (i.e. cytochromes c or quinones) are transferred to NAD^+ which can subsequently be used to fix CO_2. This means less electrons are transferred to O_2. For the LOR, 5.2% of the obtained electrons with sulfide oxidation were used for assimilation. If the O_2/H_2S supply was increased to 2 mol/mol, 17% of the electrons were used for assimilation; this was called the full oxygen route (FOR) [28]. It was shown that the growth yield was proportional to the amount of sulfate formed and it was assumed that no energy is available for growth at 100% S^0 formation.

In a recent study using a feed-forward O_2/H_2S control strategy in a dual-reactor system, a selectivity for S^0 formation of 97.7 ± 3.0 % was achieved with an O_2/H_2S supply ratio of 0.63 mol mol^{-1} [18]. This was a similar O_2/H_2S supply as in the experiments of van den Bosch et al.) and Klok et al. [3, 28] in the traditional 1-bioreactor line-up where the selectivity for S^0 was 83-88%. Thus, it remains a question what the specific oxygen consumption would be at a selectivity for S^0 formation of (close to) 100%. This, amongst others, depends on the amount of electrons used for assimilation. In Chapter 2 it has been suggested that certain SOB are limited to S^0 formation, meaning these SOB should be able to generate metabolic energy from sulfide oxidation to elemental sulfur. Furthermore, if other components are present in the feed gas stream, such as organic (sulfur) components, the specific oxygen consumption increases.

8.6 CONTROLLING PRODUCT FORMATION

In the traditional 1-bioreactor biodesulfurization process, process control is based on the O_2 dosing rate. In full-scale systems this is controlled via the online ORP measurement [29], which is an indirect measure for the O_2/H_2S supply ratio [30]. While air dosage based on an ORP feedback control strategy is a proven concept in the biological desulfurization, the work described in this thesis shows the ORP control strategy has limitations. Apart from the applied ORP setpoint, the microbial community is a determining factor in the obtained product selectivities. In a recent study by Kiragosyan et al., it was shown that the product selectivities are very different with other microbial communities at identical applied process conditions, e.g. volumetric sulfide loading rate, pH and ORP setpoint [4]. This

observation is in line with the observations in Chapter 2 of this thesis. In Chapter 2 it was shown that the selectivity for S^0 formation increased when the microbial community composition changed (while ORP setpoint remained constant). The microbial community in a biodesulfurization system is initially determined by the inoculum, but will change based on the applied process conditions, such as the O_2/H_2S supply and feed gas composition. Therefore, to optimize product formation, it is essential to apply a selection pressure to control the microbial community composition. This cannot be controlled optimally by the ORP alone.

In addition to the selection pressure, in Chapter 7 it was shown that the ORP measurement is dominated by the total charge storage in SOB, and not only by sulfide and oxygen. Furthermore, it was shown that product formation is dependent on the specific stored charge, i.e. more SO_4^{2-} is formed at a lower specific stored charge. The ORP and specific stored charge are both determined by the combination of the total charge storage and the biomass concentration. This further confirms that ORP is not sufficient for optimal process control. In addition, the biomass concentration is also a factor that plays a role in product formation.

In this thesis we showed that specific process conditions can be applied by the addition of a sulfidic bioreactor that imposes a selection pressure on the bacteria. This results in an extra control mechanism. Further improvements could be made by applying a feed-forward O_2 supply control strategy [18] and/or optimization of the specific stored charge in the bacteria by applying electrochemical measurements.

8.7 Final remarks

In 2012, Klok et al. predicted that a selectivity for S^0 formation of 98% should be possible [14], which would make the application of the biological gas desulfurization process for gas streams with a sulfur load up to 100 ton-S day^{-1} economically feasible [31]. In this work, we showed that the incorporation of an anaerobic, sulfidic bioreactor in the process line-up increases the selectivity for sulfur formation to 97%. With further improvements a selectivity of 98% could be achieved. Currently, the first full-scale dual-reactor biodesulfurization installations are under construction. When treating industrial gas streams, these full-scale facilities should prove the benefits of dual-reactor system in practice and will provide useful information to further improve biological gas desulfurization.

8.8 REFERENCES

[1] J.B. Klok, G. Van Heeringen, P. Shaunfield, Desulfurization of amine acid gas under turndown: performance of the biological desulfurization process, in: Laurence Reid Gas Conditioning Conference, Norman, Oklahoma USA, 2018.

[2] P.L. van den Bosch, Application of the redox potential to control product formation. Biological sulfide oxidation by natron-alkaliphilic bacteria: application in gas desulfurization - PhD thesis, Wageningen University., 2008.

[3] P.L. Van Den Bosch, O.C. van Beusekom, C.J. Buisman, A.J. Janssen, Sulfide oxidation at halo-alkaline conditions in a fed-batch bioreactor, Biotechnology and bioengineering, 97 (2007) 1053-1063.

[4] K. Kiragosyan, J.B. Klok, K.J. Keesman, P. Roman, A.J. Janssen, Development and validation of a physiologically based kinetic model for starting up and operation of the biological gas desulfurization process under haloalkaline conditions, Water research X, 4 (2019) 100035.

[5] D.Y. Sorokin, M.S. Muntyan, A.N. Panteleeva, G. Muyzer, *Thioalkalivibrio sulfidiphilus* sp. nov., a haloalkaliphilic, sulfur-oxidizing gammaproteobacterium from alkaline habitats, International journal of systematic and evolutionary microbiology, 62 (2012) 1884-1889.

[6] P.L. Van den Bosch, D.Y. Sorokin, C.J. Buisman, A.J. Janssen, The effect of pH on thiosulfate formation in a biotechnological process for the removal of hydrogen sulfide from gas streams, Environmental science & technology, 42 (2008) 2637-2642.

[7] D.Y. Sorokin, T.P. Tourova, O.L. Kovaleva, J.G. Kuenen, G. Muyzer, Aerobic carboxydotrophy under extremely haloalkaline conditions in *Alkalispirillum/Alkalilimnicola* strains isolated from soda lakes, Microbiology, 156 (2010) 819-827.

[8] D.Y. Sorokin, T.N. Zhilina, A.M. Lysenko, T.P. Tourova, E.M. Spiridonova, Metabolic versatility of haloalkaliphilic bacteria from soda lakes belonging to the *Alkalispirillum–Alkalilimnicola* group, Extremophiles, 10 (2006) 213-220.

[9] C. Griesbeck, G. Hauska, M. Schütz, Biological sulfide oxidation: sulfide-quinone reductase (SQR), the primary reaction, Recent research developments in microbiology, 4 (2000) 179-203.

[10] T. Berben, L. Overmars, D.Y. Sorokin, G. Muyzer, Diversity and distribution of sulfur oxidation-related genes in *Thioalkalivibrio*, a genus of chemolithoautotrophic and haloalkaliphilic sulfur-oxidizing bacteria, Frontiers in microbiology, 10 (2019) 160.

[11] G. Muyzer, D.Y. Sorokin, K. Mavromatis, A. Lapidus, A. Clum, N. Ivanova, A. Pati, P. d'Haeseleer, T. Woyke, N.C. Kyrpides, Complete genome sequence of "*Thioalkalivibrio sulfidophilus*" HL-EbGr7, Standards in genomic sciences, 4 (2011) 23-35.

[12] J.P. Collman, S. Ghosh, A. Dey, R.A. Decréau, Using a functional enzyme model to understand the chemistry behind hydrogen sulfide induced hibernation, Proceedings of the National Academy of Sciences, 106 (2009) 22090-22095.

[13] P. Nicholls, D.C. Marshall, C.E. Cooper, M.T. Wilson, Sulfide inhibition of and metabolism by cytochrome c oxidase, Biochemical Society Transactions, 41 (2013) 1312-1316.

[14] J.B. Klok, M. de Graaff, P.L. van den Bosch, N.C. Boelee, K.J. Keesman, A.J. Janssen, A physiologically based kinetic model for bacterial sulfide oxidation, Water research, 47 (2013) 483-492.

[15] H. Banciu, D.Y. Sorokin, R. Kleerebezem, G. Muyzer, E.A. Galinski, J.G. Kuenen, Growth kinetics of haloalkaliphilic, sulfur-oxidizing bacterium *Thioalkalivibrio versutus* strain ALJ 15 in continuous culture, Extremophiles, 8 (2004) 185-192.

[16] A. Slobodkin, G. Slobodkina, Diversity of sulfur-disproportionating microorganisms, Microbiology, 88 (2019) 509-522.

[17] J.M. Visser, L.A. Robertson, H.W. Van Verseveld, J.G. Kuenen, Sulfur production by obligately chemolithoautotrophic *Thiobacillus* species, Applied and Environmental Microbiology, 63 (1997) 2300.

[18] K. Kiragosyan, P. Roman, K.J. Keesman, A.J. Janssen, J.B. Klok, Stoichiometry-driven heuristic feedforward control for oxygen supply in a biological gas desulfurization process, Journal of Process Control, 94 (2020) 36-45.

[19] W.E. Kleinjan, J.N. Lammers, A. de Keizer, A.J. Janssen, Effect of biologically produced sulfur on gas absorption in a biotechnological hydrogen sulfide removal process, Biotechnology and bioengineering, 94 (2006) 633-644.

[20] A. Poser, R. Lohmayer, C. Vogt, K. Knoeller, B. Planer-Friedrich, D. Sorokin, H.-H. Richnow, K. Finster, Disproportionation of elemental sulfur by haloalkaliphilic bacteria from soda lakes, Extremophiles, 17 (2013) 1003-1012.

[21] G. Ni, P. Harnawan, L. Seidel, A. Ter Heijne, T. Sleutels, C.J. Buisman, M. Dopson, Haloalkaliphilic microorganisms assist sulfide removal in a microbial electrolysis cell, Journal of hazardous materials, 363 (2019) 197-204.

[22] K.S. Aiyer, How does electron transfer occur in microbial fuel cells?, World Journal of Microbiology and Biotechnology, 36 (2020) 1-9.

[23] H.V. Hamelers, A. Ter Heijne, T.H. Sleutels, A.W. Jeremiasse, D.P. Strik, C.J. Buisman, New applications and performance of bioelectrochemical systems, Applied microbiology and biotechnology, 85 (2010) 1673-1685.

[24] D. Call, B.E. Logan, Hydrogen production in a single chamber microbial electrolysis cell lacking a membrane, Environmental science & technology, 42 (2008) 3401-3406.

[25] A. Prange, R. Chauvistre, H. Modrow, J. Hormes, H.G. Trüper, C. Dahl, Quantitative speciation of sulfur in bacterial sulfur globules: X-ray absorption spectroscopy reveals at least three different species of sulfur, Microbiology, 148 (2002) 267-276.

[26] J.G. Kuenen, Colourless sulfur bacteria and their role in the sulfur cycle, Plant and soil, 43 (1975) 49-76.

[27] I. Pikaar, E.M. Likosova, S. Freguia, J. Keller, K. Rabaey, Z. Yuan, Electrochemical abatement of hydrogen sulfide from waste streams, Critical reviews in environmental science and technology, 45 (2015) 1555-1578.

[28] J.B. Klok, P.L. van den Bosch, C.J. Buisman, A.J. Stams, K.J. Keesman, A.J. Janssen, Pathways of sulfide oxidation by haloalkaliphilic bacteria in limited-oxygen gas lift bioreactors, Environmental science & technology, 46 (2012) 7581-7586.

[29] A. Janssen, S. Meijer, J. Bontsema, G. Lettinga, Application of the redox potential for controling a sulfide oxidizing bioreactor, Biotechnology and bioengineering, 60 (1998) 147-155.

[30] P. Roman, M.F. Bijmans, A.J. Janssen, Influence of methanethiol on biological sulphide oxidation in gas treatment system, Environmental technology, 37 (2016) 1693-1703.

[31] J.B.M. Klok, Modeling studies of biological gas desulfurization under haloalkaline conditions, PhD thesis, Wageningen University, Wageningen, 2015.

SUPPORTING INFORMATION

SI 1 SUPPORTING INFORMATION FROM CHAPTER 2

SI 1.1 DETAILED INFORMATION ON EXPERIMENTAL SET-UP (H_2S ABSORBER, LIQUID FLOWS, PUMPS AND PUMP CONTROLS)

Stream 1 was driven with eccentric screw pump P1 (Verderpro, Verder BV, the Netherlands), controlled by a flow meter (Promass A, Endress+Hauser, Reinach, Switzerland). The desired flow was set in the programmable logic controller.

Stream 2 was driven by the pressure difference between the pressurized H2S absorber and the atmospheric-pressure anaerobic bioreactor. A level control in the bottom of the H2S absorber acts on a valve (Flowserve, Kämmer Valves, Pittsburg, USA) in the line of that stream. Keeping the level in the H_2S absorber bottom at a preset value ensures that stream 2 was constant and equal to stream 1.

Stream 3 was driven by peristaltic pump P3 (505S, Watson Marlow, Wilmington, USA), of which the inlet was installed at the overflow level of anaerobic bioreactor. The pump keeps the level constant (thereby also transferring some headspace gas, which was N_2/H_2S).

Stream 4 was an overflow (gravity).

Stream 5 was driven by peristaltic pump P5, of which the pause/pulse time was set manually with a timer clock.

Streams 6 and 7 are driven by peristaltic pumps P3 and P4, of which the pause/pulse time was controlled via a programmable logic controller.

The H_2S absorber was a stainless steel column, with an inner diameter of 5 cm and a height of 4 m. It contained two beds of 1 m with random packing. The pressure in the H_2S absorber was measured with a pressure meter (Rosemount, Emerson Electric co., St. Louis, USA) and kept between 3 and 4 bar(g) with a Tescom Europe backpressure regulator (Emerson Electric co., St. Louis, USA).

SI 1.2 SCHEMATIC REPRESENTATION OF THE CONVENTIONAL AND THE NEW PROCESS LINE-UP

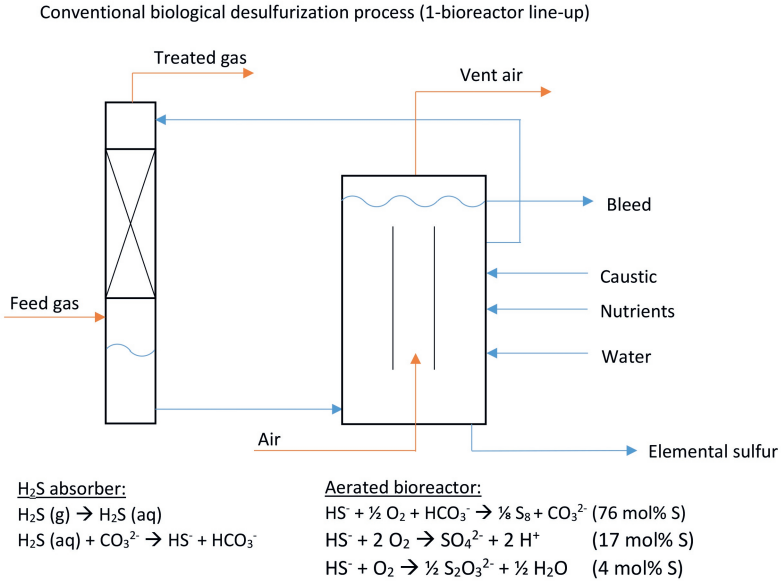

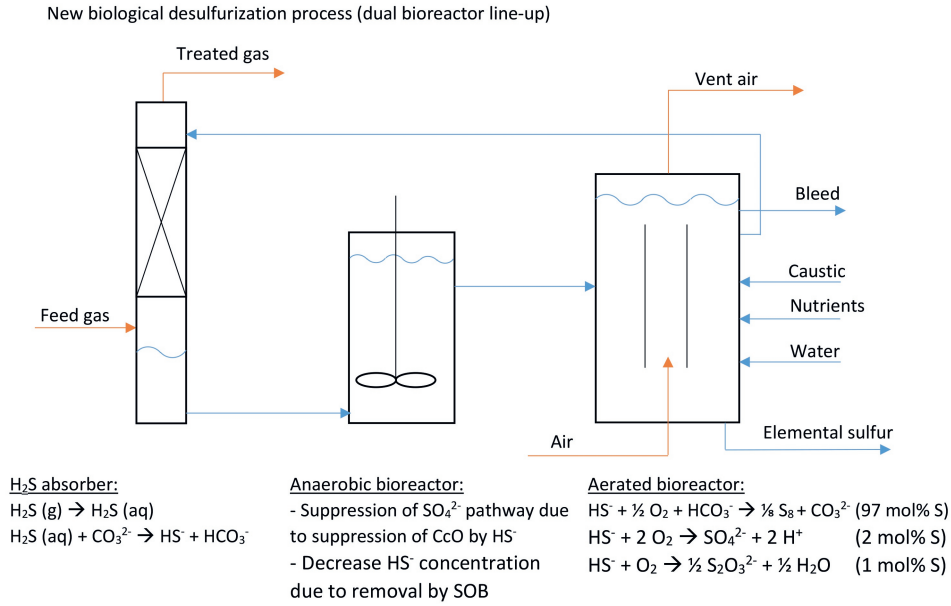

Figure SI1.1: Overview of the conventional biological desulfurization process (1-bioreactor line-up) (top) and new biological desulfurization process (dual bioreactor line-up) (bottom). Orange lines indicate gas flows, blue lines indicate liquid flows.

SI

SI 1.3 Calculation of caustic consumption and bleed formation based on product selectivities

The process selectivity and consumables of a full scale plant are calculated via the following procedure. From the total bleed flow and the composition of the bleed flow, the total production rate of SO_4^{2-} and $S_2O_3^{2-}$ can be calculated, via:

$$P_{SO_4^{2-}} = [SO_4^{2-}] \cdot Q_{bleed} \quad \text{(Equation SI1.1)}$$

$$P_{S_2O_3^{2-}} = [S_2O_3^{2-}] \cdot Q_{bleed} \quad \text{(Equation SI1.2)}$$

where P_* is the formation rate of product (in mol day^{-1}), $[*]$ the concentration of product in the bleed (mol L^{-1}) and $Q_{bleed}$the bleed flow (in L day^{-1}). When the production rates are known, the selectivity of the process can be calculated according to:

$$S_{SO_4^{2-}} = \frac{P_{SO_4^{2-}}}{H_2S\ load} \cdot 100\% \quad \text{(Equation SI1.3)}$$

$$S_{S_2O_3^{2-}} = \frac{2 \cdot P_{S_2O_3^{2-}}}{H_2S\ load} \cdot 100\% \quad \text{(Equation SI1.4)}$$

where S_* is selectivity for the product (in %) and $H_2S\ load$ the total H_2S load to the full scale unit (in mol day^{-1}).

The total caustic consumption can be calculated based on the bleed flow, according to:

$$C_{NaOH} = \frac{[Na^+] \cdot Q_{bleed}}{H_2S\ load} \cdot \frac{u_{NaOH}}{u_S} \quad \text{(Equation SI1.5)}$$

where C_{NaOH} is the caustic consumption (in kg NaOH kg^{-1} S), $[Na^+]$ the concentration of sodium in the bleed (in mol L^{-1}). Na^+ is the counter ion for SO_4^{2-}, $S_2O_3^{2-}$ and HCO_3^-/CO_3^{2-} (alkalinity). u_{NaOH} and u_S are the molar mass of NaOH and S respectively.

In case process selectivity of the process is known, but the bleed flow is not, the total bleed flow can be calculated via reformulating equations SI1.1 and SI1.3, following:

$$Q_{bleed} = \frac{S_{SO_4^{2-}} \cdot H_2S\ load}{[SO_4^{2-}] \cdot 100\%} \quad \text{(Equation SI1.6)}$$

As part of the sulfur cake contains bleed ($Q_{bleed,cake}$ is 30-40% weight of the produced sulfur cake), the required observed bleed ($Q_{bleed,obs}$) can be calculated by:

$$Q_{bleed,obs} = Q_{bleed} - Q_{bleed,cake}$$ (Equation SI1.7)

Where $Q_{bleed,cake}$ is defined as

$$Q_{bleed,cake} = \frac{1-DW}{DW}\frac{MP_{cake,S}}{\rho_{bleed}}$$ (Equation SI1.8)

Where DW is the fraction of dry weight of the produced sulfur cake (-), $M_{cake,S}$ the total mass production of sulfur in the sulfur cake (kg day^{-1}) and ρ_{bleed} the density of the bleed solution (kg L^{-1}).

SI 1.4 DETAILED INFO NGS RESULTS

Table SI1.1: Details NGS resuls. At least all species with >1% abundance are shown.

	Accession number	day 3	day 19	day 73
Alkalilimnicola ehrlichii MLHE-1	CP000453	2.18%	3.16%	58.86%
Thioalkalivibrio		**53.84%**	**59.76%**	**0.85%**
Thioalkalivibrio sulfidiphilus HL-EbGr7	CP001339	53.73%	59.72%	0.85%
Thioalkalivibrio thiocyanodenitrificans ARhD 1	AQZO01000005	0.11%	0.04%	0.01%
Thioalkalimicrobium		**0.37%**	**0.13%**	**0.01%**
Thioalkalimicrobium cyclicum ALM1	CP002776	0.20%	0.11%	0.00%
Thioalkalimicrobium aerophilum AL3	CP007030	0.17%	0.02%	0.00%
Thiohalobacter thiocyanaticus	FJ024318	0.00%	0.01%	0.73%
Halomonas sp		**33.88%**	**30.91%**	**16.50%**
Halomonas desiderata	HM438493	13.78%	23.23%	4.54%
Halomonas sp. HB.br	JX075114	4.12%	1.32%	4.99%
Halomonas sp. IB-G4	FJ469349	3.06%	0.92%	1.98%
Halomonas sp. IB-G4	JX075151	0.39%	0.07%	0.41%
Halomonas sp. PJ-18	KC261282	2.76%	1.15%	2.56%
Halomonas sp. Ko501	JQ032015	2.07%	1.11%	0.20%
Halomonas sp. Ap-5	JQ427049	0.01%	0.01%	0.03%
Halomonas sp. Ap-5	HM438481	1.53%	0.29%	0.16%
Halomonas sp. Ap-5	EU305583	1.33%	0.28%	0.20%
Halomonas sp. Ap-5	HM438496	1.07%	0.16%	0.03%
Halomonas sp. 146Z8-2	JQ032379	1.33%	1.09%	0.45%
Halomonas sp. KO116	EU540063	0.84%	0.64%	0.32%
Halomonas sp. Ijh-18	GU217701	0.71%	0.24%	0.39%
Halomonas muralis	EF157249	0.45%	0.30%	0.06%
Halomonas muralis	KM108690	0.43%	0.10%	0.18%
Desulfurispirillum indicum S5	CP002432	0.62%	0.76%	0.00%
Fodinicurvata sediminis DSM 21159	KF836196	0.00%	0.09%	15.64%
gamma proteobacterium E-113	FJ764789	3.37%	1.97%	2.25%
gamma proteobacterium E-036	FJ764788	0.90%	0.58%	1.28%
others		4.77%	2.50%	3.83%

SI 1.5 DATA CONTROL EXPERIMENT WITHOUT ANAEROBIC BIOREACTOR

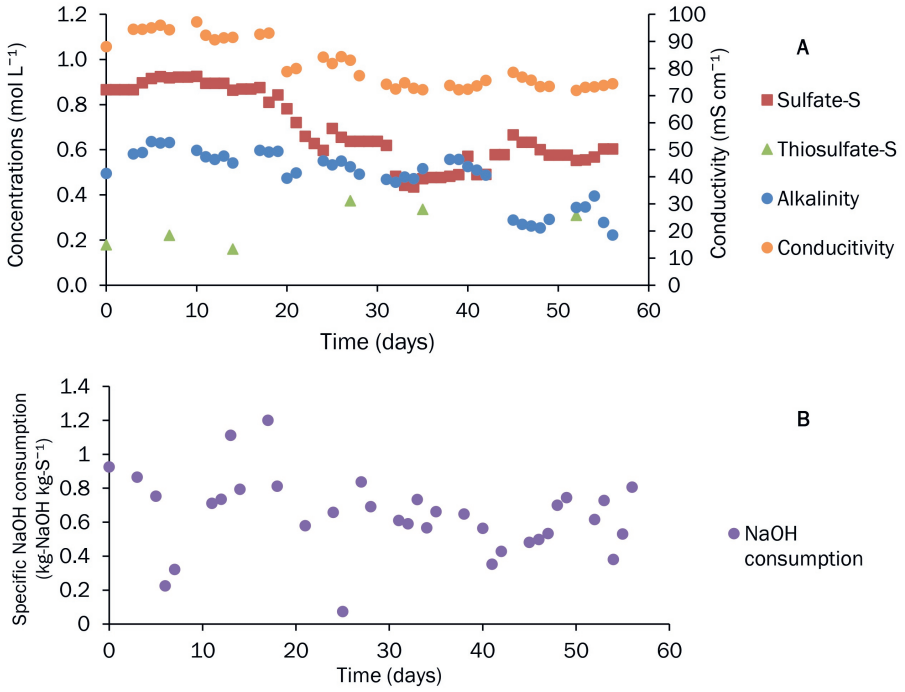

Figure SI1.2: Results of the continuous experiment of the control experiment, i.e. the original 1-bioreactor system. Figure A shows the measured concentrations of SO_4^{2-} and $S_2O_3^{2-}$, the measured alkalinity and the conductivity in the effluent of the aerated bioreactor. In Figure B the NaOH consumption is shown.

SI 2 SUPPORTING INFORMATION FROM CHAPTER 3

SI 2.1 EXPERIMENTAL SET-UP

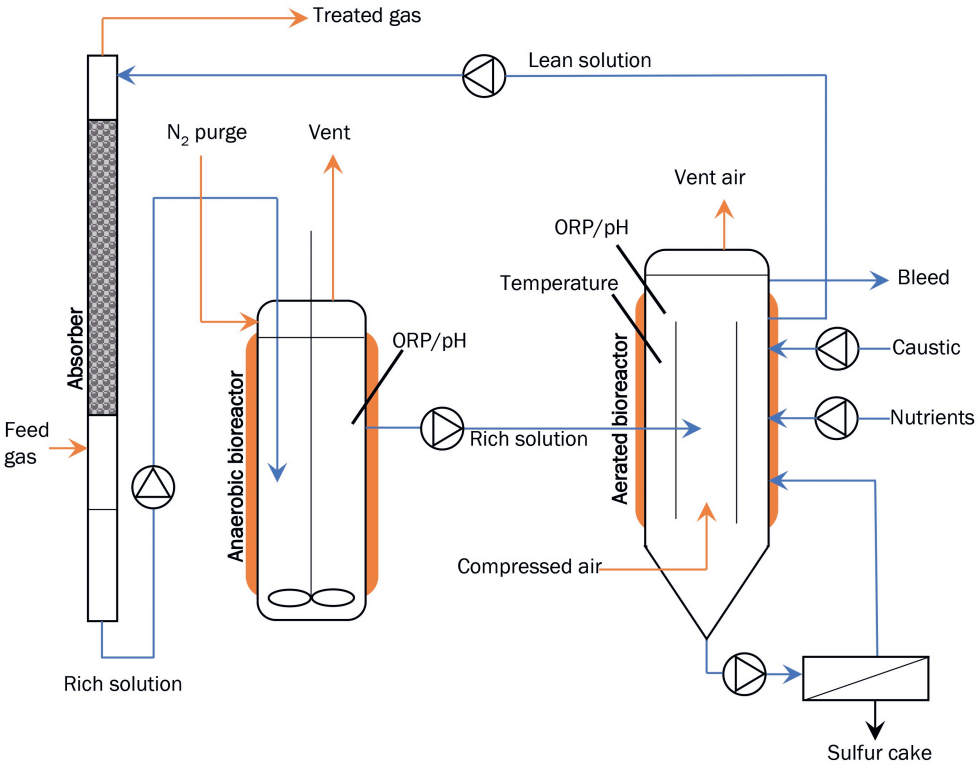

Figure SI2.1: Schematic overview of the experimental set-up. Orange lines represent gaseous flows; blue lines represent liquid flows.

SI 2.1.1 ABSORBER

Feed gas, containing H_2S, CO_2 and N_2 gas dosed via separate mass flow controllers (Brooks instrument, USA), was supplied to the absorber column. The absorber was stainless steel column of 4 m height and contained 2 meter of packing material (glass spheres with a diameter of 1 cm) in which gas and liquid were counter-currently contacted. Solution from the aerated bioreactor (which was free of sulfide and is therefore called 'lean solution') was pumped to the top of the absorber by an eccentric screw pump (Verder BV, the Netherlands). The solution flowed downwards through the packing. The sulfide containing solution ('rich solution') was collected at the bottom of the absorber column. Treated gas (i.e. gas low in H_2S) was leaving the absorber at the top. The H_2S content in the treated gas

was not analyzed, since from previous research it is know that under the applied conditions practically all H_2S is absorbed [1]. The absorber was operated at a pressure of 3 bar(g). The flow of rich solution from the absorber bottom to the anaerobic bioreactor was controlled via a piston pump (Pompe Cucchi, Italia).

SI 2.1.2 BIOREACTORS

The anaerobic reactor was a glass vessel with a mechanical agitator (rzr2020, Heidolph Instruments, Germany) to mix the inventory. The liquid level in this reactor was adjusted to change the liquid volume between 1 and 6 L. A stream of N_2 was supplied to the headspace of the anaerobic reactor to ensure anaerobic conditions. The pH and ORP were measured online by a combined SE552/2 Inducon ORP/pH sensor, connected to a Stratos Pro Transmitter (Knick, Germany). An integrated Ag/AgCl electrode was used as reference for ORP and pH. The flow of rich solution from the anaerobic bioreactor to the aerated bioreactor was driven by a peristaltic pump (Watson and Marlow).

The aerated bioreactor was a glass vessel with a volume of 11.4 L, with dimensions 690/150 mm (H/D). This was a gas lift reactor with a riser / downer system. Compressed air was injected via an air sparger at the bottom of an internal cylinder and the rich solution from the anaerobic bioreactor was injected just above the air inlet. A combined ORP/pH probe was measuring the pH and ORP in the bioreactor. The ORP in the aerated bioreactor was maintained at a constant pre-set value via a PI feedback controller that controlled the air flow rate with a mass flow controller (Brooks Instruments, USA). Warm water from a thermostatic bath was routed through the water jackets of the aerated and anaerobic bioreactor. The temperature of the solution was measured online in the aerated bioreactor and was always between 37 and 38 °C. The presence of dissolved sulfide (HS^- and polysulfide) in the aerated bioreactor was regularly checked with lead acetate paper (Merck). The aerated bioreactor had a conical bottom where elemental sulfur settled. The slurry in the conical bottom was circulated by a peristaltic pump (Watson and Marlow) to prevent blockage.

SI 2.1.3 INFLUENTS AND EFFLUENTS

Caustic and nutrients were dosed to the aerated bioreactor via a pulse/pause timer. Bleed was leaving the aerated bioreactor via an overflow to maintain the level in the aerated bioreactor. A slipstream of the circulation flow over the conical bottom of the aerated bioreactor was routed to a decanter centrifuge (Lemitech, Germany) via a pump (Master

flex). The centrate from the decanter was routed back into the aerated bioreactor. Elemental sulfur was recovered from the decanter as a sulfur cake. To determine the liquid influent and effluent streams, the vessels for storing and collecting nutrients, caustic, bleed water and sulfur cake were weighed each time a sample was taken, using a scale.

Liquid samples for analyses were taken from two sampling points located at (i) the sample port at the bottom of the anaerobic bioreactor, and (ii) the sample port of the lean solution from the aerated bioreactor.

SI 2.2 Materials and methods NGS analysis

Samples for microbial community analysis were taken from the aerated bioreactor at the end of each experiment. Also a sample of the inoculum was analyzed. 2 mL sample was centrifuged for 10 minutes at 14000 g. The biomass pellets were preserved by snap-freezing in liquid nitrogen and stored at -80 °C. DNA was extracted using the Powersoil DNA isolation kit (Qiagen) according to the manufacturer's instructions. Subsequently, PCR was used to amplify the V3 and V4 region of the 16S rRNA gene, using primers as described by [2]. These primers are targeting both the bacterial and the archaeal 16s rRNA gene. The DNA was sequenced using the Illumina platform and MiSeq sequencer. The paired-end MiSeq reads were merged based on the overlap between the two reads. Only merged sequences were used in subsequent analyses and the non-overlapping pairs were discarded. The 16S-based metagenomics analyses were performed using QIIME [3] version 1.9.1. After primer sequences were removed from the merged sequence reads, these were placed in a single fasta file using the add_qiime_labels.py script with the options 'cutadapt -m 100 -u 17 -u -21'. OTU picking was performed with the script pick_open_reference_otus.py using the SILVA version 128 [4]. 16S reference database and uclust [5]. The RDP classifier (version 2.2) [6] was trained with the same SILVA reference database and subsequently used to classify the OTUs.

SI 2.3 Results of all experimental runs

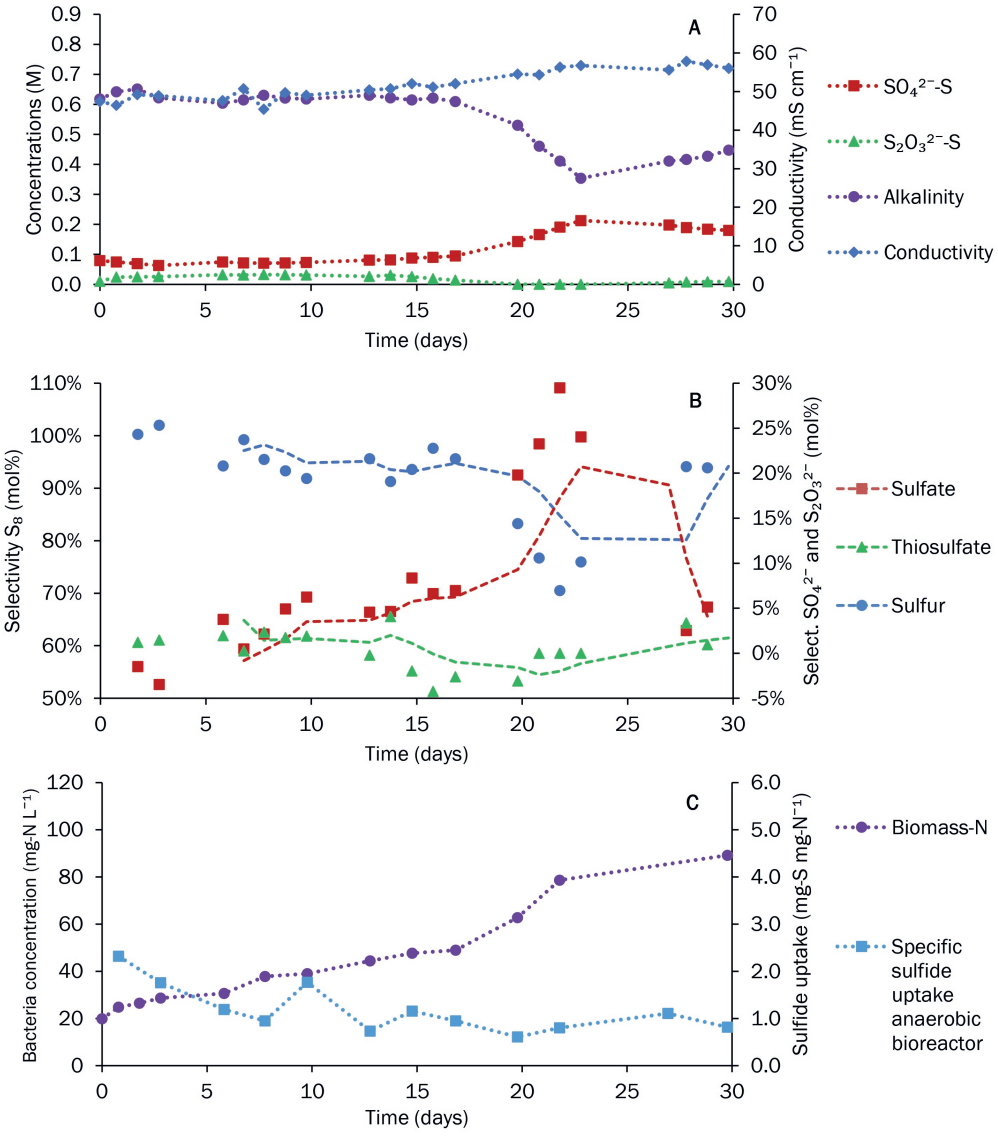

Figure SI2.2: Experimental results experiment 1. Fig A shows the concentrations of the SO_4^{2-}, $S_2O_3^{2-}$, the alkalinity and the conductivity. Fig B shows the calculated product selectivities. The dots are the daily measurements and the dashed line indicates the moving average (average value of 5 consecutive measurements). Fig C shows the biomass concentration in the process solution and the specific sulfide uptake by the bacteria in the anaerobic bioreactor.

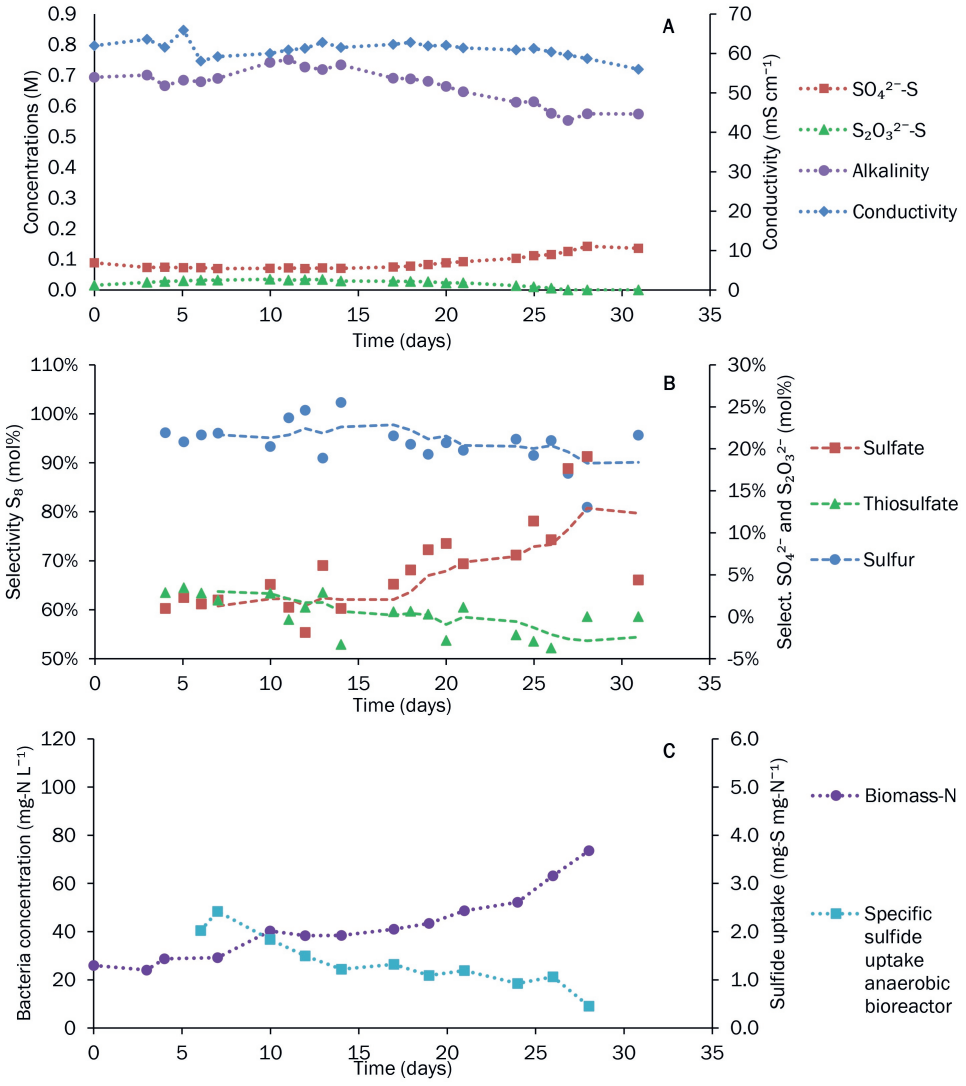

Figure SI2.3: Experimental results experiment 3. Fig A shows the concentrations of the SO_4^{2-}, $S_2O_3^{2-}$, the alkalinity and the conductivity. Fig B shows the calculated product selectivities. The dots are the daily measurements and the dashed line indicates the moving average (average value of 5 consecutive measurements). Fig C shows the biomass concentration in the process solution and the specific sulfide uptake by the bacteria in the anaerobic bioreactor.

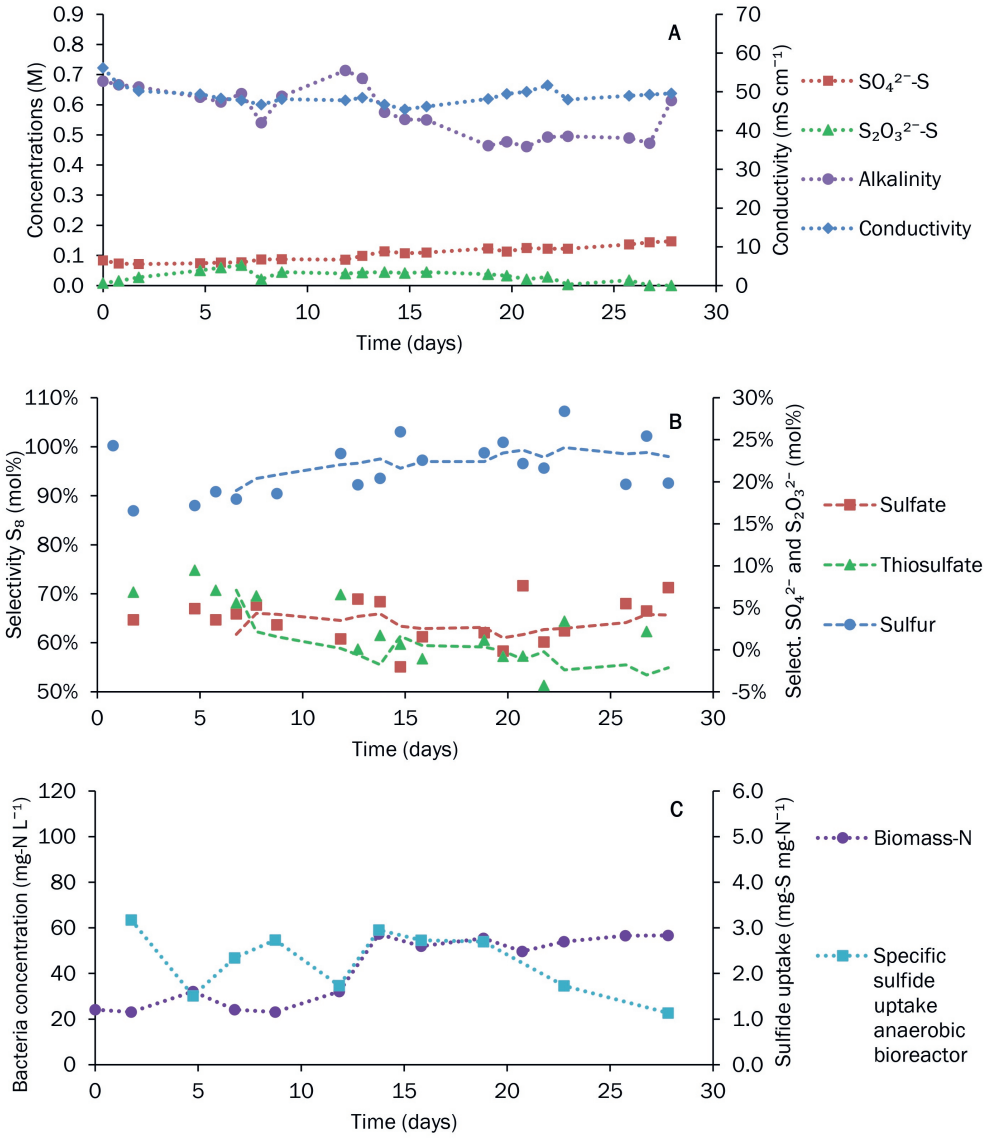

Figure SI2.4: Experimental results experiment 4. Fig A shows the concentrations of the SO_4^{2-}, $S_2O_3^{2-}$, the alkalinity and the conductivity. Fig B shows the calculated product selectivities. The dots are the daily measurements and the dashed line indicates the moving average (average value of 5 consecutive measurements). Fig C shows the biomass concentration in the process solution and the specific sulfide uptake by the bacteria in the anaerobic bioreactor.

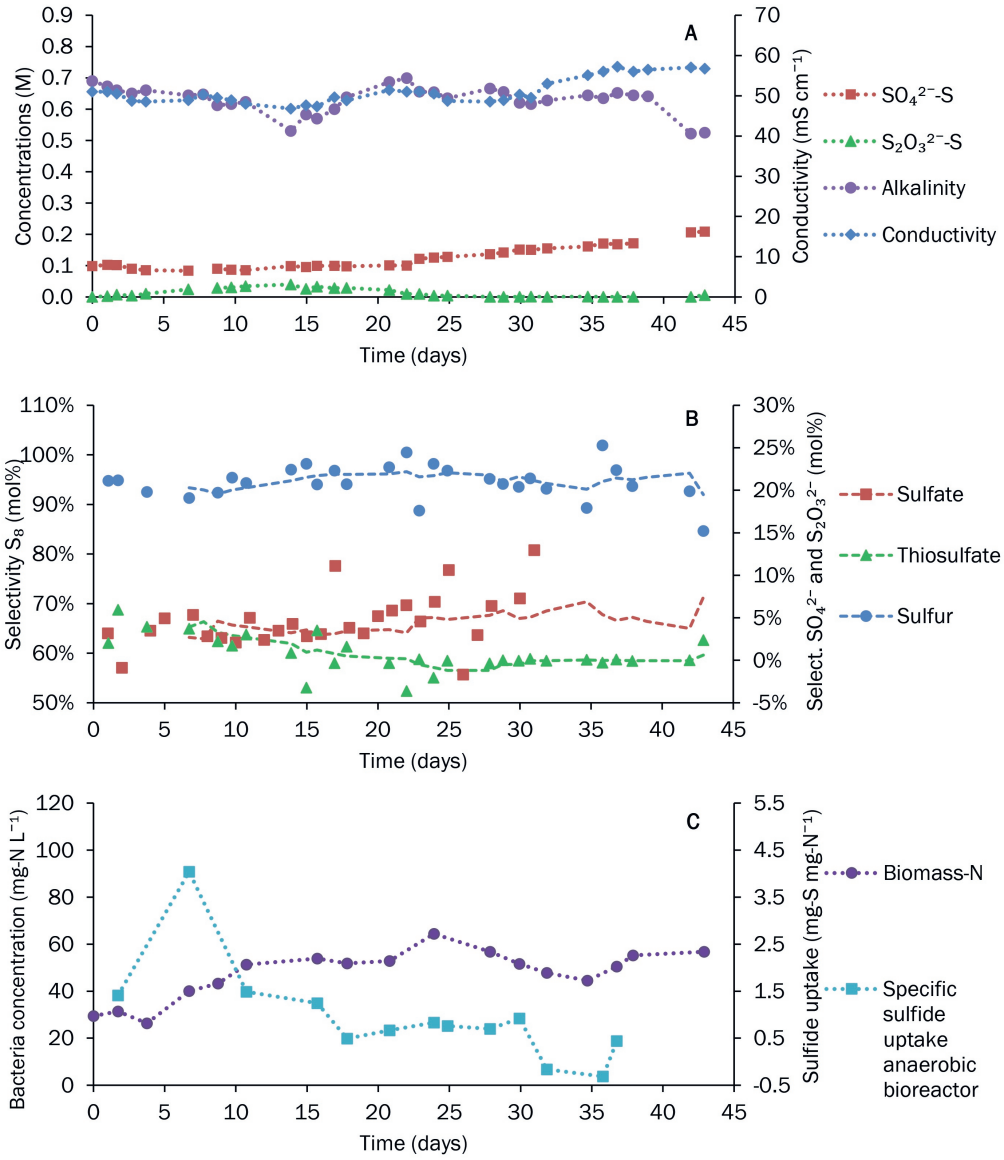

Figure SI2.5: Experimental results experiment 5. Fig A shows the concentrations of the SO_4^{2-}, $S_2O_3^{2-}$, the alkalinity and the conductivity. Fig B shows the calculated product selectivities. The dots are the daily measurements and the dashed line indicates the moving average (average value of 5 consecutive measurements). Fig C shows the biomass concentration in the process solution and the specific sulfide uptake by the bacteria in the anaerobic bioreactor.

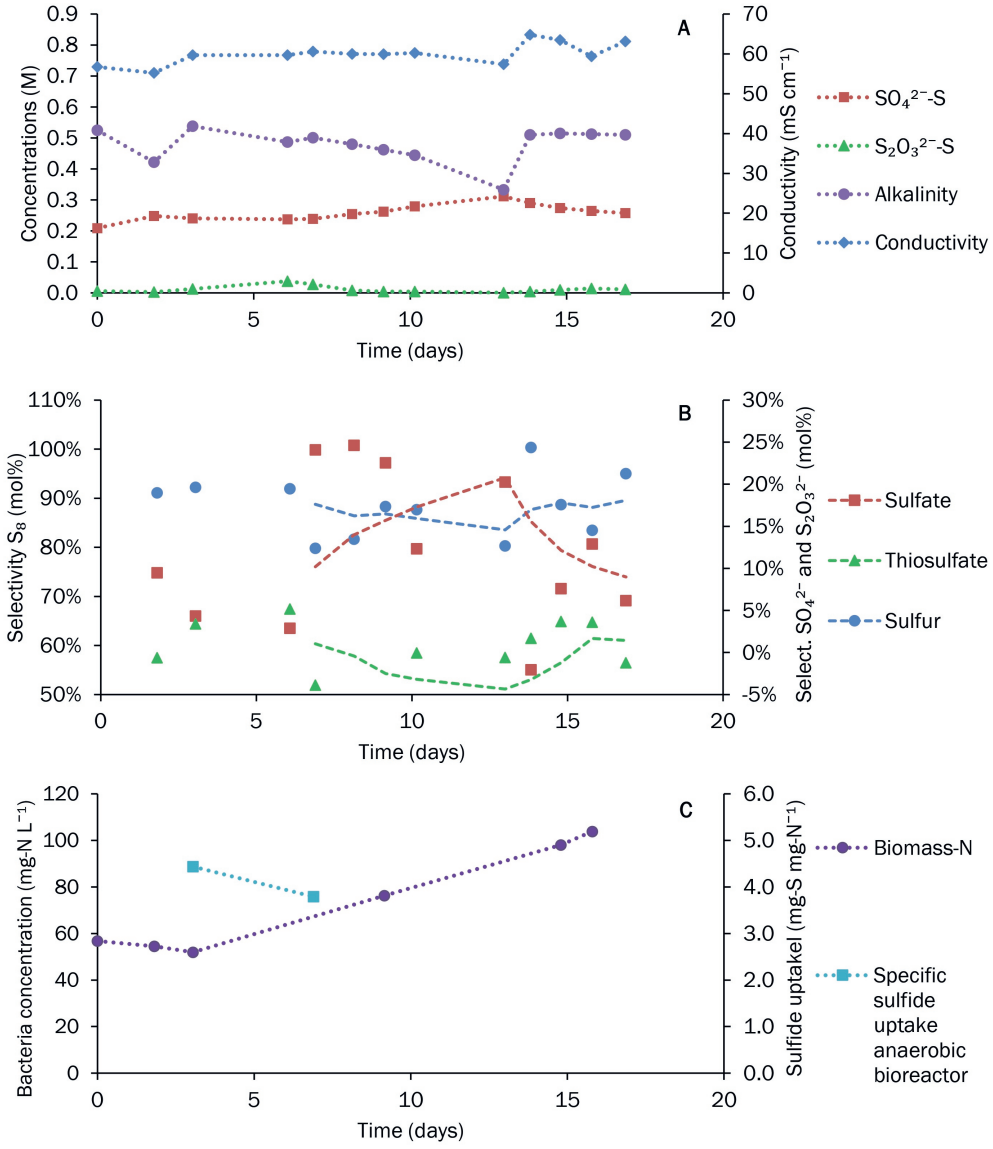

Figure SI2.6: Experimental results experiment 6. Fig A shows the concentrations of the SO_4^{2-}, $S_2O_3^{2-}$, the alkalinity and the conductivity. Fig B shows the calculated product selectivities. The dots are the daily measurements and the dashed line indicates the moving average (average value of 5 consecutive measurements). Fig C shows the biomass concentration in the process solution and the specific sulfide uptake by the bacteria in the anaerobic bioreactor.

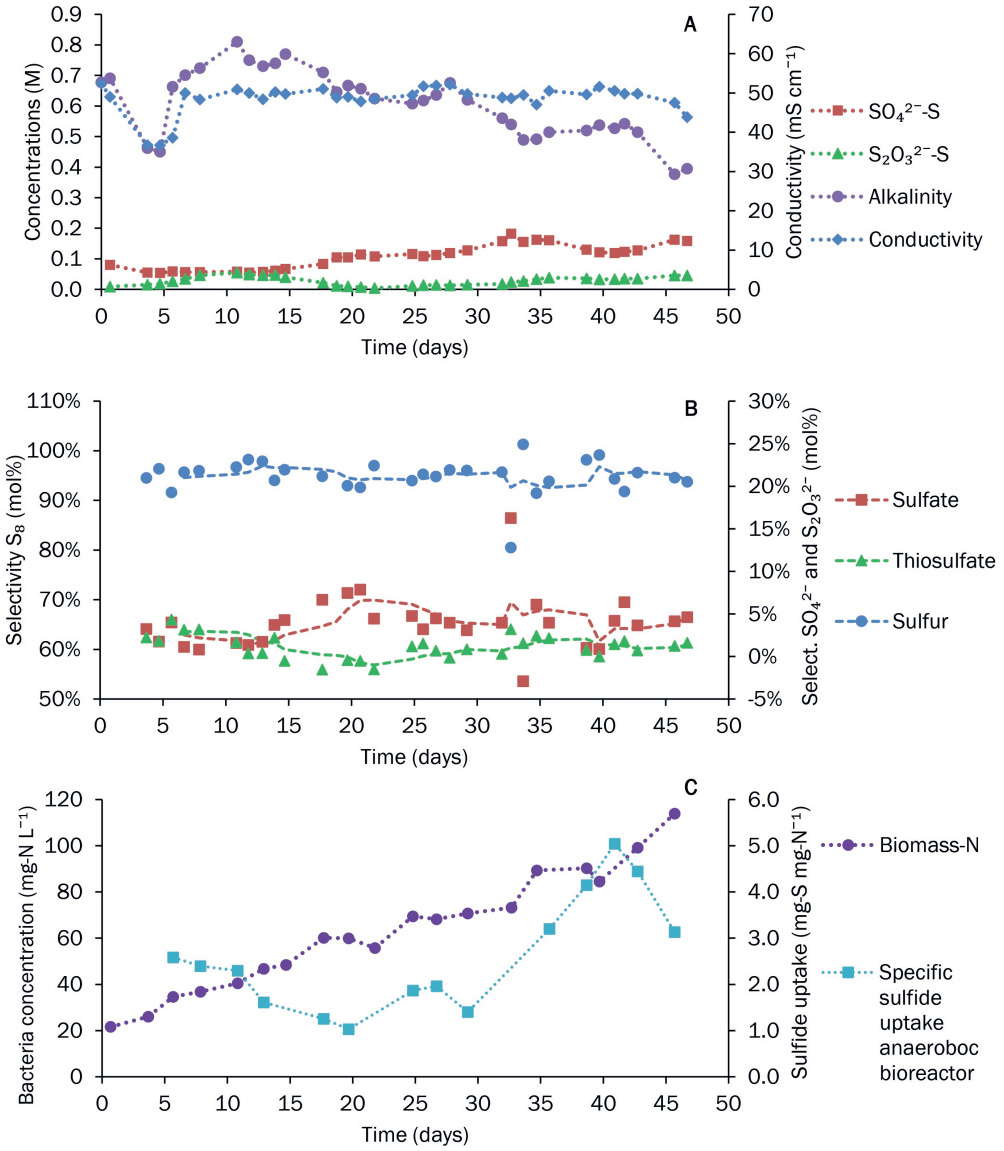

Figure SI2.7: Experimental results experiment 7. Fig A shows the concentrations of the SO_4^{2-}, $S_2O_3^{2-}$, the alkalinity and the conductivity. Fig B shows the calculated product selectivities. The dots are the daily measurements and the dashed line indicates the moving average (average value of 5 consecutive measurements). Fig C shows the biomass concentration in the process solution and the specific sulfide uptake by the bacteria in the anaerobic bioreactor.

SI 3 SUPPORTING INFORMATION CHAPTER4

SI 3.1 DETAILS EXPERIMENTAL SET-UP

The pilot-scale biodesulfurization installation consisted of an H_2S absorber, an anaerobic bioreactor, an aerated bioreactor and auxiliary vessel (Figure 4.1). The feed gas supplied to the H_2S absorber (stream A in Figure SI3.1) was a mixture of H_2S (8.9 vol% H_2S, 91.1 vol% N_2) and CO_2 (99.995 vol%). These gases were supplied as separate streams using mass flow controllers (Profibus, Brooks instrument, Hatfield, USA) to the main feed gas line. The feed gas entered the absorber just below the packed bed. Process solution (stream 1 in Figure 4.1) containing no sulfide ('lean solution') was continuously pumped to the absorber top by an eccentric screw pump (P1 in Figure SI3.1). The liquid flow was measured and controlled by a flow meter (Endress+Hausser, Reinach, Switzerland). The pressure in the absorber was controlled with a Tescom Europe backpressure regulator (Emerson Electric co., St. Louis, USA) and measured with a pressure meter (Endress+Hausser, Reinach, Switzerland), located at the outlet gas line. A sub stream of the treated gas was routed to a gas chromatograph (GC) (EnCal 3000, Honeywell, USA), by a diaphragm vacuum pump (knf, Freiburg, Germany) for analysis of the treated gas composition.

The liquid which has absorbed the H_2S ('rich solution'), was collected in the absorber bottom (total volume approximately 1 L). The flow of rich solution from the bottom of the absorber to the anaerobic bioreactor (stream 2) was controlled with a valve and driven by the pressure difference between the pressurized absorber and the atmospheric anaerobic bioreactor. A Level indictor (Endress+Hausser, Reinach, Switzerland), acting on the control valve, kept the liquid level on a constant pre-set value. The anaerobic bioreactor solution (liquid volume of 5.3 L) was continuously mixed by an installed mechanical mixer (rzr2020, Heidolph Instruments, Schwabach, Germany). The effluent of the anaerobic bioreactor was directed to the aerated bioreactor (stream 3) with a peristaltic pump (P2). The aerated bioreactor was a gas-lift bioreactor with a liquid volume of 11.4 L. Compressed air (stream D) was supplied to the aerated bioreactor using a mass flow controller (Profibus, Brooks instrument, Hatfield, USA). The airflow was controlled via the ORP measurement in the aerated bioreactor, using a PID controller in the PLC [7]. The ORP was maintained at -360 mV. Under these conditions, SOB oxidize HS^- mainly to S_8, which regenerates the process solution. In addition, a sensor for measuring dissolved O_2 (PSt 6 Presens, Regensburg, Germany) was positioned in the aerated bioreactor. The produced S_8 was settling in the

cone-shaped bottom of the aerated bioreactor. This S_8 slurry was removed with a pump (P6) (101 U/R, Watson Marlow, Wilmington USA) (stream 8). To compensate for the removed slurry, diluted nutrient solution (stream 7) and a 5 w/w % NaOH solution (stream 6) were continuously supplied to the aerated bioreactor with pumps P5 and P4 (both 101 U/R, Watson Marlow, Wilmington, USA). The nutrients contained 28.6 g L^{-1} nitrogen as urea, 20 g L^{-1} potassium as KNO_3, 6.5 g L^{-1} P as H_3PO_4 and trace metals as described by Pfennig & Lippert[8]. These components are required for growth of the SOB. Caustic soda (NaOH) was supplied to maintain a constant alkalinity. Furthermore, the flow from the aerated bioreactor to anaerobic bioreactor (stream 4) was set a flow rate of 10 L h^{-1}, using pump P3.

SI 3.2 NGS ANALYSIS MICROBIAL COMMUNITY COMPOSITION

The microbial community composition of the system was analyzed using *by 16S rRNA gene Amplicon Sequencing*. The sample, taken from the aerated bioreactor, was conserved immediately after sampling by addition of ethanol up to 50 % (v/v). DNA was extracted with the MPbio FastDNA™ SPIN Kit for Soil. Subsequently, PCR was used to amplify the V3 and V4 region of the 16S rRNA gene of bacteria giving a 400 bp product. The library prep, sequencing and data analysis was performed via the 16S BioProphyler® method [9], using the Illumina MiSeq sequencer. The obtained sequences were compared with the online nt database with the aid of the BLAST algorithm. Low abundance reads were not removed from the dataset and no correction on differences in library sized was applied. The reported species name is the species most related to the detected sequence. Results are shown in Figure SI3.1.

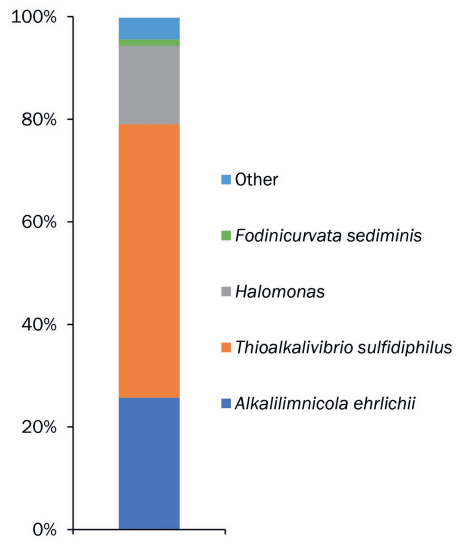

Figure SI3.1: Mapping of bacterial diversity in the system during the temperature and biomass concentration experiments. Sample taken from aerated reactor.

SI 3.3 DYNAMIC MODEL TO DESCRIBE BIOMASS CONCENTRATIONS IN ALL PROCESS VESSELS

SI 3.3.1 NOMENCLATURE AND INDICES

Xb biomass concentration, in mg-N L^{-1}

Q flow solution, in kg h^{-1}

t time, h

ρ density of the solution, in kg L^{-1}

θ parameter vector

abs absorber

aux auxillary vessel

BR1 bioreactor 1, anaerobic bioreactor

BR2 bioreactor 2, aerated bioreactor

rec recycle flow from BR2 to BR1

lean lean solution from auxiliary vessel to top absorber

SI 3.3.2 MODEL DESCRIPTION

The model describing the concentrations of biomass in the system (see Figure 4.4) is presented as a set of ordinary differential equations. Assumed is that the volume of the tubing between all vessels is neglectable and all reactor vessels are ideally mixed. The differential equation, describing the dynamic biomass concentration in the absorber is given by Equation SI3.1.

$$\frac{dXb_{abs}(t)}{dt} = \frac{Q_{lean}}{\rho \cdot V_{abs}} \cdot \left(Xb_{aux}(t) - Xb_{abs}(t)\right) \quad \text{(Equation SI3.1)}$$

The differential equation, describing the dynamic biomass concentration in bioreactor 1, the anaerobic bioreactor, is given by Equation SI3.2.

$$\frac{dXb_{BR1}(t)}{dt} = \frac{Q_{lean}}{\rho \cdot V_{BR1}} \cdot Xb_{abs}(t) + \frac{Q_{rec}}{\rho \cdot V_{BR1}} \cdot Xb_{BR2}(t) - \frac{Q_{lean}+Q_{rec}}{\rho \cdot V_{BR1}} \cdot Xb_{BR1}(t) \quad \text{(Equation SI3.2)}$$

The differential equation, describing the dynamic biomass concentration in BR 2, the aerated bioreactor, is given by Equation SI3.3.

$$\frac{dXb_{BR2}(t)}{dt} = \frac{Q_{lean}+Q_{rec}}{\rho \cdot V_{BR2}} \cdot \left(Xb_{BR1}(t) - Xb_{BR2}(t)\right) \quad \text{(Equation SI3.3)}$$

The differential equation, describing the dynamic biomass concentration in the auxiliary vessels is given by Equation SI3.4.

$$\frac{d(t)}{dt} = \frac{Q_{lean}}{\rho \cdot V_{aux}} \cdot \left(Xb_{BR1}(t) - Xb_{aux}(t)\right) \quad \text{(Equation SI3.4)}$$

SI 3.3.3 Initial conditions and process parameters

The initial conditions for the concentrations of the biomass concentrations are given by the following vector:

$$\begin{pmatrix} Xb_{abs,0} \\ Xb_{BR1,0} \\ Xb_{BR2,0} \\ Xb_{aux,0} \end{pmatrix} = \begin{pmatrix} Xb_0 \\ Xb_0 \\ Xb_0 \\ 0 \end{pmatrix}$$

Where Xb_0 was 56.55 mg-N L^{-1} in Run 1 and 43.4 mg-N L^{-1} in Run 2. The parameter vector θ, containing all process parameters, is defined as:

$$\theta = \begin{pmatrix} Q_{lean} \\ Q_{rec} \\ \rho \\ V_{abs} \\ V_{BR1} \\ V_{BR2} \\ V_{aux} \end{pmatrix} = \begin{pmatrix} 6 \\ 10.5 \\ 1.05 \\ 1.0 \\ 5.3 \\ 11.4 \\ 5 \end{pmatrix}$$

SI 3.4 Theoretical physico-chemical H_2S and CO_2 absorption at different temperatures

The relationship between temperature and liquid/vapour fractions for CO_2 and H_2S was assessed with Aspen Technology software, using the electrolyte non-random two-liquid model. For both gases the model shows that at lower temperatures leads to lower equilibrium partial pressures of H_2S and CO_2. Hence, at lower temperatures, a higher absorption of these gases into the liquid is expected.

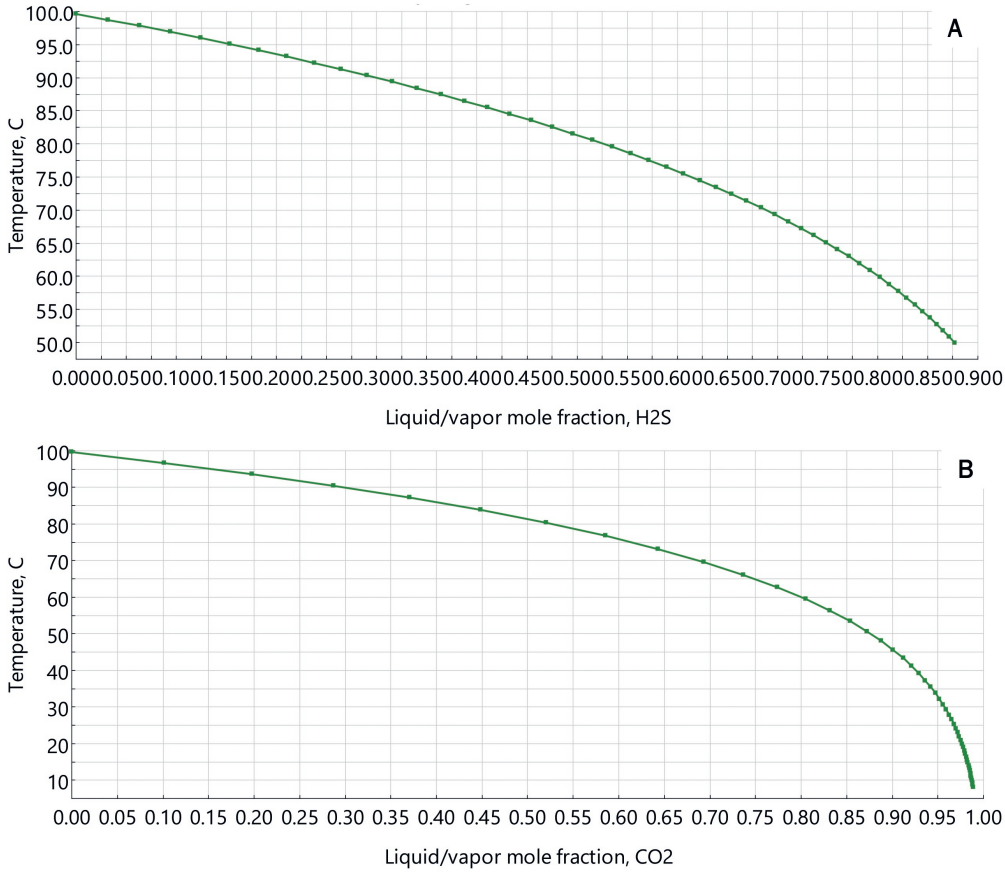

Figure SI3.2: Model predictions of the liquid/vapour mol fractions of H_2S (A) and CO_2 (B) at different temperatures.

SI 4 SUPPORTING INFORMATION FROM CHAPTER 5

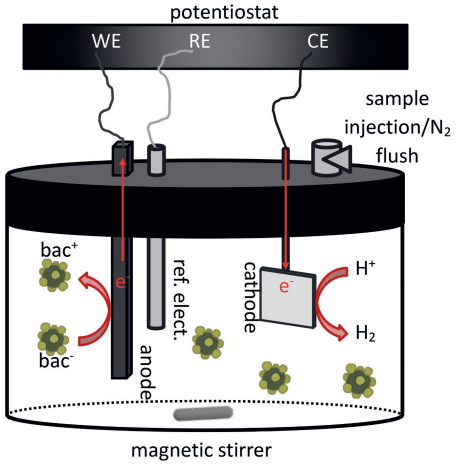

Figure SI4.1: Scheme of electrochemical cell to measure electricity recovery from HA-SOB.

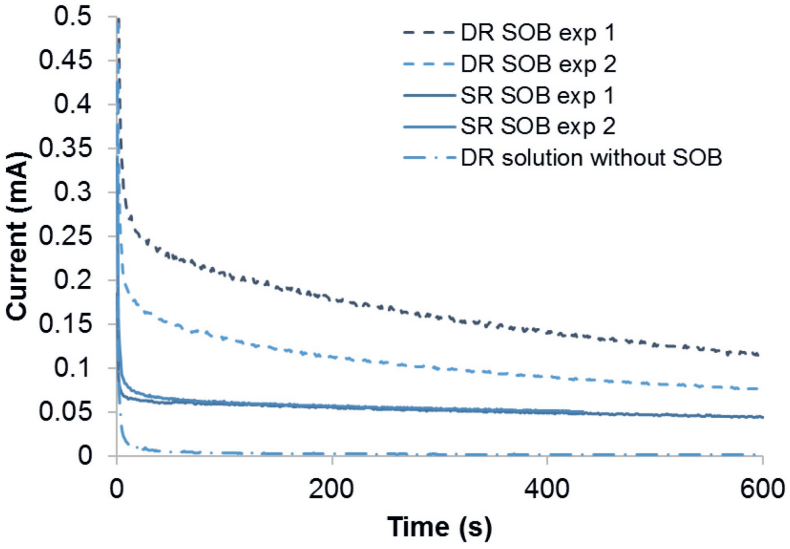

Figure SI4.2: Chronoamperograms of the 600 s discharge of SOB at anode potential of +0.1V vs Ag/AgCl. One typical curve of current production from centrifuged reactor solution without SOB at the same potential is also included and shows minimal current production. Data for SR-SOB exp 2 were obtained only during 430 seconds. The current for SR-SOB was assumed to follow the same trend as SR-SOB exp 1 to estimate the total charge obtained in 600 seconds.

Table SI4.1: Measured sulfide concentrations after 5 minutes, as measured during the sulfide uptake experiments. Exp 1 and Exp 2 are two replicate experiments with fresh solution. Initial concentration was 0.2 mM. Absence of sulfide after 5 minutes using DR solution with SOB was confirmed using lead acetate paper.

	Exp 1 (mM)	Exp 2 (mM)
DR solution with SOB	0	0
DR centrifuged reactor solution without SOB	0.153	0.155
SR solution with SOB	0.059	0.053
SR centrifuged reactor solution without SOB	0.113	0.093

MICROBIAL COMMUNITY ANALYSIS

DNA samples from sludges of both pilot and full-scale plant were extracted using the Powersoil ® DNA isolation kit (MO BIO Laboratories, Carlsbad, CA, USA). The isolated DNA was used to amplify the V3-V4 region of 16S rDNA according to the standard illumine library preparation method [2]. Bacteria and archaea was then analyzed by the same primer sets. Taxonomic analysis was processed using the QIIME [3] software (package version 1.9.1). OTU picking was performed by the SILVA 128, 16S reference database and the uclust tool [4]. The same SILVA reference database was subsequently trained by the RDP classifier (version 2.2) for OTUs classification [6].

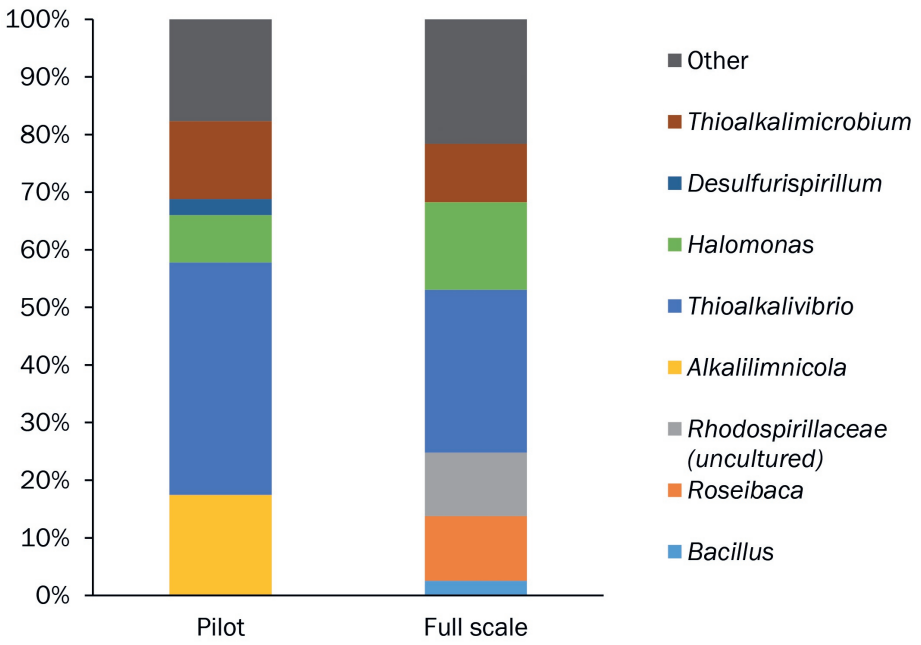

Figure SI4.3: Microbial community composition of the sludge from pilot and full-scale plant. *Alkalilimnicola* were the dominant SOB in the pilot plant, whereas *Thioalkalivibrio* were the dominant SOB in the full-scale plant.

SI 5 SUPPORTING INFORMATION FROM CHAPTER 6

SI 5.1 OVERVIEW OF LIQUID FLOW RATES AND HRT'S

An overview of the applied liquid flow rates, liquid volumes in different parts of the system and the HRT's in the different experiments, is provided in Table SI5.1.

Table SI5.1: overview of the applied liquid flow rates, liquid volumes in different parts of the system and the HRT's in the different experiments

	Exp 1	Exp 2	Exp 3
Recirculation flow rate (L h^{-1})	0.6	0.42	0.42
Influent flow rate (L h^{-1})	$0.23 \cdot 10^{-3}$	$0.41 \cdot 10^{-3}$	$0.23 \cdot 10^{-3}$
Volume entire system (incl tubing) (L)	0.5	0.5	0.5
Volume anolyte recirculation reactor (L)	0.4	0.4	0.4
Volume anode side of the electrochemical cell (L) *	0.016	0.016	0.016
HRT entire system (h)	2174	1220	1274
HRT anolyte recirculation reactor (h)	0.67	0.95	0.95
HRT electrochemical cell (h)	0.03	0.04	0.04

* The liquid volume of the anode side of the electrochemical cell has been calculated according to: Liquid volume (L) = total volume (L) · bed porosity (%)

The bed porosity was approximately 48% (calculated as described by: Pushnov [10]).

SI 5.2 NGS DETAILS

SI 5.2.1 MATERIALS AND METHODS

Samples for microbial community analysis were taken from the liquid and the graphite granules at the end of each run. Also a sample of the inoculum (planktonic biomass) was analyzed. For the analysis of planktonic biomass, 2 mL sample was centrifuged for 10 minutes at 14000 g. The biomass pellets and graphite granules were preserved by snap-freezing in liquid nitrogen and stored at -80 °C. DNA was extracted using the Powersoil DNA isolation kit (Qiagen) according to the manufacturer's instructions. Subsequently, PCR was used to amplify the V3 and V4 region of the 16S rRNA gene, using primers as described by [2]. These primers are targeting both the bacterial and the archaeal 16s rRNA gene. The DNA was sequenced using the Illumina platform and MiSeq sequencer. The paired-end

MiSeq reads were merged based on the overlap between the two reads. Only merged sequences were used in subsequent analyses and the non-overlapping pairs were discarded. The 16S-based metagenomics analyses were performed using QIIME [3] version 1.9.1. After primer sequences were removed from the merged sequence reads, these were placed in a single fasta file using the add_qiime_labels.py script with the options 'cutadapt -m 100 -u 17 -u -21'. OTU picking was performed with the script pick_open_reference_otus.py using the SILVA version 128 [4] 16S reference database and uclust [5]. The RDP classifier (version 2.2) [6] was trained with the same SILVA reference database and subsequently used to classify the OTUs.

SI 5.2.2 RESULTS

Table SI5.2: Overview of the bacterial species in the solution (planktonic biomass) and attached to the electrode (biofilm) as analyzed via 16S rRNA amplicon sequencing.

	Relative abundances					Key physiology	Occurrence (Alkaline habitat)
	Inoculum	End of exp 1 (planktonic)	End of exp 1 (biofilm)	End of exp 2 (planktonic)	End of exp 1 (biofilm)		
Sulfide oxidizing bacteria (SOB)							
Proteobacteria / Gammaproteobacteria / Chromatiales / Ectothiorhodospiraceae / Alkalilimnicola	18.48%	18.58%	4.02%	6.36%	1.94%	facultatively autotrophic and facultatively denitrifying SOB	Soda lakes and biodesulfurization plants
Proteobacteria / Gammaproteobacteria / Chromatiales / Ectothiorhodospiraceae / Thioalkalispira	0.22%	1.21%	0.12%	3.34%	0.23%	microaerophilic lithoautotrophic SOB	Soda lakes
*Proteobacteria / Gammaproteobacteria / Chromatiales / Ectothiorhodospiraceae / Thioalkalivibrio **	31.88%	2.54%	0.75%	16.40%	9.93%	Lithoautotrophic SOB	Soda lakes and Thiopaq reactors
Proteobacteria / Gammaproteobacteria / Thiotrichales / Piscirickettsiaceae / Thioalkalimicrobium	3.00%	2.90%	0.34%	0.73%	0.99%	Lithoautotrophic SOB	Soda lakes and Thiopaq reactors
Proteobacteria / Gammaproteobacteria / Oceanospirillales / Halomonadaceae Halomonas	1.27%	0.17%	0.23%	0.81%	1.63%	heterotrophic SOB forming tetrathionate	soda lakes and Thiopaq reactors
Proteobacteria / Alphaproteobacteria / Rhodobacterales / Rhodobacteraceae / Other	28.75%	2.59%	0.42%	9.38%	2.43%	Might be photoheterotrophic anaerobic SOB	Might be in soda lakes
Proteobacteria / Epsilonproteobacteria / Campylobacterales / Campylobacteraceae / Arcobacter	0.06%	3.08%	0.08%	14.30%	0.86%	Microaerophilic sulfide oxidation	Marine
Anaerobic sulfur bacteria							
*Proteobacteria / Deltaproteobacteria / Desulfobacterales / Desulfobulbaceae / Desulfurivibrio ***	1.28%	21.59%	36.97%	11.11%	43.31%	Elemental sulfur disproportionation or sulfur reduction with H_2	Biodesulfurization plants
Chrysiogenetes / Chrysiogenetes / Chrysiogenales / Chrysiogenaceae / Desulfurispirillum	0.35%	1.10%	6.03%	0.35%	1.38%	Sulfur reduction; dissimilatory ammonification	Soda lakes

* Until recently, *Thioalkalivibrio* was classified as a member of the family *Ectothiorhodospiraceae* (*Gammaproteobacteria*). It has been suggested to reclassify the genus *Thioalkalivibrio* into its own family *Thioalkalivibrionacea* within the order *Ecthothiorhodospirales* on the basis of the emerging phylogenetic taxonomy (https://gtdb.ecogenomic.org).

** The higher taxonomy recently has been changed to *Desulfobulbia>Desulfobulbales:Desulfurivibrionaceae*.

	Relative abundances					Key physiology	Occurrence (Alkaline habitat)
	Inoculum	End of exp 1 (planktonic)	End of exp 1 (biofilm)	End of exp 2 (planktonic)	End of exp 1 (biofilm)		
Fermentative bacteria							
Tenericutes / Mollicutes / Acholeplasmatales / Acholeplasmataceae / Acholeplasma	0.58%	6.10%	0.67%	3.44%	1.99%	Fermentative	Found in soda lake metagenomes
Firmicutes / Clostridia / Clostridiales / Clostridiaceae 2 / Anoxynatronum	0.83%	0.92%	1.30%	0.28%	2.73%	Fermentative	Soda lakes
Firmicutes / Clostridia; / Clostridiales / Clostridiaceae 2 / Tindallia	0.40%	0.14%	1.89%	0.16%	1.51%	Acetogenic, can use H_2 and reduce thiosulfate	Soda lakes
Cloacimonetes / MSBL8 / uncultured bacterium / uncultured bacterium / uncultured bacterium	0.00%	2.12%	2.84%	0.10%	0.40%	Fermentative	Found in soda lake metagenomes
Tenericutes / Mollicutes / NB1-n / Other / Other	0.43%	1.71%	0.79%	0.97%	0.42%	fermentative	found in soda lake metagenomes
Firmicutes / Clostridia / Clostridiales / Clostridiaceae 1 / uncultured	0.11%	0.72%	3.25%	0.05%	0.26%	?	?
Firmicutes / Clostridia / ML635J-38 / uncultured bacterium / uncultured bacterium	0.14%	0.07%	1.12%	0.07%	0.83%		
Firmicutes / Clostridia / Clostridiales / Syntrophomonadaceae / uncultured	0.02%	0.68%	0.39%	0.41%	1.04%	syntrophic oxidation of fatty acids at anaerobic conditions	there are isolates from soda lakes
Firmicutes / Erysipelotrichia / Erysipelotrichales / Erysipelotrichaceae / Erysipelothrix	0.77%	0.43%	0.69%	0.82%	1.08%		

	Relative abundances					Key physiology	Occurrence (Alkaline habitat)
	Inoculum	End of exp 1 (planktonic)	End of exp 1 (biofilm)	End of exp 2 (planktonic)	End of exp 1 (biofilm)		
Hydrolytic bacteria							
Bacteroidetes / Sphingobacteriia / Sphingobacteriales / Lentimicrobiaceae / uncultured bacterium	0.24%	15.69%	3.69%	16.13%	8.02%	Polysaccharidolytic	Soda lakes
Bacteroidetes; / Bacteroidia / Bacteroidales / Marinilabiaceae / Natronoflexus	0.00%	0.03%	7.31%	0.01%	0.45%	sugar fermentation	Soda lakes
Bacteroidetes / Bacteroidia / Bacteroidales / ML635J-40 aquatic group / uncultured bacterium	0.01%	0.65%	2.18%	0.95%	0.83%		soda lakes
Bacteroidetes / Bacteroidia / Bacteroidales / Marinilabiaceae;Ambiguous_taxa	0.00%	0.08%	2.08%	0.01%	1.24%		
Bacteroidetes / Bacteroidia / Bacteroidales / Marinilabiaceae / Alkaliflexus	0.00%	0.01%	1.20%	0.00%	0.10%	sugar fermentation	soda lake
Bacteroidetes / Bacteroidia / Bacteroidales / Rikenellaceae / Blvii28 wastewater-sludge group	0.03%	0.08%	1.63%	0.33%	1.37%		
Bacteroidetes / Bacteroidia / Bacteroidia Incertae Sedis / Draconibacteriaceae / uncultured	0.08%	0.14%	0.41%	0.35%	1.88%	sugar fermentation	

SI 5.3 XRD MEASUREMENTS

At the end of each experiment, the presence of elemental sulfur on the working electrode (i.e. the graphite granules and the graphite plate of the anolyte side of the electrochemical cell) was verified with XRD analysis. The measurements were done with a Bruker D8 Advance powder diffractometer with Lynxeye detector in Bragg Brentano geometry. Figures S5.1 and S5.2 show the XRD spectra of the granules and plate at the end of experiment 2. The XRD spectra corresponds to graphite (the electrode material), but doesn't indicate presence of S_8 sulfur. Spectra after experiment 1 and after the abiotic experiment indicate the same.

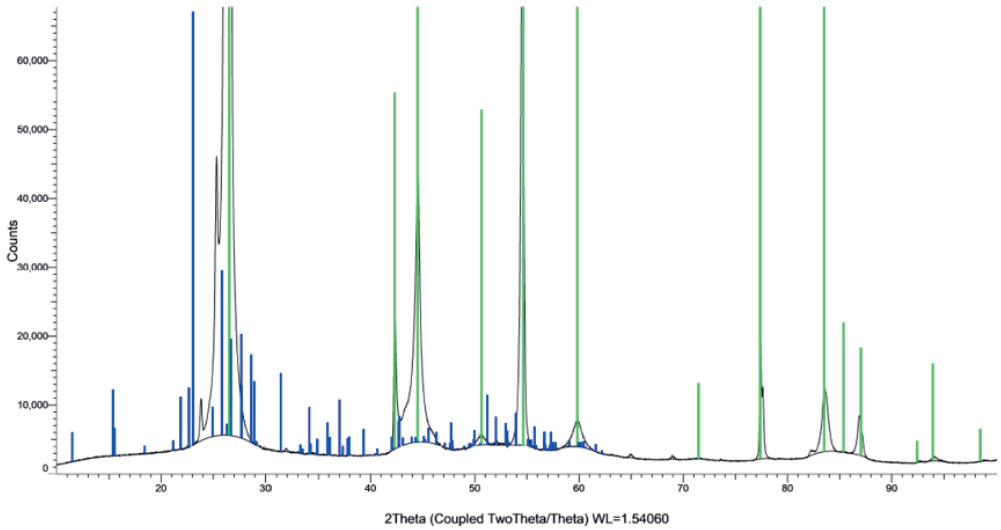

Figure SI5.1: XRD spectrum of graphite granules at end of experiment 2. The measurement was done from 10 to 100 deg 2 theta, with steps of 0.02 deg, time/step 3 s. The measured spectrum is shown by the black line. XRD spectrum of graphite is indicated in green; XRD spectrum of S_8 sulfur is indicated in blue.

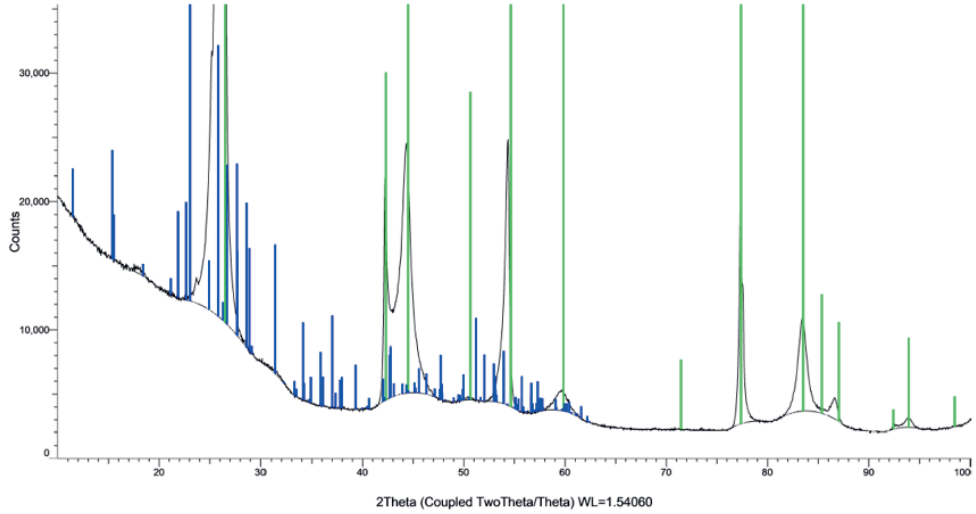

Figure SI5.2: XRD spectrum of the graphite plate at the end of experiment 2. The measurement was done from 10 to 100 deg 2 theta, with steps of 0.05 deg, time/step 1 s and xyz-sample stage. The measured spectrum is shown by the black line. XRD spectrum of graphite is indicated in green; XRD spectrum of S_8 sulfur is indicated in blue.

SI 5.4 SULFIDE CONCENTRATIONS

The sulfide uptake was determined by measuring sulfide in the in the anolyte recirculation reactor. In experiment 1, lead acetate paper was used. This indicates the presence or absence of sulfide. In experiment 2, the sulfide concentration was also measured using Hach Lange kit LCK635. The results are shown in Figure SI5.3.

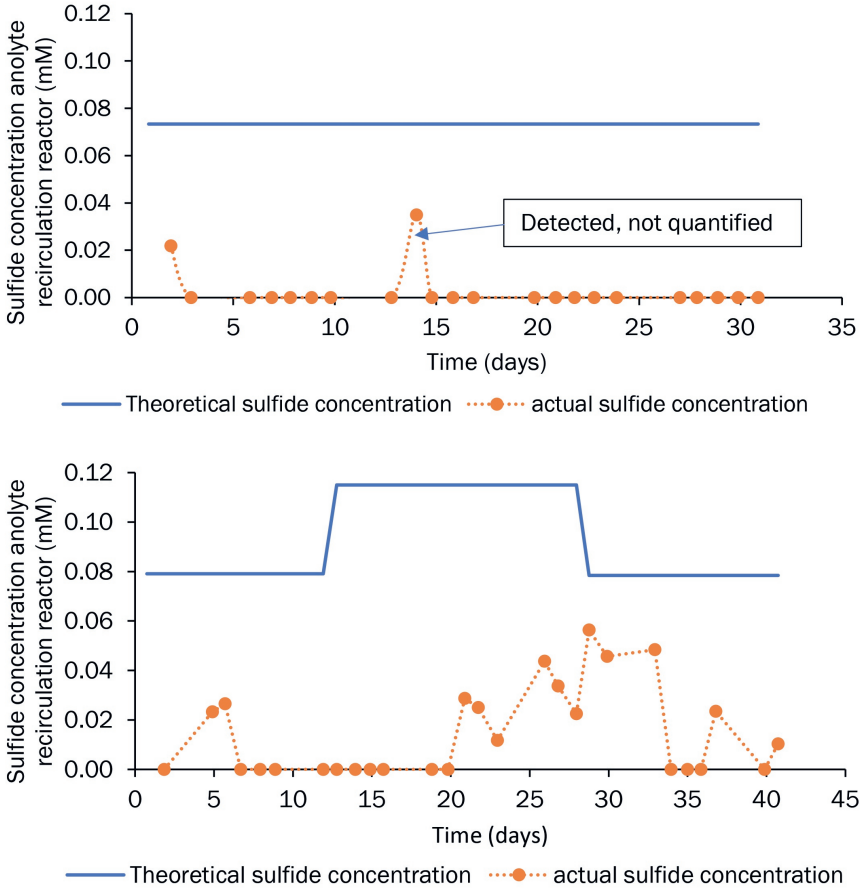

Figure SI5.3: The actual and measured sulfide concentrations in experiments 1 (top) and 2 (bottom. The blue line indicates the theoretical sulfide concentration in the anolyte recirculation reactor, which is set by the sulfide dosing rate and the recirculation flow rate. The orange dots indicate the measured sulfide concentration in the anolyte recirculation reactor.

SI 6 SUPPORTING INFORMATION FROM CHAPTER 7

SI 6.1 OPERATING CONDITIONS IN THE PILOT DURING DISCHARGE EXPERIMENTS

The bioreactor solution composition during the discharge experiments is shown in table SI 6.1. The analyses were performed as described elsewhere [11].

Table SI6.1: Composition of the solution in the aerated bioreactor of the pilot-scale installation during the discharge experiments

	Exp 1	Exp 2
pH in aerated bioreactor (-)	8.45	9.2
Alkalinity, expressed as HCO_3^- (M)	0.65	0.51
Conductivity (mS cm^{-1})	57	61
SO_4^{2-} (M)	0.17	0.26
$S_2O_3^{2-}$ (M)	0	0
Biomass concentration (mg-N L^{-1})	53	104

SI 6.2 MICROBIAL COMMUNITY COMPOSITION

Microbial community composition during the discharge experiments was analysis based on 16S rRNA gene sequencing, as described elsewhere [11]. Results are shown in Figure SI6.1.

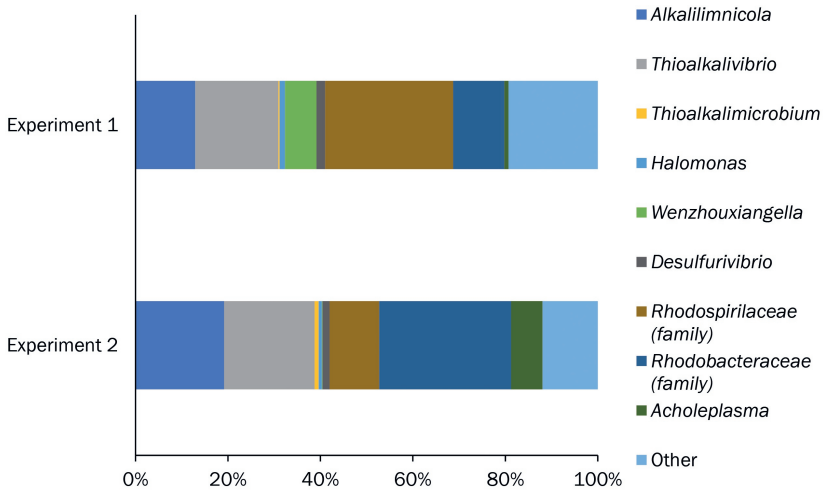

Figure SI6.1: Microbial community composition during the discharge experiments. All species (or families) with a relative abundance of at least 5% in one of the samples are shown [11].

SI 6.3 NON-LINEAR LEAST SQUARE PARAMETER ROUTINE

The unknown parameters in the model for ORP dependency of bacteria, represented by parameter vector θ, are estimated using the experimental data of the discharge tests. Via a least square routine, the estimated parameter output vector ($\hat{\theta}$) is given by:

$$\hat{\theta} = argmin_{\theta \in D} \sum_{i=1}^{N} \varepsilon(ORP_i | \theta)^2 \quad \text{(Equation SI6.1)}$$

Where $\varepsilon(\cdot \mid \theta) = y(i) - \kappa_{supernatant} - \hat{y}(\cdot \mid \theta)$ is the output error at measurement index *N* with setpoint *ORP*, $y(i)$ the harvested charge measurement at *i*, $\hat{y}(\cdot \mid \theta)$ the predicted model output given with estimated θ, $\kappa_{supernatant}$ the harvested charge of the supernatant i.e. solution without bacteria (mC) and D is the parameter domain. The measure for the model fit, error variance ${\sigma_\varepsilon}^2$, is given by:

$${\sigma_\varepsilon}^2 = \frac{\sum_{i=1}^{N} \varepsilon(ORP_i | \theta)^2}{N-p} \quad \text{(Equation SI6.2)}$$

With p the number of parameters. The standard deviation for each parameter is found by the square root of the diagonal of the covariance matrix (COV), which is defined by:

$$COV = {\sigma_\varepsilon}^2 \cdot (SENS^T \, SENS) \quad \text{(Equation SI6.3)}$$

where SENS is the (N x p) sensitivity matrix with elements $\frac{\partial \varepsilon(ORP_i | \theta)}{\partial \theta_j}$. The index j=1,..,p.

SI 6.4 ONLINE DATA DURING DISCHARGE EXPERIMENTS

Online data of air flow rate and ORP in the aerated bioreactor during discharge experiment 1 is shown in Figure SI6.2.

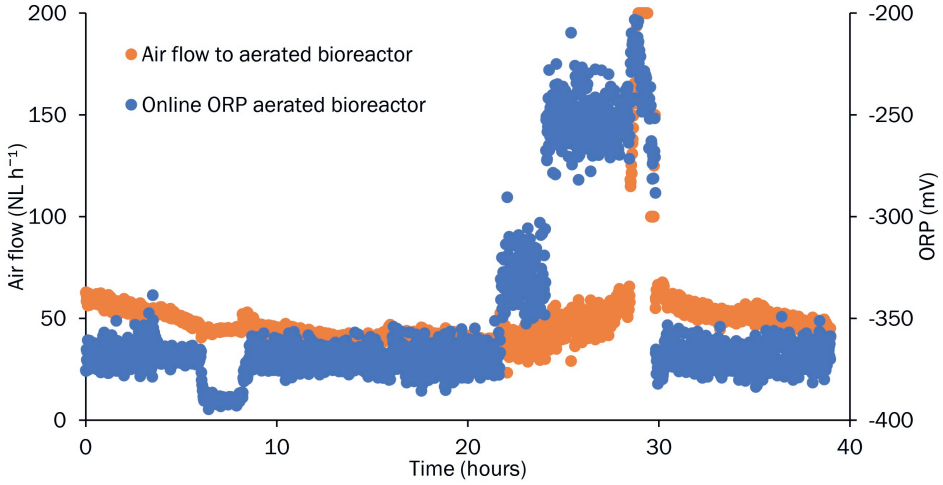

Figure SI6.2: Online data of ORP and airflow rate in the aerated bioreactor of the pilot-scale installation during discharge experiment 1.

REFERENCES

[1] R. De Rink, J.B. Klok, G.J. Van Heeringen, D.Y. Sorokin, A. Ter Heijne, R. Zeijlmaker, Y.M. Mos, V. De Wilde, K.J. Keesman, C.J. Buisman, Increasing the selectivity for sulfur formation in biological gas desulfurization, Environmental science & technology, 53 (2019) 4519-4527.

[2] S. Takahashi, J. Tomita, K. Nishioka, T. Hisada, M. Nishijima, Development of a prokaryotic universal primer for simultaneous analysis of Bacteria and Archaea using next-generation sequencing, PloS one, 9 (2014) e105592.

[3] J.G. Caporaso, J. Kuczynski, J. Stombaugh, K. Bittinger, F.D. Bushman, E.K. Costello, N. Fierer, A.G. Pena, J.K. Goodrich, J.I. Gordon, QIIME allows analysis of high-throughput community sequencing data, Nature methods, 7 (2010) 335-336.

[4] C. Quast, E. Pruesse, P. Yilmaz, J. Gerken, T. Schweer, P. Yarza, J. Peplies, F.O. Glöckner, The SILVA ribosomal RNA gene database project: improved data processing and web-based tools, Nucleic acids research, 41 (2012) D590-D596.

[5] R.C. Edgar, Search and clustering orders of magnitude faster than BLAST, Bioinformatics, 26 (2010) 2460-2461.

[6] Q. Wang, G.M. Garrity, J.M. Tiedje, J.R. Cole, Naive Bayesian classifier for rapid assignment of rRNA sequences into the new bacterial taxonomy, Applied and environmental microbiology, 73 (2007) 5261-5267.

[7] A. Janssen, S. Meijer, J. Bontsema, G. Lettinga, Application of the redox potential for controling a sulfide oxidizing bioreactor, Biotechnology and bioengineering, 60 (1998) 147-155.

[8] N. Pfennig, K.D. Lippert, Über das vitamin B 12-bedürfnis phototropher Schwefelbakterien, Archiv für Mikrobiologie, 55 (1966) 245-256.

[9] B. Geurkink, S. Doddema, H. de Vries, G.J. Euverink, E. Croese, Value of Next Generation Sequencing as Monitoring Tool For Microbial Corrosion-A Practical Case from Bioprophyling to Tailor made MMM Analysis, in: CORROSION 2016, OnePetro, 2016.

[10] A. Pushnov, Calculation of average bed porosity, Chemical and Petroleum Engineering, 42 (2006) 14-17.

[11] R. de Rink, S. Gupta, F. Piccioli de Carolis, D. Liu, A. Ter Heijne, J.B. Klok, C.J. Buisman, Effect of process conditions on the performance of a dual-reactor biodesulfurization process [unpublished manuscript, chapter 3 of this thesis], (2021).

Summary

Samenvatting

SUMMARY

Hydrogen sulfide (H_2S) is a toxic, odorous and corrosive gas that can be present in various gas streams, such as natural gas, synthesis gas, petroleum refinery gas streams and biogas. To prevent emission of sulfur compounds, such as sulfur dioxide, these gas streams require treatment before combustion. As a cost-effective and environmentally friendly alternative to physico-chemical processes, a biological gas desulfurization process has been developed. This process uses a mildly alkaline sodium (bi)carbonate solution to remove H_2S from gas streams in an absorber column. In an aerated bioreactor, a mixed population of sulfide oxidizing bacteria (SOB) converts dissolved sulfide, (HS^-) and polysulfide (S_x^{2-}), into predominantly elemental sulfur (S^0) using oxygen. Biological formation of sulfate (SO_4^{2-}) and chemical formation of thiosulfate ($S_2O_3^{2-}$) are enhanced at higher oxygen levels. These by-products impair the sustainability of the process as they consume caustic (NaOH). In addition, (thio)sulfate formation requires removal via a bleed stream. Although the bioreactor is operated under oxygen-limited conditions, formation of (thio)sulfate is inevitable in the current process.

In **Chapter 2** a new process line-up for biological gas desulfurization was investigated at pilot-scale level. In this 'dual-reactor line-up', an anaerobic bioreactor with sulfidic conditions was placed in between the absorber column and the aerated bioreactor. With this line-up, the selectivity for elemental sulfur formation of 97% was achieved, compared to 76% in the traditional 1-bioreactor line-up. This increase in elemental sulfur formation resulted in a reduction of 90% in NaOH consumption and bleed stream formation. A short-term effect of the addition of the anaerobic bioreactor was the decrease in sulfate formation, likely due to suppression of metabolic routes by sulfide. On longer term, the selection pressure in the anaerobic bioreactor resulted in a shift of the microbial population. The bacteria that became dominant were suggested to be limited to elemental sulfur formation and could not form sulfate. This further reduced the tendency for sulfate formation. A very interesting finding was that bacteria removed part of the sulfide in the anaerobic bioreactor, thereby shuttling sulfide and / or electrons from the anaerobic to the aerated bioreactor. This indicated that the oxidation of sulfide and the reduction of oxygen can be spatially separated due to the 'sulfide shuttling capacity' of the bacteria that are active in this process. Moreover, the sulfide uptake capacity of the bacteria increased over the course of the experiment. A direct effect of the sulfide uptake in the anaerobic

bioreactor is a lower sulfide concentration entering the aerated bioreactor, reducing chemical formation of thiosulfate.

In order to apply the 'dual-reactor line-up' in industry, more insight is required in the effect of the conditions in the anaerobic bioreactor on the process performance. These conditions are dependent on the specifications of the gas stream that needs to be treated and design choices. This was the topic of the work in **Chapter 3.** It was hypothesized that the selection pressure of the anaerobic bioreactor is dependent on a combination of the sulfide concentration and the hydraulic retention time (HRT). Therefore, several experiments at different combination of sulfide concentrations and HRT were performed. Furthermore, the effect of pH was investigated. To achieve a high selectivity for elemental sulfur formation (>95%), either the HRT in the anaerobic bioreactor should be at least 20 minutes, or the sulfide concentration should be at least 0.5 g L^{-1}. A higher pH resulted in lower selectivity for elemental sulfur formation (the selectivity for elemental sulfur formation was 88% at pH 9.1 and 96% at pH 8.5). Furthermore, the sulfide uptake in the anaerobic bioreactor was studied. The biological sulfide uptake increased at higher sulfide concentrations and at higher pH. The concentration of polysulfides, which are formed due to an equilibrium reaction between HS^- and elemental sulfur, increases at higher sulfide concentrations and higher pH. Hence, the results suggest that biological sulfide uptake in the anaerobic bioreactor is related to polysulfide.

The finding that bacteria can remove sulfide from solution under anaerobic conditions, lead to another hypothesis, namely that bacteria play a role the absorption of H_2S from the gas stream in the absorber column (**Chapter 4**). Previously, the absorption of H_2S into the process solution was considered to be purely physico-chemical. First, it was shown that activity of SOB increases with temperature between 25-45 °C. Subsequently, the H_2S absorption efficiency at different temperatures was determined. Whereas chemical absorption improves at lower temperatures, in our experiment the H_2S absorption efficiency increased at higher temperatures. Also when the biomass concentration in the stream to the absorber increased, the H_2S absorption efficiency improved. These results show that SOB enhance the absorption of H_2S and thus play a role in the removal of H_2S from gas streams. in the absorber. Thus, besides the aerated bioreactor, the bacteria are also active in the absorber.

In the biological desulfurization process (as described in chapters 2-4), bacteria use oxygen as electron acceptor for sulfide oxidation. In **Chapter 5** it was shown that bacteria taken from the biodesulfurization process can also use the anode of an electrochemical cell as electron acceptor. In batch tests it was shown that bacteria remove sulfide from solution under anaerobic conditions (without presence of an electron acceptor), similar to the removal in the anaerobic bioreactor. When these 'charged' SOB were subsequently transferred to an electrochemical cell, electric current was produced in the absence of dissolved sulfide. We called this ability of the bacteria to take up sulfide and release electrons at the anode 'electron shuttling'. Furthermore, it was shown that bacteria taken from the dual-reactor line up have a higher sulfide uptake capacity and produced more current than bacteria taken from a traditional 1-bioreactor line up.

In **Chapter 6** the electron shuttling principle as demonstrated in chapter 5 were applied in a continuous system, consisting of an anolyte uptake chamber and an electrochemical cell. Sulfide was continuously supplied to the anaerobic anolyte uptake chamber and removed from solution by bacteria. This solution, containing the charged bacteria and no dissolved sulfide, was circulated over the anode side of the electrochemical cell, where bacteria continuously released electrons. It was found that growth of bacteria occurred, mainly in the form of a biofilm on the anode. Furthermore, after a certain time of operation, the main end product became sulfate and not elemental sulfur. The results indicated that, most likely, planktonic bacteria oxidized sulfide to sulfur and that the biofilm oxidized sulfur to sulfate.

In **Chapter 7** an electrochemical cell was used to recover electrons the bacteria in the aerated bioreactor. In the aerated bioreactor, the air flow for oxygen supply to the aerated bioreactor is controlled via online measurement of the oxidation / reduction potential (ORP). The ORP was considered to be mainly dependent on the concentration of sulfide and oxygen in the bioreactor. However, both sulfide and oxygen are rapidly consumed and their concentrations in the aerated bioreactor are normally below the detection limit. In batch tests, it was shown that the ORP is not only dependent on sulfide or oxygen, but is influenced by the bacteria. Furthermore, the aerated bioreactor of the pilot-scale biodesulfurization installation that was also used for the experiments as described in chapters 2-4, was operated at various redox setpoints. Bacteria from the aerated bioreactor were transferred to an electrochemical cell and current was measured, demonstrating that bacteria release more electrons (i.e. contain more charge) when the

redox setpoint was lower. These measurements were subsequently used to calibrate a model to describe the relation between redox and charge storage. The model showed that selectivity for sulfate formation increases when bacteria contain less charge.

Throughout this PhD thesis it is shown that haloalkaliphilic sulfide oxidizing bacteria can store and shuttle sulfide and / or electrons. In the new process line-up, bacteria shuttle sulfide from the anaerobic bioreactor to the aerated bioreactor. The sulfide shuttling capacity also results in biological enhancement of H_2S from gas streams in the absorber. Furthermore, electricity production in an electrochemical cell can take place without dissolved sulfide being present. The new process line-up decreases chemical consumption and waste stream formation of biological gas desulfurization considerably, which is especially important when treating gas streams with a high sulfur load. The ability of bacteria to release electrons to an electrode in the absence of dissolved sulfide provides new opportunities to recover energy from sulfide, which potentially could further increase the sustainability of biological gas desulfurization.

SAMENVATTING

Waterstofsulfide (H_2S) is een zeer giftig en corrosief gas, dat stinkt naar rotte eieren. Het komt algemeen voor in allerlei gasstromen, zoals aardgas, biogas, gas dat gevormd wordt bij de vergassing van steenkool en biomassa ('syngas') en verschillende gasstromen die vrijkomen bij de winning en raffinage van aardolie. Bij verbranding van H_2S komt zwaveldioxide (SO_2) vrij. Dit is een giftig gas dat tevens zorgt voor de vorming van zure regen. Om de uitstoot van deze giftige zwavelcomponenten te voorkomen, is 'ontzwaveling' van H_2S houdende gassen noodzakelijk.

Eind jaren '80 van de vorige eeuw is op de vakgroep milieutechnologie van de Wageningen Universiteit een begin gemaakt met de ontwikkeling van een biologisch ontzwavelingsproces. In dit proces worden van nature voorkomende bacteriën gebruikt om giftig H_2S om te zetten in elementair zwavel (S^0), een vaste stof dat doormiddel van bezinking of centrifugatie afgescheiden kan worden. Dit 'biozwavel' heeft bovendien nuttige toepassingen, zoals gebruik in de landbouw. De eerste commerciële fabriek is in 1993 in bedrijf gesteld voor de ontzwaveling van biogas, dat gevormd wordt bij de verwerking van afvalwater van een aantal papierfabrieken. Deze fabriek staat in Eerbeek.

De eerste stap van het biologisch ontzwavelingsproces vindt plaats in een absorber, waar H_2S houdend gas volgens het tegenstroomprincipe in contact wordt gebracht met procesmedium. Dit procesmedium is een natrium(bi)carbonaatoplossing. Hierin reageert H_2S naar bisulfide (HS^-) en polysulfide (S_x^{2-}). De sulfidische stroom wordt vervolgens naar een bioreactor gebracht, waar sulfide oxiderende bacteriën de sulfide omzetten met behulp van zuurstof dat wordt toegevoerd via perslucht. Naast elementair zwavel worden ook de bijproducten sulfaat (SO_4^{2-}) en thiosulfaat ($S_2O_3^{2-}$) gevormd via respectievelijk biologische en chemische reacties. Het nadeel van de vorming van sulfaat en thiosulfaat is dat ze een verzurende werking op het procesmedium hebben waardoor er natriumhydroxide (NaOH) toegevoegd moet worden om de alkaliniteit van het procesmedium te behouden. Omdat sulfaat en thiosulfaat in de opgeloste vorm aanwezig zijn, kunnen deze alleen verwijderd worden via een spuistroom ('bleed'). Zowel de consumptie van NaOH als de vorming van een spuistroom komen de duurzaamheid van het proces niet ten goede en verhogen tevens de operationele kosten. Hoewel het proces onder zuurstof limiterende condities geopereerd wordt, wordt er altijd sulfaat en thiosulfaat gevormd. Het hoofddoel van dit onderzoek was het verminderen van sulfaat en thiosulfaat vorming zodat de consumptie van NaOH en de spuistroom verlaagd worden.

In **Hoofdstuk 2** wordt een nieuwe procesopstelling onderzocht waarin een anaerobe bioreactor is geplaatst tussen de bestaande absorber en beluchte bioreactor. Met deze nieuwe opstelling werd een hele hoge selectiviteit voor zwavel vorming gehaald (97% tov 76% in de traditionele opstelling zonder anaerobe reactor). De verhoogde selectiviteit voor zwavelvorming leidt tot een 90% verlaging van het NaOH verbruik en vorming van de spuistroom. In de anaerobe bioreactor verblijven de bacteriën onder sulfidische condities, wat zorgt voor selectiedruk. Het korte-termijn effect hiervan is een lagere sulfaat vorming, omdat sulfide sulfaatvorming onderdrukt. Op de langere termijn werd een verandering van de microbiologische populatie waargenomen. Van de bacteriën die dominant werden, wordt gedacht dat ze geen sulfaat kunnen maken en sulfide alleen kunnen oxideren naar elementair zwavel. Dit zorgde voor een verdere verlaging van de sulfaat vorming in het proces. Een andere opvallende observatie was dat bacteriën een deel van de sulfide al in de anaerobe bioreactor opnamen (zonder de aanwezigheid van zuurstof). Hierbij 'shuttelen' de bacteriën sulfide en/of elektronen van de anaerobe bioreactor naar de aerobe bioreactor. Dit duidt aan dat de oxidatie van sulfide en de reductie van zuurstof aparte processen zijn die gescheiden plaats kunnen vinden. Een direct effect van de sulfideopname is een verlaging van de sulfideconcentratie in de stroom van de anaerobe naar de beluchte bioreactor. Hierdoor wordt de chemische reactie tussen sulfide en zuurstof verlaagd en vindt er minder thiosulfaatvorming plaats.

Op de nieuwe procesopstelling met 2 bioreactor in de praktijk te kunnen toepassen is meer inzicht nodig in de invloed van de procescondities, met name in de anaerobe bioreactor, op de productvorming. In de praktijk zijn de procescondities afhankelijk van de gasstroom die behandeld moet worden en het ontwerp van de fabriek. Dit is onderzocht in **Hoofdstuk 3**. De hypothese was dat de selectiedruk van de anaerobe bioreactor afhankelijk is van de sulfideconcentratie en de verblijftijd. Er zijn 7 experimenten uitgevoerd waarbij de sulfideconcentratie en verblijftijd in de anaerobe bioreactor werden gevarieerd. Tevens werd het effect van de pH onderzocht. Om een hoge selectiviteit voor zwavelvorming te bereiken (>95%) moet de verblijftijd minimaal 20 minuten bedragen, of moet de sulfideconcentratie minimaal 0.5 g L^{-1} zijn. Een verhoging van de pH in de beluchte bioreactor van 8.5 naar 9.1 leidde tot een lagere selectiviteit voor zwavelvorming (96% bij pH 8.6 en 88% bij pH 9.1). Verder is de biologische opname van sulfide in de anaerobe bioreactor onderzocht. Er werd meer sulfide opgenomen naarmate de sulfide concentratie hoger was. Ook werd er meer sulfide opgenomen als de pH hoger was. Polysulfidevorming, dat plaatsvindt door een evenwichtsreactie tussen HS^- en elementair zwavel, is hoger bij

een hogere sulfide concentratie en bij een hogere pH. De verkregen resultaten duiden er dus op dat de biologische opname van sulfide in de anaerobe bioreactor te maken heeft met polysulfide.

De bevinding dat bacteriën sulfide opnemen uit het procesmedium onder anaerobe condities leidde tot nog een hypothese, namelijk dat bacteriën een rol spelen bij de absorptie van H_2S uit het gas in de absorber kolom (**Hoofdstuk 4**). Vanwege de afwezigheid van zuurstof in de absorber werd er altijd aangenomen dat de absorptie van H_2S een fysisch-chemisch proces is waarbij bacteriën geen rol speelden. Ten eerste is de activiteit van sulfide oxiderende bacteriën onderzocht in het temperatuurbereik van 25-40°C. De biologische activiteit van bacteriën neemt toe als de temperatuur stijgt. Hierna is de efficiëntie van H_2S absorptie bepaald bij verschillende temperaturen. Hieruit bleek dat H_2S absorptie verbeterde bij hogere temperaturen. Fysisch-chemische absorptie wordt juist beter als de temperatuur lager wordt. Ook bleek dat er meer H_2S geabsorbeerd werd als de concentratie bacteriën in het procesmedium naar de absorber, hoger was. Uit deze experimenten blijkt dat bacteriën ook in de absorber actief zijn en niet alleen in de beluchte bioreactor.

In het biologische ontzwavelingsproces, zoals beschreven in hoofdstukken 2-4, gebruiken bacteriën zuurstof als elektronenacceptor bij het oxideren van sulfide. In **Hoofdstuk 5** wordt laten zien dat de bacteriën in het biologische ontzwavelingsproces ook de anode van een elektrochemische cel kunnen gebruiken als elektronenacceptor. Uit batchexperimenten blijkt dat de bacteriën sulfide opnemen onder anaerobe condities zonder aanwezigheid van elektronenacceptor, zoals bijvoorbeeld zuurstof (vergelijkbaar met de sulfideopname in de anaerobe bioreactor). Deze 'opgeladen' bacteriën zijn vervolgens overgebracht naar een elektrochemische cel, waar elektrische stroom gemaakt werd zonder dat er vrije sulfide aanwezig was. De eigenschap van bacteriën om sulfide op te nemen en elektronen af te staan aan een elektrode noemen we 'electron shuttling'. Verder viel het op dat de bacteriën uit de nieuwe procesopstelling met anaerobe bioreactor meer sulfide konden opnemen en meer stroom produceerden dan bacteriën uit de traditionele processopstelling zonder anaerobe bioreactor.

In **Hoofdstuk 6** wordt het elektronen shuttling principe uit Hoofdstuk 5 toegepast in een continue proces, bestaande uit een sulfide opname reactor en een elektrochemische cel. Sulfide werd continue toegevoerd aan de sulfide opname reactor, waar dit werd

opgenomen door de bacteriën. Het medium, die de 'opgeladen' bacteriën en geen vrije sulfide bevatte, werd continue gecirculeerd over de anode van de elektrochemische cel. Aan de anode werden de bacteriën continue ontladen, waardoor er een constante elektrische stroom geproduceerd werd. Het bleek dat er groei van bacteriën plaatsvond, voornamelijk op de anode in de vorm van een biofilm. Na een aantal dagen operatie werd er voornamelijk sulfaat gevormd. Uit de resultaten blijkt dat het waarschijnlijk is dat de planktonische (gesuspendeerde) bacteriën sulfide naar zwavel omzetten en de biofilm zwavel naar sulfaat.

In **Hoofdstuk 7** is er, met behulp van een elektrochemische cel, gekeken naar elektronenopslag in de bacteriën uit de beluchte bioreactor van het biologische ontzwavelingsproces. De luchttoevoer (en daarmee de zuurstoftoevoer) naar deze bioreactor wordt gestuurd middels online meting van de oxidatie / reductie potentiaal (ORP). De ORP in de beluchte bioreactor werd geacht voornamelijk afhankelijk te zijn van de opgeloste sulfide- en zuurstofconcentraties. Echter, zowel sulfide- als zuurstof zijn normaal gesproken niet detecteerbaar in de beluchte bioreactor. Uit batchexperimenten blijkt dat de ORP, naast sulfide en zuurstof, ook bepaald wordt door de bacteriën. De beluchte bioreactor uit de proefinstallatie die ook gebruikt is tijdens de experimenten zoals beschreven in hoofdstukken 2-4, is geopereerd op verschillende ORP setpoints. Voor elk setpoint zijn er bacteriën uit de beluchte bioreactor overgebracht naar een elektrochemische cel en werd gemeten hoeveel elektrische stroom er geproduceerd werd. Het bleek dat hoe lager het ORP setpoint, hoe meer stroom er geproduceerd werd. Dit laat zien dat bacteriën meer 'lading' bevatten bij een lager ORP setpoint. Deze metingen zijn vervolgens gebruikt om een wiskundig model te kalibreren om de relatie tussen ORP en de hoeveelheid lading te beschrijven. Dit model laat zien dat de selectiviteit voor zwavel toeneemt als de lading in de bacteriën hoger is. De methode kan gebruikt worden bij verdere optimalisatie van zuurstoftoevoer naar de bioreactor om de zwavelvorming te verhogen.

LIST OF PUBLICATIONS

Bacteria as electron shuttle for sulfide oxidation - Annemiek ter Heijne, Rieks de Rink, Dandan Liu, Johannes B. M. Klok, and Cees J. N. Buisman, *Environmental Science & Technology Letters* 2018 *5* (8), 495-499

Increasing the selectivity for sulfur formation in biological gas desulfurization - Rieks de Rink, Johannes B.M. Klok, Gijs J. van Heeringen, Dimitry Y. Sorokin, Annemiek ter Heijne, Remco Zeijlmaker, Yvonne M. Mos, Vinnie de Wilde, Karel J. Keesman, and Cees J.N. Buisman, *Environmental Science & Technology* 2019 *53* (8), 4519-4527

Biologically enhanced hydrogen sulfide absorption from sour gas under haloalkaline conditions, Rieks de Rink, Johannes .B.M. Klok, Gijs J. van Heeringen, Karel J. Keesman, Albert J.H. Janssen, Annemiek ter Heijne, Cees J.N. Buisman, *Journal of hazardous materials*, 383 (2020) 121104.

ACKNOWLEDGEMENTS

The past 6 years have been a great adventure. I would like to express my sincere gratitude to all the people that contributed to this thesis.

First of all I would like to thank my supervisors: Jan, Annemiek and Cees.
Jan, your ideas have been the basis for this research and I'm glad we have been able to demonstrate a few of those ideas in the lab. This thesis would never have been possible without your efforts and I'm very grateful for your support during the past 6 years. When I was again pessimistic about experiments, you were always able to convince me of the value of the obtained results. Also thanks to your wife Susanne for her patience when we had scheduled meetings in the late evening.
Annemiek, I'm very happy to have had you as my supervisor. Thank you for all your valuable input during meetings, manuscript (re)writing and rebuttals, and for giving me the trust that I would be able to make it to this point. I especially liked the summer diners at your place and the times that I played chess with your son Wietse.
Cees, I was very happy when you provided the (unexpected) opportunity to do my PhD research at Environmental Technology. I enjoyed the nice discussions we've had during the AIO meetings, lunch walks and the yearly biorecovery meetings. Your ideas, suggestions and advice were very valuable, although sometimes it took me the rest of the day to digest your input.

I would also like to thank other people from Paqell and Environmental Technology for their contributions. Gijs, I remember the many Facetime sessions and your visits to 'Hal 5' during the initial year in Groningen, which were very helpful. I appreciate your help and guidance in all the other Paqell work.
Dandan, I'm grateful for everything you learned me about bioelectrochemistry when I just started at ETE. Many experiments would have been impossible without your help.
Special thanks to the technical and analytical staff from ETE for all their support with performing experiments and analysis: Vinnie, Bert, Jean, Pieter, Livio, Ilse, Julian, Jill, Katja and Hans.
Annemerel, we started at ETE around the same time and on the same topic; I'm happy that you are paranymph during my defense. Thanks for all your help, especially with the microscope and PSD measurements.

Margo and Sanne, I enjoyed the time in Bath during the electrochemistry course. Thanks for the nice discussions about our research.
I'm grateful to all people from ETE for the pleasant atmosphere and all the nice borrels, department trips and celebrations. A special thanks for this to the secretary team: Liesbeth, Marjolein and Wies.

The members of the sulfur theme are gratefully acknowledged for the stimulating discussions during the theme meetings: Dimitry, Albert, Gerard, Karel, Caroline, Pawel, Renata, Jaap, Razvan, Karine and Suyash. Dimitry, your enormous knowledge on sulfur bacteria is impressive and so valuable for all sulfur theme researchers. Thanks for the interesting discussions and your contributions to the first dual line-up paper and the electrochemistry work. Albert, I enjoyed the discussions we've had on the absorber experiments, your detailed feedback was very helpful. Karel, thank you for your input on the dual line-up- and absorber paper. Suyash, thanks for the nice cooperation with the pilot plant experiments in Wageningen.

During the past 6 years, I've had the pleasure to work with many students, whom I like to thank for the collaboration and their contributions: Luc, Jasper, Marijke, Pieter, Flavia, Micaela, Thomas, Mark and Sean.

I would like to thank my colleagues at Paqell for their support and cooperation: Joost, Hans, Desiree, Jan-Henk, Uli, Elsbeth and Sandra. Joost, I appreciate the freedom you gave me to do my PhD research within my job at Paqell.

Angelique, thank you for creating this book, the nice lay-out and your support during the final stage of my PhD.

Finally, I like to thank my family. Lieve papa en mama, lieve Bake, ik wil jullie bedanken voor jullie onvoorwaardelijke steun en liefde. Lieve Wes, ik hoop dat mijn gepieker iets minder wordt nu dit erop zit. Dankjewel dat je er altijd voor mij bent. En onze allerliefste Siem, je maakt ons zo gelukkig! Ik hou van jullie.

Rieks

ABOUT THE AUTHOR

Frederikus (Rieks) de Rink was born on July 27, 1990 in the city of Groningen, the Netherlands. Growing up in the village Zuidhorn, he attended high school (VWO) at the Kamerlingh Onnes College in Groningen where he graduated in 2008. The same year, he started studying at Wageningen University, where he obtained his MSc degree in biotechnology with a specialization in process technology. In 2015, he started working at the company Paqell as process engineer. While employed at Paqell, Rieks started his PhD research at the department of Environmental technology of Wageningen University in 2016, of which the results are described in this dissertation. During his PhD, Rieks combined research with his job as process engineer at Paqell, providing (on-site) technical support for companies operating the Thiopaq O&G technology, which he will continue after obtaining his PhD.

The research described in this thesis was financially supported by Paqell B.V.

Financial support from Wageningen University for printing this thesis is gratefully acknowledged.

Cover painting by Antje Dijk
Lay-out by Angelique Wammes-Bouman
Printed by Proefschriftmaken